Amplitude squeezed states of the radiation field

by

KASIVISHWANATHAN SUNDAR

A THESIS IN PHYSICS

Presented to the University of Madras in partial fulfillment of the requirements for the degree of Doctor of Philosophy

April 1996

The Institute of Mathematical Sciences
C.I.T. Campus, Taramani
Madras 600113 INDIA

எப்பொருள் எத்தன்மைத் தாயினும் அப்பொருள்
மெய்பொருள் காண்ப தறிவு.

— குறள்

Intellect is one which seeks the essentials of anything whatever be its nature.

— Kural

எப்பொருள் : *epporul* – anymatter, anything ; எத்தன்மைத் தாயினும் : *eththanmaith thaayinum* – be it of any kind, of any nature ; அப்பொருள் : *apporul* – of that matter, of that thing ; மெய்பொருள் : *meyporul* – the subtle or inner meaning, essentials, the truth ; காண்பது : *kanbhadhu* – to see, to seek ; அறிவு : *aarivu* – mind, intellect.

CERTIFICATE

This is to certify that the Ph.D. thesis titled ***Amplitude squeezed states of the radiation field*** submitted by KASIVISHWANATHAN SUNDAR is a record of bonafide research work done under my supervision. The research work presented in this thesis has not formed the basis for the award to the candidate of any Degree, Diploma, Associateship, Fellowship or other similar titles. It is further certified that the thesis represents independent work by the candidate and collaboration when existed was necessitated by the nature and scope of the problems dealt with.

R. Simon

Thesis Supervisor

April 1996

Abstract

In the recent decades, squeezed light, which exhibits statistics that cannot be associated with any classical stochastic process, has been experimentally generated by a number of groups in a variety of configurations. Of particular interest is the class of squeezed states known as the amplitude squeezed states, which are characterized by their photon number fluctuations being smaller than that of a coherent state. The technological implications of these states in fields such as telecommunications has been clearly demonstrated, apart from their immense importance in the field of pure physics. These states of the radiation field show many inter-related non-classical properties such as sub-poissonian statistics in photon counting experiments, noise reduction below shot-noise level in direct detection, and photon antibunching in Hanbury-Brown-Twiss type of intensity-intensity correlation experiments.

In this thesis, we propose a combination of quadratic and quartic non-linearities, viz, evolving a quadrature squeezed state through a Kerr medium, which results in a variety of states with different properties. Of great interest are the states which show substantial amplitude squeezing and whose photon number fluctuations can be minimized to a value $\langle (\Delta\hat{n})^2 \rangle < \langle \hat{n} \rangle^{1/5}$. With the existing technology this is one of the proposals which seem experimentally viable. We have also studied other amplitude squeezed states produced by the evolution of quadrature squeezed states in the Kerr medium which even if experimentally more difficult to achieve at this time are nevertheless interesting.

These proposals have stemmed from a deeper understanding of the dependence of amplitude squeezing upon the curvature of the quasi probability distributions

(QPD) such as the Q-function. The usual quadrature squeezed state, for a very high squeezing, has a QPD which is concentrated along a straight line segment in phase space. On the other hand for a Fock state, which has a vanishing photon number uncertainty, the QPD is concentrated along a circle centered at the origin of phase space. Hence states having curved QPD, such as those produced by evolving a coherent state or a quadrature squeezed state through a Kerr medium, should show reduced photon number uncertainty after a suitable displacement to an appropriate position in phase space. Simpler states with a curved QPD are superpositions of two coherent states such as $|x\rangle + e^{i\theta}|-x\rangle$. We have shown that the angle θ, called the relative phase, plays a crucial role in imparting a curvature to the quasi probability distribution. Hence this relative phase is fundamental in the understanding of amplitude squeezing, as any state can be expressed as a superposition of coherent states, and since the behavior of such superpositions can be understood and built in terms of pairwise superpositions.

This thesis is arranged into six chapters. The introductory chapter quickly recounts the tools required to pursue the subject. Quantization of the radiation field and the different representations of the quantum field are briefly presented. The coherent state representations are discussed giving a short account of the various quasi-probability distributions. The quantum noise of the electromagnetic field and the tools necessary to quantify and study it are also recollected along the way. The quadrature squeezed states are then introduced from a more conceptual point of view. Finally, the Kerr medium with its quartic interaction term and its effect on a coherent state evolving through it are presented briefly.

In the second chapter, the role of relative phase, in the sense of Pancharatnam's

classic work, is explored in the context of superposition of coherent states. In particular, it is demonstrated that one of the effects of the relative phase is to produce a curvature in the QPD. For later convenience a canonical form of the superposition of two coherent states is given. We study in detail the effect of the relative phase on the QPD of the canonical form. The noise matrix for the canonical form is then calculated and the presence of various kinds of squeezing for different relative phases are studied. A general superposition of two coherent states is then studied by reducing and relating it to the canonical form.

In the third chapter, the relationship between amplitude squeezing and relative phase is analyzed using the superposition of two coherent states. We show that one can optimize the amplitude squeezing by displacing the superposition with a given relative phase to a proper position in phase space. The real role the relative phase plays in producing amplitude squeezing is then studied by fixing a superposition of two coherent states at a given distance from the origin and varying the relative phase between the component states. We also show that for small squeezing the quadrature squeezed state, whose QPD is not curved, is equivalent to a in-phase superposition of two coherent states.

The fourth chapter studies the evolution of a quadrature squeezed state in a Kerr medium. The calculations involving this are considerably simplified if one expresses the quadrature squeezed state as a superposition of coherent states. The pictorial representation of this evolution is given using the Q-function, which is then compared with that of the coherent state case. The expectation values of various field quantities are then calculated to assess the noise properties of the field and certain interesting limiting cases are pointed out.

The fifth chapter presents the study of amplitude squeezing in the superposition of quadrature squeezed states. The evolution in a Kerr medium can give rise to Yurke-Stoler type of superposition of quadrature squeezed states, and such a state shows considerable amplitude squeezing when displaced to a proper position in phase space. The photon number properties of these displaced states are then studied. One particular case of getting amplitude squeezed states from a Yurke-Stoler type of superposition of phase squeezed states is then studied in detail and it is shown analytically that $\langle (\Delta\hat{n})^2 \rangle < \langle \hat{n} \rangle^{2/3}$ in this case. Finally, the feasibility of getting amplitude squeezed states from other Yurke-Stoler type superpositions is briefly considered.

The sixth chapter proposes a scheme for getting highly amplitude squeezed states through the evolution of a quadrature squeezed state in a Kerr medium. The scheme is first outlined and the photon number fluctuation of the out-coming beam is then calculated. The photon number fluctuation is then minimized first by optimizing the scaled time of evolution inside the Kerr medium for a given quadrature squeezing. The presence of a minimum here enables one to optimize the initial quadrature squeezing too. After this complete optimization of the parameters involved, the photon number fluctuation is shown to go as $\langle \Delta\hat{n})^2 \rangle < \langle \hat{n} \rangle^{1/5}$, which is two orders of magnitude smaller than those obtained in previous similar schemes. Finally, the experimental feasibility of this scheme, and its potential as a candidate for getting experimentally the smallest photon number fluctuation as of date, are discussed.

Parts of the research work leading to this thesis have been published, some of which (*) are not included in this thesis.

"Generation of amplitude squeezed states of light from phase squeezed coherent states",

Kasivishvanathan Sundar, *J. Mod. Opt.*, in press (1996).

"Amplitude-squeezed quantum states produced by the evolution of a quadrature-squeezed coherent state in a Kerr medium", Kasivishvanathan Sundar, *Phys. Rev.* **A53**, 1096-1111 (1996).

"Highly amplitude squeezed states of the radiation field", Kasivishvanathan Sundar, *Phys. Rev. Lett.* **75**, 2116 (1995).

(*) *"Twisted Gaussian Schell-model beams : I. Symmetry structure and normal-mode spectrum"*, R. Simon, K. Sundar and N. Mukunda, *J. Opt. Soc. Am.* **A10**, 2008-2016 (1993).

(*) *"Twisted Gaussian Schell-model beams : II. Spectrum analysis and propagation characteristics"*, K. Sundar, R. Simon and N. Mukunda, *J. Opt. Soc. Am.* **A10**, 2017-2023 (1993).

(*) *"Coherent-mode decomposition of general anisotropic Gaussian Schell-model beams"*, K. Sundar, N. Mukunda and R. Simon, *J. Opt. Soc. Am.* **A12**, 560-569 (1995).

To my wife ***K. S. Shobana***

and

To my daughter ***K. S. Anamica***

without whose unfailing sympathy and encouragement

this work would have never been

made possible.

Acknowledgments

I am indebted to my thesis supervisor Prof. R. Simon for the patience he has shown in guiding me through these six years. I shall always envy the thoroughness with which he looks at any problem, and I am grateful for the open mindedness he has shown in giving me absolute freedom to do things to my liking. He had always given his full attention and had been of great support in many ways. I thank Srinath for his assistance in proof reading.

I refrain from mentioning any name of the office and library staff, since I knew every one of them personally, and each one has offered his/her help at many times. I extend my thanks to all of them.

I take this opportunity to thank Prof. W. Schleich, University of Ulm, Germany, and Prof. P. Mandel, University of Brussels, Belgium, for the hospitality that they showed me when I was visiting these places.

Finally, I wish to thank all my friends here for the kind of unadulterated fun that we had in Matscience.

Contents

Chapter 1

Introduction

In this introductory chapter, we briefly summarize the concepts and techniques needed to pursue our study. We first recollect the usual way in which the electromagnetic field is quantized. The usual representations of the quantized electromagnetic field in terms of the Fock states and coherent states are then briefly summarized. Along the way, we introduce the quantum noise of the electromagnetic field and the tools needed to quantify this noise. We briefly discuss the density operator and the various quasi-probability distributions. The quadrature squeezed state is then introduced from a more conceptual point of view and its properties listed. Finally, the Kerr medium, which gives rise to another kind of squeezing in which the noise in the photon number is squeezed, is reviewed, and its effect on a coherent state is summarized.

1.1 Quantization of the Electromagnetic field

The quantum theory of light grew out of Max Planck's [1] proposal that the electromagnetic radiation is made up of discrete lumps of energy, where the energy of each lump is postulated to be proportional to the frequency of radiation. Planck made this proposal at that time to explain the experimentally observed spectral energy distribution of a radiating black body, which was inexplicable in terms of the classical

theories. This proposal was consequently used to explain the phenomenon of photo-electric-current, first observed by Hertz in 1877 and further studies of which were conducted by Lenard between 1899 – 1902. It was experimentally observed that in the phenomenon of photo-electric-current, the energy carried off by the electrons is independent of the intensity and, moreover, this carried off energy was proportional to the frequency of the radiation, which was in contradiction to the predictions of classical theory of radiation. Starting from Planck's hypothesis, Einstein explained the nature of photo-electric current and introduced the term *photon* [2, 3] to mean the discrete lump of energy of the radiation field. He and others extended the same treatment to other undulatory phenomena such as sound waves in a solid [4, 5, 6], which resulted in the solution to the long standing problem of specific heat of solids.

Around this time, the field of spectroscopy [7] had matured enough to identify the signature of the atoms in line spectra. Even the existence of a mathematical relationship between the lines had been recognized [8, 9]. The evidence of the planetary model of an atom, due to the investigations of Rutherford [10], could not explain the structure of the line spectra on the basis of classical electromagnetic theory. Once again, the quantum hypothesis was used successfully to explain the spectra of (at least the simplest) atoms [11]. The adhoc 'quantum' conditions used in the above process were refined by Sommerfeld [12]. This paved way for a more analytical approach based on the earlier work by Hamilton, and Heisenberg [13], and Born and Jordan [14], among themselves [15] developed the theory further into what was then known as Matrix mechanics. In parallel, De Broglie's proposal that all matter must also have a wave counterpart [18], led to the development of a mechanics for this 'waves' by Schrödinger [19]. Dirac took the work on Matrix

mechanics to a more abstract level in this period [16, 17], which finally led him to the formulation of quantum mechanics in a unified way [20] that we use now. In 1928, Dirac developed the relativistic quantum theory of electron [21], which was soon followed by attempts to quantize other fields [22].

In 1909, Einstein proposed a phenomenological theory of radiation [72], in which he introduced the concept of stimulated emission of photons apart from the spontaneous emission. It could be said that the *quantum* theory of absorption and emission of photons was first formulated when Dirac [73] in 1927 could obtain the A and B coefficients earlier introduced by Einstein. At present we use a similar but non-covariant formulation [23, 24], to quantize the radiation field. The starting point [23, 24, 25, 26, 27, 28] is the Maxwell's equation for the electromagnetic field, which itself was the result of earlier work by Coulomb, Ampère, Faraday and Biot. These equations give the relationship between the electromagnetic field vectors $\vec{E}$ and $\vec{B}$, and their sources, namely the charge density ρ and the current density $\vec{J}$. If one knows the scalar field ρ and the vector field $\vec{J}$ at every point in a given domain, then the Maxwell's equations in principle provides one with the solution of the polar vector field $\vec{E}$, and the axial vector field $\vec{B}$. The Maxwell's equation themselves are given by

$$\begin{aligned}
\vec{\nabla}\cdot\vec{E} &= \frac{\rho^f}{k_e\epsilon_0} && \text{(Gauss Law)} \\
\vec{\nabla}\cdot\vec{B} &= 0 && \text{(No Magnetic Monopoles)} \\
\vec{\nabla}\times\vec{E} &= -\frac{\partial\vec{B}}{\partial t} && \text{(Faraday's Law)} \\
\vec{\nabla}\times\vec{B} &= k_m\mu_0\vec{J}^f + \frac{k_e k_m}{c^2}\frac{\partial\vec{E}}{\partial t} && \text{(Modified Ampère's Law),}
\end{aligned} \tag{1.1}$$

where c is the velocity of light in vacuum, and ϵ_0, μ_0 are the permittivity and per-

meability of vacuum. k_e and k_m are relative permittivity and relative permeability of the medium. The modification of the Ampère's law to include the displacement current was the contribution of Maxwell, which led to the completion of the theory, and to identify Light as an electromagnetic field.

The source terms ρ^f and $\vec{J}^f$ stand for the free charge and free current, which *does not* include the bound charges of the medium[30, 31]. The electromagnetic properties of the medium due to the existence of the bound charges are generally incorporated into the relative permittivity and relative permeability of the medium. In linear anisotropic media , k_e and k_m are represented by second rank tensors [29, 31], as the direction of the induced field may be different from that of the inducing field. In very strong fields, such as those produced by a laser, k_e and k_m are interpreted as functions of $\vec{E}$ and $\vec{B}$ respectively to take into account the non-linearities [32] exhibited by the medium at such strong fields.

We consider as an illustration to the method of quantizing the radiation field, the quantization of radiation in a source free region ($\rho^f = 0$, $\vec{J}^f = 0$). In the source free region, which we will call as the cavity, the first and second of the Maxwell's equations will be identically satisfied if one takes

$$\begin{aligned} \vec{B} &= \vec{\nabla} \times \vec{A} \\ \vec{E} &= -\frac{\partial \vec{A}}{\partial t} - \vec{\nabla} V \quad , \end{aligned} \tag{1.2}$$

where $\vec{A}$ is the vector potential and V, the scalar potential. Since the Maxwell's equations are gauge invariant, and since one mainly works in the non-relativistic regime in quantum optics, one usually chooses the *Coulomb gauge* [23], described by the conditions $\vec{\nabla} \cdot \vec{A} = 0$ and $V = 0$, and which implies that both $\vec{E}$ and $\vec{B}$ are

determined by the transverse vector potential $\vec{A}$ alone. Substituting for the electric and magnetic field in terms of the potentials, and incorporating the Coulomb gauge condition, we get a wave equation for the vector potential, the solutions of which are the solutions of the Maxwell's equation.

The total energy contained in the field inside the cavity is the hamiltonian, given by

$$H = \frac{1}{2}\int(\epsilon_0 \vec{E}\cdot\vec{E} + \frac{1}{\mu_0}\vec{B}\cdot\vec{B})dV \quad , \tag{1.3}$$

where dV is the volume element, and the integration is done over the entire volume of the cavity. The electric and the magnetic fields at each point inside the cavity are specified by giving values to the components of $\vec{A}$ at each point in the cavity. If one treats these as the variables describing the field, then it is obvious that these are infinite and continuous. One can make this countably infinite, by assuming that the cavity is of finite size L^3, and by finding the entire set of functions that satisfy the wave equation for some given boundary condition. One can then express $\vec{A}$ as a superposition of these functions, and use the coefficients as the dynamical variables describing the field. Thus, the static aspects of the problem such as the boundary conditions are included in the solutions, and the dynamic aspects such as the time variation of the fields are built into the coefficients. Hence one can make an ansatz for the solution of the wave equation as

$$\vec{A}(\vec{r},t) = \frac{1}{\sqrt{\epsilon_0}}\sum_m q_m(t)\vec{u}_m(\vec{r}) \quad , \tag{1.4}$$

where the constant outside the sum is for normalization purposes. The functions $\vec{u}_m(\vec{r})$ can be chosen to be orthonormal. The coefficients, or amplitudes q_m, satisfy

a differential equation analogous to that of the simple harmonic oscillator. Each function $\vec{u}_m$ of the orthonormal set is called a *mode*.

One set of orthonormal functions which are solutions to the wave equation are the cosine or the sine functions, depending on the boundary conditions. But note that these solutions are standing wave solutions and one is often interested in travelling waves. The usual procedure to get travelling waves is to require periodic boundary condition at the walls of the cavity. One may also get travelling waves by observing the fact that a standing wave can be made up of a superposition of two travelling waves, travelling in *opposite* directions. Hence one can choose a set of complex mode functions, which in the simplest case can be plane waves, in which case the amplitudes too become complex and are denoted by a_m and a_m^*. Introducing the polarizations also into the mode functions, we can have

$$\vec{u}_{m\sigma}(\vec{r}) = \frac{\hat{e}_{m\sigma} \exp(i\vec{k}\cdot\vec{r})}{\sqrt{V}} \quad . \tag{1.5}$$

One can now write the vector potential in terms of these as

$$\vec{A}(\vec{r},t) = \sum_m \sum_{\sigma=1}^{2} \sqrt{\frac{\hbar}{2\omega_m \epsilon_0 V}} \hat{e}_{m\sigma} \left(a_{m\sigma} e^{-i\omega_m t} e^{i\vec{k}\cdot\vec{r}} + a_{m\sigma}^* e^{i\omega_m t} e^{-i\vec{k}\cdot\vec{r}} \right) \quad . \tag{1.6}$$

It is obvious that each term in the series is a solution to the wave equation if

$$\vec{k}_m \cdot \vec{k}_m = \left|\vec{k}_m\right|^2 = \frac{\omega_m^2}{c^2} \quad . \tag{1.7}$$

The coulomb gauge condition $\vec{\nabla}\cdot\vec{A} = 0$ imposes that

$$\hat{e}_{m\sigma} \cdot \vec{k}_m = 0 \quad , \tag{1.8}$$

which is called the transversality condition. Here the direction of $\vec{k}_m$ is the direction of propagation of the plane wave. Hence we see that $\vec{A}$, and hence $\vec{E}$ (since $\vec{E}$ is the

time derivative of $\vec{A}$), are perpendicular to the direction of propagation. Note also that the summations now run over $-\infty$ to ∞, and $\vec{k}_{-m} = -\vec{k}_m$ and $\omega_{-m} = \omega_m$.

Now, if one sets $a_{m\sigma}\exp(-i\omega_m t) = a_{m\sigma}(t)$, we can write the electric and the magnetic fields as

$$\begin{aligned}
\vec{E}(\vec{r},t) &= i\sqrt{\frac{\hbar\omega_m}{2\epsilon_0 V}}\hat{e}_{m\sigma}\left(a_{m\sigma}(t)e^{i\vec{k}\cdot\vec{r}} + a^*_{m\sigma}(t)e^{-i\vec{k}\cdot\vec{r}}\right) \\
\vec{B}(\vec{r},t) &= \frac{i}{c}\sqrt{\frac{\hbar}{2\omega_m\epsilon_0 V}}\frac{(\hat{e}_{m\sigma}\times\vec{k}_m)}{|\vec{k}_m|}\left(a_{m\sigma}(t)e^{i\vec{k}\cdot\vec{r}} + a^*_{m\sigma}(t)e^{-i\vec{k}\cdot\vec{r}}\right) \quad , \qquad (1.9)
\end{aligned}$$

where we have done a little bit of vector algebra. The hamiltonian of the field given in Eq. (1.3) can now be written as

$$\begin{aligned}
H &= \frac{1}{2}\sum_{m,\sigma}\hbar\omega_m(a_{m\sigma}a^*_{m\sigma} + a^*_{m\sigma}a_{m\sigma}) \\
&= \frac{1}{2}\sum_{m,\sigma}\left(p^2_{m\sigma} + \omega^2_m q^2_{m\sigma}\right) \quad , \qquad (1.10)
\end{aligned}$$

where we have used

$$a_{m\sigma} = \frac{1}{\sqrt{2\hbar\omega_m}}(\omega_m q_{m\sigma} + ip_{m\sigma}) \quad , \qquad (1.11)$$

and its complex conjugate. The details of this derivation can be found in many books (See in particular, appendix B of [27]) and hence is not reproduced here.

We have shown that the problem of the radiation field in vacuum can be reduced to a problem of infinitely many non-interacting harmonic oscillators. Since one is familiar with the quantum mechanics of simple harmonic oscillators, all one has to do is to promote the complex amplitudes α, α^* to non-hermitian operators $\hat{a}$ and $\hat{a}^\dagger$. Since it is experimentally known that photons are bosons, one promotes $p_{m\sigma}$, $q_{m\sigma}$ to hermitian operators obeying the boson commutation relations. These operators $\hat{p}_{m\sigma}$ and $\hat{q}_{m\sigma}$ are called the quadrature operators, since one can express the electric and

the magnetic fields directly in terms of them. The bosonic commutation relations for the quadrature operators imply that the non-hermitian operators for the amplitudes $a_{m\sigma}$ and there complex conjugate satisfy

$$\begin{aligned} [\hat{a}_{m\sigma}, \hat{a}^{\dagger}_{m'\sigma'}] &= \delta_{mm'}\delta_{\sigma\sigma'} \\ [\hat{a}_{m\sigma}, \hat{a}_{m'\sigma'}] = 0 &= [\hat{a}^{\dagger}_{m\sigma}, \hat{a}^{\dagger}_{m'\sigma'}] \quad , \end{aligned} \tag{1.12}$$

which again implies that the radiation oscillators for all modes are independent of each other, and the annihilation and creation operators for different modes commute. Hence the hamiltonian for the quantized radiation field can be written as

$$\widehat{H} = \frac{1}{2}\sum_{m,\sigma} \hbar\omega_m \left(\hat{a}^{\dagger}_{m\sigma}\hat{a}_{m\sigma} + \hat{a}_{m\sigma}\hat{a}^{\dagger}_{m\sigma}\right) = \sum_{m,\sigma} \hbar\omega_m \left(\hat{a}^{\dagger}_{m\sigma}\hat{a}_{m\sigma} + \frac{1}{2}\right) \quad . \tag{1.13}$$

In this section we have summarized the method for quantizing the radiation field in vacuum. What has been done here is but a trivial example of quantization. There is an extensive literature on quantizing some non-trivial configurations. One can quantize a box filled with uniform dielectric [33] and also a box filled with two uniform media with different permittivities [34], the natural extension of which will be to consider a cavity with output coupling [35]. There are more general theories of light propagation, in linear media [36] and in inhomogeneous media [37, 38]. There are recent works on the complete theory of general dispersive inhomogeneous nonlinear media by Drummond [39] and by Glauber [40]. Work has also been done on non-linear time dependent media [41]. Recently cavities with moving walls has attracted attention [42] in relation to squeezed state generation [142]. The direct consequence of quantizing the radiation field is the force felt by two parallel plates, which was discussed by Casimir [43], and an excellent account of which is given in

the appendix of Power's book [25], and as such the method can be used to calculate the Casimir force even when one assumes squeezed states of the radiation field. A recent review of Casimir force is available in the context of QED [44]. In the context of Quantum Optics one calculates this as radiation pressure [45], a brief account of which is given in relation to squeezed states in [91].

We have recollected the bare basics to quantize the radiation field. After the calculation of the Einstein coefficients [72] by Dirac [73] using the quantum theory of the radiation field, there was an attempt to understand many a problem related to radiation [74, 23]. Attempts to get the rate equation in the quantized form [78], led to the invention of maser [75] and the laser [76], which in turn led to the expansion of many fields such as holography [77]. It took many more years to get the full quantum theory of laser, since one had to include the losses in a quantum mechanical way. This was finally done and the complete quantum theory of laser was established by Haken [79, 80], Fleck [81], Lax [82] and Scully and Lamb [83], using various approaches such as quantum stochastic and density operator methods. With this, we now turn to the solutions of the radiation field hamiltonian, and a suitable way of representing the quantized radiation field.

1.2 Representations of the Electromagnetic field

In this section, we will consider the representations of the quantized electromagnetic field. These representations can be in terms of Fock states, coherent states or some suitable quasi probability distribution function. The complete state vector of the quantized radiation field can be written in terms of products of the state vectors

of each mode making up the field, as these modes are independent of each other. Hence we look more closely at the single mode field for each of these basis states. In what follows we briefly summarize the properties of these basis states.

Fock States

We have earlier said that the single mode of the quantized radiation field is a simple harmonic oscillator. The hamiltonian of the single mode is written as

$$\widehat{H} = \hbar\omega\left(\hat{a}^\dagger\hat{a} + \frac{1}{2}\right) \quad . \tag{1.14}$$

One can solve the Schrödinger equation for this hamiltonian, and one finds that these state vectors can be denoted by an abstract ket which is labeled by an integer. These eigen kets which are labeled by an integer n, are the normalized hermite polynomials of order n in the coordinate representation, apart from a gaussian factor which is independent of n. These are usually called the single mode Fock states or number states.

We briefly summarize the properties of these energy eigen kets $|n\rangle$. The action of the annihilation and creation operators on these kets are specified by

$$\begin{aligned} \hat{a}\,|n\rangle &= \sqrt{n}\,|n-1\rangle \\ \hat{a}^\dagger\,|n\rangle &= \sqrt{(n+1)}\,|n+1\rangle \quad . \end{aligned} \tag{1.15}$$

Hence $\hat{a}\,|0\rangle = 0$, where $|0\rangle$ is the vacuum state and the annihilation operator completely annihilates the vacuum to a vector of vanishing norm. Due to the way they act on the number states they are also called the ladder operators. The number

states are the eigen states of the hamiltonian and hence of the operator $\hat{n} = \hat{a}^{\dagger}\hat{a}$, which is called the number operator, since its action on the Fock state

$$\hat{n}\,|n\rangle = n\,|n\rangle \quad , \tag{1.16}$$

gives the occupation number of the state. The number states are orthonormal, and one can have the resolution of the Identity operator in terms of them as given below :

$$\begin{aligned} \langle m\,|n\rangle &= \delta_{mn} \\ \hat{I} &= \sum_{n=0}^{\infty} |n\rangle\langle n| \quad . \end{aligned} \tag{1.17}$$

Also, the photon number operator can be resolved in terms of the Fock states as

$$\hat{n} = \sum_{n=0}^{\infty} n\,|n\rangle\langle n| \quad . \tag{1.18}$$

An arbitrary state of a single mode can be expressed as a superposition of number states, given by

$$|\psi\rangle = \sum_{n=0}^{\infty} \mathcal{C}_n\,|n\rangle \quad , \qquad \mathcal{C}_n = \langle n\,|\psi\rangle \quad . \tag{1.19}$$

One uses these Fock states extensively in calculations even though ideal Fock states have not been produced in the laboratory. The radiation field in a Fock state implies that each mode has a precisely fixed number of photon, whereas in real sources (as of date) they fluctuate. Since an arbitrary quantum state of a single mode can be expressed as a superposition of number states, the probability amplitude of getting n photons in such a state is trivially found by projecting that state to the n photon fock state, and the probability is just the modulus square of

this amplitude. It is given by

$$P_{nn} = \langle n \mid \psi \rangle \langle \psi \mid n \rangle \quad , \qquad \sum_n P_{nn} = 1 \quad . \tag{1.20}$$

The general matrix element

$$P_{mn} = \langle m \mid \psi \rangle \langle \psi \mid n \rangle \quad , \tag{1.21}$$

is also often used. Note that the extension of these definitions for the multi-mode case is quite straight forward. P_{nn} is usually called the photon number distribution of the mode, since it gives the probabilities for observing different number of photons in a mode specified by a given quantum state. The mean of the photon number operator for a given state is the weighted sum of the photon number distribution P_{nn}, since

$$\begin{aligned} \langle \hat{n} \rangle &= \langle \psi \mid \hat{n} \mid \psi \rangle \\ &= \langle \psi \mid \left(\sum_{n=0}^{\infty} n \mid n \rangle \langle n \mid \right) \mid \psi \rangle \\ &= \sum_{n=0}^{\infty} n P_{nn} \quad , \end{aligned} \tag{1.22}$$

where we have used the resolution of the number operator in terms of the number states, and the definition of P_{nn}. To quantify the magnitude of deviations from this mean one usually considers the photon number uncertainty, which is the expectation value of the operator $(\Delta\hat{n})^2$, in the given state, and where $\Delta\hat{n}$ is defined as $\Delta\hat{n} = \hat{n} - \langle \hat{n} \rangle$. Note that for a fock state this photon number uncertainty is zero. It is a usual practice to consider the photon number uncertainty of a state normalized with respect to its mean, and this normalized photon number uncertainty is known as the Fano factor. This is related to the Q-parameter introduced by Mandel [234], and this relationship is given by $Q = f_n - 1$.

Coherent States

An equally often used other representation of the quantized radiation field is in terms of the coherent states. These states were first considered by Schrödinger in 1926 [53]. Like the photon number, the electric and the magnetic fields also have an associated quantum noise and both these cannot be specified simultaneously with unlimited accuracy. One can get unique quantum states, by demanding the uncertainties to be the minimum possible value allowed by quantum mechanics for both these quadratures [54, 55], and such states are defined to be the coherent states. These states are introduced in quantum optics [56, 57, 64] as a neat way of solving various problems. At present there are various approaches to coherent states [64, 65, 66]. An excellent overview of coherent states can be had from Ref. [68]. There are some recent review articles too [69]. Here we briefly summarize the properties of coherent states. The coherent states can also be defined as the eigen states of the non-hermitian annihilation operator,

$$\hat{a}\,|\alpha\rangle = \alpha\,|\alpha\rangle \qquad\qquad \langle\alpha\,|\,\hat{a}^{\dagger} = \langle\alpha\,|\,\alpha^{*} \quad , \tag{1.23}$$

and hence are essentially indexed by a complex number α. The coherent states are expanded in terms of the number states as

$$|\alpha\rangle = e^{-|\alpha|^2/2} \sum_{n=0}^{\infty} \frac{\alpha^n}{\sqrt{n!}} |n\rangle \quad . \tag{1.24}$$

Hence the photon number distribution of the coherent states is given by

$$P_{nn} = \langle n\ |\alpha\rangle\,\langle\alpha\ |n\rangle = e^{-|\alpha|^2} \frac{\alpha^{2n}}{n!} \quad , \tag{1.25}$$

which is a Poissonian. The photon number uncertainty of the coherent states is given by

$$\left\langle (\Delta\hat{n})^2 \right\rangle = |\alpha|^2 = \langle\,\hat{n}\,\rangle \quad , \tag{1.26}$$

Hence the Fano factor for any coherent state takes the value unity. On the other hand, the Fock state has zero photon number uncertainty and hence the Fano factor takes the value zero. The Fano factor is a very convenient quantity to characterize the photon number properties of a quantum state, since a value of Fano factor in the range $0 \leq f_n < 1$ implies amplitude squeezing.

The coherent states are not orthogonal and their inner product is given by

$$\langle \beta \mid \alpha \rangle = e^{-(|\alpha|^2+|\beta|^2)/2+\alpha\beta^*} \quad . \tag{1.27}$$

Nevertheless, coherent states form a complete set, and indeed an over-complete set [64]. Hence one can write the resolution of the Identity operator as

$$\hat{I} = \int |\alpha\rangle\langle\alpha| \, \frac{d^2\alpha}{\pi} \quad , \tag{1.28}$$

where if $\alpha = x + iy = re^{i\theta}$, then $d^2\alpha = dx\,dy = r dr\, d\theta$. One could write the quadrature operators in terms of the boson annihilation and creation operators, which in the single mode case is given by

$$\hat{q} = \sqrt{\frac{\hbar}{2\omega}} \left(\hat{a}^\dagger + \hat{a}\right) \tag{1.29}$$

$$\hat{p} = i\sqrt{\frac{\hbar\omega}{2}} \left(\hat{a}^\dagger - \hat{a}\right) \quad . \tag{1.30}$$

As mentioned earlier, the electric and the magnetic fields have quantum noise which are reflected in these quadrature operators, since one can write the electric and magnetic fields in terms of these operators (in the way we have done, $\hat{E}$ in terms of $\hat{p}$, and $\hat{B}$ in terms of $\hat{q}$). The noise is again quantified by taking the second moment of these operators, and for a coherent state these are given by

$$\begin{aligned} \left\langle (\Delta\hat{q})^2 \right\rangle &= \frac{\hbar}{2\omega} \\ \left\langle (\Delta\hat{p})^2 \right\rangle &= \frac{\hbar\omega}{2} \quad , \end{aligned} \tag{1.31}$$

and the product of the uncertainties is given by

$$\Delta q \cdot \Delta p = \frac{\hbar}{2} \quad , \tag{1.32}$$

where $\Delta q = \sqrt{\langle (\Delta \hat{q})^2 \rangle}$ and $\Delta p = \sqrt{\langle (\Delta \hat{p})^2 \rangle}$. This is the minimum possible value for two conjugate variables (here $\hat{q}$ and $\hat{p}$), and the one which saturates the Heisenberg uncertainty relation.

The coherent state has a symmetric noise and hence this uncertainty relation is sufficient. But for states having an asymmetric noise like the quadrature squeezed states (which are minimum uncertainty states again, even though they have different noises in different quadratures), one defines a noise matrix [233], which is given by

$$\mathcal{M} = \begin{pmatrix} \langle (\Delta \hat{q})^2 \rangle & \left\langle \frac{1}{2} \{ \Delta \hat{q}, \Delta \hat{p} \} \right\rangle \\ \left\langle \frac{1}{2} \{ \Delta \hat{q}, \Delta \hat{p} \} \right\rangle & \langle (\Delta \hat{p})^2 \rangle \end{pmatrix} \quad , \tag{1.33}$$

and defines the uncertainty relation as $(\det \mathcal{M}) \leq \hbar/2$. The off-diagonal element is the expectation value of the anticommutator of $\Delta \hat{q}$ and $\Delta \hat{p}$. In the simple case, such as in the coherent states, the off-diagonal elements are zero. In a quadrature squeezed state with an arbitrary direction of squeezing, the off-diagonal elements are non-zero.

The coherent states can also be defined as those states that are got by rigidly displacing the vacuum in phase space [60, 62]. By rigid displacement one means that one changes only the first moment or the mean and none of the higher moments. There is a simple operator, called the displacement operator, to do that, and in terms of this, the coherent state is given by

$$|\alpha\rangle = \widehat{D}(\alpha)|0\rangle = e^{\alpha \hat{a}^\dagger - \alpha^* \hat{a}} |0\rangle \quad . \tag{1.34}$$

The action of the displacement operator on a coherent state results in another coherent state. One can use the simple version [27] of the general Baker-Campbell-Hausdorff (BCH) formula [270, 271, 272, 273, 274, 275], to get

$$\widehat{D}(\alpha)\,|\,\beta\,\rangle = \widehat{D}(\alpha)\widehat{D}(\beta)\,|\,O\,\rangle = e^{(\alpha\beta^{*}-\alpha^{*}\beta)/2}\,|\,\alpha+\beta\,\rangle \quad . \tag{1.35}$$

The action of displacement on the annihilation operator is given by [27]

$$\widehat{D}^{\dagger}(\alpha)\,\hat{a}\,\widehat{D}(\alpha) = \hat{a}+\alpha \quad , \tag{1.36}$$

from which the action on any other operator can be discerned. Also, the normal ordered form of the displacement operator is easy to find, and is given by

$$\widehat{D}(\alpha) = e^{\alpha\hat{a}^{\dagger}-\alpha^{*}\hat{a}} = e^{-|\alpha|^{2}/2}e^{\alpha\hat{a}^{\dagger}}e^{\alpha^{*}\hat{a}} \quad . \tag{1.37}$$

Another facet of the coherent states is the coherence properties [60, 62, 63] of these states. In general, the correlation function is defined as the correlation between the fields at different space time points. If $x=(\vec{r},t)$ and $x'=(\vec{r}',t')$, then the nth order correlation function between the fields at these points is defined as

$$G^{(n)}(x_1,\cdots,x_n;x_1',\cdots,x_n') = Tr\,[\hat{\rho}\hat{E}^{(-)}(x_1)\cdots\hat{E}^{(-)}(x_n)\hat{E}^{(+)}(x_1')\cdots\hat{E}^{(+)}(x_n')] \quad , \tag{1.38}$$

where $\hat{\rho}$ is the density operator which will be discussed shortly. The $\hat{E}^{(+)}$ is the field operator (not necessarily the electric field) for the positive frequency part and is given by

$$\hat{E}^{(+)}(x) = \hat{E}^{(+)}(\vec{r},t) = \frac{1}{\sqrt{V^{3}}}\sum_{m\sigma} I(\omega_m)\hat{e}_{m\sigma}\hat{a}_{m\sigma}e^{i(\vec{k}_m\cdot\vec{r}-\omega_m t)} \quad . \tag{1.39}$$

Here, $I(\omega)$ is some simple function of frequency (for the electric field $I(\omega) = i(\hbar\omega/2\epsilon_0)^{1/2}$) and it depends on which field vector is being expanded. The field

operator for the negative frequency is given by the hermitian conjugate of the positive frequency operator. If for a given quantum state of the system, the nth order correlation function factories into

$$G^{(n)}(x_1, \cdots, x_n; x'_1, \cdots, x'_n) = \mathcal{E}^{(-)}(x_1) \cdots \mathcal{E}^{(-)}(x_n)\mathcal{E}^{(+)}(x'_1)\mathcal{E}^{(+)}(x'_n) \quad , \qquad (1.40)$$

then the system is said to posses nth order coherence. It could be immediately seen that if the system is in a coherent state, then from the definition of the field operator, the above factorization does take place for any order, since the coherent states are the right eigen states of the $\hat{E}^{(+)}(x)$ operator. Note that $G^{(1)}(x, x)$ gives the intensity of the field at the space-time point x. The second and higher order correlation functions are measured in Hanbury-Twiss type of intensity-intensity correlation experiments.

Density Operator and Quasi-Probability Distributions

Apart from the quantum state vector representation, an alternate way of representing the field is through the density operator $\hat{\rho}$, which is defined as the outer product of the state vector in the simplest case. A quantum mechanical system can be completely specified in terms of its density operator $\hat{\rho}$, which is given by,

$$\hat{\rho} = \sum_i p_i \, |\psi_i\rangle\langle\psi_i| \, , \qquad \sum_i p_i = 1, \qquad 0 \leq p_i \leq 1 \quad , \qquad (1.41)$$

where $|\psi_i\rangle$'s are the possible state vectors of the system, and p_i's are the probability that the system is in the state $|\psi_i\rangle$. Given a density operator, if one can factorise it to an outer product of state vectors, as

$$\hat{\rho} = |\psi\rangle\langle\psi| \qquad (1.42)$$

then such a system is said to be in a *pure state*. For a pure state one has

$$Tr\,\hat{\rho}^2 = Tr\,\hat{\rho} = 1 \quad . \tag{1.43}$$

Conversely the above equation implies that the system having such a density operator is in a pure state, and one can factorise such a density operator. For a statistical ensemble, we can tell only the probabilities with which the system might be in different states $|\psi_i\rangle$ and in which case we always have,

$$Tr\,\hat{\rho}^2 < 1 \quad . \tag{1.44}$$

Such a density operator cannot be factorised, and such systems are said to be in a *mixed state*.

The expectation values of operators representing physical observables, say $\hat{F}$, can be obtained using the density operator as,

$$\left\langle \hat{F} \right\rangle = Tr\,(\hat{\rho}\hat{F}) \quad . \tag{1.45}$$

Note that if the system is in a pure state, then $\hat{\rho} = |\psi\rangle\langle\psi|$ and $Tr\,(\hat{\rho}\hat{F})$ reduces to the usual definition $\langle\psi|\,\hat{F}\,|\psi\rangle$. One can express any operator as a function of the boson annihilation and creation operators. Finding the expectation values in many cases is simplified if we can cast $\left\langle \hat{F} \right\rangle$ in the form,

$$\left\langle \hat{F} \right\rangle = Tr\,(\hat{\rho}\hat{F}) = \int d^2\alpha\, \mathcal{W}(\alpha)\, f(\alpha) \quad . \tag{1.46}$$

The 'weight function' $\mathcal{W}(\alpha)$ in the classical sense of the above equation can be called the probability distribution function, but since here $\mathcal{W}(\alpha)$ doesn't satisfy all the requirements of such a function, such as taking non-positive values, it is called

a quasi-probability distribution function. Since the coherent states are minimum uncertainty states, they are the closest to the classical states. Hence one can define quasi-phase spaces in terms of these, and such a approach will simplify many calculations. One of the earliest quasi-probability distribution functions is the Wigner function [58], a review of which can be found in Ref. [59]. Another problem is in associating,

$$\hat{F}(\hat{a},\hat{a}^\dagger) \longrightarrow f(\alpha,\alpha^*) \quad , \tag{1.47}$$

since for any given $\hat{F}(\hat{a},\hat{a}^\dagger)$, such as, say, the number operator, all the forms $\hat{a}^\dagger\hat{a}$ (normal ordering) or $\hat{a}\hat{a}^\dagger$ (antinormal ordering) or $\frac{1}{2}\{\hat{a},\hat{a}^\dagger\}$ (symmetric or Weyl ordering) can be associated with $\alpha\alpha^*$. Hence for each such ordering one has to have a different weight function.

It is possible to write a s-parameterized quasi probability distribution function [70, 71] given by

$$\mathcal{W}(\alpha,s) = \frac{1}{\pi^2}\int d^2\xi Tr\,[\hat{\rho}e^{\xi\hat{a}^\dagger-\xi^*\hat{a}+s|\xi|^2/2}]e^{(\alpha\xi^*-\alpha^*\xi)} \quad , \tag{1.48}$$

which when $s=+1$ corresponds to normal ordering of $\hat{F}(\hat{a},\hat{a}^\dagger)$ before associating it with $f(\alpha,\alpha^*)$ and $\mathcal{W}(\alpha,+1)$ corresponds to the P-function, $P(\alpha)$ [60, 61]. The $s=0$ case corresponds to symmetric ordering of $\hat{F}(\hat{a},\hat{a}^\dagger)$ and $\mathcal{W}(\alpha,0)$ is the Wigner function $W(\alpha)$. The $s=-1$ case corresponds to anti-normal ordering and $\mathcal{W}(\alpha,-1)$ is called the Q-function $Q(\alpha)$. There is an infinity of quasi-probability distribution functions for different values of s in the range $-1 \le s \le 1$.

Note that $\mathcal{W}(\alpha,s)$ is a well behaved function when $\mathrm{Re}(s) < 0$. When $s=-1$ it corresponds to the Q function given by,

$$Q(\alpha) = \frac{1}{\pi}\langle\alpha\,|\,\hat{\rho}\,|\,\alpha\rangle \quad , \tag{1.49}$$

where $|\alpha\rangle$ is the coherent state. As we can see, the Q function is always positive, well behaved and is normalisable. In that sense, the Q function is the smoothest of all the quasi-probability distribution functions. The problem here is that there are operators $\hat{F}(\hat{a}, \hat{a}^\dagger)$ for which the anti-normally ordered counter part is highly singular. On the other hand, in the case of the P-function, normally ordered counter part exists for every $\hat{F}(\hat{a}, \hat{a}^\dagger)$, but $P(\alpha)$ is singular for most $\hat{\rho}$ operators. The Wigner function, which corresponds to the association of symmetrically ordered operators to c-numbers, can be written for all $\hat{\rho}$, and is given in integral form as,

$$W(\alpha) = \frac{1}{2\pi\hbar} \int_{-\infty}^{+\infty} d\sigma \left\langle q - \frac{\sigma}{2} \middle| \hat{\rho} \middle| q + \frac{\sigma}{2} \right\rangle e^{ip\sigma/\hbar} \quad . \tag{1.50}$$

These quasi-probability distribution functions can also be used as a visual aid to discern certain properties of quantum states. The Q function is usually well suited for this purpose and the reason might well be the extreme smoothness of the projection operator $|\alpha\rangle\langle\alpha|$. $P(\alpha)$ is good when we are considering $\hat{\rho}$ operator's that represent classical-like states, like highly chaotic systems and thermal states, whose behavior can be well approximated by classical methods. On the other hand, for non-classical states the P-function becomes highly singular, and the Wigner function becomes extremely oscillatory, obscuring the essentials. But in this limit the Q-function is quite well suited. The Wigner function can be used when we need some of the subtleties of the interference to be exhibited. We went to lengths to compare these functions, even though they give the same information, because when used as a visual aid some are more descriptive then others. Thus our comparison should be taken in a heuristic sense.

We conclude this section by pointing out some other representations of the radiation field. We have seen earlier that the quadrature operators are canonically conjugate. But the operator canonically conjugate to the number operator called the phase operator, is ill-defined [73]. Attempts were being made to construct phase operators [46], many of which turn out to be non-hermitian. A review and comparison of various phase operators that were considered up to 1968 can be found in [49]. Recently, an hermitian phase operator has been successfully constructed [50, 51], using the techniques of discrete-time Fourier transforms [52]. Here one does the calculations in a finite s-dimensional fock space, and finally takes the limit $s \to \infty$. But still there is a controversy regarding whether this is measurable, or whether this is what one measures in a lab. Other schemes have been introduced [47, 48] and different schemes are now being compared. Hence the advantages that might exist in using a phase eigen state representation of the radiation field are yet to materialize. In passing, we wish to note that one might also use the quadrature squeezed states as a basis to represent the radiation field. With this, we turn now to a brief summary of the quadrature squeezed states and the Kerr states, which we will be using throughout this thesis.

1.3 Quadrature squeezed states

The quadrature squeezed states in the form that is now prevalent in the literature of quantum optics was first introduced by Stoler [85, 86] in the seventies, even though these states were studied as early as the fifties, beginning with the work of K. Husimi [84]. These states are usually defined in the single mode case as the

minimum uncertainty states associated with the generalized Heisenberg inequality [95, 96, 97, 98], which is equivalent to the two-photon state definition [89]. The generalization to the multi-mode case is quite straightforward [99, 100].

The first experimental observation of squeezing was made in 1985 in the AT&T Bell Labs [104]. They used a four-wave mixing scheme in sodium vapor, and were able to get noise reductions up to 10% below the shot noise level. The four wave mixing is a non-linear process [101, 102] involving the $\chi^{(3)}$ non-linearity, in which squeezing had been predicted [103] earlier. In four-wave mixing, two intense beams of the same frequency ω (degenerate case) are used to excite the non-linear medium to get a signal and idler beams at frequencies ω_1 and ω_2, where the conservation law $2\omega = \omega_1 + \omega_2$ is obeyed. The interaction hamiltonian is essentially of the form $\chi^{(3)}\hat{a}_s^\dagger \hat{a}_i^\dagger \hat{a}_e \hat{a}_e$, where s, i, e stands for the signal, idler and the exciting beam's photons.

Quadrature squeezed light can also be generated using a parametric down conversion process. Here, an intense beam of frequency ω is used to excite a $\chi^{(2)}$ non-linear medium, which produces two beams called the signal and the idler whose frequencies match the condition $\omega = \omega_i + \omega_s$. Unlike the case of four-wave mixing the frequencies of these beams are quite different from each other. The degenerate case corresponds to the signal and idler photon having the same frequency. The process of spontaneous parametric down conversion was known right from the early sixties. References to these early works can be found in [105, 106]. Extensive theoretical work has been done in this field [107, 108, 109, 110, 111]. It had been shown that quadrature squeezed light could be generated using the parametric oscillator operating in the sub-threshold regime [112, 113, 114]. The non-linearity and hence the squeezing is enhanced if the medium is placed inside a cavity [115, 116]. A system

using $\chi^{(2)}$ non-linearity of the $LiNbO_3$ inside a cavity and pumped by a single-mode YAG laser can reduce the quantum noise of one of the quadratures by as much as 64% [117].

The basic phenomena in parametric generation is the annihilation of a single exciting beam's photon to create two signal photons at the same time. This pair emission gives specific correlation between the photons of the two signal beam and the associated statistical features for any combined measurement made on both the beams [118, 119]. The twin photons emerge simultaneously with no more time lag than 100 ps [120]. The two beams have noise which are copies of each other and hence the difference should show substantial squeezing. Usually the difference of the intensities of the twin beams show squeezing due to the pair correlation of photons [121]. Noise reduction up to 75% below the standard quantum noise has been observed [122].

On the other hand, quadrature squeezed light can be produced using Second-harmonic generation[127], where a non-linear $\chi^{(2)}$ material is excited at frequency ω_0 to generate a signal at $2\omega_0$. The Second-harmonic generation was one of the oldest examples [123, 124] of the use of non-linear media and has a well established theory [125, 126]. The Second-harmonic as well as the field at the fundamental frequency are squeezed at the output of the non-linear medium and if the non-linear material is inside a cavity that is resonant for both the pump and the signal fields, then the same amount of squeezing results in both the modes [128, 196]. Experiments using MgO-doped $LiNbO_3$ have demonstrated squeezing in the fundamental mode [129], as well as in the up-converted mode [130].

Squeezing can also be produced in the short cavity limit. One has a short cavity limit when the decay rates of atomic polarization matches with those of the cavity modes. The theory of the short cavity limit in connection with optical bistability can be found in Ref. [131]. This theory can now be thoroughly done without using any adiabatic elimination[132, 133, 134]. These experiments are difficult to perform since the cavity has to be very small in length. Around 30% squeezing has been achieved using sodium vapor [135, 136]. Even without a cavity, broad band squeezed light can be achieved by using a pulsed laser. The pulsed laser concentrates the energy in pulses, which is enough in some non-linear materials to give rise to a squeezed signal. An optimum squeezing of 13% using $KTiOPO_4$ (KTP) [137] and 24% using $Ba_2NaNb_5O_{15}$ (BNN) [138] has been obtained using pulsed laser beams to pump these crystals.

The Optical fibers exhibit a certain amount of $\chi^{(3)}$ non-linearity which has been utilized to produce quadrature squeezed light [139]. This can be modelled as a Kerr medium, and the self-phase modulation of this medium [175, 174, 176, 177, 178, 179] is used to shape the field fluctuations. Even though the Kerr medium produces a different kind of squeezing, for very low non-linearities it is quite similar to quadrature squeezing, and there are many proposals for generating quadrature squeezed light using this [140, 141]. We will see more about the Kerr medium in the next section. In the present section we only briefly summarize the properties of the quadrature squeezed states, since there are a number of excellent review articles [90, 96, 91, 92, 93, 94] describing this.

The coherent states that we have seen in the last section form a particular class of minimum uncertainty states, in the sense that the noise of the conjugate variables

are equal. The minimum uncertainty states themselves, as defined earlier, are a class of quantum states for which the product of the noise in a given pair of conjugate variables is minimum. Hence there can be minimum uncertainty states whose noise in a particular quadrature may be smaller than the coherent state value at the expense of increased noise in the other quadrature. Let us assume that their is an operator $\hat{S}(r)$, which when acting on a coherent state changes the quadrature noises. Let us further assume that the expectation values of the second moment of the quadrature operators $\hat{q}$ and $\hat{p}$ taken in the state $\hat{S}(r)\,|\,\alpha\,\rangle$ have the form

$$\begin{aligned} \langle\,\alpha\,|\,\hat{S}^{\dagger}(r)(\Delta\hat{q})^2\hat{S}(r)\,|\,\alpha\,\rangle &= \frac{\hbar}{2\omega}\mathcal{Z}^2(r) \\ \langle\,\alpha\,|\,\hat{S}^{\dagger}(r)(\Delta\hat{p})^2\hat{S}(r)\,|\,\alpha\,\rangle &= \frac{\hbar\omega}{2}\frac{1}{\mathcal{Z}^2(r)} \quad , \end{aligned} \tag{1.51}$$

where $\mathcal{Z}(r)$ is some real function of a real parameter r. This could be simply achieved if the quadrature operators $\hat{q}$ and $\hat{p}$ transform as

$$\begin{aligned} \hat{S}^{\dagger}(r)\,\hat{q}\,\hat{S}(r) &= \hat{q}\mathcal{Z}(r) \\ \hat{S}^{\dagger}(r)\,\hat{p}\,\hat{S}(r) &= \hat{p}\frac{1}{\mathcal{Z}(r)} \quad . \end{aligned} \tag{1.52}$$

Now since the quadrature operators are expressed in terms of the sum and difference of the boson annihilation and creation operators, this function should be a sum of two other functions, whose difference is the inverse of this function. Since $\mathcal{Z}(r)$ is real, one can immediately assign the exponential function for $\mathcal{Z}(r)$. To stay in accordance with convention we choose $\mathcal{Z}(r) = e^r$. These would imply that the annihilation operator itself should transform as

$$\hat{S}^{\dagger}(r)\,\hat{a}\,\hat{S}(r) = \hat{a}\cosh(r) - \hat{a}^{\dagger}\sinh(r) \quad . \tag{1.53}$$

Whether the form of $\hat{S}(r)$ could be obtained directly from the above transformation, assuming that $\hat{S}$ is an operator function of the boson annihilation and creation operators, is a question to ponder over. Nevertheless, the form of the right hand side of the equation is well known in many areas of physics [232], and one could have judged the form of $\hat{S}(r)$.

The above operator only squeezes along the q or the p quadrature and one can easily go over to a general squeeze operator which squeezes along any direction in phase space by using a rotation matrix whose effect is to make the parameter complex. The usual way in which the squeeze operator is written [85, 86, 87, 88, 89, 145, 146] is given by

$$\hat{S}(z) = e^{(z\hat{a}^{\dagger 2} - z^{*}\hat{a}^{2})/2} \quad , \tag{1.54}$$

where z is taken to be a complex number $z = re^{2i\theta}$. Before we proceed further, we wish to point out that we have chosen to take 2θ as the argument rather than θ, since as we will see, squeezing has a symmetry in the sense that z and $-z$ correspond to the same squeezing. This means that the argument of z in an half-period completes all the squeezing directions. Hence, if one visualize this in phase space the angle subtended by the major axis of the uncertainty ellipse with the q quadrature is half the argument of z. Hence our choice of putting the factor 2 in defining z is more satisfactory since θ will now directly correspond to the angle subtended by the major axis of the uncertainty ellipse with the positive q direction. Also, squeezing along a particular direction, say along θ is the same as squeezing along the $\pi + \theta$ direction in our convention, which is ideal. Under this unitary operator the full transformation of the annihilation operator is given by

$$\hat{S}^{\dagger}(re^{2i\theta})\hat{a}\hat{S}(re^{2i\theta}) = \hat{a}\cosh(r) - \hat{a}^{\dagger}\sinh(r)e^{-2i\theta} \quad , \tag{1.55}$$

and that of the creation operator can be obtained by complex conjugation of the above equation.

We had started by considering a squeeze operator acting on a coherent state [Eq. (1.51)], which is akin to the two-photon coherent state [89]. On the other hand one could have squeezed the vacuum and displaced the resulting state, which is sometimes called in the literature as *ideal squeezed state* [146]. If the squeeze operator acting on a coherent state is given by

$$|\psi_s\rangle = \hat{S}(z)\,|\alpha'\rangle = \hat{S}(z)\widehat{D}(\alpha')\,|0\rangle \quad , \tag{1.56}$$

and the displacement of the squeezed vacuum is given by $|\alpha, z\rangle = \widehat{D}(\alpha)\hat{S}(z)\,|0\rangle$, then these two are connected by [237]

$$\alpha' = \alpha\cosh(r) - \alpha^{*}\sinh(r)e^{-2i\theta} \quad . \tag{1.57}$$

One generally specifies the quadrature squeezed states by

$$|\alpha, z\rangle = \widehat{D}(\alpha)\hat{S}(z)\,|0\rangle \quad , \tag{1.58}$$

and we follow this convention throughout the thesis.

Expressing a given quantum state as a superposition of some other quantum state whose properties are well known, often simplifies many calculations apart from providing insight and connectivity. The squeeze operator has been applied to the number states [239], and the squeezed number states thus obtained can be expressed as a superposition of displaced number states [252]. Similarly, the quadrature squeezed state can be expressed as a superposition of coherent states [246, 247, 248, 219], which was based on the observation that a continuous superposition of coherent

states along a straight line [245] leads to squeezing of the perpendicular quadrature. We will see how the quadrature squeezed state can be expressed as a continuous superposition of coherent states in greater detail in Chapter 4, but we just state the result here :

$$\begin{aligned} |\alpha, z\rangle &= \widehat{D}(\alpha = \rho e^{i\phi})\widehat{S}(z = re^{2i\theta})\,|O\rangle \\ &= [2\pi \sinh(r)]^{-\frac{1}{2}} \int_{-\infty}^{\infty} dy\, e^{-\frac{1}{2}(\coth(r)-1)y^2 - i\rho y \sin(\theta-\phi)} \left|\rho e^{i\phi} + y e^{i\theta}\right\rangle_{\rm coh} \end{aligned} \quad (1.59)$$

The Q function for the quadrature squeezed state can be written easily using this integral representation, and we have

$$Q_S(\beta = ke^{i\tau}) = \frac{1}{\cosh(r)} e^{-k^2-\rho^2+\tanh(r)[\rho\cos(\theta-\phi)+k\cos(\theta-\tau)]+2k\rho\cos(\phi-\tau)} \quad . \quad (1.60)$$

The mean photon number of the quadrature squeezed state is given by

$$\langle \widehat{n} \rangle = \langle \alpha, z \,|\, \widehat{n} \,|\, \alpha, z \rangle = |\alpha|^2 + \sinh^2(r), \quad (1.61)$$

and the photon number uncertainty by

$$\left\langle (\Delta\widehat{n})^2 \right\rangle = \sinh^2(r)\,[1 + \sinh(2r)] + \rho^2 \sinh(2r)\,[1 + \cos(2\theta - 2\phi)] \quad . \quad (1.62)$$

Here we have parameterized z as $z = re^{2i\theta}$ and the displacement α as $\alpha = \rho e^{i\phi}$. It is obvious from the above equation that the photon number uncertainty depends on the angle between the squeezing direction and the direction of coherent excitation. The expression goes to a minimum when $\theta - \phi = \pi/2$, where the direction of squeezing is along the direction of excitation. We choose to call such a state as an *amplitude squeezed coherent state*, whose Q function is illustrated in Fig. (1.1b). The expression is maximum when $\theta - \pi = 0$ which happens when the direction of

squeezing is perpendicular to the direction of excitation. We call these states as *phase squeezed coherent states*, since these are squeezed in the phase sector. The Q function for this state is illustrated in Fig. (1.1c), and one can see that the noise in the phase is smaller than in a coherent state. For comparison we have also given the

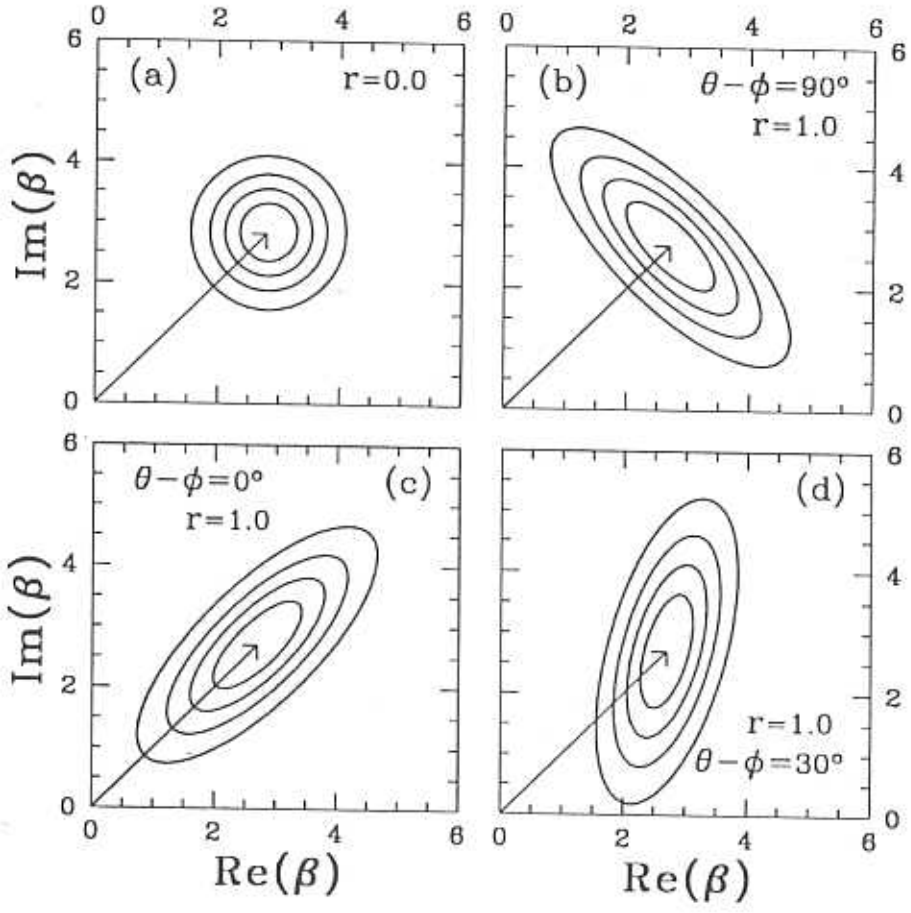

Fig. 1.1. Plot of the Contours of Q function for different directions of squeezing.

Q function of a coherent state [Fig. (1.1a)] and a squeezed state with an arbitrary direction of squeezing [Fig. 1.1d].

The squeeze operator can be normal ordered by identifying the $\hat{a}^{\dagger 2}$, $\hat{a}^2$ and $\hat{a}^\dagger\hat{a}$ as SU(1,1) operators. In fact a general exponential quadratic in the boson creation

and annihilation operators can be normal ordered [276, 277]. We give here only the normal ordered squeeze operator without going through the derivation :

$$\widehat{S}(z = re^{2i\theta}) = \cosh^{-\frac{1}{2}}(r)\, e^{\frac{1}{2}e^{2i\theta}\tanh(r)\widehat{a}^{\dagger 2}}\, e^{-\ln(\cosh(r))\widehat{a}^{\dagger}\widehat{a}}\, e^{-\frac{1}{2}e^{-2i\theta}\tanh(r)\widehat{a}^{2}} \quad . \qquad (1.63)$$

The squeezed state itself was proposed to increase the sensitivity of the interferometers used in the detection of gravitational waves [85, 86, 145]. The amount of effort put in understanding and generating these states of the radiation field is justified by the practical importance of these states. Numerous applications have been envisaged where the squeezed light would be of great use. Here we restrict ourselves to those class of applications which are either directly or indirectly connected with interferometry. Injection of the squeezed vacuum into the empty port of the Michelson type of interferometers [146] used in the gravitational wave detection [147] would considerably increase the sensitivity of these and also enable them to work at lower optical powers. There are other proposals for increasing the sensitivity of instruments measuring the phase using quadrature squeezed light [148, 149], some of which have been experimentally attempted [150]. In addition, the interferometers can be described in a natural way using the formalism used for squeezed states, and hence, as the squeezed light is used to increase the sensitivity of the interferometer, the interferometer can in turn be used to measure the degree of squeezing [151]. There are many gedanken experiments proposed in connection with the conceptual foundations of quantum mechanics, that can now be tested in the lab using squeezed light. In this connection the generalized Horne-Shimony-Zeilinger two photon momentum-position interferometer had been proposed [152] and experimentally implemented [153]. There are proposals for a similar three particle version too [154].

Two particle gedanken interferometers that use the interference between two possible states, each of which belongs to a different emission time have been proposed [155], and were later experimentally realized [156, 157].

A time honored paradox, which was put forward by Einstein, Podolsky and Rosen[162], has occupied much attention of people concerned with the foundations of quantum mechanics[163]. There are alternative formulations of quantum mechanics, such as the hidden variable theories with a more classical philosophy. Experimental observation of the difference between these formulations has been made possible by the Bell type of inequalities [164], an excellent review of which can be found in Ref. [166]. These earlier experiments and their modern counterparts [167, 168, 169] were based on using light from atomic cascade decays. But for many this had not been a compelling test of Bell's inequality since one can alway argue that the photons detected were not correlated. In parametric down conversion, we have seen that the signal and idler photon are emitted simultaneously and hence are highly correlated. In fact the quantum states of these are highly entangled[165], and can be used to test the inequalities[170, 171]. It has also been shown that multi-photon correlations can lead to an exponential increase in the violation of Bell type inequalities [160, 161]. It is realized now that multi-photon correlations can lead to much more quadrature squeezing [158] and anti-bunching [159]. With this, we will now turn to the nonlinear Kerr medium, which gives rise to another kind of squeezing in the noise of the radiation field, and which is different from the quadrature squeezing.

1.4 Non-linear Kerr medium

A Kerr medium is an isotropic, third order non-linear medium which belongs to a class of non-linear media where the self-action effects of strong beams are dominant. Unlike the more well known non-linear media, where coupling of photons at different frequencies is more dominant, the self-action process exhibits quasimonochromaticity. There are many self-action effects which had been studied earlier in the literature, such as self-focusing [172], self-trapping [173] and self-phase modulation [174]. The Kerr medium in particular is mainly a self-phase modulating medium.

In Photonics, the use of Kerr medium is well known. Apart from optical fibers which exhibit this non-linearity being used in propagating optical pulses which do not spread – known in the literature as optical solitons [180, 181] and quantum solitons [182], there are media which exhibit optical bistability [183], which can find many important applications where this property can be used, as in optical switches, logical gates, and memory elements [184]. The Kerr effect can be used to do optical non-demolition measurements [185, 186, 187]. Most important of all is that the Kerr medium can be used to generate non-classical states, such as amplitude squeezed states [191, 192, 193, 218, 219]. It can also be used in the detection of non-classical states [220, 221].

In quantum optics, the Kerr medium is usually treated in the single mode case as a third order nonlinear oscillator[194, 195, 196, 197]. The statistical properties of this oscillator were studied by Drummond [194]. If one neglects losses, the system can be solved exactly[194, 195, 197]. For many proposals involving the generation of amplitude squeezed light [191, 218, 219], a coherent beam evolves for a very small

duration of time in the Kerr medium, and hence one can neglect the loss and the associated noise due to it. The effect of loss can be easily included in the calculations and had been done so for a reservoir at zero temperature[198, 199], even for a general initial state [200]. Recently, calculations involving the bath at finite temperature has been done for both an initial coherent state [201], and a general initial state [202, 203] evolving through a Kerr medium. In this thesis and in the proposals that we make for the generation of amplitude squeezed light we have neglected the losses and the associated quantum noise, since in our opinion these can be incorporated quite readily, and such inclusions might obscure more fundamental issues.

In this section we recollect the main results of the calculations involving the Kerr medium, and we restrict ourselves to giving only references for treatments involving losses. If one assumes that the optical wave travelling through the Kerr medium is plane polarized and monochromatic, and if this travelling wave is treated as a sequence of localized wave packets [175], then each wave packet corresponds to a single mode quantized field given by

$$\hat{E}(z,t) = i\left[\frac{\hbar\omega_0}{2\epsilon v}\right]^{\frac{1}{2}} \hat{a}(z)e^{i(kz-\omega_0 t)} + \text{h.c.}, \tag{1.64}$$

where ω_0 is the frequency, $k = \omega_0/v$ is the propagation constant, $v = c/n_0$ is the velocity of the packet in the medium, and n_0 is the linear refractive index of the medium. The dielectric constant is given by $\epsilon = n_0^2\epsilon_0$, where ϵ_0 is the dielectric constant of the vacuum. The quantization volume is given by $V = AL$, where A is the cross-sectionl area of the beam, and L is the length traversed by the beam.

The hamiltonian for the single mode radiation field in the Kerr medium is given

by

$$\widehat{H} = \hbar\omega\hat{a}^{\dagger}\hat{a} + \hbar\chi_{NL}\hat{a}^{\dagger 2}\hat{a}^{2} \quad , \tag{1.65}$$

where χ_{NL} is the non-linearity experienced by the field in the medium. It should be observed that this is the effective hamiltonian for the field in the Kerr medium and the physical process which gives rise to this effective hamiltonian for the field is generally considered to belong to the purview of condensed matter physics. Note that the interaction part of the hamiltonian commutes with the free evolution part, and hence the solution to the problem of any state evolution through the Kerr medium can be found.

In a slightly different way of looking at this hamiltonian, χ_{NL} is the anhormonicity parameter. The parameter χ_{NL} is proportional to the third-order nonlinear susceptibility $\chi^{(3)}$ [185]. In terms of the nonlinear refractive index n_2 of the Kerr medium, we have

$$\chi_{NL} = \frac{\hbar\omega_0^2 n_2}{2c\epsilon_0 n_0^2 A\tau} \quad . \tag{1.66}$$

In fact the effect of the Kerr medium can be visualized in terms of the intensity-dependent refractive index [176], which is given by $n(|\mathcal{E}|^2) = n_0 + (1/2)n_2|\mathcal{E}|^2$, where $|\mathcal{E}|$ is the complex field amplitude as defined through $E(z,t) = (1/2)|\mathcal{E}(z,t)|\exp(i(kz - \omega_0 t)) + c.c.$. In the quantum case, this will be given by the mean field strength. The above hamiltonian is valid only when there is a large detuning from any transition level that may be present in the Kerr medium around the incident light's frequency ω_0 [179]. Also there are saturation effects and of course the losses which we have neglected.

The time evolution of any state inside the Kerr medium is usually given in terms

of the spatial length L transversed inside the Kerr medium [175]. We assume that this length L can always be mapped into a time-like parameter t and hence the output state of the Kerr medium can be written as

$$|\psi(t)\rangle = \hat{U}_K(t)\,|\psi_i\rangle \quad , \tag{1.67}$$

where $|\psi_i\rangle$ is the quantum state of the radiation field incident on the Kerr medium. The unitary operator $\hat{U}(t)$ is the time evolution operator and is given by

$$\hat{U}(t) = e^{i\hat{H}t} = e^{i\hbar\chi_{NL}\hat{a}^{\dagger 2}\hat{a}^2} \tag{1.68}$$

neglecting the free evolution part. We could do this since the free evolution part commutes with the interaction part. A closed form can be found for the annihilation operator conjugated with the above unitary operator as follows

$$\begin{aligned}
\hat{U}^\dagger(\gamma)\hat{a}\hat{U}(\gamma) &= e^{-i\frac{\gamma}{2}\hat{n}(\hat{n}-1)}\hat{a}e^{i\frac{\gamma}{2}\hat{n}(\hat{n}-1)} \\
&= \hat{a} + i\gamma\hat{n}\hat{a} - \frac{\gamma^2\hat{n}^2\hat{a}}{2!} - \frac{i\gamma^3\hat{n}^3\hat{a}}{3!} + \cdots \\
&= e^{i\gamma\hat{n}}\hat{a} \quad .
\end{aligned} \tag{1.69}$$

We will look into the evolution of a coherent state inside the Kerr medium. The expectation value of the annihilation operator for a coherent state that has evolved through the Kerr medium is given by

$$\langle\,\alpha\,|\,\hat{U}^\dagger\hat{a}\hat{U}\,|\,\alpha\,\rangle = \alpha e^{-4|\alpha|^2\sin^2(\gamma/2)}e^{i|alpha|^2\sin\gamma} \quad . \tag{1.70}$$

The Q function for this state $\hat{U}_K(\gamma)\,|\,\alpha\,\rangle$ can be calculated to be

$$Q(\beta) = \frac{e^{-\rho^2-|\beta|^2}}{\pi}\left|\sum_{n=0}^{\infty} e^{i\frac{\gamma}{2}n(n-1)}\frac{(\alpha\beta^*)^n}{n!}\right| \tag{1.71}$$

Even though the photon number uncertainty and the photon number properties of a state evolving through a Kerr medium remains unchanged, the Kerr medium changes the state in a subtle way as can be seen from the plot of the Q function given in Fig. (1.2). Here, we have plotted the Q-function against the real and imaginary parts of its argument, for different γ values. This figure can be taken as the visualization of the evolution of the state inside the Kerr medium. The mean $|\alpha|^2$ remains at

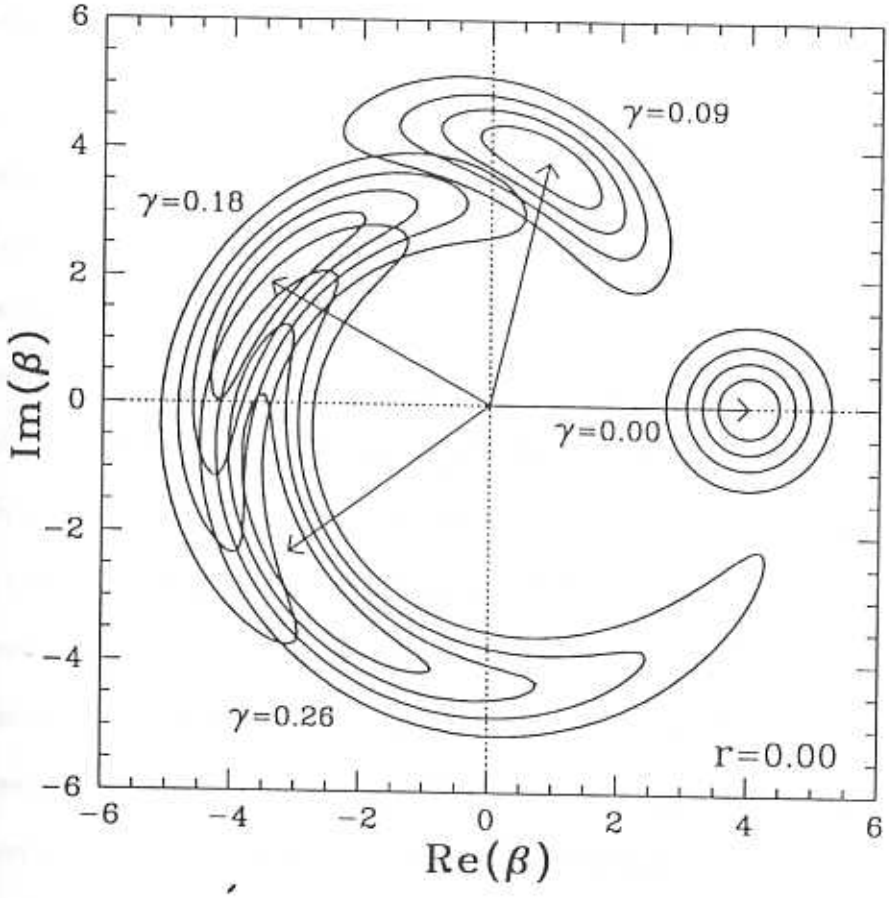

Fig. 1.2. Plot of the contours of the Q-function of the evolution of a coherent state ($r = 0$) in a Kerr medium. The different γ values are indicated in the figure. The mean $|\alpha|^2$ is fixed at 16, and the arrows connect the phase space origin and the maximum of the Q-function. The contours are drawn at 0.2, 0.4, 0.6, and 0.8 times the maximum value.

16, and the contours are drawn at 0.2, 0.4, 0.6, and 0.8 times the maximum of the Q-function, for four values of γ. The arrows connect the maximum of these to the origin of phase space. It can be seen from the figure that the state that is evolving through a Kerr medium has a very different Q function compared to a coherent state. Also, there is a larger spread in the phase, and the crescent seems to be thin in the middle. But still the photon number properties doesn't change because the crescent is slightly rotated about its center so that the radius of curvature of this crescent is not along the line joining the center of the distribution to phase space origin.

The reason the Q function shears in this way can be easily understood. The hamiltonian giving rise to this state has a intensity dependent term $\hat{n}^2$, which means that areas of the phase space at different radial distances from the origin evolve with different angular velocity. Points farther way from the origin move faster. Considerable squeezing can be got by slightly displacing this state, in which case the photon number uncertainty goes as the cube root of the mean photon number [191]. Our contention is that if one takes an initial state with a gaussian distribution having a lesser radial spread than the coherent state, the photon number uncertainty might be much lower. In fact the amplitude squeezed coherent state fulfills exactly this, and we will see that when this state evolves through a Kerr medium, one can achieve photon number uncertainties that go as the fifth root of the mean photon number [218].

The amplitude squeezed state has a wide range of applications, both in technology and pure physics, an excellent review of which can be found in Ref. [188]. A more recent review about the Kerr medium itself, its properties and applications

can be found in Ref. [189].

To conclude this chapter, we wish to point out that these are not the only schemes where one can get squeezing of noise, whether it is along some quadrature or in the photon number. There are considerations which show that a cavity with a moving wall [42] can give rise to squeezed states [142]. It has also been shown that there is squeezing in harmonic oscillators with time-dependent frequencies [143, 144]. It is known that by making the noise of the pumping current sub-poissonian, one can get amplitude squeezed light in a semi-conductor laser [206]. In general, if one could make the noise of the pump sub-poissonian, one can get amplitude squeezed light [208, 207, 209]. It can be done by using another sub-poissonian light as the pump, or by using electronics to get pulses whose noise is sub-poissonian. There had also been proposals for getting amplitude squeezed states using a combination of quantum non-demolition measurement of photon number and negative feedback [210]. Sub-Poissonian photon statistics has been observed in negative feedback semiconductor lasers with a destructive photon detector [211]. There were proposals for getting more amplitude squeezing [190, 191, 216], which have varying degree of experimental feasibility. This thesis is in fact concerned about one such proposal we have made to generate highly amplitude squeezed states of the radiation field [218, 219], and which seems to be experimentally feasible with existing technology. There have been other recent proposals [217], some of which are more concerned with Fock state generation [216, 217] rather than an amplitude squeezed state. Note that in a Fock state the phase information is completely lost, whereas in an amplitude squeezed state, the phase information is only less precise than in a coherent state.

There is also a related concept of amplifying a squeezed state. In particular,

whether one could achieve a photon number amplifier [222], which preserves the number-phase noise of the original state is an intriguing problem which has received only moderate attention [223, 224].

Apart from these there are other types of squeezing too, which at present have not been attempted experimentally. The amplitude squared squeezing introduced by Hillery [226, 243], has been rebuilt in terms of the properties of the SU(1,1) group as SU(1,1) squeezing [225, 227]. The representations of this can be used to study higher order squeezing [228, 229, 230]. There is also difference squeezing introduced again by Hillery [231], which corresponds to the SU(2) group. In fact many of the states also show higher order squeezing in the sense of Hong and Mandel [235, 236], and some states which do not show squeezing or sub-poissonian statistics can still be a non-classical [238] and show quantum properties. The squeeze operator itself cannot be generalized naively [237] to higher degree in the photon creation and annihilation operators, since such operators are not unitary. This is because the combination $\hat{a}^{\dagger k} + \hat{a}^k$ is not self-adjoint. By this we mean that a state got by acting with the exponential of this operator on a state in the Hilbert space will lie outside the Hilbert space. Hence the inner product of such a state with any state in the Hilbert space will diverge. But it should be noted that this study was done only for the above combination of operators. It would be more fruitful if it could be done for combination of quadrature operators $\hat{q}$ and $\hat{p}$.

In this chapter, we have briefly presented the usual way in which the electromagnetic field is quantized. We then gave some considerations

into the representations of the quantized field in terms of Fock states and coherent states. We have mentioned about the noise in the quantum field, which is quantum mechanical in origin, and the various tools required to quantify this noise. A brief review of the quadrature squeezed states, and the Kerr medium which gives rise to a different kind of squeezing, was then made. With this background material, we move on to the next chapter where we concern ourselfs with the relative phase between quantum states, whose presence gives rise to a curved quasi-probability distribution, and which in turn is responsible for amplitude squeezing.

Chapter 2

Relative phase in superposition of coherent states

In this chapter, the concept of relative phase is formulated. The relative phase first defined in Pancharatnam's classic work is adopted here to the superposition of two coherent states. For later convenience a canonical form of the superposition of two coherent states is constructed. We study in detail the effect of the relative phase on the QPD for the canonical form. The noise matrix for the canonical form is then calculated and the presence of various kinds of noise squeezing for different relative phases is studied. A general superposition of two coherent states is then studied by reducing and relating it to the canonical form.

2.1 Definition of relative phase

The overall phase of a quantum state generally doesn't reflect in the calculated physical observables. But there are comparatively many cases where the difference between the phases of individual quantum states, called the relative phase, enters calculated quantities. One such instance is the superposition of quantum states. If one considers two states $e^{i\chi_1}|\psi_1\rangle$ and $e^{i\chi_2}|\psi_2\rangle$, where χ_1 and χ_2 are phases of

quantum states $|\psi_1\rangle$ and $|\psi_2\rangle$, then one can construct a superposition

$$|\psi\rangle = \mathcal{N} e^{ix_1}(|\psi_1\rangle + e^{i(x_2-x_1)}|\psi_2\rangle) \quad , \tag{2.1}$$

where $\mathcal{N}$ is the normalization constant. From the way the superposition is written, it is clear that even those quantities which are unaffected by the overall phase e^{ix_1} will involve the relative phase $e^{i(x_2-x_1)}$.

In this context, the Pancharatnam [263] way of defining the relative phase is very appropriate, since it is based on the inner product between the states and hence has deep mathematical consequences [266, 267]. Pancharatnam originally used it in polarization states, but its connection to Berry phase [258, 259] has been pointed out by many people [260, 261, 262]. The Berry-Pancharatnam phase is now being used cleverly in many experimental situations [268, 269]. In the Pancharatnam sense, the phase of a quantum state $|\psi_1\rangle$ over another quantum state $|\psi_0\rangle$ is defined as

$$\mathrm{Ph}_{(|\psi_0\rangle)}(|\psi_1\rangle) = \mathrm{Arg}[\langle\psi_0|\psi_1\rangle] \quad . \tag{2.2}$$

Note that $\mathrm{Ph}_{(|\psi_0\rangle)}(|\psi_1\rangle) = -\mathrm{Ph}_{(|\psi_1\rangle)}(|\psi_0\rangle)$, and hence the phase defined in this way has a orientation. Two quantum states are said to be *in-phase* when they have vanishing relative phase in the sense of Eq. (2.2), which will happen when their inner product is real positive. One should also carefully note the non-transitivity property, in the sense that if two quantum states $|\psi_1\rangle$ and $|\psi_2\rangle$ are in-phase and again if $|\psi_1\rangle$ and $|\psi_3\rangle$ are in-phase, then in the general case $|\psi_1\rangle$ need not be in-phase with $|\psi_3\rangle$. Hence, 'being in phase' is not an equivalence relation. Note that the relative phase between two orthogonal states is not defined by Eq. (2.2).

The way the coherent states are defined [64, 65], one is free to choose an arbitrary overall phase for each coherent state. But by convention, the phases are so chosen

that their inner product with the vacuum state is real. The usual expansion of coherent states in terms of the Fock states [62, 63],

$$|\alpha\rangle = e^{-|\alpha|^2/2} \sum_{n=0}^{\infty} \frac{\alpha^n}{\sqrt{n!}} |n\rangle \quad , \tag{2.3}$$

has this convention built into it. Using the definition of relative phase, the relative phase of a coherent state $|\beta\rangle$ with respect to another coherent state $|\alpha\rangle$ is given by,

$$\mathrm{Ph}_{(|\alpha\rangle)}(|\beta\rangle) = \mathrm{Arg}[\langle\alpha\ |\beta\rangle] = \mathrm{Im}(\alpha^*\beta) \quad . \tag{2.4}$$

Any coherent state $|\alpha\rangle$, as noted earlier, has $\langle 0\ |\alpha\rangle$ real and hence every coherent state $|\alpha\rangle$ is in-phase with the vacuum state $|0\rangle$. It can also be immediately seen that all coherent states lying along a straight line passing through the origin of phase space, which can be parameterized as $\left|r_j e^{i\phi}\right\rangle$ are in-phase with one another. This is so, since for two states $\left|r_1 e^{i\phi}\right\rangle$ and $\left|r_2 e^{i\phi}\right\rangle$, we have

$$\left\langle r_1 e^{i\phi}\ \middle|\ r_2 e^{i\phi}\right\rangle = e^{-(r_1^2+r_2^2)/2+r_1 r_2} = e^{-\frac{1}{2}(r_1-r_2)^2} \tag{2.5}$$

which is real. We can generalize this to coherent states lying on any straight line in phase space, which we will do now.

Two coherent states $|\alpha_1\rangle$ and $|\alpha_2\rangle$ can be made in-phase by choosing an overall phase for one of the states. Thus $|\alpha_1\rangle$ and $e^{-i\,\mathrm{Im}(\alpha_1^*\alpha_2)}|\alpha_2\rangle$ will have no relative phase. Note that the argument can not be extended to three or more coherent states in general, since if we choose another coherent state $|\alpha_3\rangle$ which we want to be in-phase with $|\alpha_1\rangle$, we have to consider the state $e^{-i\,\mathrm{Im}(\alpha_1^*\alpha_3)}|\alpha_3\rangle$. But then in the general case $e^{-i\,\mathrm{Im}(\alpha_1^*\alpha_2)}|\alpha_2\rangle$ will not be in-phase with $e^{-i\,\mathrm{Im}(\alpha_1^*\alpha_3)}|\alpha_3\rangle$. The question that immediately arises is, when can one choose these states $|\alpha_1\rangle$, $|\alpha_2\rangle$,

and $|\alpha_3\rangle$, to be in-phase with each other? It is obvious that these states can be in-phase with each other if and only if

$$\mathrm{Im}(\alpha_1^*\alpha_2) + \mathrm{Im}(\alpha_2^*\alpha_3) + \mathrm{Im}(\alpha_3^*\alpha_1) = 0 \quad . \tag{2.6}$$

That this is so can easily be checked by noting the condition required to make $e^{-i\,\mathrm{Im}(\alpha_1^*\alpha_2)}\,|\alpha_2\rangle$ and $e^{-i\,\mathrm{Im}(\alpha_1^*\alpha_3)}\,|\alpha_3\rangle$ in-phase.

If one parameterizes α_i as $\alpha_i = \alpha_i^{(x)} + i\alpha_i^{(y)}$ the above relation reduces to

$$\left(\alpha_3^{(x)} - \alpha_2^{(x)}\right)\alpha_1^{(y)} + \left(\alpha_1^{(x)} - \alpha_3^{(x)}\right)\alpha_2^{(y)} + \left(\alpha_2^{(x)} - \alpha_1^{(x)}\right)\alpha_3^{(y)} = 0 \quad . \tag{2.7}$$

We can see that this relation is readily satisfied if one chooses

$$\alpha_k^{(y)} = m\alpha_k^{(x)} + C \quad . \tag{2.8}$$

This implies that the α_k's must lie on a straight line in phase space whose slope is m and whose intercept with the imaginary axis is at C. Hence we have shown that the coherent states lying along any straight line in phase space can be made in-phase and vice-versa. It is easy to see that this argument can be extended to any number of coherent states.

To elucidate the concept of relative phase between coherent states further, let us look at a more geometrical picture. One can represent the coherent states $|\alpha\rangle$ as points in the complex α-plane. This parameter space is called the complex α-plane. A coherent state $|\alpha\rangle$ can be represented by a point $(\alpha^{(x)}, \alpha^{(y)})$ in the complex plane, where $\alpha = \alpha^{(x)} + i\alpha^{(y)}$. The origin of the complex plane is chosen to be the vacuum state $|0\rangle$. Let us consider two coherent states $|\alpha_1\rangle$ and $|\alpha_2\rangle$. These are represented in the complex plane by the points $(\alpha_1^{(x)}, \alpha_1^{(y)})$ and $(\alpha_2^{(x)}, \alpha_2^{(y)})$. These

two points are connected to the origin by arrows as shown in Fig. (2.1). The relative phase of $|\alpha_2\rangle$ with respect to $|\alpha_1\rangle$ is given by $\mathrm{Ph}_{(|\alpha_1\rangle)}(|\alpha_2\rangle) = \mathrm{Arg}(\langle\alpha_1|\alpha_2\rangle) = \mathrm{Im}(\alpha_1^*\alpha_2) = (\alpha_1^{(x)}\alpha_2^{(y)} - \alpha_1^{(y)}\alpha_2^{(x)})$. But note that this is just twice the area enclosed in the triangle formed by the states $|0\rangle$, $|\alpha_1\rangle$ and $|\alpha_2\rangle$ in the parameter space, as indicated in the figure by the shaded area. The geometric phase is precisely defined

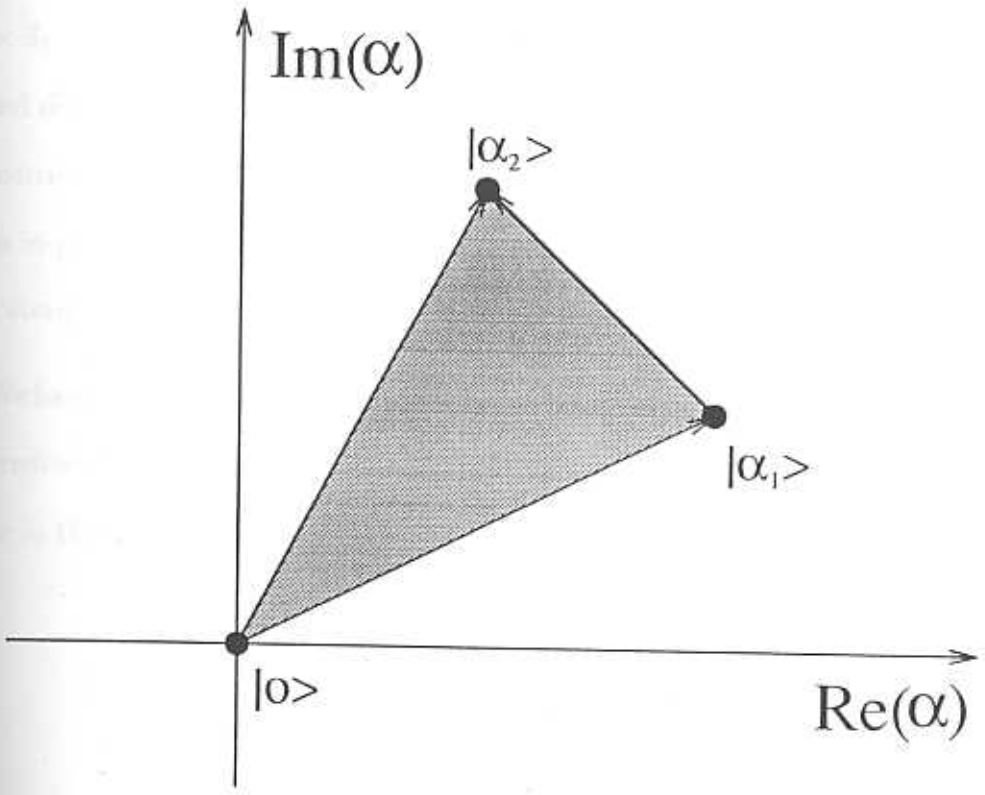

Fig. 2.1. The Coherent states $|o\rangle$, $|\alpha\rangle$ and $|\beta\rangle$ are represented in the complex-α plane.

in the same way [264, 265, 266, 267] and in general if these states $|\alpha_1\rangle$, $|\alpha_2\rangle$ and $|\alpha_3\rangle$ formed a closed figure then we have

$$\begin{aligned}\mathrm{Ph}_{(|\alpha_1\rangle)}(|\alpha_2\rangle) + \mathrm{Ph}_{(|\alpha_2\rangle)}(|\alpha_3\rangle) + \mathrm{Ph}_{(|\alpha_3\rangle)}(|\alpha_1\rangle) &= \text{geometric phase} \\ &= 2 \times (\text{area enclosed}). \qquad (2.9)\end{aligned}$$

One should note the analogy with vector cross product, since if one denotes the quantum state $|\alpha_i\rangle$ as a three dimensional vector $(\alpha_i^{(x)}, \alpha_i^{(y)}, 0)$, then we can define

$$\mathrm{Ph}_{(|\alpha_1\rangle)}(|\alpha_2\rangle) = (\vec{\alpha}_1 \times \vec{\alpha}_2) \cdot \hat{k} \tag{2.10}$$

where $\vec{k}$ is the unit vector perpendicular to the plane containing $\vec{\alpha}_1$ and $\vec{\alpha}_2$. In fact, it is obvious from vector algebra and the way we have defined these vectors that $(\vec{\alpha}_1 \times \vec{\alpha}_2 + \vec{\alpha}_2 \times \vec{\alpha}_3 + \vec{\alpha}_3 \times \vec{\alpha}_1) \cdot \hat{k}$ will give twice the area enclosed by the vectors $\vec{\alpha}_1$, $\vec{\alpha}_2$ and $\vec{\alpha}_3$, which is consistent with what we said earlier. It is also obvious from the geometric phase concept that three quantum states $|\alpha_1\rangle$, $|\alpha_2\rangle$, and $|\alpha_3\rangle$ cannot be made in-phase with each other since they enclose an area, unless they happen to lie on a straight line.

We have discussed the concept of relative phase in quantum states in general and coherent states in particular. We will use this knowledge in introducing the relative phase in the superposition of coherent states.

2.2 Relative phase in superposition of two coherent states – canonical form

Consider the superposition of two coherent states of the form

$$|\psi\rangle = \mathcal{N}\Big(|\alpha\rangle + |\beta\rangle\Big) \quad , \tag{2.11}$$

where $\mathcal{N}$ is the normalization constant. From the considerations of the previous section It is clear that $|\alpha\rangle$ and $|\beta\rangle$ are not in-phase in the general case. In fact the phase of $|\beta\rangle$ with respect to $|\alpha\rangle$ is given by $\mathrm{Ph}_{(|\alpha\rangle)}(|\beta\rangle) = \mathrm{Im}(\alpha^*\beta)$. it is not obvious from the way the superposition is written above that there is this relative phase

between the states. It would be quite nice if we can reduce the above superposition to a simpler one where the relative phase is apparent. The idea is that one should be able to go over from this simple superposition to the general one by operating it with some specific operators which doesn't change the relative phase between the states.

The coherent state is also defined as the state that is got by displacing the vacuum using the displacement operator [63]. Thus a coherent state $|\gamma\rangle$ can be written as,

$$|\gamma\rangle = \widehat{D}(\gamma)\,|0\rangle \quad , \tag{2.12}$$

where

$$\widehat{D}(\gamma) = e^{\gamma\hat{a}^\dagger - \gamma^*\hat{a}} \quad . \tag{2.13}$$

The displacement operator is unitary since $\widehat{D}^\dagger\widehat{D} = 1 = \widehat{D}\widehat{D}^\dagger$. In the above superposition, if one displaces both the component states by the same amount, say by $\widehat{D}(\gamma)$, then the relative phase between the displaced states $\widehat{D}(\gamma)\,|\alpha\rangle$ and $\widehat{D}(\gamma)\,|\beta\rangle$ will be the same as the relative phase between $|\alpha\rangle$ and $|\beta\rangle$. This is so since the relative phase of $\widehat{D}(\gamma)\,|\beta\rangle$ with respect to $\widehat{D}(\gamma)\,|\alpha\rangle$ is given by

$$\mathrm{Ph}_{(\widehat{D}(\gamma)|\alpha\rangle)}(\widehat{D}(\gamma)\,|\beta\rangle) = \langle\alpha|\,\widehat{D}^\dagger(\gamma)\widehat{D}(\gamma)\,|\beta\rangle = \langle\alpha\,|\beta\rangle = \mathrm{Ph}_{(|\alpha\rangle)}(|\beta\rangle) \quad . \tag{2.14}$$

This argument can be easily extended to a superposition of many coherent states. The relative phase between any two component states in such a superposition is preserved on displacement. Note that the above argument is essentially based on the unitarity property and as such holds for any unitary operator provided that it acts in the same way on all the component states. Hence, even if one applies a squeeze operator [85, 86, 89] to a superposition of coherent states, the relative phase

between the now squeezed component states will be the same as the relative phase between the component coherent states of the initial superposition.

The superposition given above in Eq. (2.11) can hence be a displaced version of some superposition where the relative phase is apparent. This could be done if one chooses a superposition whose component states are on a straight line passing

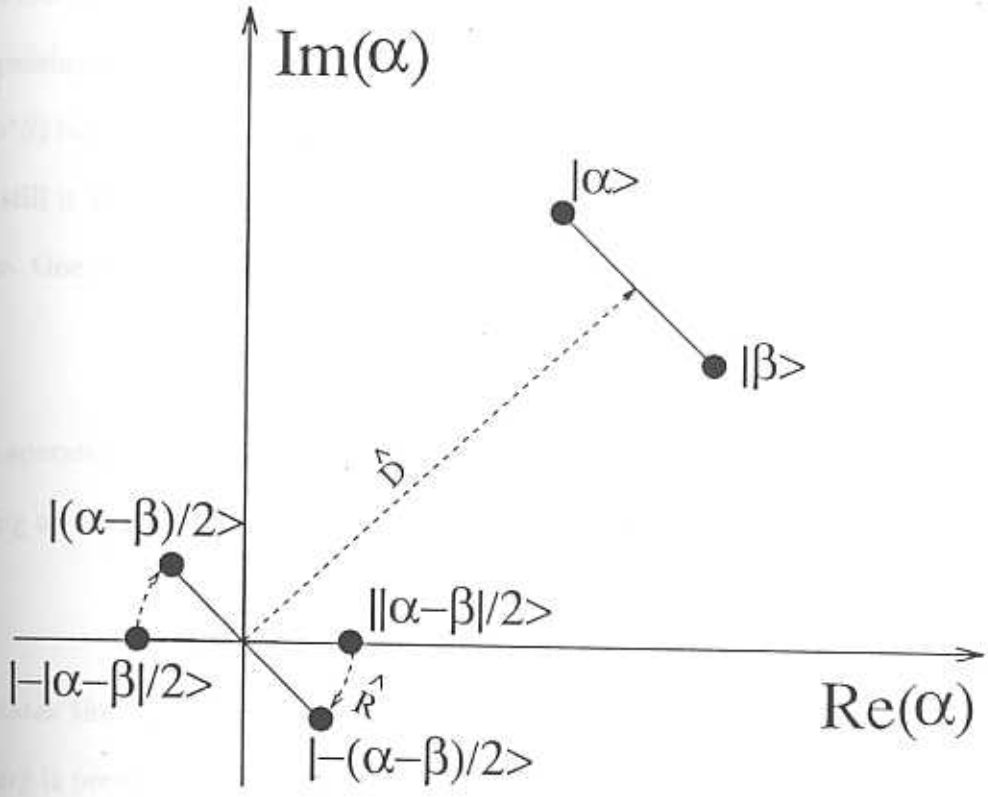

Fig. 2.2. The way the superposition of coherent states $|\alpha\rangle$ and $|\beta\rangle$ obtained from the canonical form is illustrated.

through the origin. Such a scheme can be readily achieved if one visualizes [Fig. 2.2] these in the complex α-plane introduced earlier. The mid-point of the line joining the points representing the states $|\alpha\rangle$ and $|\beta\rangle$ must be moved to the origin of phase space, since a displacement operator acting on the superposition with its mid-point

at the phase space origin will be able to move it back to the earlier position. It can be written as

$$\begin{aligned} |\psi\rangle &= \mathcal{N}\big(|\alpha\rangle + |\beta\rangle\big) \\ &= \mathcal{N}e^{-\frac{i}{2}\,\mathrm{Im}(\alpha^*\beta)}\widehat{D}\left(\frac{\alpha+\beta}{2}\right)\left[\left|\left(\frac{\alpha-\beta}{2}\right)\right\rangle + e^{i\,\mathrm{Im}(\alpha^*\beta)}\left|-\left(\frac{\alpha-\beta}{2}\right)\right\rangle\right] . \end{aligned} \tag{2.15}$$

It can be seen that the states $|(\alpha-\beta)/2\rangle$ and $|-(\alpha-\beta)/2\rangle$ are along a straight line passing through the origin and are in-phase with each other. The relative phase $\mathrm{Im}(\alpha^*\beta)$ between the component states of the original superposition is now manifest. But still it would be better to bring these states on the real axis of the complex α-plane. One could do that using the operator $\widehat{R}(\tau)$ which is defined as

$$\widehat{R}(\tau) = e^{i\tau\hat{a}^\dagger\hat{a}} \quad . \tag{2.16}$$

This operator $\widehat{R}(\tau)$ rotates every point in phase space by an angle τ about the origin. Acting on a coherent state

$$\widehat{R}(\tau)\,|\alpha\rangle = \left|\alpha e^{i\tau}\right\rangle \quad , \tag{2.17}$$

it rotates the state to a new position in phase space. Since this operator is also unitary it preserves the relative phase between the component states in a superposition.

Hence our superposition can be brought to the form

$$|\psi\rangle = \mathcal{N}e^{-\frac{i}{2}\,\mathrm{Im}(\alpha^*\beta)}\widehat{D}\,(\gamma)\,\widehat{R}(\tau)\,\big(\,|-x\rangle + e^{i\chi}\,|x\rangle\,\big) \quad , \tag{2.18}$$

where

$$\gamma = \frac{\alpha+\beta}{2} \quad ; \quad e^{i\tau} = -\frac{\alpha-\beta}{|\alpha-\beta|} \quad ; \quad x = \frac{|\alpha-\beta|}{2} \quad ; \quad \chi = \mathrm{Im}(\alpha^*\beta) \quad . \tag{2.19}$$

The component states now lie along the real axis. The parameter x is called the *half-separation* and χ is called the *relative phase*, γ the *displacement*, and τ the *orientation*. These four quantities form the basic parameters of any superposition of two coherent states. The original superposition is specified by four real numbers, whereas if the displacement is taken as a complex quantity there are now five real numbers. But note that the displacement occurs in a fixed direction and the argument of γ is related to the angle τ.

There are many benefits of casting the superposition in this way, since rotation and displacement act "trivially"; if one knows the quantities of interest for the state

$$|\psi_c\rangle = \mathcal{N}\left(\,|-x\rangle + e^{i\chi}|x\rangle\,\right) \quad , \tag{2.20}$$

where

$$\mathcal{N}^2 = \frac{1}{2\left(1+e^{-2x^2}\cos\chi\right)} \quad , \tag{2.21}$$

then one can easily write down the quantities corresponding to any superposition of two coherent states. We wish to call the state $|\psi_c\rangle$ as the *canonical* state. Note that one cannot do the above were it not for the presence of the relative phase in the canonical state. This relative phase plays a crucial role in many of the properties of $|\psi_c\rangle$ and hence in any superposition.

2.3 Effect of relative phase on the quasi probability distribution

In this section we would like to visualize the effect of relative phase in a superposition of two coherent states. We do it by plotting the contours of the Q-quasi probability

distribution. We have earlier seen that it is the smoothest of the quasi probability distributions and never goes singular [70, 71]. The Q function of an arbitrary state $|\psi\rangle$ is calculated using the definition

$$Q(\beta) = \frac{1}{\pi} |\langle \beta \ | \psi \rangle|^2 \quad , \tag{2.22}$$

where $|\beta\rangle$ is a coherent state. In the case of a superposition of two coherent states in the canonical form [Eq. (2.20)], the Q function is given by

$$Q_c(\beta) = \frac{e^{-(q^2+p^2+x^2)}}{\pi(1 + e^{-2x^2} \cos\chi)} \{\cosh(2xq) + \cos(\chi + 2xp)\} \tag{2.23}$$

where $q = \mathrm{Re}(\beta)$ and $p = \mathrm{Im}(\beta)$.

It can be seen from the above equation that $Q(\beta)$ is oscillatory with respect to and p, with a heavy damping factor in the front. Hence, essentially what we observe will only be the first oscillation in p. In the q variable, the $\cosh(2xq)$ implies that there will be two peaks symmetrically situated about the origin of phase space. In the absence of χ, the first oscillation in p has a peak at $p = 0$. Hence we would expect the quasi-probability distribution to be like an elongated ellipse with its major axis along the q-direction if the half-separation x is small, or as two separate peaks along the q-direction if x is large. When χ is non-zero, the p-oscillation peak is shifted along the positive p-direction, the shift in turn depending on the q-value. Hence we will get a crescent shaped Q function if the half-separation x is small enough. In the extreme case of $\chi = \pi$, the crescent expands into a circle centered at the origin of phase space – the mid-point of the line joining the two superposed states. For $\chi > \pi$, the process is repeated, but with the crescent now in the negative p-direction. In fact, the Q function for this superposition has a symmetry with respect to χ, in

the sense that χ and $2\pi - \chi$ correspond to mirror reflections about the q-axis – the line joining the two component states.

We wish to first discern the effect of the (half-)separation of the states on the Q function before we proceed to study in detail the effect of the relative phase. In Fig. (2.3, 2.4, 2.5), we plot the Q function for different half-separation, for three different values of the relative phase. In Fig. (2.3), we have plotted the Q function of the superposition for the relative phase $\chi = 0°$, which is called as the even-coherent state [243] in the literature. Starting from the half-separation value of $x = 0.1$, we have plotted the Q function for this value of χ for half-separations that are in steps of 0.3. It could be seen that when the half-separation is very small ($x = 0.1$), the Q function resembles that of a coherent state. As the x value increases there is squeezing in the direction perpendicular to the line joining the component states. This squeezing is maximum around the half-separation value of $x = 0.7$. When the half-separation is increased further, the individual coherent states start separating, as in the figure when $x = 1.0$, and one can see the consequent increase in the noise along the perpendicular direction. Further increase in x leads to a decrease in the interference between the two states. When $x = 1.6$, for all practical purpose the superposition is rather like a statistical mixture of two coherent states.

In Fig. (2.4), we have fixed the relative phase at $\chi = 90°$. This state corresponds to the Yurke-Stoler state [241, 197, 198] and has similar characteristics as that of a coherent state. It shows no squeezing, but still its Q function is very different from that of the coherent state. It would show very different photon number characteristics if it is displaced to a proper position in phase space [242]. We will come to this in Chapter 3. Here too, it may be seen that the ideal half-separation is around the

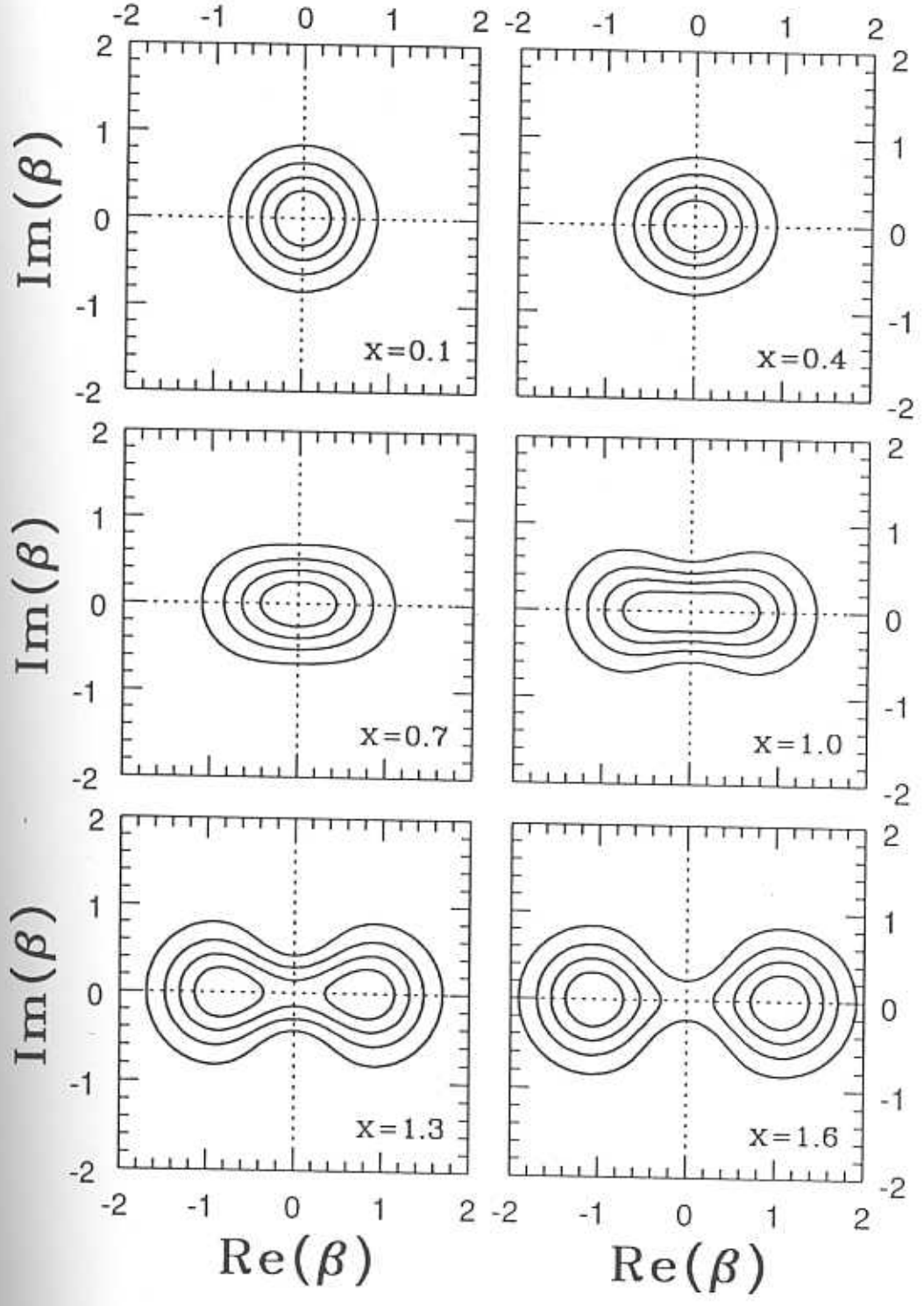

Fig. 2.3. Plot of the contours of the Q-function of a superposition of two coherent states for different half-separation when the relative phase $\chi = 0^{\circ}$.

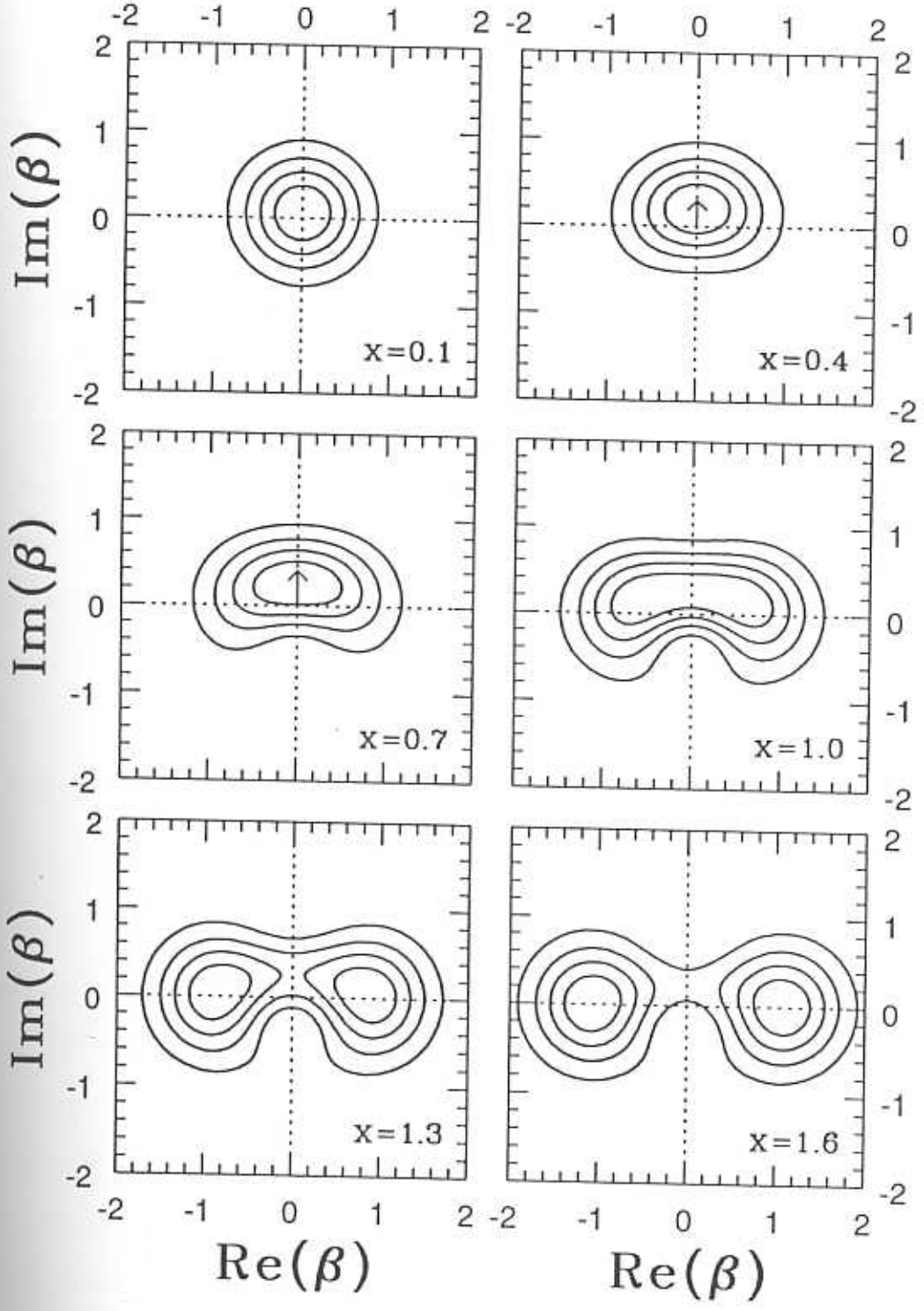

Fig. 2.4. Plot of the contours of the Q-function of a superposition of two coherent states for different half-separation when the relative phase $\chi = 90°$.

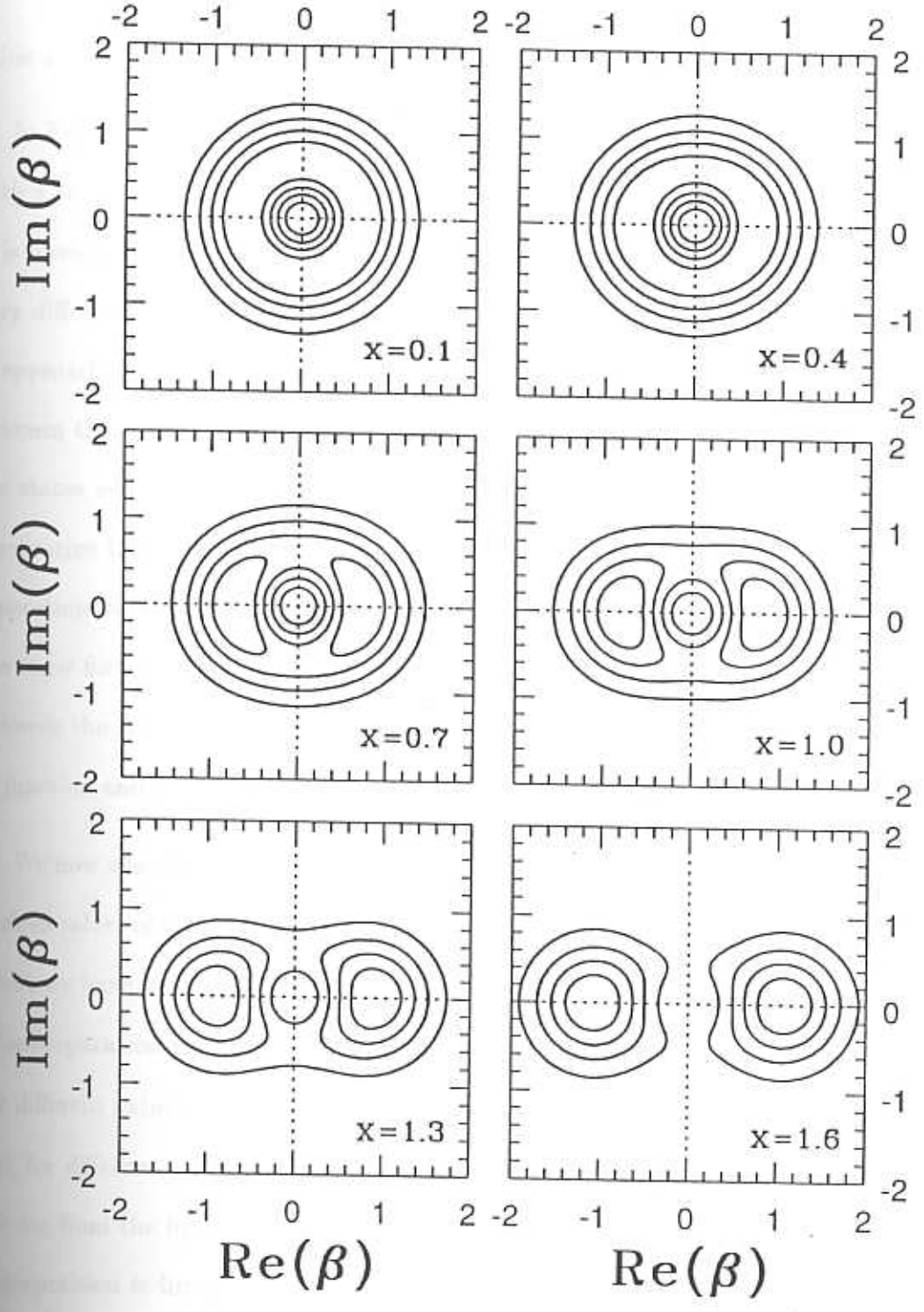

Fig. 2.5. Plot of the contours of the Q-function of a superposition of two coherent states for different half-separation when the relative phase $\chi = 180°$.

value $x = 0.7$.

In Fig (2.5), we plot the Q function for the superposition of two coherent states with a relative phase fixed at $\chi = 180°$, called the odd-coherent state [243]. Here it is obvious that if the half-separation is small enough, then the superposition is very different from a coherent state. Actually, we will see later (Chapter 3) that it approaches the Fock state $|1\rangle$. As the half-separation increases, the interference between the component states weakens, and as in the previous cases when $x > 1$, the states are separated enough to behave as a statistical mixture. Hence we can summarize that as far as the *strength* of the interference is concerned, the half-separation between the states plays a crucial role and it seems to be more or less the same for any relative phase. For small half-separations, where the interference between the states is quite high, the relative phase plays an important role, and the Q function and many other properties crucially depend on it.

We now wish to give the Q function for a superposition of two coherent states for various values of the relative phase for a given half-separation. We do so in Fig. (2.6), where we have plotted the Q function for a superposition of two coherent states with a half-separation (arbitrarily chosen near the optimum half-separation) of $x = 0.7$, for different values of relative phase. There are 24 plots in the figure (Pages 57 – 60), for different relative phase values in steps of 15°, in the range $0 \leq \chi < 2\pi$. We see from the figures that when the relative phase $\chi = 0$, the Q function of the superposition is linear[247], in the sense that it is along a straight line joining the component states in phase space. Also one can visually judge that it is quadrature squeezed in the perpendicular direction [243, 247] to the line joining the component states. This squeezing arises because of the way the component states interfere in

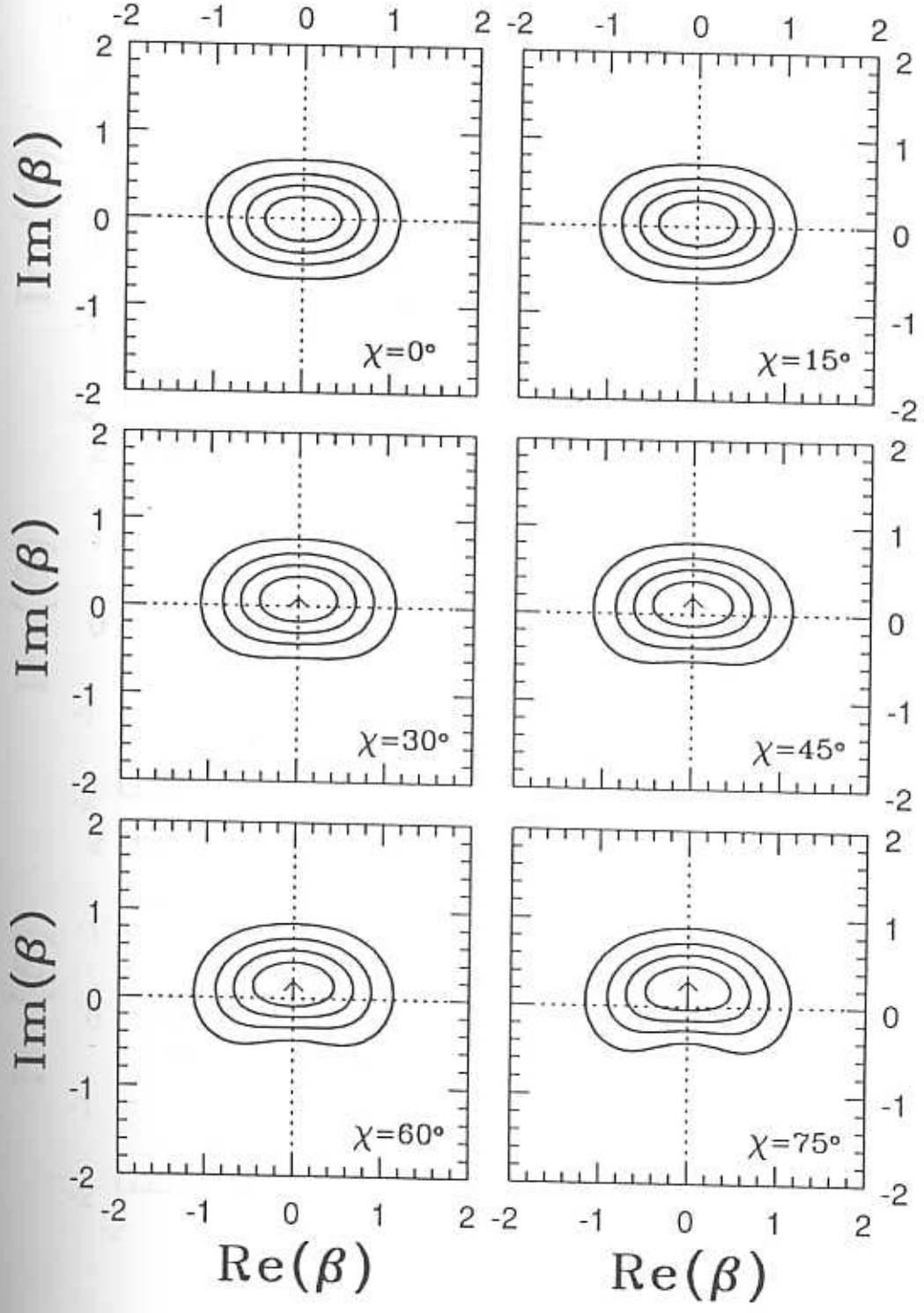

Fig. 2.6. Plot of the contours of the Q-function of a superposition of two coherent states for different values of the relative phase. The half-separation is fixed at $x = 0.7$ in these plots.

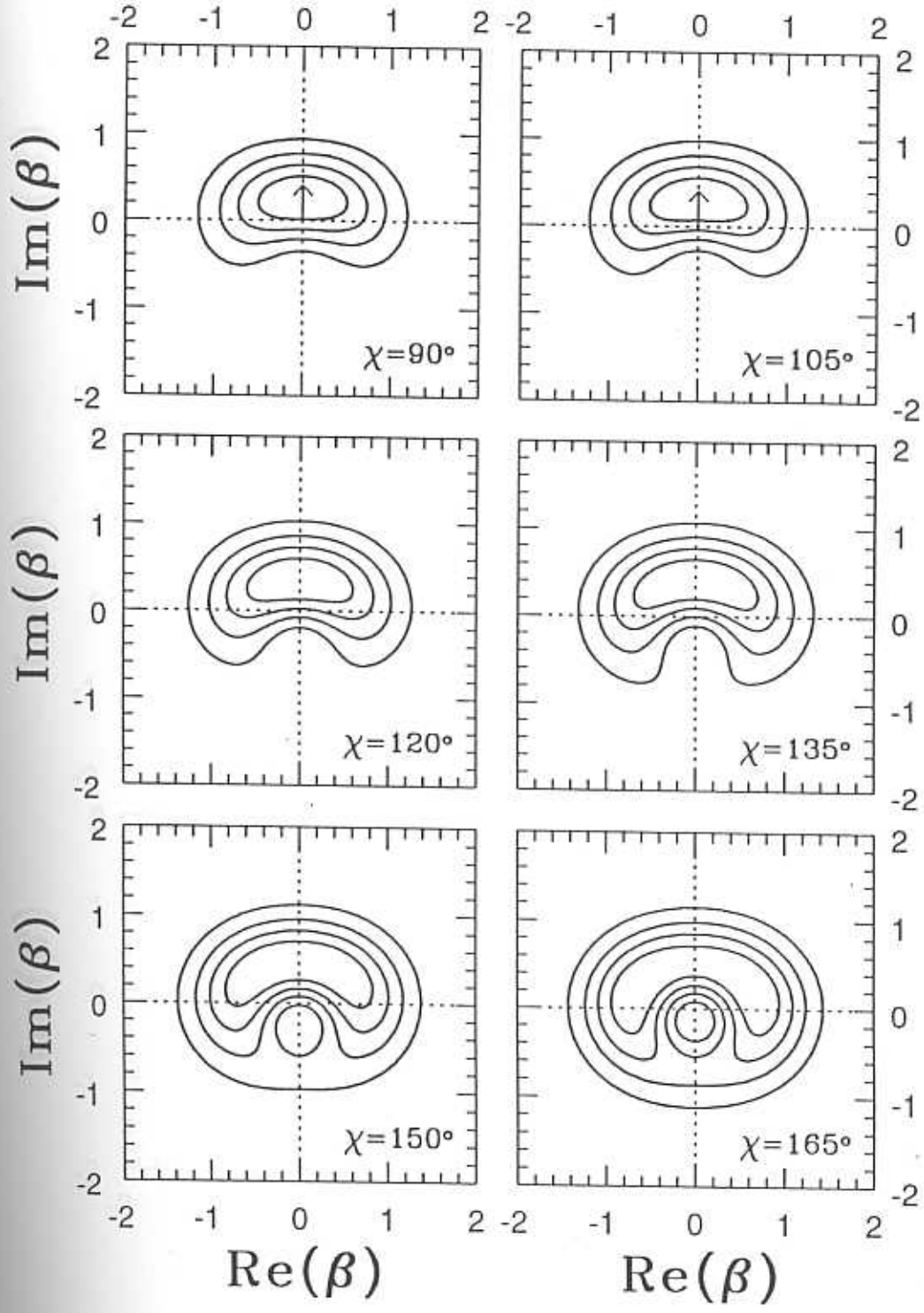

Fig. 2.6. (Cont.) Plot of the contours of the Q-function of a superposition of two coherent states for different values of the relative phase. The half-separation is fixed at $x = 0.7$ in these plots.

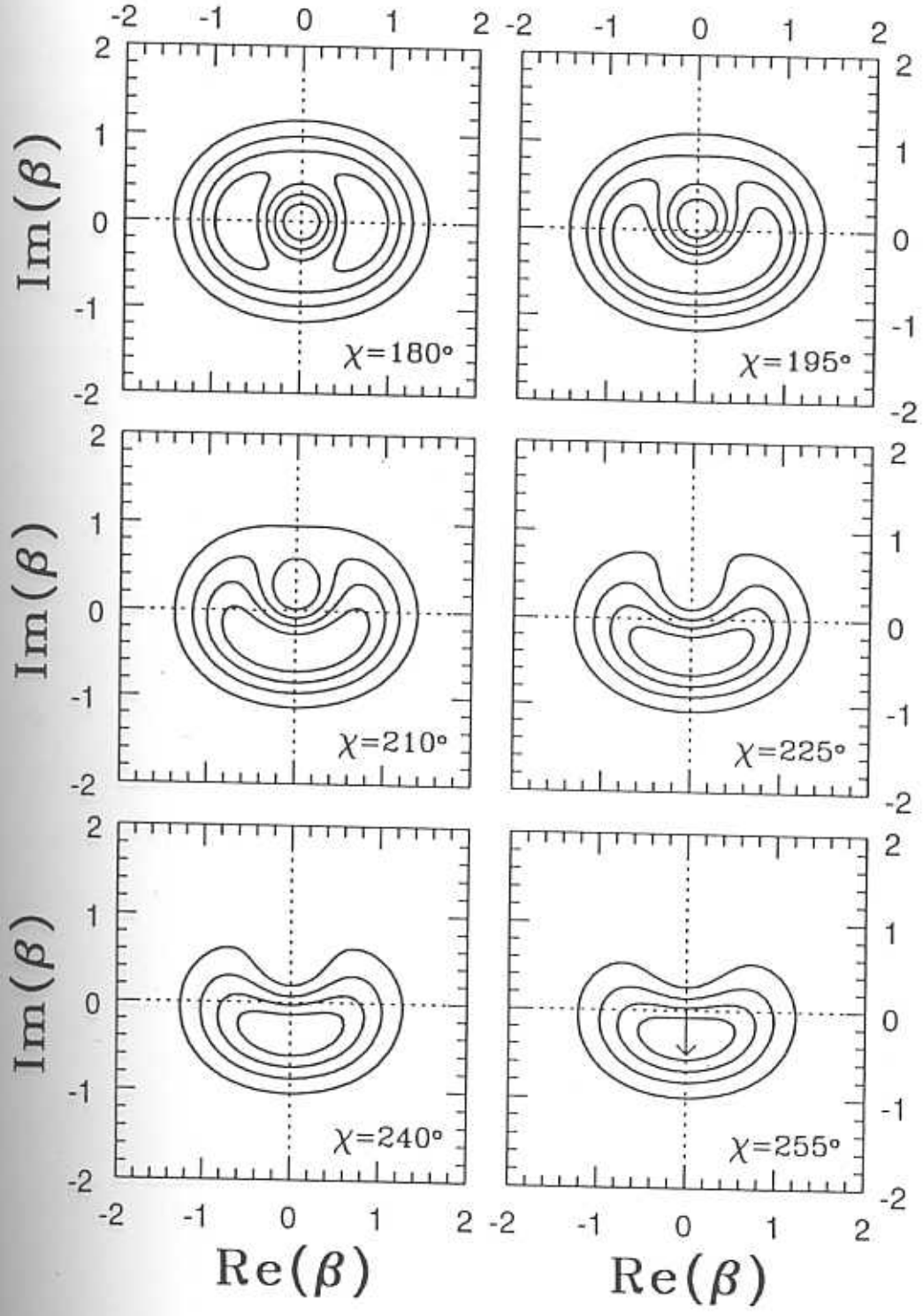

Fig. 2.6. (Cont.) Plot of the contours of the Q-function of a superposition of two coherent states for different values of the relative phase. The half-separation is fixed at $x = 0.7$ in these plots.

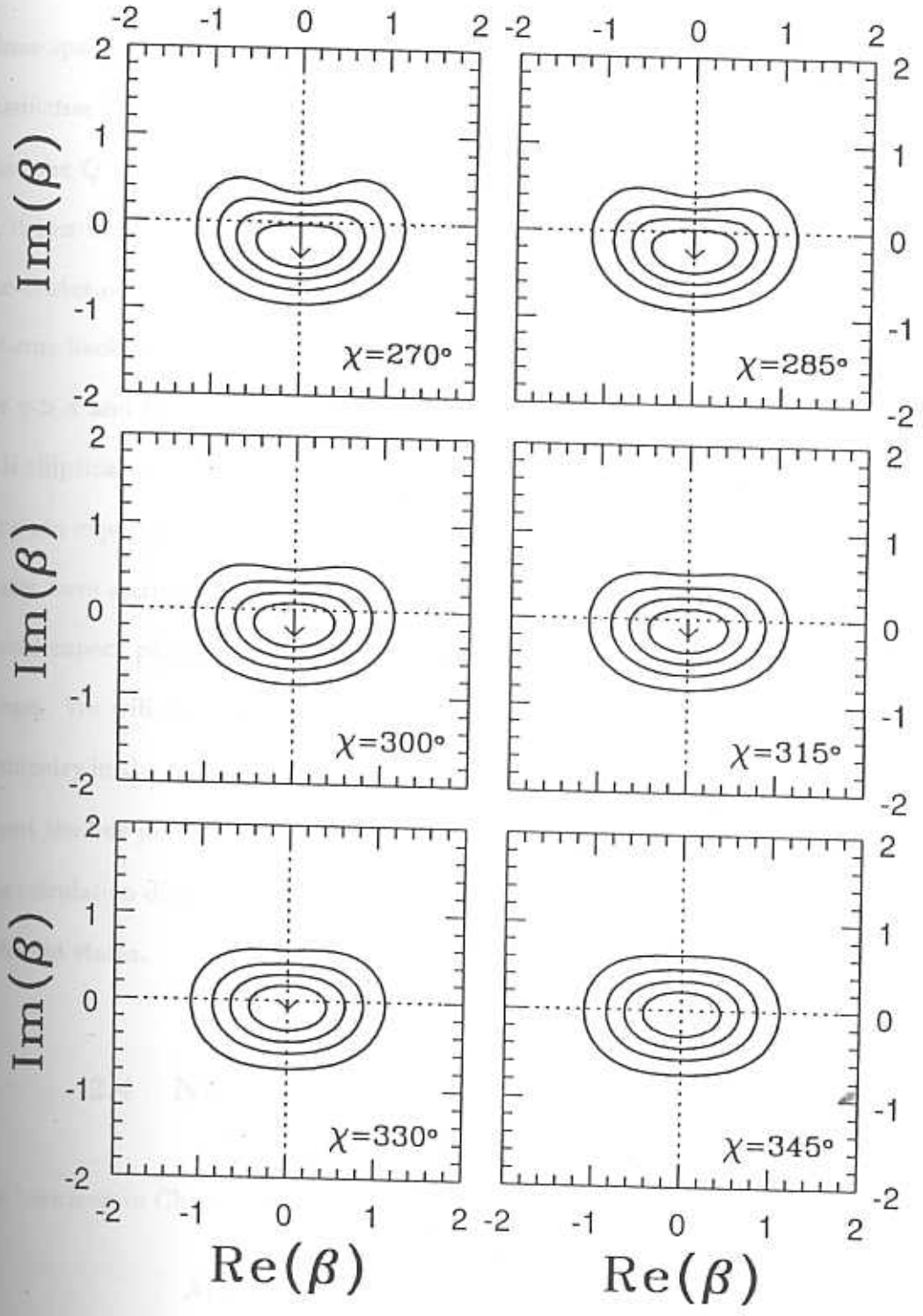

Fig. 2.6. (Cont.) Plot of the contours of the Q-function of a superposition of two coherent states for different values of the relative phase. The half-separation is fixed at $x = 0.7$ in these plots.

phase space [253, 254]. Its center of distribution is at the origin of phase space. The *distinctive* feature one notices from these plots as one increases the relative phase is that the Q function acquires a curved shape. For this value of the half-separation x, it can be seen that with increasing relative phase in the range $0 \leq \chi < 2\pi/3$, the center of the distribution starts moving along the positive Imaginary axis. It returns back to the origin at $\chi = \pi$ and moves along the negative Imaginary axis for $\chi > \pi$ and then returns back to the origin at $\chi = 2\pi$. We also see that at $\chi = \pi$ it is elliptical in shape. For smaller half-separations x, it will become more circular. One can expect photon number squeezing here, since as seen in Chapter 1, the Fock states have a circular Q function centered at the origin of phase space. In fact one would expect photon number squeezing as soon as the Q function takes a curved shape. We will discuss this in detail in Chapter 3. As stated earlier, there is a symmetry in the relative phase, in the sense that χ and $2\pi - \chi$ are mirror reflections about the line joining the two component states. We will now turn our attention to the calculation of noise properties of this canonical from of the superposition of two coherent states.

2.4 Noise matrix of the Canonical form

We have seen in Chapter 1 that the uncertainty matrix [233] of any state is given by

$$\mathcal{M} = \begin{pmatrix} \langle (\Delta\hat{q})^2 \rangle & \left\langle \frac{1}{2}\{\Delta\hat{q}, \Delta\hat{p}\} \right\rangle \\ \left\langle \frac{1}{2}\{\Delta\hat{q}, \Delta\hat{p}\} \right\rangle & \langle (\Delta\hat{p})^2 \rangle \end{pmatrix} , \tag{2.24}$$

where $\hat{q}$ and $\hat{p}$ are called the quadrature operators, and $\{\hat{A}, \hat{B}\}$ is the anticommutator of the operators $\hat{A}$ and $\hat{B}$. The operators $\hat{q}$ and $\hat{p}$ are given in terms of the usual

boson operators by the relations

$$\begin{aligned} \hat{q} &= \frac{1}{\sqrt{2}}\left(\hat{a}^{\dagger}+\hat{a}\right) \\ \hat{p} &= \frac{i}{\sqrt{2}}\left(\hat{a}^{\dagger}-\hat{a}\right) \quad , \end{aligned} \tag{2.25}$$

which we have seen earlier in Chapter 1. Here, $(\Delta\hat{A})$ stands for $(\Delta\hat{A}) = \hat{A} - \langle\hat{A}\rangle$. The aim of this section is to calculate the noise matrix, and to study in some detail the noise in different quadratures. With the above definition of the quadrature operators, $\langle(\Delta\hat{q})^2\rangle$ and $\langle(\Delta\hat{p})^2\rangle$ can be written as

$$\begin{aligned} \left\langle(\Delta\hat{q})^2\right\rangle &= \frac{1}{2}+\frac{1}{2}\left\langle(\Delta\hat{a})^2\right\rangle+\frac{1}{2}\left\langle(\Delta\hat{a}^{\dagger})^2\right\rangle+\left\langle\hat{a}^{\dagger}\hat{a}\right\rangle-\left\langle\hat{a}^{\dagger}\right\rangle\left\langle\hat{a}\right\rangle \\ \left\langle(\Delta\hat{p})^2\right\rangle &= \frac{1}{2}-\frac{1}{2}\left\langle(\Delta\hat{a})^2\right\rangle-\frac{1}{2}\left\langle(\Delta\hat{a}^{\dagger})^2\right\rangle+\left\langle\hat{a}^{\dagger}\hat{a}\right\rangle-\left\langle\hat{a}^{\dagger}\right\rangle\left\langle\hat{a}\right\rangle \quad . \end{aligned} \tag{2.26}$$

We calculate first the expectation values of the needed powers of the annihilation and creation operators in the canonical state. Thus we have

$$\begin{aligned} \langle\hat{a}\rangle &= ix\left(\frac{e^{-2x^2}\sin\chi}{1+e^{-2x^2}\cos\chi}\right) \\ \left\langle\hat{a}^2\right\rangle &= x^2 \\ \left\langle\hat{a}^{\dagger}\hat{a}\right\rangle &= x^2\left(\frac{1-e^{-2x^2}\cos\chi}{1+e^{-2x^2}\cos\chi}\right) \end{aligned} \tag{2.27}$$

and $\left\langle\hat{a}^{\dagger}\right\rangle = \left\langle\hat{a}\right\rangle^*$ and $\left\langle\hat{a}^{\dagger 2}\right\rangle = \left\langle\hat{a}^2\right\rangle^*$. Hence we see that

$$\left\langle(\Delta\hat{a}^{\dagger})\right\rangle^2 = \left\langle(\Delta\hat{a})\right\rangle^2 = x^2\left[\frac{1+e^{-4x^2}+2e^{-2x^2}\cos\chi}{(1+e^{-2x^2}\cos\chi)^2}\right] \quad . \tag{2.28}$$

The uncertainty in the quadrature operators is then given by

$$\begin{aligned} \left\langle(\Delta\hat{q})^2\right\rangle &= \frac{1}{2}+2x^2\left[\frac{1}{(1+e^{-2x^2}\cos\chi)}\right] \\ \left\langle(\Delta\hat{p})^2\right\rangle &= \frac{1}{2}-2x^2\left[\frac{e^{-2x^2}\cos\chi+e^{-4x^2}}{(1+e^{-2x^2}\cos\chi)^2}\right] \quad . \end{aligned} \tag{2.29}$$

We now look into these set of expressions in more detail. The mean value of the annihilation operator, as we have seen earlier, gives an estimate of the center of the distribution of the state, in the q-p phase space. The Q function we have plotted uses the real and imaginary parts of its argument. The q-p phase space is got from

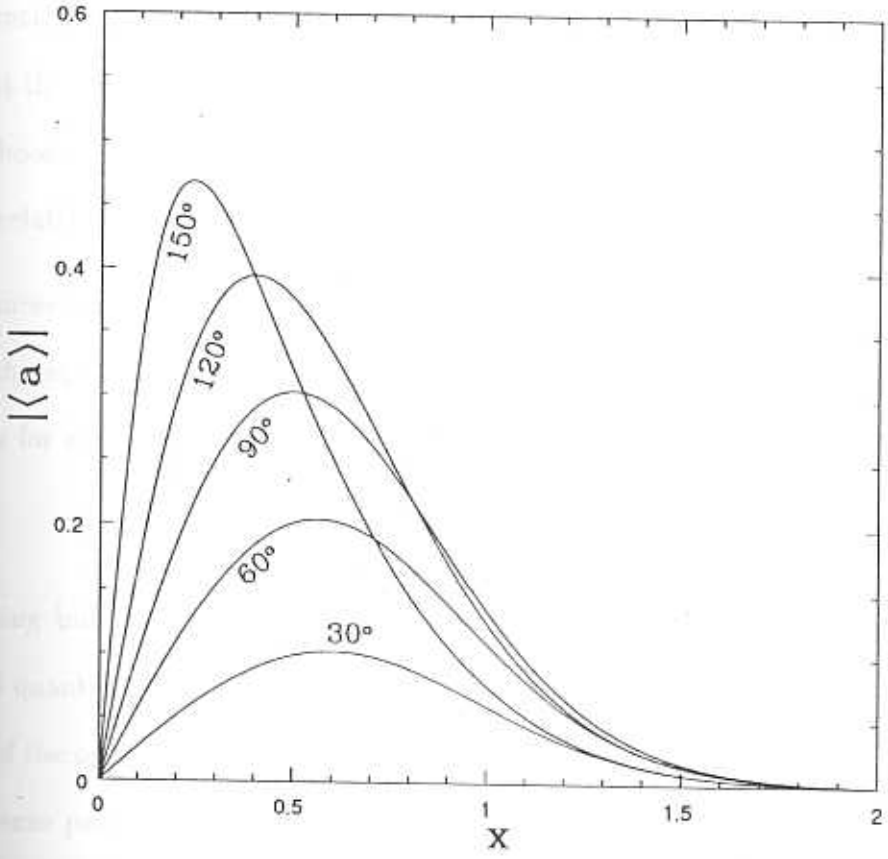

Fig. 2.7. Plot of the magnitude of the mean value of the annihilation operator with respect to the half-separation x for various values of the relative phase χ indicated in the figure. Note that for $\chi = 0$ and $\chi = \pi$ the mean value is zero for any half-separation x.

this by scaling each point by a factor of $\sqrt{2}$ [See Eq. (2.25)]. It is obvious from the Q function plots [Fig. (2.6)] and the equation for the mean value of the annihilation operator [First equation of Eq. (2.27)] that the center of the distribution moves

along the imaginary axis. Note that for $\chi = 0, \pi$ the mean $\langle \hat{a} \rangle$ is zero and the center coincides with the origin of phase space. For large values of x, the maximum of $\langle \hat{a} \rangle$ is at $\chi = \pi/2$, whereas when $\chi = \pi$, even though both the numerator and the denominator tends to zero, the limiting value of $\langle \hat{a} \rangle$ is zero. In Fig. (2.7), we have plotted the magnitude of the mean of the annihilation operator as a function of the half-separation x, for various values of the relative phase χ. It can be seen in the figure that the above arguments are substantiated. For the values of half-separation that we choose to plot Fig. (2.6) ($x = 0.7$), the shift of the center of the distribution with the relative phase can be correlated with this figure.

The uncertainties in the quadrature operators $\hat{q}$ and $\hat{p}$ can be better studied through the squeeze parameter introduced in Chapter 1. The m th order squeeze parameter for any operator $\hat{A}$ is defined [235, 236] for any quantum state $|\psi\rangle$ as

$$S_{\hat{A}}^{(m)} = \frac{\left\langle (\Delta \hat{A})^m \right\rangle_{|\psi\rangle}}{\left\langle (\Delta \hat{A})^m \right\rangle_{|\mathrm{coh}\rangle}} - 1 \quad . \tag{2.30}$$

It is nothing but the difference of the m th order variance of the operator in the concerned quantum state and in the coherent state, normalized with the m th order variance of the operator in the coherent state. Hence, for a coherent state, the m th order squeeze parameter of any operator is zero, and it serves as a reference. If the squeeze parameter takes negative values then the operator and the observable it represents has a squeezed noise in that state, compared to the coherent state. We now write the 2nd order squeeze parameter for the quadrature operators $\hat{q}$ and $\hat{p}$. These are given by

$$\begin{aligned} S_{\hat{q}}^{(2)} &= \frac{4x^2}{1 + e^{-2x^2} \cos\chi} \\ S_{\hat{p}}^{(2)} &= -\frac{x^2 e^{-2x^2} (\cos\chi + e^{-2x^2})}{(1 + e^{-2x^2} \cos\chi)^2} \quad . \end{aligned} \tag{2.31}$$

It can be immediately seen that the 2nd order squeeze parameter for the quadrature operator $\hat{q}$ is always positive. Hence its noise is greater than that of the coherent state irrespective of the half-separation and the relative phase. On the other hand, there are regions of the half-separation and the relative phase where the 2nd order squeeze parameter of the p-quadrature operator $\hat{p}$ becomes negative. This implies that in those regions of the parameter space the superposition state shows squeezing of noise for this operator. It should be noted that the line joining the component states of the superposition is along the q-quadrature and the noise along this direction in phase space is always greater than the coherent state. On the other hand the noise along the perpendicular direction to the line joining the component states, which in this case is the p-quadrature, is squeezed at least in some regimes of the parameter space.

In Fig. (2.8), a plot of the 2nd order squeeze parameter $S_{\hat{p}}^{(2)}$ Vs. the half-separation is given for various relative phase values for the canonical form of the superposition of two coherent states. It can be seen that the maximum squeezing occurs when the relative phase is zero. Note that [Fig. (2.6)] at this value of relative phase, the Q function is not curved and has its major axis along the q-quadrature. As the relative phase is increased from 0 to π, we see that the noise in this quadrature increases. For values of relative phase χ not equal to π there is a region of small half-separation where there is some squeezing, as can be seen from the figure. This is so because, even though the presence of relative phase makes its distribution curved, for very small half-separation x, the distribution itself is quite compact and doesn't spread much along the p direction in phase space. To end this discussion we will also look at the 4th order squeeze parameter for this superposition state.

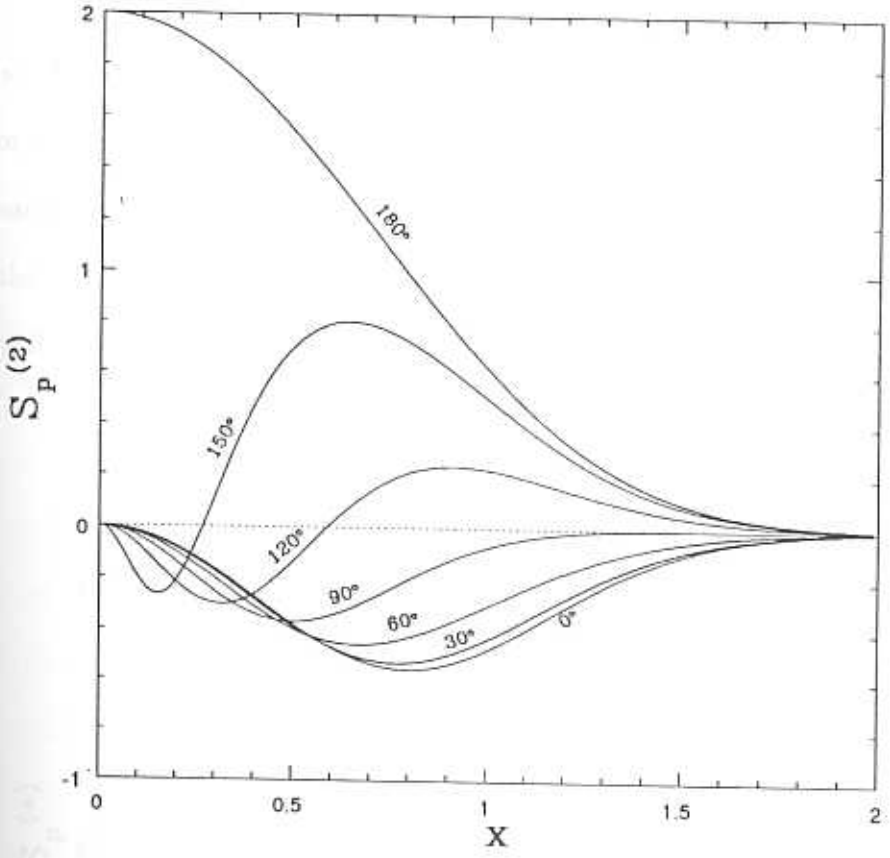

Fig. 2.8. Plot of the second order squeeze parameter $S_{\hat{p}}^{(2)}$ for the $\hat{p}$ quadrature operator Vs. the half-separation x for different values of the relative phase χ indicated in the figure.

We give here the 4th order squeeze parameters of the quadrature operators for completeness :

$$
\begin{aligned}
S_{\hat{p}}^{(4)} &= \frac{16x^4e^{-2x^2}\cos\chi - 24x^2e^{-2x^2}\cos\chi}{3(1+e^{-2x^2}\cos\chi)} \\
&+ \frac{8x^2e^{-4x^2}\sin^2\chi\left[1+8x^2+(1-4x^2)e^{-2x^2}\cos\chi\right]}{3(1+e^{-2x^2}\cos\chi)^3} \\
&- \frac{48x^4e^{-8x^2}\sin^4\chi}{3(1+e^{-2x^2}\cos\chi)^4}
\end{aligned}
$$

$$S_{\widehat{q}}^{(4)} = \frac{16x^2 + 24x^2}{3(1 + e^{-2x^2}\cos\chi)} \quad . \tag{2.32}$$

It can be seen that the 4th order squeeze parameter of the $\widehat{q}$ quadrature operator is positive for all values of half-separation x, and relative phase χ. This is so because, the component states of the superposition are along the q axis of the phase space. Not only the 4th order, but any higher order squeeze parameter of the $\widehat{q}$ quadrature operator will not be squeezed because of this. On the other hand, there may be

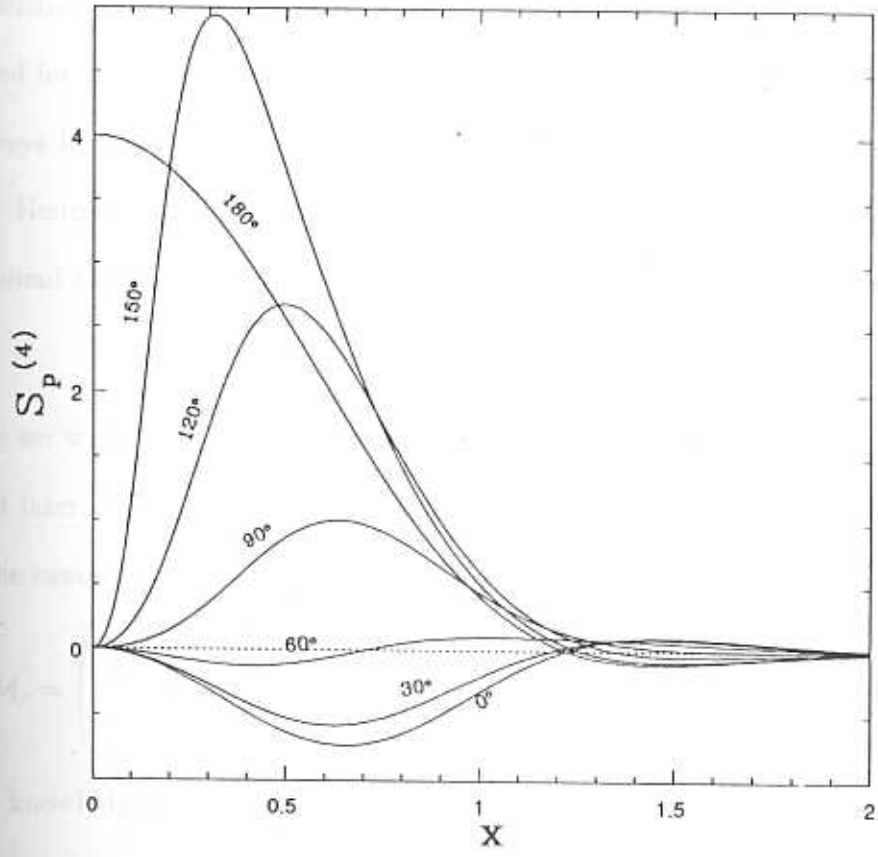

Fig. 2.9. Plot of the fourth order squeeze parameter $S_{\widehat{p}}^{(4)}$ for the $\widehat{p}$ quadrature operator Vs. the half-separation x for different values of the relative phase χ indicated in the figure.

a range of values of half-separation x and relative phase χ for which the 4th order

squeeze parameter for the $\widehat{p}$ quadrature operator is squeezed.

In Fig. (2.9), we plot the fourth order squeeze parameter for the $\widehat{p}$ quadrature operator against the half-separation x, for various values of the relative phase χ. It can be seen from the figure that there are regions of the half-separation x above or below which the noise in the p quadrature is squeezed, except when $\chi = \pi/2$. Again the relative phase $\chi = 0$ is ideal for quadrature squeezing even at this higher order (See [244]). One can show that for all even orders the p quadrature, which is perpendicular to the line joining the component states of the superposition will be squeezed for some values of half-separation x and some relative phase χ. Also, it will always be the $\chi = 0$ which will be the ideal relative phase for quadrature squeezing. Hence one can summarize that quadrature squeezing is maximum when the component states are in-phase with each other. We will be using this fact later on.

Finally we wish to write the noise matrix of the canonical form, since we will be using it later. Since the anticommutator $\{\Delta\widehat{q}, \Delta\widehat{p}\}$ has a vanishing expectation value in the canonical state, one can write the entire noise matrix as

$$\mathcal{M}_c = \begin{pmatrix} \frac{1}{2} + \left[\frac{2x^2}{(1+e^{-2x^2}\cos\chi)}\right] & O \\ O & \frac{1}{2} - \left[\frac{2x^2(e^{-2x^2}\cos\chi + e^{-4x^2})}{(1+e^{-2x^2}\cos\chi)^2}\right] \end{pmatrix} . \tag{2.33}$$

With this knowledge of the canonical form of the superposition, we will now turn to the general superposition of two coherent states.

2.5 General superposition of two coherent states

The general superposition of two coherent states, as mentioned earlier, is got from the canonical form by

$$|\psi_g\rangle = \widehat{D}(\alpha)\hat{R}(\tau)\,|\psi_c\rangle \quad , \tag{2.34}$$

where

$$\begin{aligned} |\psi_c\rangle &= \mathcal{N}\left(|-x\rangle + e^{ix}\,|x\rangle\right) \quad , \\ \widehat{D}(\alpha) &= e^{\alpha\hat{a}^\dagger - \alpha^*\hat{a}} \quad , \\ \hat{R}(\tau) &= e^{i\tau\hat{a}^\dagger\hat{a}} \quad . \end{aligned} \tag{2.35}$$

The properties of this general superposition can be easily calculated from those of the canonical form.

We will first calculate the Q function of the general superposition of two coherent states. It is given by

$$\begin{aligned} Q_g(\beta) &= \frac{1}{\pi}\,|\langle\beta\,|\psi_g\rangle|^2 = \frac{1}{\pi}\left|\langle\beta|\,\widehat{D}(\alpha)\,\hat{R}(\tau)\,|\psi_c\rangle\right|^2 \\ &= \frac{1}{\pi}\left|e^{(\alpha\beta^*-\alpha^*\beta)/2}\,\langle\beta-\alpha|\,\hat{R}(\tau)\,|\psi_c\rangle\right|^2 \\ &= Q_c\left((\beta-\alpha)e^{-i\tau}\right) \quad , \end{aligned} \tag{2.36}$$

where Q_c is the Q function of the canonical form, given in Eq. (2.23). Thus, the Q function of a general superposition is obtained from the Q function of the canonical form by a rigid translation α and rotation τ in phase space. Since we have already computed the Q function of the canonical form, we can get the Q function of any general superposition of two coherent states. We now wish to calculate the

noise properties of the general superposition of two coherent states from the noise properties of the canonical form.

It has been pointed out in Chapter 1 that the displacement moves only the mean of the distribution without affecting the shape. It means that only the first moment of the distribution is changed, while all the higher moments remain intact under the operation of the displacement operator. Hence the noise of the quantum state is unaffected by the action of the displacement. Hence we have to bother only about the rotation operator. This can be easily figured out, since the rotation operator rigidly rotates the distribution as a whole in phase space. Hence one simply goes to a rotated phase space after the action of the rotation operator. So the noise matrix of the general superposition of coherent state can be written as,

$$\mathcal{M}_g = \mathcal{R}^T(\tau)\mathcal{M}_c\mathcal{R}(\tau) \quad , \tag{2.37}$$

where $\mathcal{M}_c$ is the noise matrix of the canonical state as given in Eq. (2.33) and where $\mathcal{R}(\tau)$ is the corresponding rotation matrix given by

$$\mathcal{R}(\tau) = \begin{pmatrix} \cos\tau & \sin\tau \\ -\sin\tau & \cos\tau \end{pmatrix} \quad . \tag{2.38}$$

Hence one can easily calculate the noise matrix and the noise properties of the general superposition. The noise matrix $\mathcal{M}$ is defined modulo a displacement, which makes this choice of the canonical form rather good.

To illustrate the above method, let us consider the state that was introduced earlier by Schleich [250]. We will calculate the noise properties of this state using the noise matrix of the canonical form. It can be noticed in Fig. (2.10) that the

component states of this superposition are $\left|\alpha e^{i\varphi/2}\right\rangle$ and $\left|\alpha e^{-i\varphi/2}\right\rangle$, which are superposed without any other 'additional' relative phase. Let us denote this superposition as

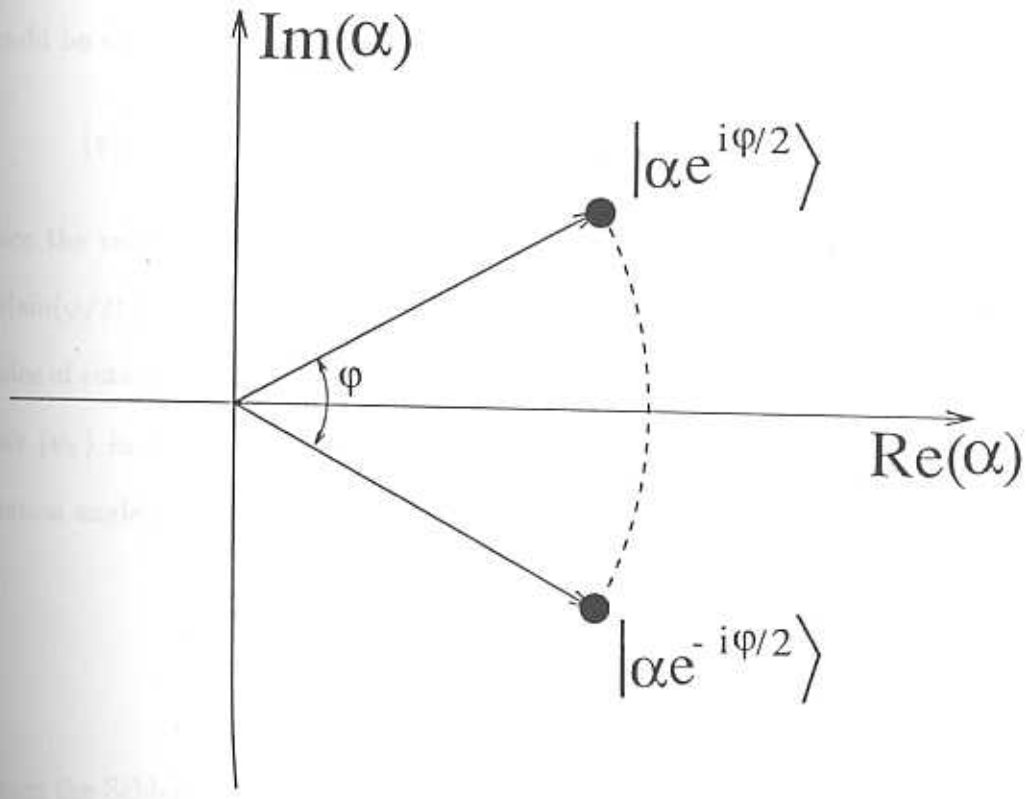

Fig. 2.10. The superposition of coherent states introduced by Schleich [250]. The two coherent states subtends an angle φ in the origin and are placed symmetrically about the q axis of phase space.

$$|\psi_s\rangle = \mathcal{N}\left(\left|\alpha e^{i\varphi/2}\right\rangle + \left|\alpha e^{-i\varphi/2}\right\rangle\right) \quad . \tag{2.39}$$

The relative phase between the component states is given by

$$\chi = \mathrm{Arg}[\left\langle \alpha e^{-i\varphi/2} \right| \left.\alpha e^{\varphi/2}\right\rangle] = |\alpha|^2 \sin(\varphi) \quad , \tag{2.40}$$

which is actually the relative phase of $\left|\alpha e^{i\varphi/2}\right\rangle$ with respect to $\left|\alpha e^{-i\varphi/2}\right\rangle$. The

half-separation between the states is given by

$$x = |\alpha| \sin(\varphi/2) \quad , \tag{2.41}$$

as can be figured out from Fig. (2.10). Hence the basic or the canonical form that should be chosen for this state is

$$|\psi_b\rangle = \mathcal{N} \left(|-|\alpha| \sin(\varphi/2)\rangle + e^{i|\alpha|^2 \sin(\varphi)} \, ||\alpha| \sin(\varphi/2)\rangle \right) \quad . \tag{2.42}$$

Since the relative phase in the exponential comes along with the coherent state $||\alpha|\sin(\varphi/2)\rangle$, this state should go over to the coherent state $\left|\alpha e^{i\varphi/2}\right\rangle$ with a proper choice of rotation angle τ and displacement. Since the rotation operator rotates this state $|\psi_b\rangle$ in the anti clock-wise direction [Eq. (2.17)], the proper choices of the rotation angle and the displacement are

$$\begin{aligned} \tau &= \pi/2 \quad , \\ \xi &= |\alpha| \cos(\varphi/2) \quad . \end{aligned} \tag{2.43}$$

Hence the Schleich state is given by

$$|\psi_s\rangle = \widehat{D}\left[|\alpha| \cos(\varphi/2)\right] \hat{R}(\pi/2) \, |\psi_b\rangle \quad . \tag{2.44}$$

Since the displacement doesn't affect the noise matrix the noise matrix of the Schleich state can be immediately written down as

$$\mathcal{M}_s = \begin{pmatrix} 0 & -1 \\ 1 & 0 \end{pmatrix} \mathcal{M}_b \begin{pmatrix} 0 & 1 \\ -1 & 0 \end{pmatrix} \quad . \tag{2.45}$$

The action of this rotation is to switch the diagonal elements of the noise matrix of the canonical form in Eq. (2.33), which means the noise in the q and p quadrature

are exchanged. Hence for the Schleich state we have

$$\begin{aligned}
\left\langle (\Delta\widehat{q})^2 \right\rangle &= \frac{1}{2} - 2x^2 \left[\frac{e^{-2x^2}\cos\chi + e^{-4x^2}}{(1+e^{-2x^2}\cos\chi)^2} \right] \\
\left\langle (\Delta\widehat{p})^2 \right\rangle &= \frac{1}{2} + 2x^2 \left[\frac{1}{(1+e^{-2x^2}\cos\chi)} \right] \\
x &= |\alpha|\sin(\varphi/2) \\
\chi &= |\alpha|^2 \sin(\varphi)
\end{aligned} \tag{2.46}$$

The effectiveness of the above method should be compared with the straightforward method used in Ref. [250].

We have elucidated in this chapter the concept of relative phase between two quantum states. Starting from Pancharatnam's phase, we defined the relative phase and elaborated it using the coherent states as an example. We then introduced the relative phase in two coherent superposition, which enabled us to choose a canonical form from which one can get any general two coherent superposition by 'trivial' actions of displacement and rotation. We then studied the canonical form of the superposition and had illustrated the effect of relative phase in the Q function. The noise properties of the canonical form are then studied and the various kinds of squeezing shown by the two coherent superposition for different values of the relative phase are described. Finally, we considered the quantum state introduced by Schleich, and illustrated the ease with which one could get this superposition's noise properties from those of the canonical form, as an example. Having

seen that the relative phase produces a curved Q function, we will study the relationship between this curved Q function and the photon number noise properties of a quantum state in the next chapter.

Chapter 3

Amplitude squeezing and superposition of coherent states

In this chapter the relationship between amplitude squeezing and relative phase in the superposition of coherent states is analyzed. First, the amplitude squeezing of the canonical form of the superposition of two coherent states introduced in the last chapter is studied in detail. We then study the change in the amplitude squeezing as this state is displaced in phase space. This leads to an understanding of the relationship between the positioning of the state in phase space and amplitude squeezing. The real role the relative phase plays in producing amplitude squeezing is then studied by fixing a superposition of two coherent states at a given distance from the origin of phase space and varying the relative phase between the component states.

3.1 Amplitude squeezing in superposition of two coherent states

Amplitude squeezing, as we have already seen in Chapter 1, is characterized by the photon number uncertainty of a quantum state being smaller than its mean photon number. In this section, we will concentrate on the photon number properties of the canonical form of superposition of two coherent states introduced in the last chapter. We have studied the (quadrature) noise properties of the canonical form in

general, but we will now concentrate on the noise in photon number. More attention will be paid to describe the way in which the relative phase changes this noise.

The mean photon number of the canonical form

$$|\psi_c\rangle = \mathcal{N}\left(|-x\rangle + e^{i\chi}|x\rangle\right) \quad , \tag{3.1}$$

is given by

$$\langle\hat{n}\rangle = \left\langle\hat{a}^\dagger\hat{a}\right\rangle = x^2\left(\frac{1-e^{-2x^2}\cos\chi}{1+e^{-2x^2}\cos\chi}\right) \quad . \tag{3.2}$$

From this expression it is obvious that when $\chi = \pi/2$, the mean photon number of the superposition is the same as that of a coherent state. Indeed with this special value of χ the entire photon number distribution of this non-classical state is identical to that of a coherent state. For any other relative phase, the superposition is still seen to behave like a coherent state for large half-separation x. However for a small half-separation the mean is greater than the coherent state value when $\pi/2 < \chi \leq \pi$, and it is smaller than the coherent state value for $0 \leq \chi < \pi/2$.

The expectation value of $\left\langle\hat{a}^{\dagger 2}\hat{a}^2\right\rangle$ for the canonical form of the two coherent state superposition is calculated to be

$$\left\langle\hat{a}^{\dagger 2}\hat{a}^2\right\rangle = x^4 \quad , \tag{3.3}$$

which is independent of the relative phase χ. The photon number uncertainty for the superposition is given by

$$\begin{aligned}\left\langle(\Delta\hat{n})^2\right\rangle &= \left\langle\hat{n}^2\right\rangle - \left\langle\hat{n}\right\rangle^2 \\ &= \left\langle\hat{a}^{\dagger 2}\hat{a}^2\right\rangle + \left\langle\hat{a}^\dagger\hat{a}\right\rangle - \left\langle\hat{a}^\dagger\hat{a}\right\rangle^2 \\ &= \frac{4x^4e^{-2x^2}\cos\chi + x^2(1-e^{-4x^2}\cos^2\chi)}{(1+e^{-2x^2}\cos\chi)^2} \quad .\end{aligned} \tag{3.4}$$

It is usual practice to consider the normalized photon number uncertainty, which is called in the literature as the *Fano factor*. This normalization is with respect to the mean photon number and hence the Fano factor is given by

$$f_n = \frac{\langle (\Delta\hat{n})^2 \rangle}{\langle \hat{n} \rangle}, \tag{3.5}$$

and which when calculated for the canonical form gives

$$f_n = 1 + \frac{4x^2 e^{-2x^2} \cos\chi}{1 - e^{-4x^2} \cos^2\chi} \quad . \tag{3.6}$$

We have seen earlier that the Fano factor takes the value of one for a coherent state and zero for a Fock state. Hence the Fano factor is bounded from below by the value of zero. One way of characterizing amplitude squeezing is to say that the Fano factor has a value in the range $0 \leq f_n < 1$. A poissonian photon statistics is associated with the Fano factor value of one. The photon statistics is super-poissonian if $f_n > 1$ and sub-poissonian if $f_n < 1$. It is seen from Eq. (3.6), that in the range $0 \leq \chi < \pi/2$, the Fano factor $f_n > 1$, and hence the superposition state is super-poissonian. It is not amplitude squeezed in this range, and its photon number noise is greater than that of a coherent state. On the other hand, when $\chi = \pi/2$, we have $f_n = 1$. This means that the superposition state at this value of the relative phase is the same as that of a coherent state as far as its photon number noise is concerned. This state is called the Yurke-Stoler state [241] in the literature, and we have earlier seen that this state can be produced in a Kerr medium. For χ values in the range $\pi/2 < \chi \leq \pi$, we see that $f_n < 1$, and hence the canonical form of the superposition of two coherent states is amplitude squeezed for this range of values of χ.

These results can be understood in a simple way. If one looks at the mean photon number, it is obvious that as a function of χ the mean increases as χ increases from 0 to π. When $0 \leq \chi < \pi/2$, the mean is smaller than in a coherent state. At $\chi = \pi/2$, the mean photon number of the superposition equals that of the coherent state. In the range $\pi/2 < \chi \leq \pi$, the mean is larger than in a coherent state. In fact, the mean photon number of the superposition is largest when $\chi = \pi$. On the other hand, the photon number uncertainty also keeps decreasing slightly as χ increases from 0 to π when the half-separation is small. This change comes about by the x^4 term in the numerator of Eq. (3.4). But this is more or less compensated by the decreasing value of the denominator and hence the decrease in the photon number uncertainty is quite small. Hence we can say that the Fano factor decreases in a overall way for small x with χ is in the range $\pi/2 < \chi \leq \pi$, mainly due to the increase of the mean.

In Fig. (3.1), we plot the mean photon number as a function of the half-separation for various values of the relative phase. Note that we have normalized the mean photon number by dividing it with x^2, which is the mean of the coherent state. Hence this normalized mean, when it takes the value of one signifies that the state concerned behaves like a coherent state as far as the mean is concerned. It could be seen in Fig. (3.1) that when the relative phase is $\chi = \pi/2$, the mean for all values of half-separation is one. As we have said earlier, the mean photon number for χ values in the range $0 \leq \chi < \pi/2$ is less than the coherent state value for small half-separations, as can be seen in the figure. For values of the relative phase in the range $\pi/2 < \chi \leq \pi$, again we see that the mean photon number is larger than the coherent state value. The value of mean for this range of relative phase when

the half-separation approaches zero is quite large to be included in the figure. But they are all finite except when $\chi = \pi$, which corresponds to the odd-coherent state [243]. We will later return to this quite exceptional behavior of the photon number properties of the superposition state for the relative phase $\chi = \pi$. But one should note the rapid increase of the mean photon number for the relative phase in the

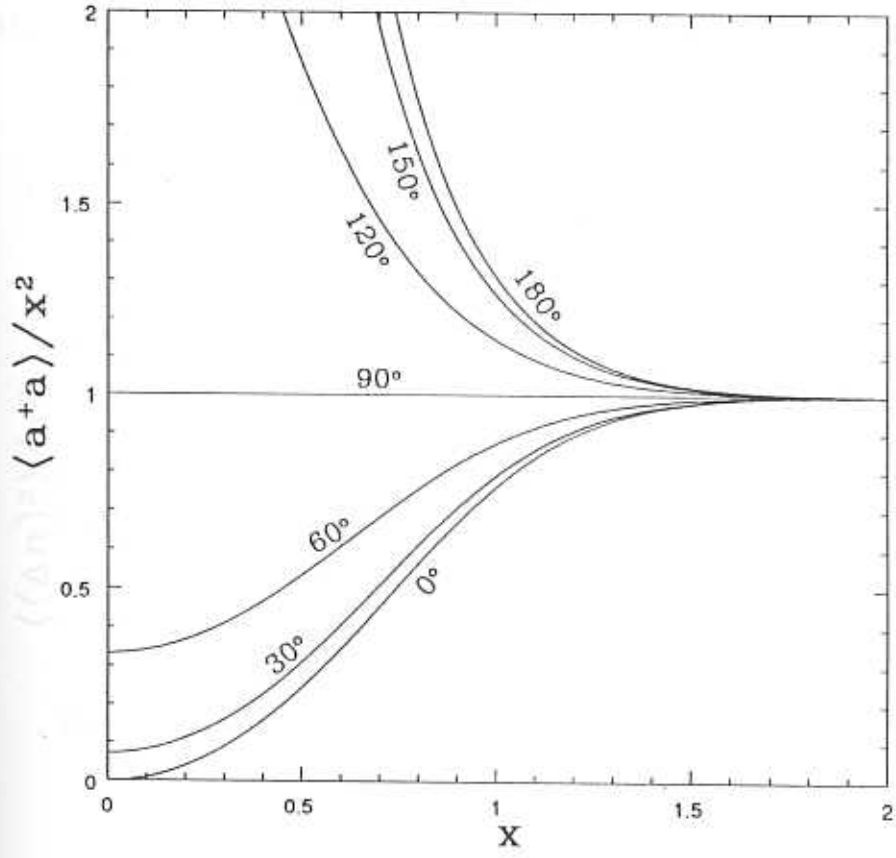

Fig. 3.1. Plot of the mean photon number of the superposition state as a function of half-separation x for different values of relative phase indicated in the figure. The mean photon number plotted here is normalized by dividing it by x^2.

range $\pi/2 < \chi \leq \pi$, a point to which we will be returning.

In Fig. (3.2), we have plotted the photon number uncertainty of the superposition

state as a function of half-separation for different values of the relative phase. Again this photon number uncertainty is normalized by x^2, so that it remains one for a coherent state. This is done to aid comparison with the coherent state case. When the half-separation $x = 0$, the photon number uncertainty equals its mean for all values of the relative phase except when $\chi = \pi$. Moreover, this normalized photon number uncertainty, for a range of values of the half-separation x and for those states with relative phase in the range $0 \leq \chi < \pi/2$, becomes greater than one and

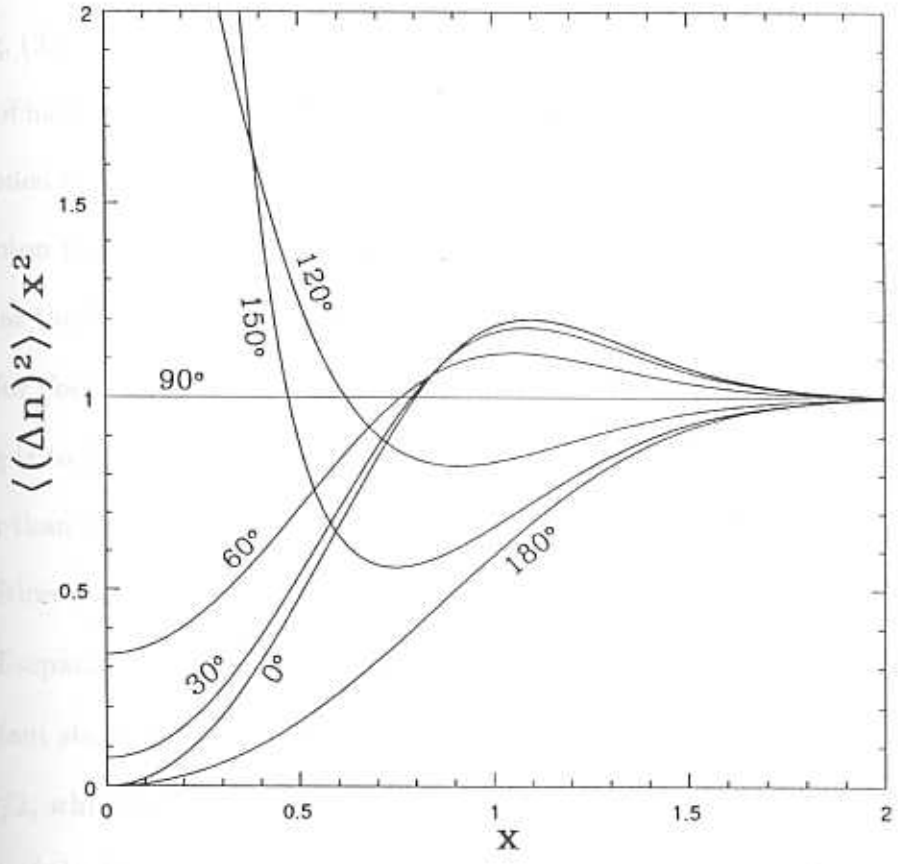

Fig. 3.2. Plot of the photon number uncertainty of the superposition state as a function of half-separation x for different values of relative phase indicated in the figure. The photon number uncertainty plotted here is normalized by dividing it by x^2.

hence has a larger uncertainty than the coherent state. This implies that they will show super-poissonian statistics. On the other hand for those states with relative phase in the range $\pi/2 < /\chi \leq \pi$, there is a range of half-separation where the uncertainty is smaller than the coherent state. These also have the mean photon number greater than the coherent state value in the same range of x, and hence are amplitude squeezed. One can expect that their photon number distribution will be sub-poissonian in this range. Note that the photon number uncertainty goes to zero when the relative phase is π, whereas the mean blows up in this limit.

In Fig. (3.3), the plot of the Fano factor for the superposition state is given as a function of half-separation, for different values of the relative phase. The Fano factor as mentioned earlier is defined as the ratio of the photon number uncertainty to the mean photon number of the state under consideration. It had also been mentioned earlier that the Fano factor for coherent states takes the value one, and on the other extreme for Fock states it takes the value zero. Hence one way of defining amplitude squeezing is to demand that the Fano factor of the quantum state has a value that is smaller than one. It can be seen from the figure that for large half-separations the superposition behaves like a coherent state. This can be readily understood since at large half-separations there is very little interference in phase space [253, 254], and the resultant state looks more like a statistical mixture of coherent states. The case of $\chi = \pi/2$, which is the Yurke-Stoler state [241], behaves like a coherent state for all values of the half-separation. One could say that this is rather accidental, since we have seen that this state has a curved quasi-probability distribution and may show amplitude squeezing when displaced to a proper position in phase space [242]. It can also be seen that for the values of relative phase in the range $\pi/2 < \chi \leq \pi$,

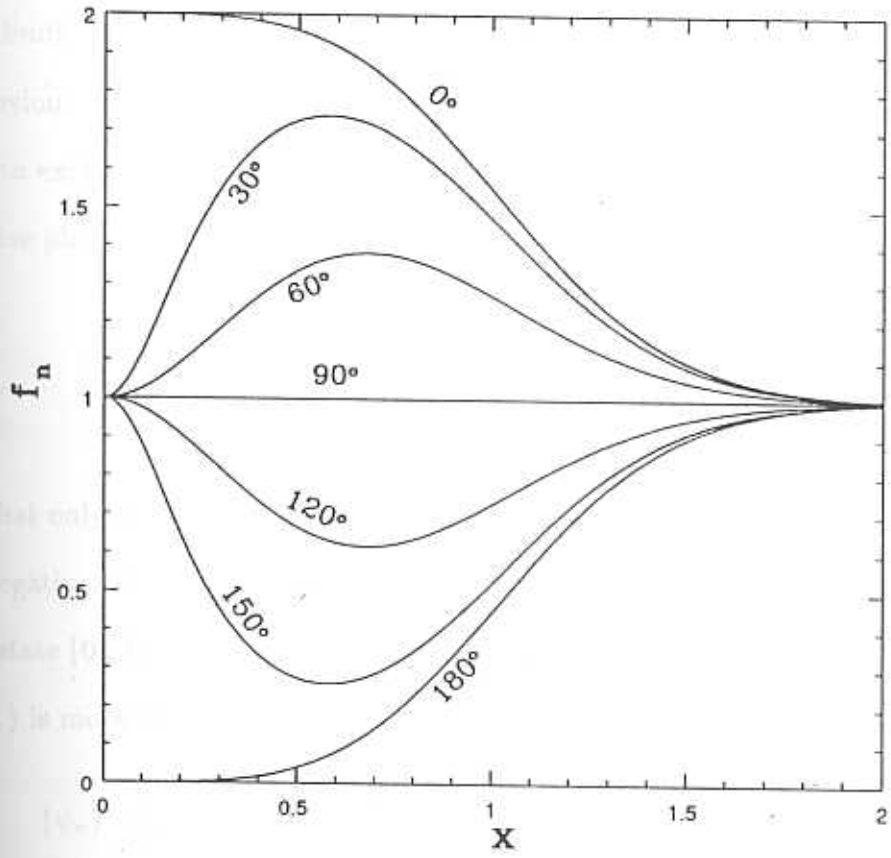

Fig. 3.3. Plot of the Fano factor of the superposition state as a function of half-separation x for different values of relative phase indicated in the figure.

the superposition state has a Fano factor less than one for small x, and hence is amplitude squeezed in this range.

Of particular interest is the quantum state when the relative phase is $\chi = \pi$. This state is well known in the literature as the odd coherent state [243]. When one considers such a quantum state and takes the limit $x \to 0$, it can be seen that the Fano factor goes to zero. But on the other hand, at the quantum state level, what one gets is superposition of two vacua with a phase difference π. But we do know that the properties of a state superposed with itself are the same. The above

superposition is not even the vacuum but a null vector in the Hilbert space. But still, the limiting process seems to indicate that it goes over to Fock state $|1\rangle$! The not so obvious error is the inclusion of the point $x = 0$. Before ending this section, we wish to explore this limit in a more careful way. The superposition state when the relative phase is π, when written in terms of the Fock states, looks as

$$\begin{aligned} |\psi_o\rangle &= \mathcal{N}\left(|-x\rangle - |x\rangle\right) \\ &= \frac{e^{-x^2/2}}{\sqrt{1-e^{-2x^2}}} \sum_{n=0}^{\infty} -\frac{x^{2n+1}\sqrt{2}}{\sqrt{(2n+1)!}} |2n+1\rangle \quad . \end{aligned} \tag{3.7}$$

We see that only the odd Fock states are involved since the even ones get cancelled by the negative sign before the second ket. Note that this means that there is no vacuum state $|0\rangle$ in the expansion. Hence as one takes the limit $x \to 0$ $(x \neq 0)$ the state $|\psi_o\rangle$ is more like the Fock state $|1\rangle$, since

$$\begin{aligned} |\psi_o\rangle &\xrightarrow[x\to 0]{\text{lm}} \frac{e^{-x^2/2}}{x\sqrt{2}\sqrt{1-2x^2+\cdots}} \sum_{n=0}^{\infty} -\frac{x^{2n+1}\sqrt{2}}{\sqrt{(2n+1)!}} |2n+1\rangle \\ &\xrightarrow[x\to 0]{\text{lm}} |1\rangle_{\text{Fock}} \quad . \end{aligned} \tag{3.8}$$

All other terms drop out as they contain non-vanishing powers of x in the numerator. A physical point to note is that two coherent states with vanishing amplitudes when superposed out of phase will give rise to a Fock state $|1\rangle$.

3.2 Effect of displacement on amplitude squeezing

In this section, we wish to study the effect of displacement on amplitude squeezing. The canonical state is displaced in phase space by applying a displacement operator [62, 63] to it. The effect of direction and magnitude of displacement on amplitude

squeezing is then studied. The displaced state can be written as

$$|\psi_d\rangle = \widehat{D}(\xi)\,|\psi_c\rangle \quad , \tag{3.9}$$

where the canonical form of the superposition of two coherent states is given by

$$|\psi_c\rangle = \mathcal{N}\left(|-x\rangle + e^{i\chi}\,|x\rangle\right) \quad . \tag{3.10}$$

The displacement operator acting on another coherent state can be found by using a simple form [27] of the BCH formula [270, 271, 272, 273, 274, 275], and is given by

$$\begin{aligned} \widehat{D}(\beta)\,|\alpha\rangle &= \widehat{D}(\beta)\widehat{D}(\alpha)\,|O\rangle \\ &= e^{\left[\beta\hat{a}^\dagger - \beta^*\hat{a},\alpha\hat{a}^\dagger - \alpha^*\hat{a}\right]/2}\widehat{D}(\beta+\alpha)\,|O\rangle \\ &= e^{(\beta\alpha^* - \beta^*\alpha)/2}\,|\beta+\alpha\rangle \quad . \end{aligned} \tag{3.11}$$

Hence the displaced superposition takes the form

$$|\psi_d\rangle = \mathcal{N}\left(|\xi - x\rangle + e^{i[\chi + 2xk\sin(\delta)]}\,|\xi + x\rangle\right) \quad , \tag{3.12}$$

where we have parameterized ξ as $\xi = ke^{i\delta}$ and have neglected the overall phase. It should be observed that the relative phase of $e^{i[\chi+2xk\sin(\delta)]}\,|\xi+x\rangle$ with respect to $|\xi - x\rangle$ is still χ, as can be checked easily. The displacement operator preserves the relative phase between the states of the superposition by introducing a term in the exponent which exactly cancels the additional relative phase introduced by the displacement.

The mean photon number of the displaced superposition is calculated to be

$$\left\langle \hat{a}^\dagger\hat{a}\right\rangle_d = \frac{k^2 + x^2 + (k^2 - x^2)e^{-2x^2}\cos\chi + 2xke^{-2x^2}\sin\delta\sin\chi}{1 + e^{-2x^2}\cos\chi} \quad . \tag{3.13}$$

Since the photon number uncertainty is given by

$$\begin{aligned}\left\langle (\Delta\hat{n})^2 \right\rangle &= \left\langle (\hat{a}^\dagger\hat{a})^2 \right\rangle - \left\langle \hat{a}^\dagger\hat{a} \right\rangle^2 \\ &= \left\langle \hat{a}^{\dagger 2}\hat{a}^2 \right\rangle + \left\langle \hat{a}^\dagger\hat{a} \right\rangle - \left\langle \hat{a}^\dagger\hat{a} \right\rangle^2 \quad , \end{aligned} \tag{3.14}$$

we need the expectation value $\left\langle \hat{a}^{\dagger 2}\hat{a}^2 \right\rangle$, which is calculated to be

$$\begin{aligned}\left\langle \hat{a}^{\dagger 2}\hat{a}^2 \right\rangle &= \frac{(k^2+x^2)^2 + 4x^2k^2\cos^2\delta + \left[(k^2-x^2)^2 - 4x^2\sin^2\delta\right] e^{-2x^2}\cos\chi}{1+e^{-2x^2}\cos\chi} \\ &\quad + \frac{4xk(k^2-x^2)e^{-2x^2}\sin\chi}{1+e^{-2x^2}\cos\chi} \quad . \end{aligned} \tag{3.15}$$

The Fano factor defined as

$$\begin{aligned} f_n &= \frac{\langle (\Delta\hat{n})^2 \rangle}{\langle \hat{n} \rangle} \\ &= 1 + \frac{\left\langle \hat{a}^{\dagger 2}\hat{a}^2 \right\rangle}{\langle \hat{a}^\dagger\hat{a} \rangle} - \left\langle \hat{a}^\dagger\hat{a} \right\rangle \quad , \end{aligned} \tag{3.16}$$

is calculated for the displaced superposition as

$$\begin{aligned} f_n &= 1 + \left(\frac{\left[x^2 - k^2\cos^2\delta - k^2\sin^2\delta\right]\cos\chi - 2xk\sin\delta\sin\chi - k^2e^{-2x^2}\sin^2\delta}{k^2+x^2+(k^2-x^2)e^{-2x^2}\cos\chi + 2xk(\xi)e^{-2x^2}\sin\delta\sin\chi} \right) \times \\ &\quad \times \left(\frac{4x^2e^{-2x^2}}{(1+e^{-2x^2}\cos\chi)} \right) \quad . \end{aligned} \tag{3.17}$$

We wish to first study the dependence of the Fano factor on the direction of displacement. To this end, we choose an arbitrary magnitude of displacement and plot the variation of Fano factor with the direction of displacement δ, in Fig. (3.4). Here the magnitude of displacement is chosen to be $k = 2.0$. The half-separation of the superposition is $x = 0.7$. Different curves are plotted for superpositions with different relative phases, which are indicated in the figure itself. Since the superposition is made up of coherent states lying along the q-axis of the phase

space, one would expect that the displacement along the perpendicular direction will increase the amplitude squeezing. From Fig. (3.4) we see that this is what happens for all relative phases, and the Fano factor takes its lowest values at $\delta = \pi/2$ and $\delta = 3\pi/2$. When the superposition is symmetric about the q-axis, the minima at

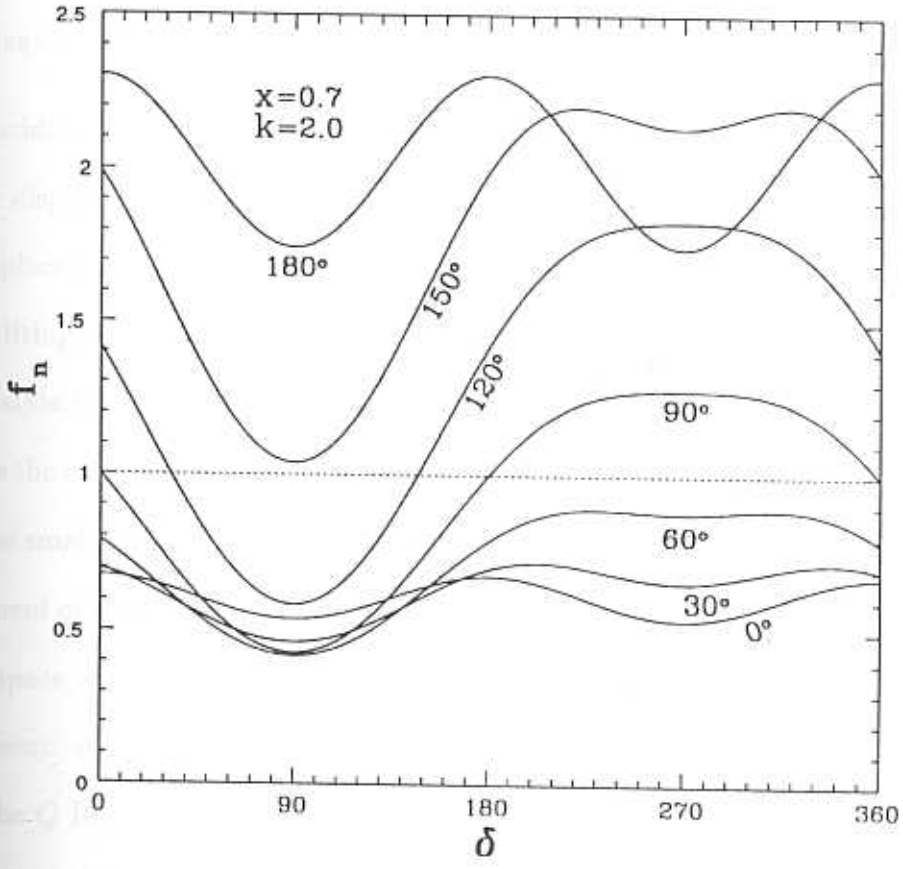

Fig. 3.4. Plot of the Fano factor of the displaced superposition state as a function of the displacement angle δ, where the displacement magnitude is $k = 2.0$. The half-separation of the state is fixed at $x = 0.7$.

these two values of δ are equal, as in the case of the relative phase being equal to 0 or π. But for other values of the relative phase χ there is no reflection symmetry about the q-axis and hence as far as amplitude squeezing is concerned the displacement along the positive p-axis of phase space is more favourable, since the center of

curvature would be towards the origin, and hence the the Q function resembles locally the Q function of the Fock states. It can be seen that when the distribution is slightly curved due to a small relative phase between the superposed states, the Fano factor has a lower value than for the state with zero relative phase and whose distribution is not curved. This can be seen in the figure even for this arbitrarily chosen magnitude of displacement.

To elucidate this further, we plot the Q function of the displaced superposition, when the displacement magnitude is fixed at $k = 4.0$ in Fig. (3.5). The Q function of the displaced state can be obtained from the Q function of the canonical form, by simply shifting the argument. This is so since the displacement operator acts on the coherent state from the left and hence $Q_d(\beta) = Q_c(\beta - \xi)$. Here the contours at the center are the contours of the Q function for the undisplaced state, viz, the canonical state. The small arrow from the origin points to the center of this distribution. The displacement operator simply shifts the center of this distribution to a new position in phase space which is illustrated in the figure by the other arrows representing the displacement. Apart from the canonical state's Q function at the center, we have plotted the Q function of four displaced states with various displacement angles δ indicated in the figure. The magnitude of the displacement as said earlier is fixed at $k = 4.0$ in all the four displaced states. The half-separation between the component states of the superposition is $x = 0.7$ and we have chosen a relative phase $\chi = \pi/2$ to illustrate the point we are trying to make. The dotted circles filling the background are the maxima of the Q functions of different Fock states. It is obvious that the states that are displaced along the q-axis of phase space for $\delta = 0, \pi$ will have more photon number uncertainty since they cut more number of Fock circles for a given

radial distance of the center of the distribution from the origin of phase space. On the other hand, when it is displaced along the p axis for $\delta = \pi/2, 3\pi/2$ it cuts less number of Fock circles. In the case of $\delta = \pi/2$ when it is displaced along the positive p axis the curvature of the distribution locally matches with the curvature of the

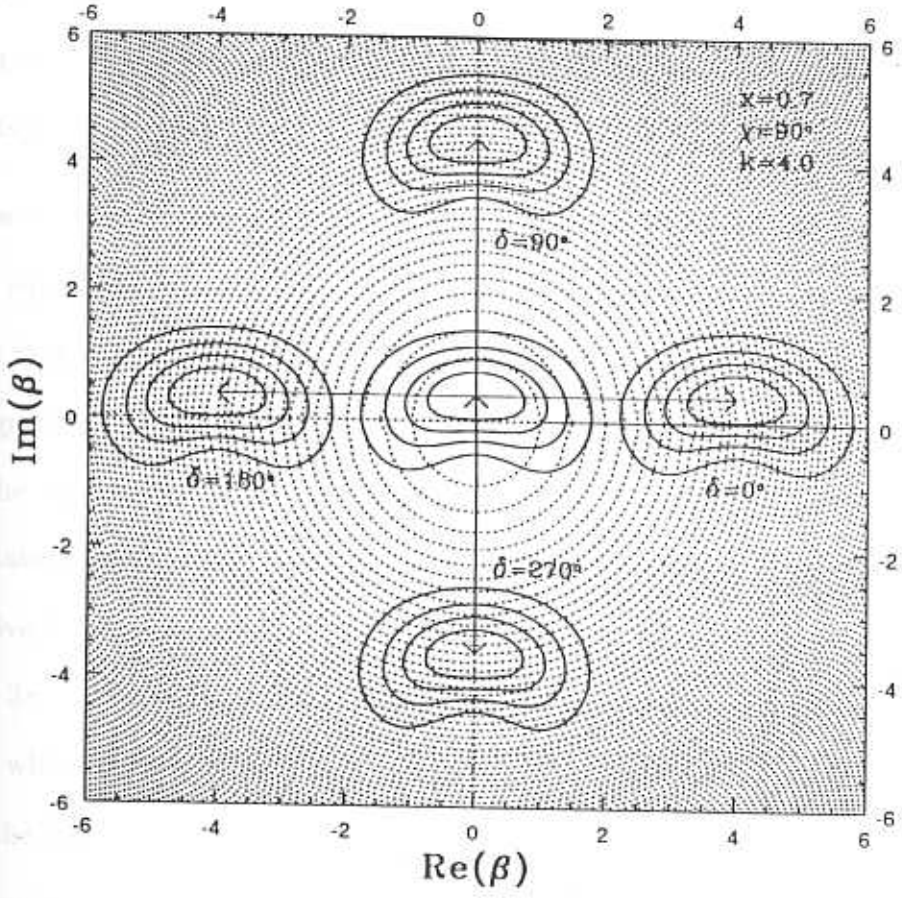

Fig. 3.5. Plot of the Q function of the displaced superposition state, for different displacement angles, when the displacement magnitude is fixed at $k = 4.0$. The arrows indicate the displacement of the center of the distribution. The background is filled with the maxima of different Fock states as dotted circles. The half-separation is fixed at $x = 0.7$ and the relative phase at $\chi = 90°$.

Fock circles, enabling it to cut a lesser number of Fock circles. Hence one can predict that the state which is displaced along the positive p-axis of phase space will have the maximum amplitude squeezing. This prediction is quite justified as one could

see in Fig. (3.4), where the Fano factor goes to a minimum at $\delta = \pi/2$. But as noted earlier, too much curvature of the distribution due to a large relative phase between the superposed states will make the distribution cut more Fock circles and hence can be worse than the case when the relative phase is zero and where there is no curvature in the distribution. Hence, we conclude by observing that the amplitude squeezing goes to a maximum when the distribution is displaced along the direction in which its curvature can locally match those of the Fock circles.

We now turn our attention to the effect of the magnitude of displacement on amplitude squeezing. Since we have seen that $\delta = \pi/2$ is the favoured direction, we will fix δ at this value and plot the variation of the Fano factor as a function of the magnitude of displacement k. In Fig. (3.6) we do this. The half-separation between the superposed states is fixed at $x = 0.7$. The different curves are for different states with different relative phases, which are indicated in the figure itself. The negative k values correspond to the displacement in the opposite direction, *i.e.* along $\delta = 3\pi/2$. Since both the states with the relative phases $\chi = 0, \pi$, have a line about which there is a reflection symmetry, the curves corresponding to these values of the relative phase have the same structure for $k < 0$ or $k > 0$. Since the distribution of the superposition state when $\chi = 0$ is a bivariate Gaussian, as one displaces this state further from the origin in phase space, the more it locally matches the curvature of the Fock circles, as can be anticipated since a line can be pictured as a circle with an infinite radius. But at increasing distances from the origin the density of Fock circles increases and hence the Fano factor will saturate at some value, as can be seen in the figure. On the other hand, if there is a curvature in the distribution, then there is an *ideal* value of the magnitude of displacement at

which the Fano factor will be minimum. For $\chi = \pi$ this ideal value is zero. With decreasing relative phase, this ideal value increases and it becomes infinite for $\chi = 0$ for which the distribution is not curved. It can also be seen that the more curved the distribution is, the more sharper is its behavior with respect to k, in the sense

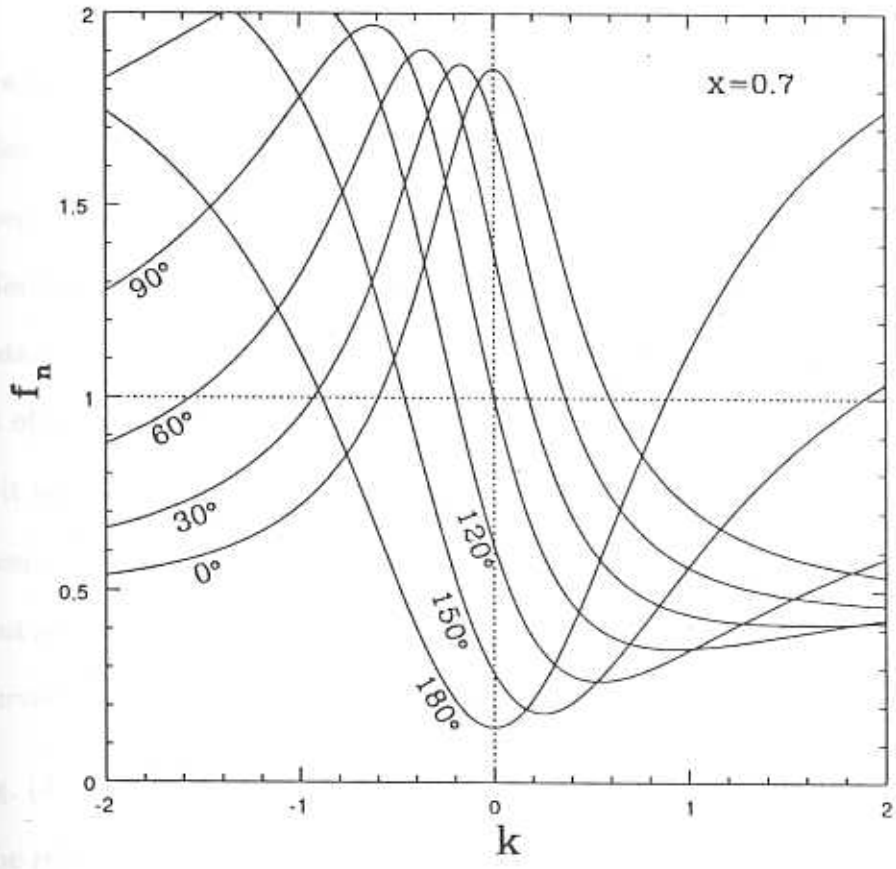

Fig. 3.6. Plot of the Fano factor of the displaced superposition state as a function of the magnitude of displacement k for different values of the relative phase indicated in the figure. The half-separation is fixed at $x = 0.7$. The direction of displacement is along the positive p-axis of the phase space.

that the maximum amplitude squeezing occurs only around a narrow range of values of k.

We have seen how the displacement affects the amplitude squeezing of a quantum

state. In the next section we wish to see the effect of relative phase in the amplitude squeezing of a displaced superposition of coherent states in more direct way.

3.3 The role of relative phase in amplitude squeezing

We have seen that the effect of the relative phase in a superposition is to make the distribution curved. We have also seen that if this curved distribution is displaced in a proper direction then there is an ideal distance at which the curvature of this distribution locally matches the curvature of the Fock circles, and consequently at which distance the amplitude squeezing is maximum. In this section we will study the effect of the relative phase in the superposition state more directly and later on compare it with a quadrature squeezed state. This is done by fixing the magnitude of displacement at a particular value and varying the relative phase between the component states. Such a study will clarify the dependence of amplitude squeezing on the curvature of the quantum state's distribution more effectively.

In Fig. (3.7), we plot the Fano factor for the displaced superposition as a function of the relative phase χ between the component states, when the magnitude of displacement is fixed at $k = 2.0$, and when the direction of displacement is along the positive p-axis of phase space. The half-separation between the component states is fixed at $x = 0.7$ again. The minima and the maxima of the curve are demarcated by drawing a dotted line parallel to the ordinate. When studying the effect of the relative phase it should be remembered that the half-separation is quite small and is less than one. Hence the effects of the curvature due to a relative phase are quite

small comparatively. In Fig (3.7), it could be seen that as one scans the range of χ values there is a minimum and a maximum. This would be true for all values of k, except that for values of k very different from the ideal value the extrema will

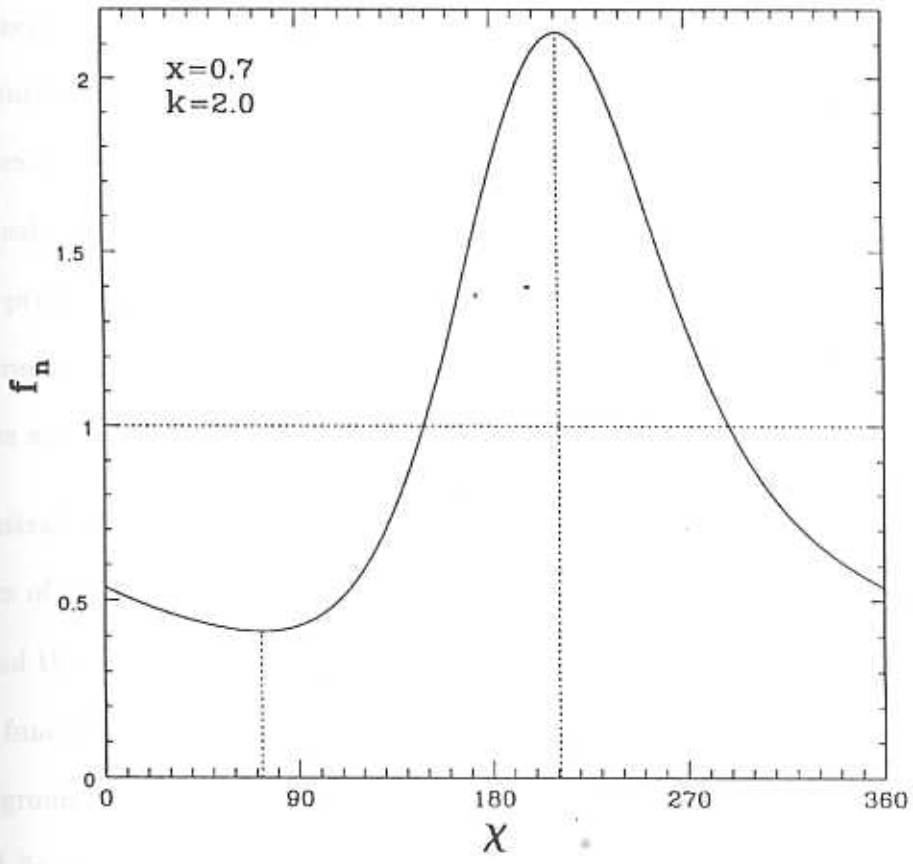

Fig. 3.7. Plot of the Fano factor of the displaced superposition state as a function of the relative phase χ. The half-separation is fixed at $x = 0.7$ and the magnitude of the displacement is fixed at $k = 2.0$. The direction of displacement is along the positive p-axis of the phase space.

be less pronounced. Note that this ideal value itself is dependent on the relative phase. For the value of magnitude of displacement $k = 2.0$ plotted in the figure the minimum of the Fano factor occurs around $\chi = 72.5°$. For values of relative phase $\chi > \pi$ the distribution is curved in the opposite direction. Note that the maximum

spread of the distribution along the p direction in phase space occurs when $\chi = \pi$. But as can be observed in the figure the maxima of the Fano factor *does not* lie at $\chi = \pi$, but rather at a higher value. As we have pointed out earlier, values of relative phase χ which are equally separated from π on either side will their distributions as mirror reflections of one another about the line joining the component states. Hence the distribution of the state when say, $\chi = 210°$, is the same as for the state when $\chi = 150°$ except that they are mirror reflections about the line joining the states. But obviously the Fano factor is not the same at these values but is larger when $\chi = 210°$, precisely for the reason that the distribution is curved in the *wrong way*. The argument can be extended to the minimum of the Fano factor which in this case occurs around $\chi = 70°$ and not around $\chi = -70°$.

To illustrate the point further, we plot the Q function of the displaced states for four values of relative phase in Fig. (3.8). Here too, the half-separation is fixed at $x = 0.7$ and the magnitude of displacement at $k = 2.0$. The contours (level curves) of the Q function are for $0.05, 0.2, 0.4, 0.6, 0.8$ times that of the maximum value. The background is filled with the maxima of the Q function of the Fock states by dotted lines. It should be observed that this is not a very good visualization of the scenario since the half-separation here, as said earlier, is too small. But this must be so for a strong interference in phase space. Unfortunately at these small separations the effect of the relative phase, even though present, is not very pronounced. These effects could be observed in a much better way if one has a superposition of many coherent states with relative phase between them and by properly modulating the superposition amplitudes. Here it is not so and hence the effect is not that pronounced. But still one can discern these effects in the figure.

In the plot where the relative phase $\chi = 0$, one can see that the distribution is straight and as the χ value is increased the distribution gets more and more bent. At $\chi = 72.5°$ it can be seen that the bending of the distribution suits the position it is sitting, in that, it is streamlined with the Fock circles, and it cuts a less number

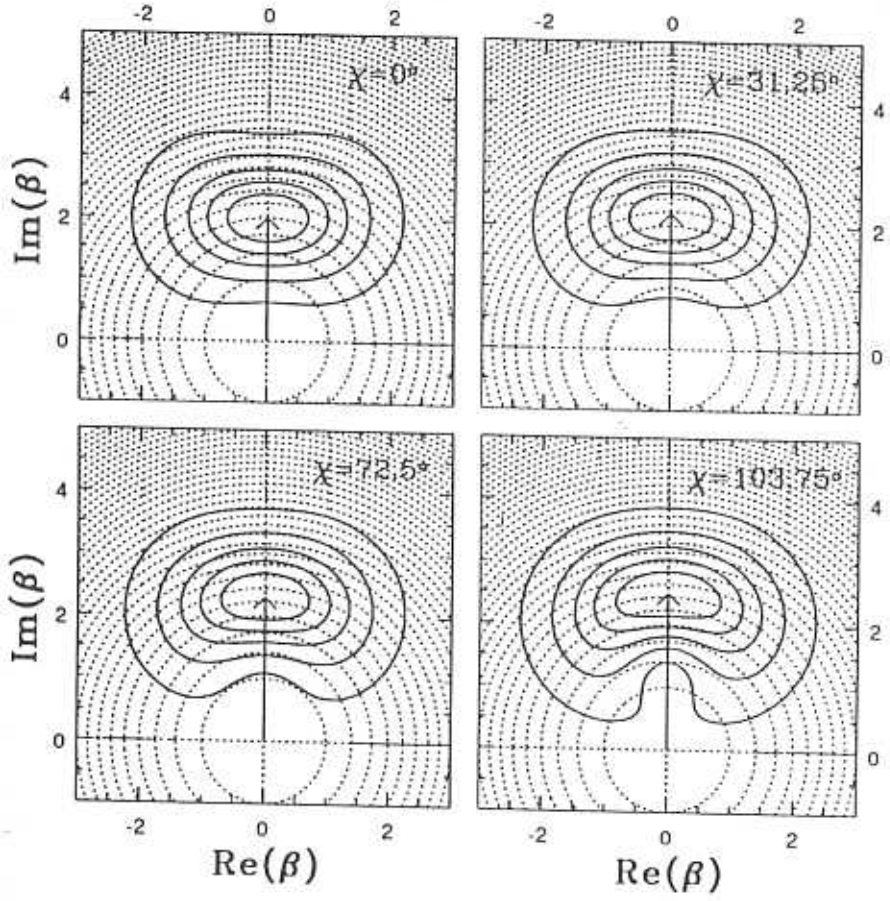

Fig. 3.8. Plot of the Q function of the superposition state. The background is filled with the maxima of different Fock states as dotted circles. The magnitude of displacement is fixed at $k = 2.0$, and the half-separation at $x = 0.7$. The plots are for different relative phases which are indicated in the figure.

of them (here only one or two less).

We have seen that a quantum state with a curved Q function is better suited as far as amplitude squeezing is concerned. We wish to show now that the quadrature

squeezed state, for a very small value of squeezing can be represented as a superposition of two coherent states with no relative phase. Since the absence of relative phase makes the distribution not curved, it is apparent that quadrature squeezed state is not that suitable when it comes to amplitude squeezing. In fact interactions which can produce quantum states with a curved Q function are better in the generation of amplitude squeezed light. We will now show that for small squeezing the quadrature squeezed state given by [85, 86, 89],

$$|\alpha, z\rangle = \widehat{D}(\alpha)\hat{S}(z)|O\rangle \quad , \tag{3.18}$$

can be represented as a superposition of two coherent states which are in-phase with one another.

We first represent the squeezed vacuum in a convenient way as

$$\begin{aligned} |z\rangle &= \hat{S}(z = re^{2i\theta})|O\rangle \\ &= \cosh^{-\frac{1}{2}}(r)\, e^{\frac{1}{2}e^{2i\theta}\tanh(r)\hat{a}^{\dagger 2}}|O\rangle \\ &= \cosh^{-\frac{1}{2}}(r)\left(1 + \frac{1}{2}e^{2i\theta}\tanh(r)\hat{a}^{\dagger 2} + \frac{1}{2.2!}e^{4i\theta}\tanh^2(r)\hat{a}^{\dagger 4} + \cdots\right)|O\rangle, \end{aligned} \tag{3.19}$$

where we had used the normal ordered form of the squeeze operator [276, 277] given in Eq. (1.63). The other two exponents of the normal ordered operator do not contribute since they are acting on the vacuum state.

On the other hand, an in-phase superposition of two coherent states in the canonical form can be written as

$$\begin{aligned} |\psi_c\rangle &= \mathcal{N}(|-x\rangle + |x\rangle) \\ &= \mathcal{N}\left(\widehat{D}(-x) + \widehat{D}(x)\right)|O\rangle \quad . \end{aligned} \tag{3.20}$$

Using the normal ordered displacement operator [27] given in Eq.(1.37), we have,

$$\begin{aligned} |\psi_c\rangle &= \frac{1}{\sqrt{\cosh(x^2)}}\left(e^{-x\hat{a}^\dagger} + e^{x\hat{a}^\dagger}\right)|O\rangle \\ &= cosh^{-\frac{1}{2}}(x^2)\left(1 + \frac{1}{2!}x^2\hat{a}^{\dagger 2} + \frac{1}{4!}x^4\hat{a}^{\dagger 4} + \cdots\right) \quad . \end{aligned} \tag{3.21}$$

This can be immediately compared with the squeezed state $|z\rangle$ for small values of x and r ($x \ll 1, r \ll 1$). One can see that for small values of r, $\tanh(r) \approx r$ and hence one can write the squeezed state as

$$|z\rangle = \hat{R}(\theta)\left(\left|-\sqrt{r}\right\rangle + \left|\sqrt{r}\right\rangle\right) \quad , \tag{3.22}$$

neglecting terms containing higher powers of r ($r \ll 1$). The operator $\hat{R}$ is the rotation operator given by $\hat{R}(\tau) = \exp(i\tau\hat{a}^\dagger\hat{a})$, and this automatically gives the correct θ coefficient for each Fock state (even when r is not small).

Hence the general squeezed state for small values of the squeezing magnitude r can be written as

$$|\alpha, z\rangle = \widehat{D}(\alpha)\hat{R}(\theta)\left(\left|-\sqrt{r}\right\rangle + \left|\sqrt{r}\right\rangle\right) \quad . \tag{3.23}$$

Neither the displacement operator nor the rotation operator changes the relative phase between the states in the superposition as we have seen earlier. The general squeezed state for small squeezing magnitudes can hence be represented by an in-phase superposition of two coherent states. But we have seen that a quantum state, which has curved Q distribution, such as those got from a superposition with a relative phase between the component states is better from the point of view of amplitude squeezing. We conclude this chapter by pointing out that interactions which

produce quantum states with a curved Q function are more suitable for producing amplitude squeezed light than the usual two photon interaction which produce states whose Q functions are not curved.

In this chapter, we have considered the role the relative phase plays in amplitude squeezing, by using the two coherent state superposition to illustrate our arguments. We have first studied the canonical form's photon number uncertainty. Since the photon number properties, unlike the quadrature noise property, are not invariant under the displacement operation, the displaced version of the canonical form is studied in detail, to discern the effect the positioning of the state in phase space has on amplitude squeezing. We have made this study both with respect to the direction and magnitude of the displacement. We have then illustrated the real role of the relative phase in amplitude squeezing in a more direct way, by considering a superposition of two coherent states at a fixed displacement and varying the relative phase between them. By this we have shown that the states with a curved Q function, when positioned properly show better amplitude squeezing than those states whose Q function is not curved. Finally, we have analytically shown that for very small squeezing, the quadrature squeezed state can be represented as an in-phase superposition of two coherent states, and hence is not very suitable when it comes to amplitude squeezing. Our conclusion is that one should look for interactions which gives rise to curved Q functions if one is looking for

higher amplitude squeezing. We proceed to look at the effect of such an interaction on the quadrature squeezed state in the next chapter.

Chapter 4

Evolution of quadrature squeezed state in a non-linear Kerr medium

This chapter studies the evolution of a quadrature squeezed state in a Kerr medium. We use the understanding gained in the previous chapters in this study. The calculations involving this evolution are considerably simplified if one expresses the initial quadrature squeezed state as a superposition of coherent states. The pictorial representation of this evolution is presented using the Q-function, which at appropriate places is compared with the coherent state case. The expectation values of field quantities which will be needed in the forthcoming chapters are then calculated. Finally some interesting limiting cases of these general expressions are pointed out.

4.1 Quadrature squeezed state as superposition of coherent states

The single mode quadrature squeeze operator is given by [85, 86, 87, 88, 89]

$$\widehat{S}(z) = \exp(\frac{1}{2}z\widehat{a}^{\dagger 2} - \frac{1}{2}z^{*}\widehat{a}^{2}) \quad , \tag{4.1}$$

where we had parameterized (Section 1.4) z as $z = r\exp(2i\theta)$ to reflect the underlying symmetry, so that the squeezed states corresponding to θ and $\theta \pm \pi$ are identified. We have also seen that when $\theta = 0, \pi$, the operator $\widehat{S}(z)$ squeezes along

the p-quadrature, and when $\theta = \pi/2, 3\pi/2$, it squeezes along the x-quadrature in phase space, and that the angle θ is the angle subtended by the major axis of the uncertainty ellipse with x-axis in the x-p phase space. The aim of this section is to write the squeezed state as a superposition of coherent states [246, 247, 248]. This will facilitate calculations involving the squeezed state to a considerable extent [219].

The process of expressing a general squeezed states $|\alpha, z\rangle = \widehat{D}(\alpha)\widehat{S}(z)|O\rangle$ as a superposition of coherent state is simplified if one first writes the squeezed vacuum defined by $\widehat{S}(z)|O\rangle$ as a coherent state superposition. This is so, since if $\widehat{S}(z)|O\rangle$ is expressed as a superposition of coherent states, then $\widehat{D}(\alpha)$ has to act only on the individual coherent states in the superposition. Hence our first task will be to write the squeezed vacuum as a superposition of coherent states.

To express the squeezed vacuum as a superposition of coherent states, we observe that the squeezed vacuum should be a superposition of coherent states along the θ direction in phase space. Again one can reason this. A squeezed vacuum specified by r and θ has the major axis of its uncertainty ellipse along the θ direction, and is squeezed in the direction perpendicular to this. For example, a squeezed vacuum squeezed in the p-quadrature will have $\theta = 0$ and its major axis will be along the x-quadrature. Now in Chapter 2, we have seen that an in-phase superposition of coherent states lying along a certain line will have squeezing in the quadrature perpendicular to that direction. Hence one has to choose the coherent states along the direction perpendicular to the direction of squeezing which, in our case is along the θ direction. Hence we choose coherent states of the form $\left|ye^{i\theta}\right\rangle$ to make the superposition.

One can try to build the squeezed vacuum as a discrete superposition by choosing coherent states $\left|y_1 e^{i\theta}\right\rangle, \cdots, \left|y_n e^{i\theta}\right\rangle$. Such a discrete superposition will be of the form $\sum_{n=-k}^{n=+k} C_n \left|y_n e^{i\theta}\right\rangle$, where k is some arbitrary integer. The form of y_n will be nx where x is a small unit of length in phase space. Note that the C_n's can be chosen to be real since we are dealing with an in-phase superposition of coherent states. One would also expect C_n to be a function of the squeezing magnitude r. On the other hand it is possible to build a continuous superposition of the form $\int_a^b dy\, \mathcal{C}(y,r) \left|ye^{i\theta}\right\rangle$. It is better to use the continuous superposition since it is not only mathematically convenient but is also more smooth.

The squeezed vacuum for a given magnitude of squeezing r, will have the same properties for both θ or $\theta \pm \pi$. But if the limits of the integral are different this cannot be true, since the upper limit gives the extension of the superposition along the θ directions and the lower limit along the $\theta \pm \pi$ direction. Hence one expects the upper and lower limits of the integral to be the same in magnitude, but differing only in sign. For simplicity we take that the superposition extends to infinity, hoping that the coefficient will turn out to be a Gaussian, which we show to be the case. These imply that the superposition will be of the form

$$\hat{S}(z = re^{2i\theta}) \left|O\right\rangle = \int_{-\infty}^{\infty} dy\, \mathcal{C}(y,r) \left|ye^{i\theta}\right\rangle \quad , \tag{4.2}$$

where $\left|ye^{i\theta}\right\rangle$ is a coherent state as noted earlier.

In order to find $\mathcal{C}(y,r)$, we expand both the superposition given above and $\hat{S}\left|O\right\rangle$ in terms of the number states. This is simple, since on normal ordering the squeeze operator [276, 277], only certain factors will act non-trivially on the vacuum. We

proceed to do this first. Normal ordering the squeeze operator, we have

$$\widehat{S}(z=re^{2i\theta}) = \cosh^{-\frac{1}{2}}(r)\, e^{\frac{1}{2}e^{2i\theta}\tanh(r)\widehat{a}^{\dagger 2}}\, e^{-\ln(\cosh(r))\widehat{a}^{\dagger}\widehat{a}}\, e^{-\frac{1}{2}e^{-2i\theta}\tanh(r)\widehat{a}^{2}} \quad . \tag{4.3}$$

Here, both the right most exponent and the middle one will not contribute when acting on the vacuum state. Only the exponent containing the $\hat{a}^{\dagger 2}$ will give rise to a series, given by

$$\widehat{S}(z=re^{2i\theta})\,|O\rangle = \cosh^{-\frac{1}{2}}(r) \sum_{n=0}^{\infty} \mathcal{S}_n\,|n\rangle \quad , \tag{4.4}$$

where

$$\begin{aligned} \mathcal{S}_n &= 0 && \text{for odd } n \\ &= \frac{e^{i\theta n}\tanh^{\frac{n}{2}}(r)2^{\frac{n}{2}}\Gamma(\frac{n+1}{2})}{\sqrt{\pi}\sqrt{n!}} && \text{for even } n \quad . \end{aligned} \tag{4.5}$$

Note that we have rearranged the coefficients so that the summation runs over all n. We would like to have it in this way since it makes the comparison with the other series obtained by expanding the coherent states in Eq. (4.2) easier.

Expanding the coherent states $\left|ye^{i\theta}\right\rangle$ in Eq. 4.2 in terms of the Fock states $|n\rangle$ we have

$$\widehat{S}(z=re^{2i\theta})\,|O\rangle = \int_{-\infty}^{\infty} dy\, \mathcal{C}(y,r) \sum_{n=0}^{\infty} e^{-y^2/2}\frac{y^n e^{in\theta}}{n!}\,|n\rangle \quad . \tag{4.6}$$

The order of summation and integration can be interchanged in the above equation, due to its convergent nature in the sense that the expectation value of the photon number is always a finite number. Comparing this with Eq. 4.4, and by noting the fact that a Gamma integral of the form

$$\int_{-\infty}^{\infty} dy\, e^{a y^2} y^m \tag{4.7}$$

vanishes for odd m, one could judge $\mathcal{C}(y,r)$ to be

$$\mathcal{C}(y,r) = [2\pi\sinh(r)]^{-\frac{1}{2}}\, e^{-\frac{1}{2}(\coth(r)-1)y^2} \quad . \tag{4.8}$$

Note that the determination of $\mathcal{C}(y,r)$ gives only the squeezed vacuum state as a superposition of coherent states, and not the squeeze operator as an integral over the displacement operators. This is so because the way we determined $\mathcal{C}(y,r)$ involved only one Fock state, namely the vacuum state. If it had been any other fock state, then the other exponents in the normal ordered squeeze operator would have contributed. This relationship can be taken as an operator identity only if it holds for all the states of the Hilbert space. Here it is not so and hence is not an operator identity.

The squeezed vacuum can hence be written as a superposition of coherent states given by

$$\widehat{S}(z = re^{2i\theta})\,|O\rangle = [2\pi \sinh(r)]^{-\frac{1}{2}} \int_{-\infty}^{\infty} dy\, e^{-\frac{1}{2}(\coth(r)-1)y^2} \left| ye^{i\theta} \right\rangle \quad , \tag{4.9}$$

The general quadrature squeezed coherent state $|\alpha, z\rangle$ can be obtained from the squeezed vacuum $\widehat{S}(z)\,|O\rangle$ by applying the displacement operator $\widehat{D}(\alpha)$ to it, as noted earlier. This operator acts directly on the individual coherent states. Note that for a general arbitrary coherent state $|\beta\rangle$, the action of the displacement operator $\widehat{D}(\alpha)$ can be written as

$$\widehat{D}(\alpha)\,|\beta\rangle = \widehat{D}(\alpha)\widehat{D}(\beta)\,|O\rangle = e^{(\alpha\beta^* - \alpha^*\beta)/2}\,|\alpha+\beta\rangle \quad , \tag{4.10}$$

using the BCH formula [270, 271, 272, 273, 274, 275], which is quite simple in this case [27]. Hence the general quadrature squeezed coherent state, after some minor algebra can be written as a superposition of coherent states given by

$$\begin{aligned} |\alpha, z\rangle &= \widehat{D}(\alpha = \rho e^{i\phi})\widehat{S}(z = re^{2i\theta})\,|O\rangle \\ &= [2\pi \sinh(r)]^{-\frac{1}{2}} \int_{-\infty}^{\infty} dy\, e^{-\frac{1}{2}(\coth(r)-1)y^2 - i\rho y \sin(\theta-\phi)} \left| \rho e^{i\phi} + ye^{i\theta} \right\rangle_{\text{coh}} \end{aligned} \tag{4.11}$$

Equipped with this integral representation of the quadrature squeezed state, we now turn our attention to the action of a non-linear Kerr medium on a squeezed coherent state.

4.2 Evolution in a Kerr medium

In this section, we study the effect of a Kerr medium on a squeezed coherent state. Earlier, numerical attempts have been made by Banerjee [215]. Our purpose here is to find analytically the state that has evolved for a given time inside the Kerr medium, when the initial state is a squeezed coherent state. By this we mean that one should be able to find analytically the expectation value of various operators for this state. Inside the Kerr medium, the Hamiltonian for the field in the rotating wave approximation is given by [194, 195, 178, 196, 185, 197],

$$H_K = \hbar\omega\hat{a}^\dagger\hat{a} + \hbar\chi_{NL}\hat{a}^{\dagger 2}\hat{a}^2 \quad , \tag{4.12}$$

where the anharmonicity parameter χ_{NL} is real, and is proportional to the third order non-linear susceptibility [185], and $\hat{a}^\dagger$, $\hat{a}$ are field boson creation and annihilation operators. This Hamiltonian is valid under the conditions that there is no saturation and no loss, and that there is a large detuning from the transition levels [179].

We have already seen (Section 1.5) that the photon number operator $\hat{n}$, is a constant of motion since

$$[\hat{n}, \widehat{H}] = 0 \quad . \tag{4.13}$$

This would immediately suggest that the photon number properties of any state that evolves through a Kerr medium will remain unchanged. Even so the state changes

in a subtle way, as we will demonstrate shortly. As we have already seen the unitary operator $\widehat{U}(\gamma)$ corresponding to the evolution inside the Kerr medium can be readily found, and is given by

$$U_K(\gamma) = e^{\frac{i}{2}\gamma\widehat{a}^{\dagger 2}\widehat{a}^2} = e^{\frac{i}{2}\gamma\widehat{n}(\widehat{n}-1)} \quad , \tag{4.14}$$

where

$$\gamma = \frac{2\chi_{NL}L}{v} \quad . \tag{4.15}$$

Here L is the length of the Kerr medium and v is the velocity of light in the Kerr medium. We have left out the free evolution part and in a sense we are working in the interaction picture. Note that the free evolution part commutes with the interaction part and hence the interaction and the Schröedinger pictures coincide in this case [191].

The state that evolves out of the Kerr medium, when the initial state is a squeezed coherent state, is given by

$$|\psi_K\rangle = U_K(\gamma)\,|\alpha, z\rangle \quad , \tag{4.16}$$

where γ is defined earlier and is akin to the scaled time. As noted earlier the photon number properties of the state $|\psi_K\rangle$ will be the same as in the state $|\alpha, z\rangle$. This means both the photon number uncertainty and the photon number distribution of the state $|\psi_K\rangle$ will be the same as those of $|\alpha, z\rangle$. As mentioned earlier, this is expected since the interaction Hamiltonian commutes with the photon number operator. But still the state changes in a subtle way, and this can be understood if one looks at the physical picture of what happens in the Kerr medium.

As briefly mentioned earlier (Section 1.5), the action of this interaction Hamiltonian can be understood if one looks at the quasi probability in phase space [191]. Under the influence of this interaction, regions of the quasi probability distribution of an initial state at different radial distances from the origin moves with different angular velocities. Regions that are farther away move slower than those regions that are near the origin. These, and other factors makes the initial distribution to get sheared. This shearing occurs in such a way that the photon number uncertainty remains preserved. On the other hand the phase uncertainty definitely increases. Note that such a shearing will produce a curved distribution. As noted earlier, one can expect amplitude squeezing with such a curved distribution by a suitable displacement in phase space. After a small duration of evolution in the Kerr medium, there exists a time at which one can get an optimal amplitude squeezing by displacing this distribution to a proper position in phase space. For an initial coherent state this results in a diminished photon number uncertainty which goes only as the cube root of the mean photon number [191]. It should be remembered that this is a huge reduction in noise since the initial coherent state has a photon number uncertainty which goes as the mean photon number itself.

The question that arises is that if one chooses a state whose quasi probability distribution is such that it has a lesser spread in the radial direction, will it lead to a much more amplitude squeezed state after it evolves through a Kerr medium? In the case of the quadrature squeezed states such a possibility of having a lesser spread in the radial direction exists when the direction of squeezing is along the direction of coherent excitation. This is the prime motive of studying the evolution of a quadrature squeezed state inside a non-linear Kerr medium [219].

The above argument at its best is only heuristic and even then is valid only for a very small duration of time. One cannot take the above argument too seriously since the assumption that regions at different radial distances move with different angular velocities cannot be established rigorously for any quasi probability distribution. Moreover after some evolution in the Kerr medium, the distribution is not symmetric over the radial line passing through the mean. These imply that many more issues are involved in the evolution. Some of these can be seen by visualizing the state using the Q-function as it evolves through the Kerr medium. We proceed to do this in the next section.

4.3 A pictorial representation of the evolution

The first task in this section will be to calculate the Q-function for the quadrature squeezed state that has evolved through a Kerr medium. From the definition of the q-function, we have

$$Q_K(\beta) = \frac{1}{\pi} |\langle \beta \mid \psi_K \rangle|^2 \quad , \tag{4.17}$$

where $|\beta\rangle$ is a coherent state. Hence the Q-function involves only the projection of the state $|\psi_K\rangle$ on the coherent state. Since $|\psi_K\rangle = \widehat{U}_K(\gamma)\,|\alpha, z\rangle$ and since we have expressed the quadrature squeezed state $|\alpha, z\rangle$ as a superposition of coherent states, $\langle \beta \mid \psi_K \rangle$ will only involve the matrix elements of the the operator $\widehat{U}_K(\gamma)$ in the coherent states basis. We have seen this already in Section 1.5, using which we can write $Q_K(\beta)$ as

$$Q_K(\beta) \;=\; \frac{e^{-\frac{1}{2}|\beta|^2}}{[2\pi \sinh(r)]} \left| \int_{-\infty}^{\infty} dy\, e^{-\frac{1}{2}(\coth(r)-1)y^2 - iy\sin(\theta-\phi)} e^{-\frac{1}{2}\left|\rho e^{i\phi} + y e^{i\theta}\right|^2} \right.$$

$$\times \sum_{n=0}^{\infty} e^{i\frac{\pi}{2}n(n-1)} \frac{(\beta^*)^n (\rho e^{i\phi} + y e^{i\theta})^n}{n!} \Bigg|^2 . \quad (4.18)$$

Interchanging the summation and integration, and doing the integral over y, we obtain the Q-function for the state $|\psi_K\rangle$ after some algebra and it is given by

$$Q_K(\beta) = \frac{e^{-\rho^2-|\beta|^2}}{\pi \cosh(r)} \Bigg| e^{\frac{1}{2}\rho^2 \tanh(r) e^{2i(\theta-\phi)}} \sum_{n=0}^{\infty} e^{i\frac{\pi}{2}n(n-1)} (\beta^*)^n \sum_{m=0}^{[n/2]} \frac{\left[\rho e^{i\phi} - \rho \tanh(r) e^{i(2\theta-\phi)}\right]^{n-2m}}{(n-2m)!\, m!} \left[\frac{1}{2}\tanh(r) e^{2i\theta}\right]^m \Bigg|^2 \quad (4.19)$$

where $[n/2]$ denotes the largest integer less than or equal to $n/2$. In all our plots of this Q-function, which we have computed numerically, we have taken a small mean photon number ($|\alpha|^2 + \sinh^2(r) = 16$). Since the interaction Hamiltonian commutes with the photon number operator, the mean photon number of the initial state doesn't change under the evolution in the Kerr medium, and in our numerical evaluation of the above function, we have terminated the infinite series at a large (compared to the initial mean photon number), but finite n. We have considered in most of the figures, an initial mean photon number of 16, and the infinite series was terminated at $n = 64$. The termination error involved is negligible due to the relatively large value of n compared to the initial mean photon number. In passing we note that taking very large value of n in the above expression will cause numerical problems.

We are more interested in the amplitude squeezed states that are produced by this evolution in the Kerr medium [218, 219, 256]. As argued in the last section, we wish to first consider the evolution of a quadrature squeezed state whose direction of squeezing is along the direction of excitation. We have called such a quadrature

squeezed state as amplitude squeezed coherent state [219]. In Fig (4.1), we plot the contours of the Q-function against the real and imaginary parts of its argument, of

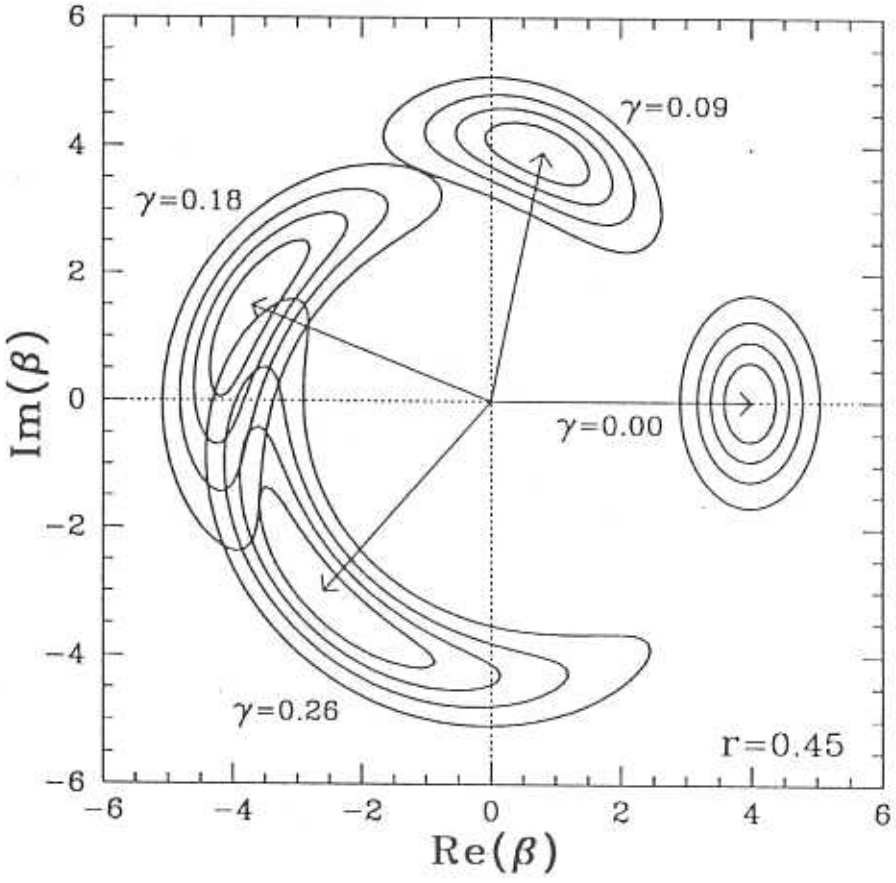

Fig. 4.1. Plot of the contours of Q-function of the evolution of the amplitude squeezed coherent state in a Kerr medium. The different γ values are indicated in the figure. The magnitude of squeezing is fixed at $r = 0.45$ and the values of ρ^2 chosen such that the mean remains at 16. The arrows connect the phase space origin and the maximum of the Q-function. The contours are drawn at 0.2, 0.4, 0.6, and 0.8 times the maximum value.

an amplitude squeezed coherent state evolving through a Kerr medium, for different γ values. This figure can be taken as the visualization of the state evolution inside the Kerr medium. Here we have chosen the magnitude of squeezing to be $r = 0.45$, and the ρ^2 value is so chosen that the mean remains at 16. The contours are at 0.2,

0.4, 0.6, and 0.8 times the maximum of the Q-function. The figure contains contours of the Q-function for four values of γ. The arrows connect the maximum of these to the origin of phase space. For comparison, we have repeated [Fig. 1.2] in Fig. (4.2), which gives the evolution of a coherent state ($r = 0$) inside a Kerr medium, for an identical set of parameter values.

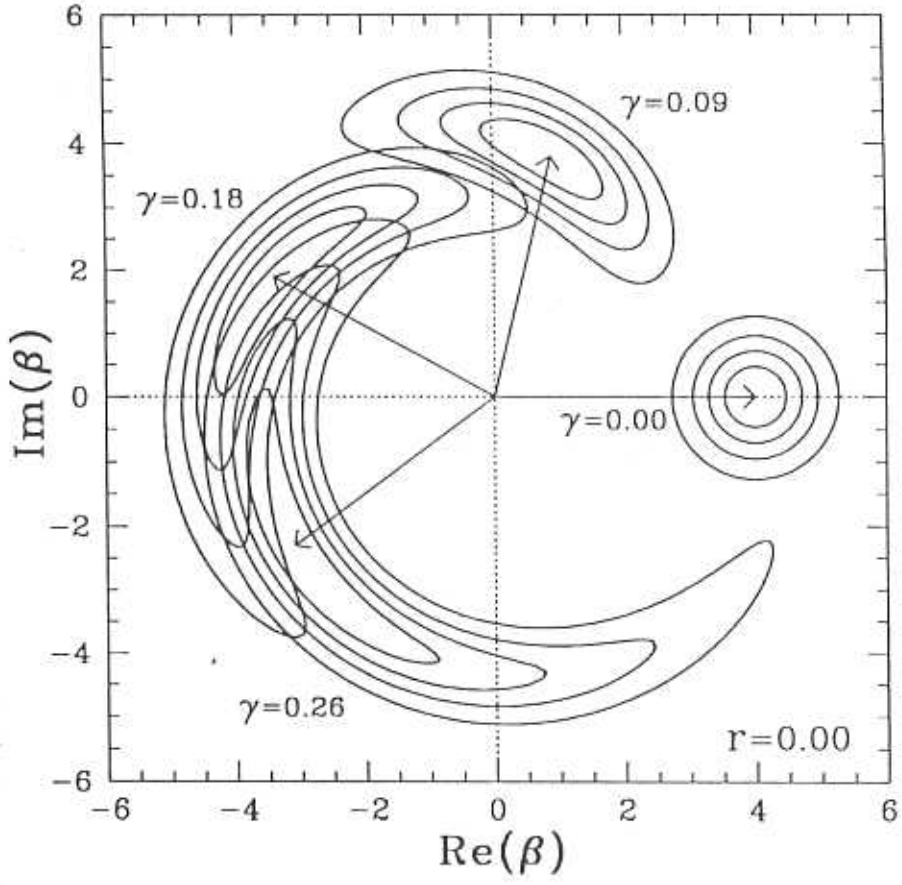

Fig. 4.2. Plot of the contours of the Q-function of the evolution of a coherent state ($r = 0$) in a Kerr medium. All other parameters are as in the earlier figure.

It can be seen from Fig. (4.2) that in the case of the evolution of a coherent state through a Kerr medium, the crescent becomes more strongly curved with increasing

γ. Moreover the tails of these are not symmetric. The increase in the squeezing

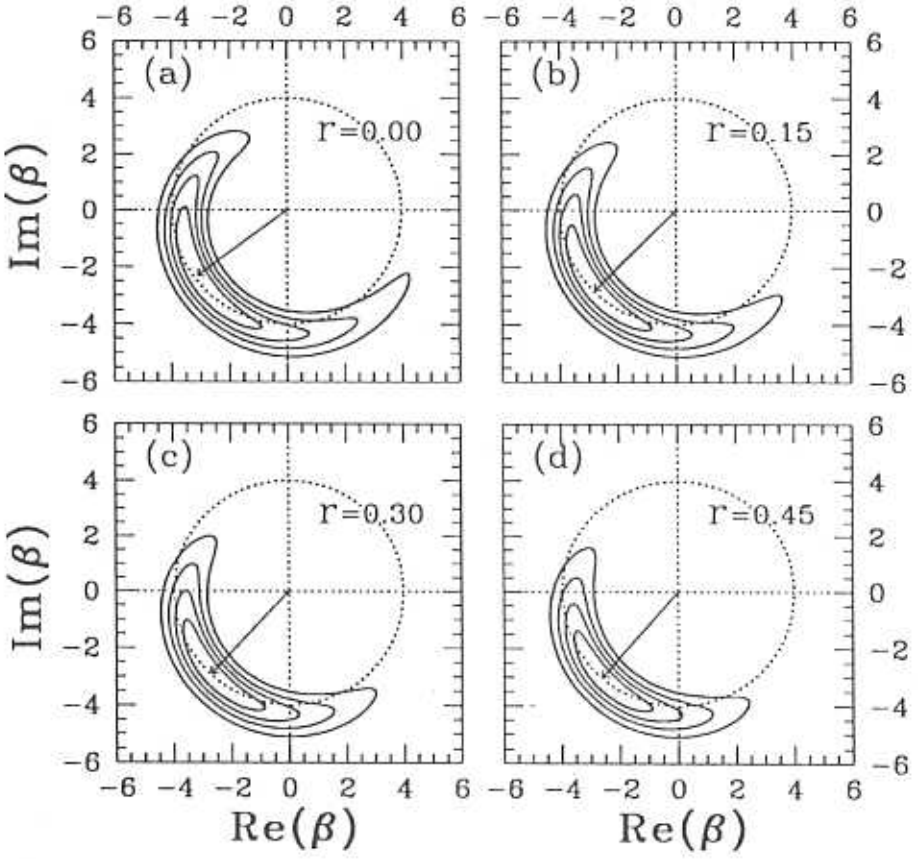

Fig. 4.3. Plot of the contours of the Q-function for the quadrature squeezed state evolved through a Kerr medium. Here the γ value is fixed at 0.26 for all the figures. The magnitude of squeezing is indicated in the figure itself. The contours are at the same level as in the previous figures.

magnitude r has the effect of flattening this distribution and at an appropriate value the tails are rather symmetric. To illustrate this point further, we plot the contours of the Q-function for various values of the magnitude of squeezing r in Fig. (4.3). Here the γ value is fixed at 0.26 in all the figures. As in the previous figures, the mean photon number is fixed at 16. The contours are plotted at the

same values as in the previous figures. It can be clearly seen in this figure that as r increases the distribution flattens and at a particular value of r (here at $r = 0.45$), the tails are nearly symmetric. We will show later that this is indeed the optimum value for this mean photon number at which the photon number uncertainty goes to an absolute minimum under a proper displacement [218, 219].

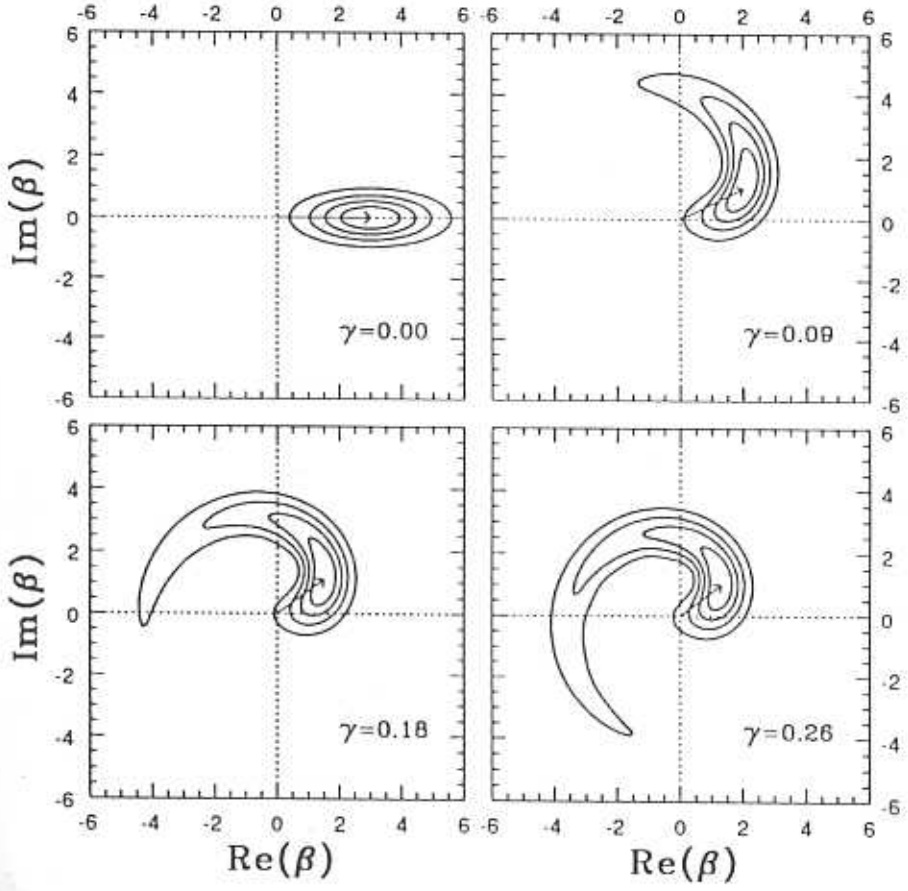

Fig. 4.4. Plot of the contours of Q-function of the evolution of the phase squeezed coherent state in a Kerr medium. The different γ values are indicated in the figure. The magnitude of squeezing is fixed at $r = 1.0$ and the values of ρ^2 so chosen that the mean remains at 16. The arrows connect the phase space origin and the maximum of the Q-function. The contours are drawn at 0.2, 0.4, 0.6, and 0.8 times the maximum value.

The evolution in the small γ limit of an initial phase squeezed coherent state is given in Fig. (4.4). Here it can be seen that since the spread in the photon number

is higher than in the coherent states, the tail of the quasi probability distribution becomes extremely asymmetric. For comparison we also give the quasi probability distribution of a quadrature squeezed state whose angle of squeezing is inclined to the angle of excitation by 45° in Fig. (4.5).

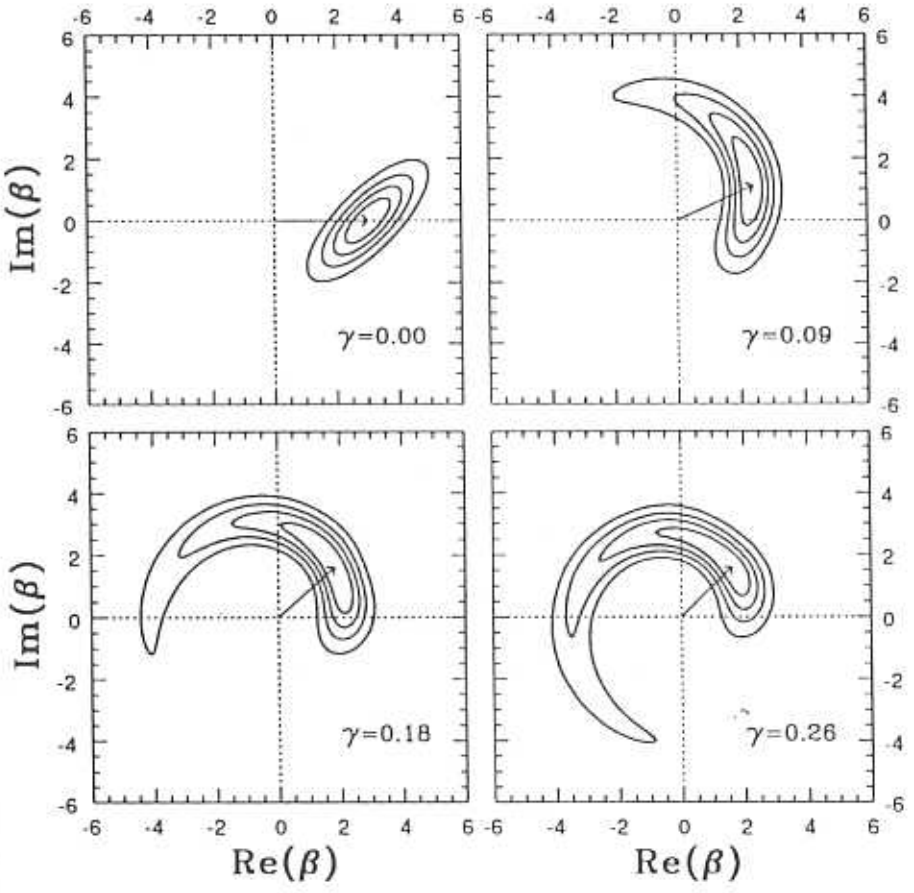

Fig. 4.5. Plot of the contours of Q-function of the evolution of the quadrature squeezed coherent state in a Kerr medium whose angle of squeezing is inclined to the angle of excitation by 45°. All the other parameters are same as in the previous figure.

We have been discussing until now the low γ limit. Even though experimentally difficult to realize, the large γ regime is nevertheless interesting. For the sake of

completeness and to gain a better understanding of this evolution, we plot the complete evolution in a Kerr medium for an amplitude squeezed coherent state in Fig. (4.6) (Pages 115 – 120). We have to content ourselves with this particular choice of quadrature squeezed state, since it will not be possible to give such detailed plots for other cases due to space constraints. One could in principle at least guess from these plots the evolution of any other case with a different initial state. Here the individual plots are for γ values which are in steps of $\pi/36$. The first plot is for $\gamma = \pi/36$, the second plot is for $\gamma = 2\pi/36$ and so on. Note that $\pi/36$ is approximately 0.09, and we have given the γ values rounded up to the first two decimal places in the plots. The initial state is the same as in Fig. (4.1). It is a quadrature squeezed state whose direction of squeezing is along the direction of excitation ($\theta - \phi = \pi/2$). The magnitude of the squeezing r is taken to be 0.45. The initial state with $\gamma = 0.0$ is not given here, but can be found in Fig. (4.1). The first three plots coincide (approximately) with the three contour plots at $\gamma = 0.09$, $\gamma = 0.18$ and $\gamma = 0.26$ of Fig. (4.1). The remaining 33 plots are, as said earlier, for different γ values in steps of $\pi/36$, up to $\gamma = \pi$. The evolution from π to 2π is the repetition of the evolution from 0 to π, but in the reverse order and with the upper and lower half plane interchanged by a mirror reflection about the x-axis of phase space.

It can be seen from these figures that there are many values of γ at which recursion occurs. To elaborate, at these values of γ, the initial state seems to have evolved into a superposition of states. The component states are made up of copies of the initial state placed at different points in phase space. Note that these component states are located at the same radial distance as the initial state. Moreover one can

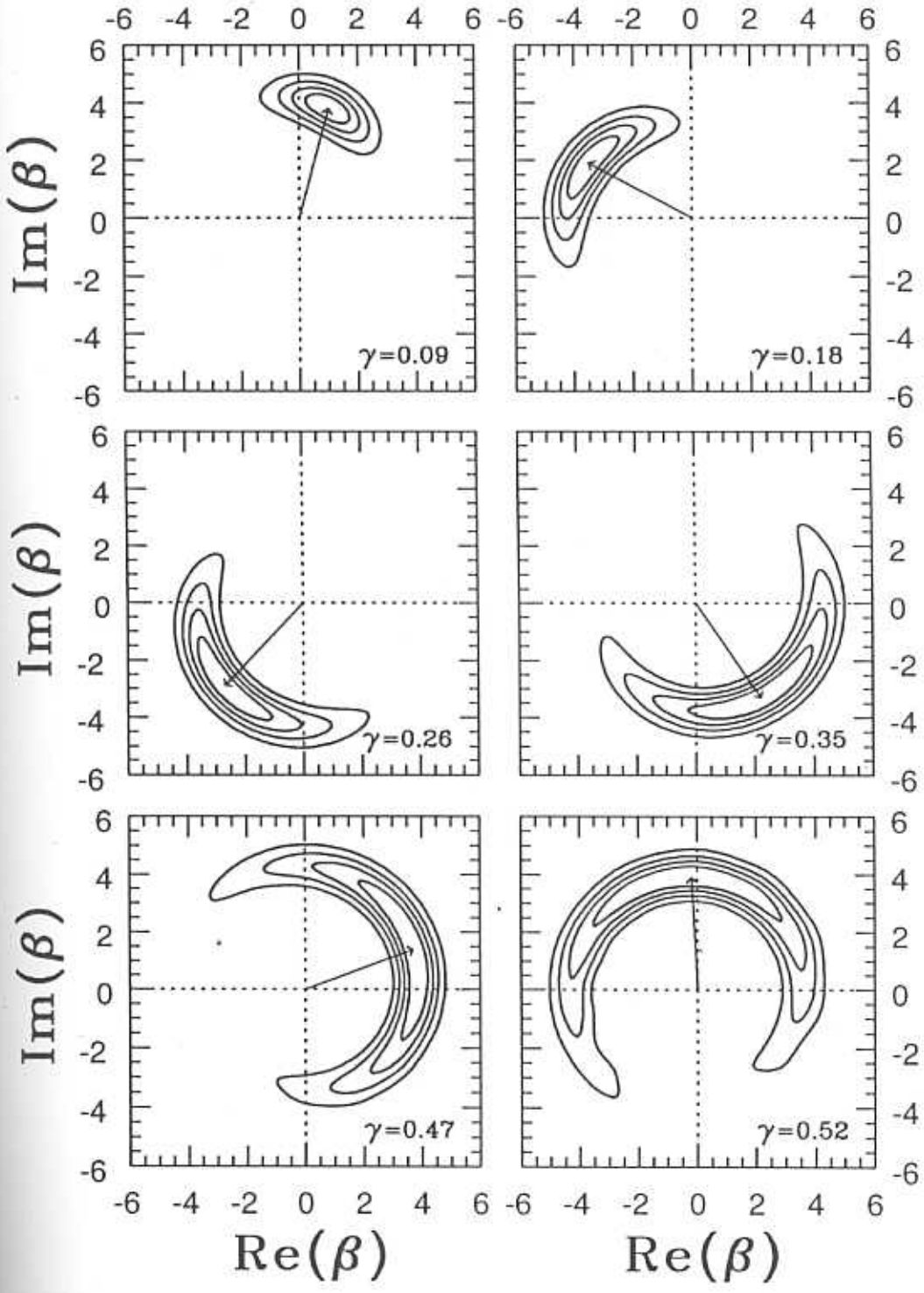

Fig. 4.6. Plot of the contours of the Q-function of the evolution of an amplitude squeezed coherent state ($r = 0.45$) in a Kerr medium. All other parameters are as in Fig. (4.1).

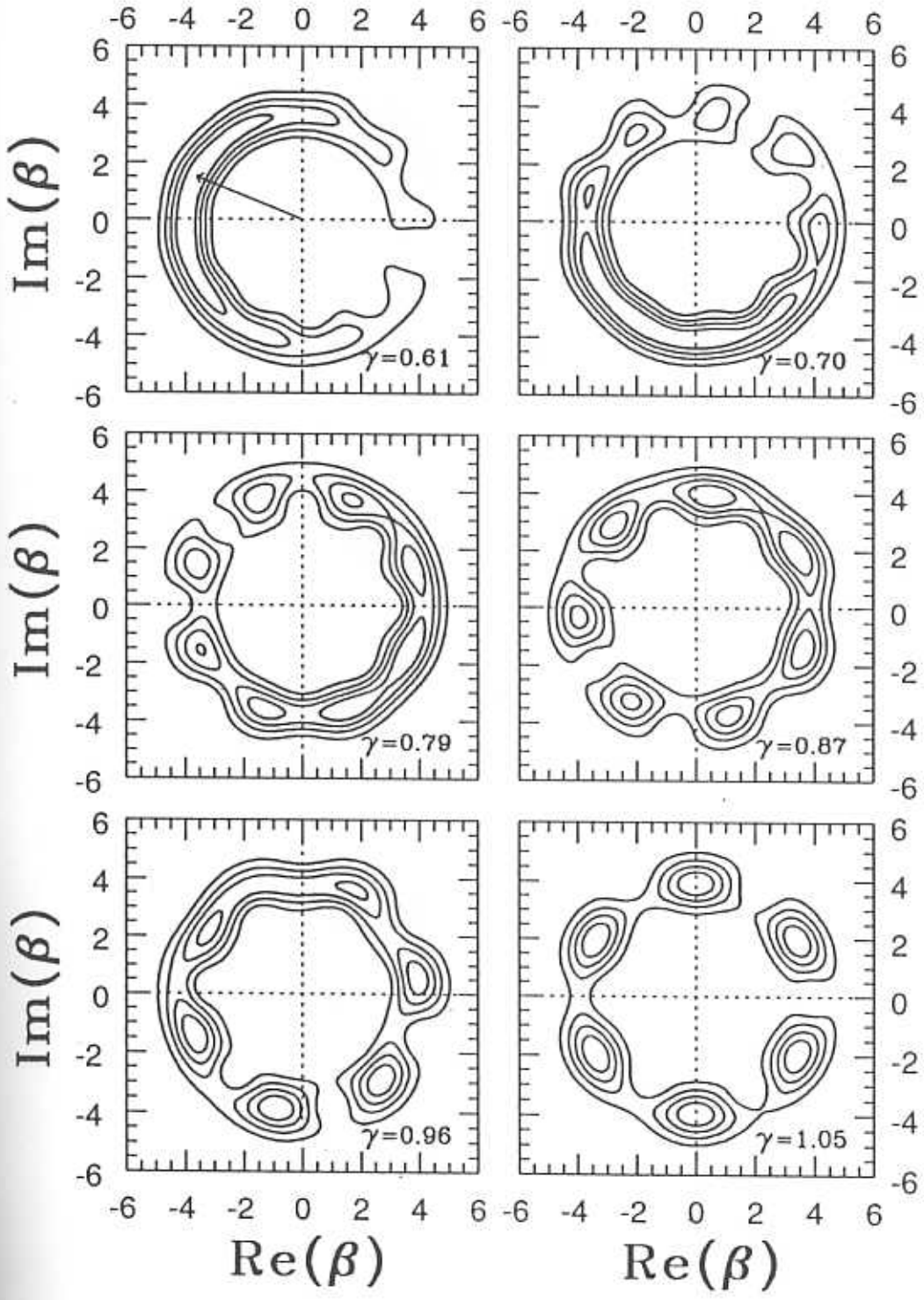

Fig. 4.6. (Cont.) Plot of the contours of the Q-function of the evolution of an amplitude squeezed coherent state ($r = 0.45$) in a Kerr medium. All other parameters are as in Fig. (4.1).

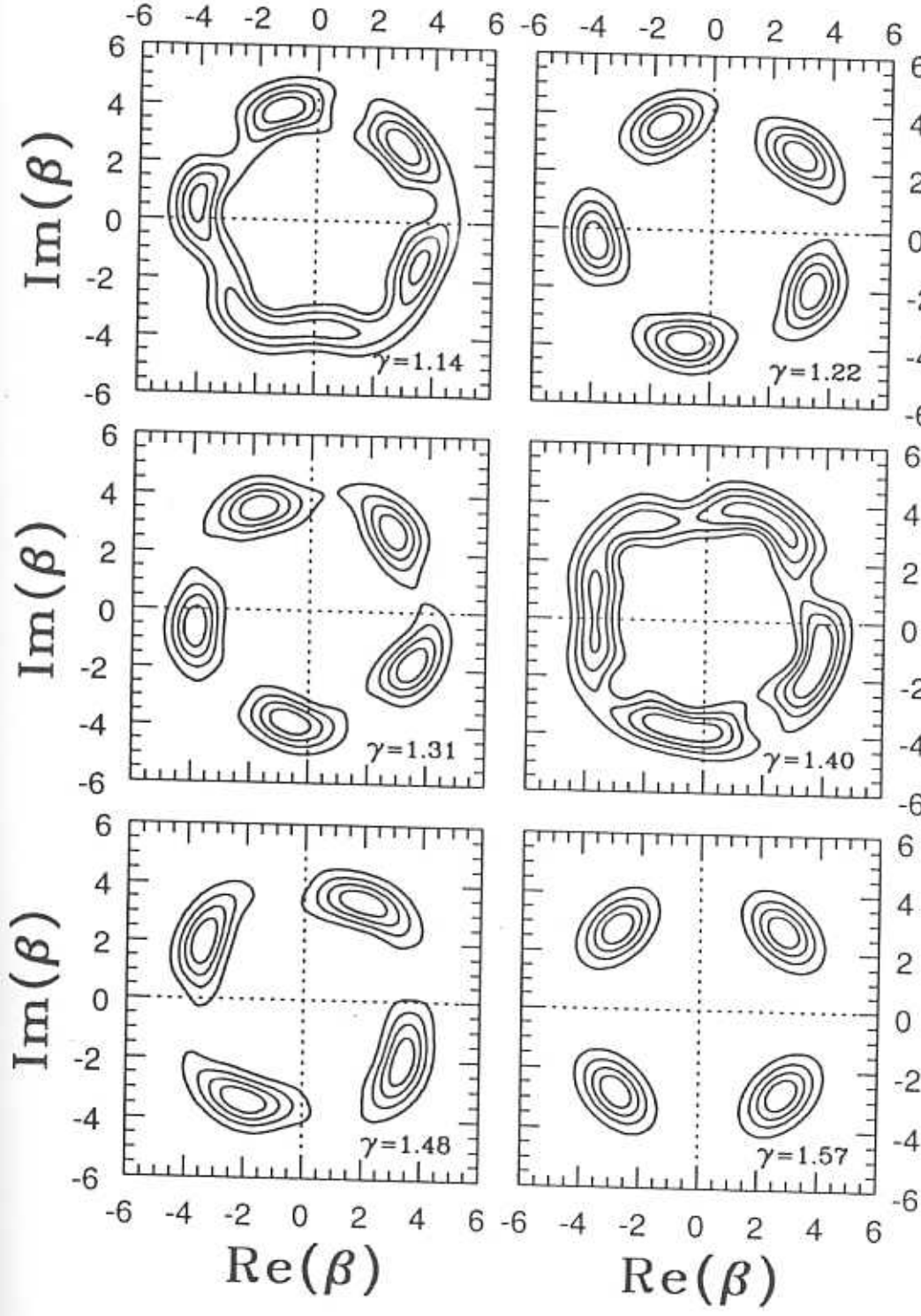

Fig. 4.6. (Cont.) Plot of the contours of the Q-function of the evolution of an amplitude squeezed coherent state ($r = 0.45$) in a Kerr medium. All other parameters are as in Fig. (4.1).

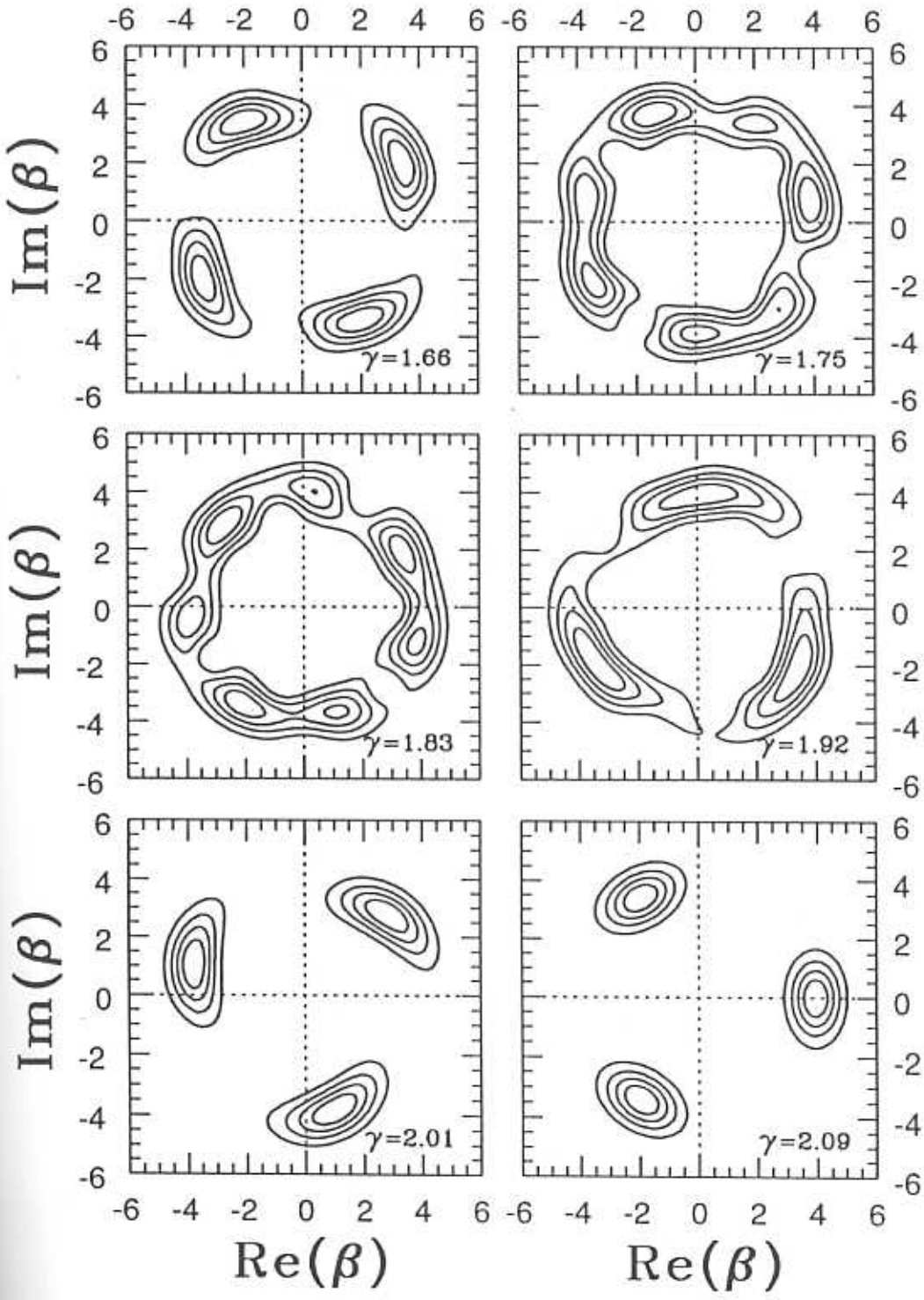

Fig. 4.6. (Cont.) Plot of the contours of the Q-function of the evolution of an amplitude squeezed coherent state ($r = 0.45$) in a Kerr medium. All other parameters are as in Fig. (4.1).

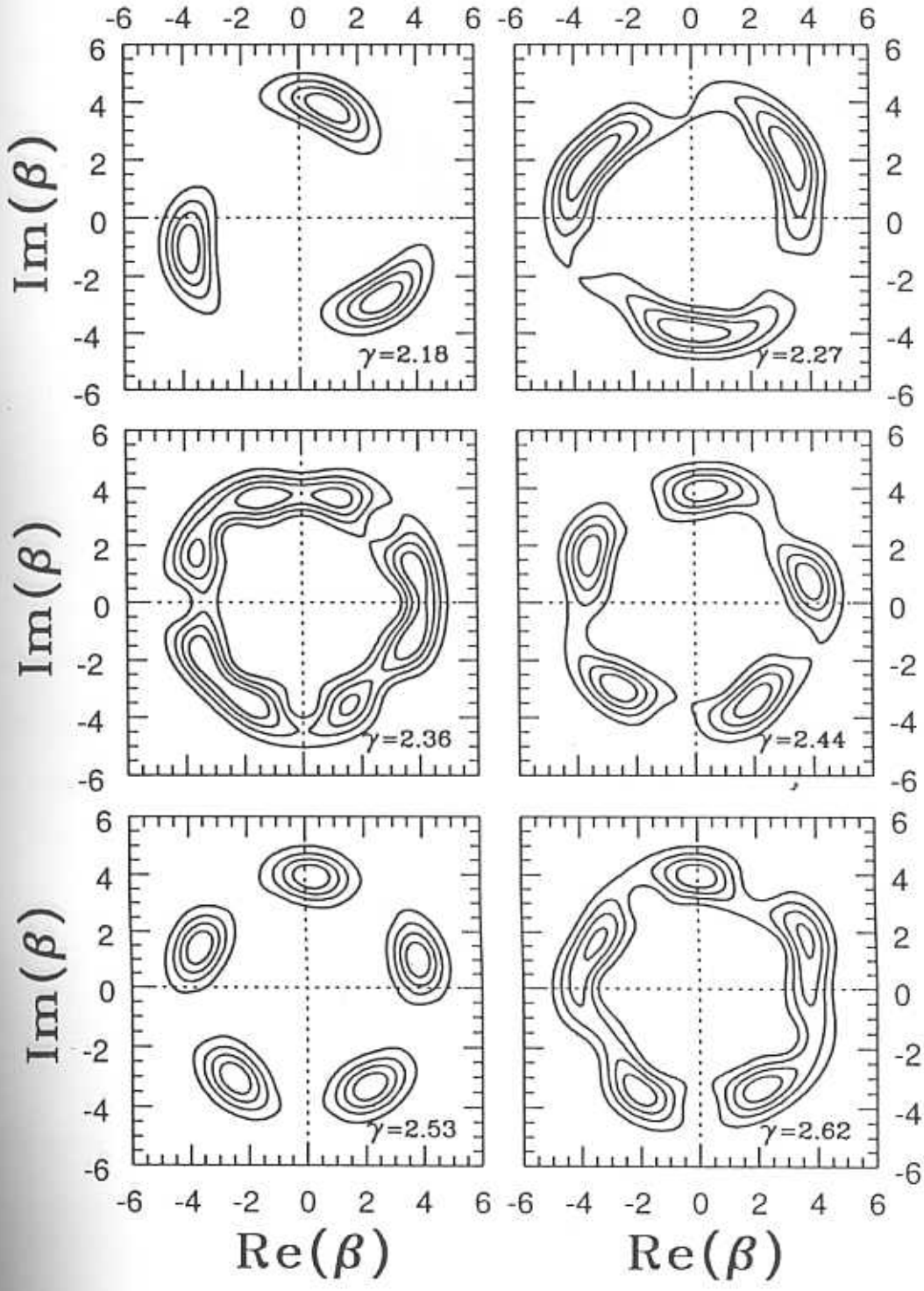

Fig. 4.6. (Cont.) Plot of the contours of the Q-function of the evolution of an amplitude squeezed coherent state ($r = 0.45$) in a Kerr medium. All other parameters are as in Fig. (4.1).

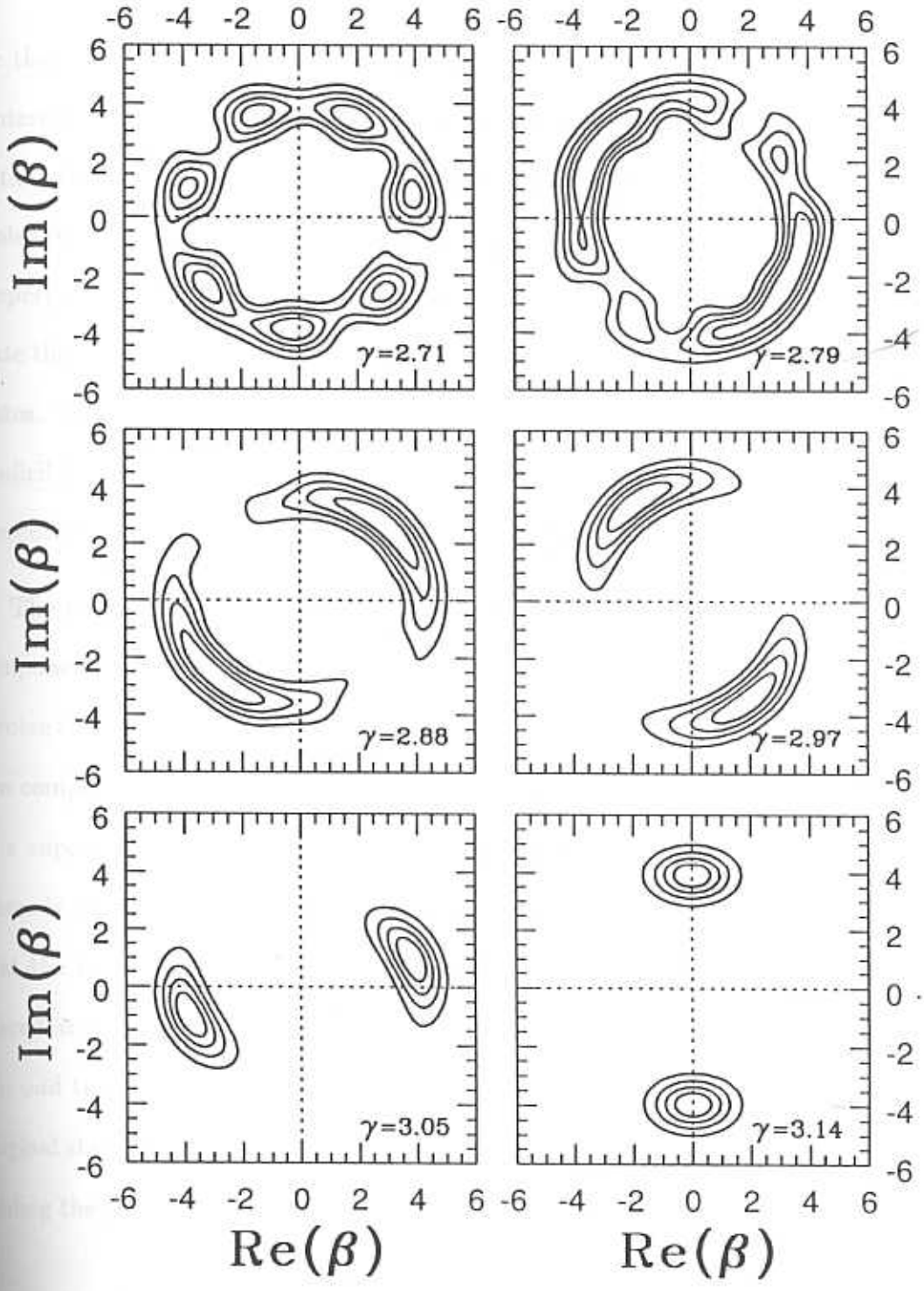

Fig. 4.6. (Cont.) Plot of the contours of the Q-function of the evolution of an amplitude squeezed coherent state ($r = 0.45$) in a Kerr medium. All other parameters are as in Fig. (4.1).

see that these components are distributed along the vertices of a regular polygon centered at the origin of phase space. One such superposition at $\gamma = \pi$ when the initial state is a coherent state, is well known in the literature [241] as the Yurke-Stoler state. These superpositions occur irrespective of the initial state and are the property of the Kerr medium itself. Thus if one takes the initial state as a coherent state then one will get the same superpositions, which will now be made of coherent states. To the best of the author's knowledge, the other superpositions have not been studied in detail. This is one of the reasons why the complete evolution is pictorially presented here. We will look at these superposition in a little more detail.

The most striking superpositions seem to occur at $\gamma = \pi/3$, which involve six components, at $\gamma = \pi/2$ which involve four components, and at $\gamma = 2\pi/3$ which involve three components. Of course at $\gamma = \pi$ there is a superposition which involves two components. There are other values of γ at which the state appears to be close to a superposition and these happen at the values $7\pi/18$, $29\pi/36$ to name a few. There is a regularity, and we can perceive a general trend from the figures. It seems that the superpositions at $\gamma = 2\pi\frac{p}{q}$ involve q components. These components are placed at the vertices of a regular polygon centered at the origin of phase space. If q is odd then one of the components is the original state itself, and if q is even the original state is not present in the components. The crux of the problem reduces to finding the phases χ's in the expansion

$$e^{2\pi i\frac{p}{q}k^2} = \sum_{l=0}^{q-1} e^{i\chi_l} e^{\frac{2\pi kl}{q}+t} \qquad \begin{cases} t = 0 & \text{when } q \text{ odd} \\ t = \pi/q & \text{when } q \text{ even} \end{cases} \tag{4.20}$$

This work is being carried on and it will appear elsewhere [249].

We will now compute the expectation values of the various field quantities when

an initial quadrature squeezed state evolves through the Kerr medium. Our expressions are purposefully general, and we will be considering particular cases of these in the later chapters.

4.4 Expectation values of the field operators

We will first calculate the expectation value of the annihilation operator $\hat{a}$ for the state $|\psi_K\rangle$. This is given by

$$\begin{aligned} \langle \hat{a} \rangle_K &= \langle \psi_K | \hat{a} | \psi_K \rangle \\ &= \langle \alpha, z | \hat{U}^\dagger(\gamma) \hat{a} \hat{U}(\gamma) | \alpha, z \rangle \quad . \end{aligned} \tag{4.21}$$

But the action of the Kerr medium on the annihilation operator can be found in a closed form, and is given by

$$\begin{aligned} \hat{U}^\dagger(\gamma) \hat{a} \hat{U}(\gamma) &= e^{-i\frac{\gamma}{2}\hat{n}(\hat{n}-1)} \hat{a} e^{i\frac{\gamma}{2}\hat{n}(\hat{n}-1)} \\ &= \hat{a} + i\gamma \hat{n}\hat{a} - \frac{\gamma^2 \hat{n}^2 \hat{a}}{2!} - \frac{i\gamma^3 \hat{n}^3 \hat{a}}{3!} + \cdots \\ &= e^{i\gamma\hat{n}} \hat{a} \quad . \end{aligned} \tag{4.22}$$

Hence, using Eq. (4.11) for $|\alpha, z\rangle$, the expectation value of the annihilation operator is calculated to be [219]

$$\langle \hat{a} \rangle_K = \rho e^{i\phi} \mathcal{N}^{-\frac{3}{2}}(\gamma) \mathcal{S}_+(\gamma) e^{\mathcal{P}(\gamma)} \quad , \tag{4.23}$$

where $\mathcal{N}$, $\mathcal{S}$ and $\mathcal{P}$ are functions of γ, which are given by

$$\begin{aligned} \mathcal{N}(\gamma) &= \cosh^2(r) - e^{2i\gamma} \sinh^2(r) \\ \mathcal{P}(\gamma) &= -\rho^2 (1 - e^{i\gamma}) \mathcal{S}(\gamma) / \mathcal{N}(\gamma) \end{aligned}$$

$$\mathcal{S}_{\pm}(\gamma) = 1 + (1 - e^{i\gamma})\left[\sinh^2(r) - \frac{1}{2}\sinh(2r)e^{\pm 2i(\theta-\phi)}\right]$$
$$\mathcal{S}(\gamma) = \frac{\mathcal{S}_{+}(\gamma) + \mathcal{S}_{-}(\gamma)}{2} \quad . \tag{4.24}$$

The expectation values of the other off-diagonal combinations of the creation and annihilation operators of degree less than four are given by

$$\left\langle \hat{a}^2 \right\rangle_K = e^{i\gamma}\mathcal{N}^{-\frac{5}{2}}(2\gamma)e^{\mathcal{P}(2\gamma)}\left[\rho^2 e^{2i\phi}\mathcal{S}_{+}^2(2\gamma) - \frac{1}{2}\sinh(2r)e^{2i\theta}\mathcal{N}(2\gamma)\right]$$
$$\left\langle \hat{a}^\dagger\hat{a}^2 \right\rangle_K = \rho e^{i\phi}e^{i\gamma}\mathcal{N}^{-\frac{7}{2}}(\gamma)e^{\mathcal{P}(\gamma)}\left[\rho^2\mathcal{S}_{+}^2(\gamma)\mathcal{S}_{-}(\gamma) + 2e^{i\gamma}\sinh^2(r)\mathcal{S}_{+}(\gamma)\mathcal{N}(\gamma)\right.$$
$$\left. - \frac{1}{2}\sinh(2r)e^{2i(\theta-\phi)}\mathcal{S}_{-}(\gamma)\mathcal{N}(\gamma)\right] \quad . \tag{4.25}$$

Note that $\left\langle \hat{a}^\dagger \right\rangle_K = \langle \hat{a} \rangle_K^*$ and similarly $\left\langle \hat{a}^{\dagger 2} \right\rangle_K = \langle \hat{a}^2 \rangle_K^*$ and $\left\langle \hat{a}^{\dagger 2}\hat{a} \right\rangle_K = \left\langle \hat{a}^\dagger\hat{a}^2 \right\rangle_K^*$, where * denotes complex conjugation. It can be seen from Eq. (4.24) that the complex conjugate of $\mathcal{N}(\gamma)$ is given by $\mathcal{N}^*(\gamma) = \mathcal{N}(-\gamma)$. Similarly, we have $\mathcal{P}^*(\gamma) = \mathcal{P}(-\gamma)$ and $\mathcal{S}^*(\gamma) = \mathcal{S}(-\gamma)$, but $\mathcal{S}_{\pm}^*(\gamma) = \mathcal{S}_{\mp}(-\gamma)$. The expectation values of the diagonal combinations of the creation and annihilation operators up to the fourth degree are given by

$$\left\langle \hat{a}^\dagger\hat{a} \right\rangle_K = \rho^2 + \sinh^2(r)$$
$$\left\langle \hat{a}^{\dagger 2}\hat{a}^2 \right\rangle_K = \rho^4 + \sinh^2(r)\left[2\sinh^2(r) + \cosh^2(r)\right]$$
$$+\rho^2\left[4\sinh^2(r) + \cos(2\theta - 2\phi)\sinh(2r)\right] \quad . \tag{4.26}$$

When $\gamma = 0$, which corresponds to the absence of the Kerr medium we see from Eq. (4.24) that $\mathcal{N}(\gamma = 0) = 1 = \mathcal{S}_{\pm}(\gamma = 0)$ and hence it follows that $\mathcal{P}(\gamma = 0) = 1$. It can be seen that in this limit, the expectation values of the off-diagonal combinations given in Eq. (4.23),(4.25) correspond to the usual quadrature squeezed state. The expectation values of the diagonal combinations are unaffected by the presence

of the Kerr medium and are independent of γ, as can be seen from Eq. (4.26). On the other hand when $\gamma = \pi$ we have again $\mathcal{N}(\gamma = \pi) = 1$. But

$$\begin{aligned} \mathcal{S}_{\pm}(\gamma = \pi) &= \cosh(2r) - e^{2i(\theta-\phi)} \sinh(2r) \\ \mathcal{S}(\gamma = \pi) &= \cosh(2r) - \cos(2\theta - 2\phi) \sinh(2r) \quad , \end{aligned} \tag{4.27}$$

and hence

$$\mathcal{P}(\gamma = \pi) = -2\rho^2 \left[\cosh(2r) - \cos(2\theta - 2\phi) \sinh(2r)\right] \quad . \tag{4.28}$$

The limit $\gamma = \pi$ can be independently checked in the following way. The unitary operator in Eq. (4.14) acting on a coherent state $|\zeta\rangle$ for $\gamma = \pi$ gives,

$$\frac{1}{\sqrt{2}}\Big(|i\zeta\rangle + e^{i\pi/2}|-i\zeta\rangle\Big) \quad . \tag{4.29}$$

Since we have written the quadrature squeezed state as a coherent state superposition (Eq. 4.11), the quadrature squeezed state $|\alpha, z\rangle$ evolves out of the Kerr medium for $\gamma = \pi$ as,

$$\begin{aligned} |\psi_K\rangle_{\gamma=\pi} &= [2\pi \sinh(r)]^{-\frac{1}{2}} \int_{-\infty}^{\infty} dy\, e^{-\frac{1}{2}(\coth(r)-1)y^2} \\ &\quad \times \frac{1}{\sqrt{2}}\Big(\Big|i\rho e^{i\phi} + iy e^{i\theta}\Big\rangle_{\rm coh} + e^{i\pi/2}\Big|-i\rho e^{i\phi} - iy e^{i\theta}\Big\rangle_{\rm coh}\Big) \quad . \end{aligned} \tag{4.30}$$

Rewriting in terms of the quadrature squeezed states, we have

$$|\psi_K\rangle_{\gamma=\pi} = \frac{1}{\sqrt{2}}\Big(|i\alpha, -z\rangle + e^{i\pi/2}|-i\alpha, -z\rangle\Big) \quad . \tag{4.31}$$

The first ket has the same relative angle between the squeezing direction and the excitation direction $(\theta - \phi)$ as the original quadrature squeezed state, whereas the second ket has a relative angle differing by π. This means that both these states are copies of the original quadrature squeezed state, with the second one displaced in

phase space in direction opposite to that of the first one. Using this quantum state, which involves only superposition of quadrature squeezed states, one can calculate the mean values of the off-diagonal combinations and check that it agrees with the expressions got in the limiting case of the more general expressions in Eq. (4.23), (4.25), by substituting Eq.(4.27,4.28) and $\mathcal{N}(\gamma = \pi) = 1$ into them.

We also see that for the evolution in a Kerr medium the Fano factor, defined as $\langle (\Delta\hat{n})^2 \rangle_K / \langle \hat{n} \rangle_K$, remains unchanged, since it involves only the expectation values of diagonal combinations of the annihilation and creation operators. Similarly the photon number distribution defined by $P_n = |\langle n \mid \psi_K \rangle|^2$ will not change in the evolution through the Kerr medium, since this evolution will only introduce a n-dependent phase in $\langle n \mid \psi_K \rangle$.

We have applied the insights got in the earlier chapters to study the evolution of the quadrature squeezed state in a non-linear Kerr medium. Consistent with our expectations, we find that the evolution of an amplitude squeezed coherent state in a Kerr medium results in a quasi probability distribution which is more suitable for producing a highly amplitude squeezed state, the further study of which we take up in Chapter 6. We have also seen that the evolution gives rise to superposition of quadrature squeezed states, some of which possess very interesting symmetries. In the next chapter, we will study in greater detail a particular type of superposition of quadrature squeezed states, called as the Y-S type superposition, which results from the Kerr medium evolution (when $\gamma = \pi$), from the point of view of amplitude squeezing.

Chapter 5

Amplitude squeezing in quadrature squeezed state superpositions

We formulate and consider a general superposition of quadrature squeezed states and reduce it to the particular class of superpositions that we are interested in. We call this particular class of superpositions as Yurke-Stoler type of superpositions, following the terminology currently vogue in the coherent state case. We then describe a scheme to generate such a superposition of quadrature squeezed states. Since we are interested in amplitude squeezing, we consider the photon number properties of these states and their displaced versions. Finally, we show that a superposition of phase squeezed coherent states, when displaced to a proper position in phase space, is amplitude squeezed, and analytically prove that its photon number uncertainty is smaller than $\langle \hat{n} \rangle^{2/3}$.

5.1 General superposition of quadrature squeezed states

In this chapter, we consider a class of superpositions of quadrature squeezed states which show amplitude squeezing. To consider this restricted class in a proper perspective, we first consider a general superposition of two quadrature squeezed states. The purpose of this section is to restrict such a general superposition to the desired

class that we are interested in. This is done in a systematic and step by step way. Less detailed studies have been carried out in the case of the superposition of squeezed states when compared to superposition of coherent states. Different superpositions of coherent states have been introduced [241, 243, 250, 251], and superpositions of finite number of Fock states have also been studied [240]. Only recently there have been some studies regarding the superposition of quadrature squeezed states [255]. Hence our desire to formulate and consider a general superposition of quadrature squeezed states, and then reduce it to the class of states we are interested in.

A general superposition of two quadrature squeezed states can be written as,

$$|\psi_g\rangle = \mathcal{N}\Big(|\alpha_1, z_1\rangle + \mu e^{i\chi'}|\alpha_2, z_2\rangle\Big) \quad , \tag{5.1}$$

where $\alpha_i = \rho_i e^{i\phi_i}$ and $z_i = r_i e^{2i\theta_i}$. The relative amplitude between the component states is denoted by μ and the relative phase by χ'. We have seen in Chapter 2 that the relative amplitude μ plays a very little role in the qualitative features of the state $|\psi_g\rangle$, except for the extreme values of μ. Hence we may assume that the states are superposed with equal amplitudes without much qualitative loss. Hence we can consider the superposition

$$|\psi''\rangle = \mathcal{N}\Big(|\alpha_1, z_1\rangle + e^{i\chi'}|\alpha_2, z_2\rangle\Big) \quad , \tag{5.2}$$

which preserves most of the qualitative features of the earlier one.

The above superposition as it stands is still quite cumbersome, especially if one wishes to understand the fundamental features of such superpositions. One drawback is that the coherent excitations of the component states are in arbitrary

directions and moreover the squeezing direction and magnitude are also arbitrary. In the coherent state case, we had considered a canonical form from which any superposition of two coherent states can be obtained by simple operations of rotation and displacement. In the superposition given in Eq. (2) such a prescription doesn't seem to sufficiently simple. From the point of view of understanding the features of the superposition of quadrature squeezed states, it is better if we only consider those superpositions whose individual components have the same angle between the direction of squeezing and the direction of coherent excitation. To elaborate, we wish to only consider superposition of two phase squeezed states or two amplitude squeezed states and so on. Note that if such is the case, the angle between the squeezing direction and the direction of excitation should be the same irrespective of where the state is situated in phase space. What we are saying amounts to the superposition in Eq.(2) with the additional condition $\phi_1 - \theta_1 = \phi_2 - \theta_2$.

Again, choosing two states with different amounts of squeezing will lead to a less clear situation because of the presence of an additional parameter. Moreover, the magnitude of squeezing of one of the components differing from the other doesn't offer many new insights, and one could judge the effect of this difference from the features of a superposition in which both components have the same magnitude of squeezing. Hence we choose the superposition

$$|\psi'\rangle = \mathcal{N}\left(\left|\alpha_1, re^{2i\theta_1}\right\rangle + e^{i\chi'}\left|\alpha_2, re^{2i\theta_2}\right\rangle\right)$$
$$\phi_1 - \theta_1 = \phi_2 - \theta_2 \qquad (5.3)$$

It should be carefully noted at this stage that the above superposition is different from the squeezed operator acting on a superposition of coherent states, as is obvious

by looking at the direction of squeezing of the two component state which are still different, the only condition being that $\phi_1 - \theta_1 = \phi_2 - \theta_2$. This superposition can now be reduced to a canonical form from which all such superpositions in this class can be obtained. The reduced or the canonical form can be written as

$$|\psi_c\rangle = \mathcal{N}\Big(|-x,z\rangle + e^{ix}|x,z\rangle\Big) \quad , \tag{5.4}$$

since, fixing $\phi_1 = \phi_2$ immediately fixes $\theta_1 = \theta_2$, and where we have used $z = re^{2i\theta}$, in accordance with our earlier convention. Note that, as before, by applying a rotation and displacement operator, one can get the whole class of superpositions given by Eq. (3).

At this stage, one can say that the above reduced form is got by applying the squeeze operator to the original coherent state case canonical form

$$|\psi_c\rangle = \hat{S}(z)\,|\psi_c\rangle_{\rm coh} \quad . \tag{5.5}$$

Hence, the class of quadrature squeezed states that we are concerned with are given by

$$|\psi\rangle = \widehat{D}(\beta)\hat{R}(\tau)\hat{S}(z)\,|\psi_c\rangle \quad , \tag{5.6}$$

where the operation of $\widehat{D}(\beta)\hat{R}(\tau)$ were explained earlier in Chapter 2.

We restrict ourselves to this form because it gives a clear picture of what the inclusion of squeezing does to a superposition. This is especially so, since we have studied in detail the coherent state case, and we can clearly hope to see the effect of the inclusion of squeezing on that. Moreover, from the knowledge gained by studying this superposition state $|\psi_c\rangle$, one can in principle at least qualitatively predict the features of a general superposition of two quadrature squeezed states. Another

important point is that a general superposition of two quadrature squeezed states has little feasibility of being experimentally realized at the current juncture, even in principle. But the form that we choose to study has a feasibility for experimental generation [257, 219, 256], at least in principle, for particular values of χ.

5.2 The Yurke-Stoler type superpositions

We have seen several times in the earlier chapters that a state evolving through a Kerr medium with the scaled time of evolution $\gamma = \pi$ results in a superposition of the initial states with a relative phase $\chi = \pi/2$ [197]. We have mentioned that this state is called a Yurke-Stoler (Y-S) [241] state when the initial state is a coherent state. We have also seen that a Y-S state on displacement shows amplitude squeezing[242]. The problem there was that there exists a specific magnitude of displacement for which the amplitude squeezing is maximum. Any further displacement will reduce the amount of amplitude squeezing. This is so since the Y-S state has a curved quasi probability distribution and beyond the optimum displacement this distribution cuts more number of Fock circles[253, 254] which reduces the amplitude squeezing. Hence one cannot have much amplitude squeezing at large intensities and this essentially reduces the scheme of using the Y-S state to get amplitude squeezed light to very low photon regime. The ideal way of improving this optimum displacement will be to reduce the curvature of the initial state. As seen in Chapter 2, this can be done by choosing a relative phase smaller than $\pi/2$. But there is no known way in which one can generate a superposition with a arbitrary relative phase, in the optical regime. The other alternative will be to try to use the quadrature squeezed

state to get a Y-S type of superposition, with the expectation that with a proper choice of direction of squeezing of the initial state, one can get a superposition state, the effective curvature of whose quasi probability distribution is small. This can be done since the Kerr medium produces a Cat state irrespective of the initial state, as it is the property of the Kerr medium evolution itself, as mention in Chapter 4.

Hence, in this chapter we wish to consider only the Y-S type of superposition of quadrature squeezed states, which is realisable experimentally, at least in principle [219, 256]. This Y-S type of superposition can be written as,

$$|\psi_K\rangle = \frac{1}{\sqrt{2}}\Big(|\alpha, z\rangle + e^{i\frac{\pi}{2}}|-\alpha, z\rangle\Big) \quad . \tag{5.7}$$

The only two additional parameters here than in the usual Y-S state is the magnitude of squeezing r and the relative angle $\theta - \phi$ between the direction of squeezing and the direction of coherent excitation. As usual $\alpha = \rho e^{i\phi}$ and $z = re^{2i\theta}$. Our interest is to show that on displacing such a Y-S type superposition of quadrature squeezed states, one can get amplitude squeezed light with high intensity. The experimental scheme for achieving these states is given in Fig. (5.1). One can start with the output of a ring laser generating light at two frequencies ω and 2ω which are orthogonally polarized, is split into two beams at the polarizer P_1. The high frequency component is used to pump the Optical Parametric Oscillator (OPO). The signal that comes out of the OPO is at a frequency ω[116]. This signal is then passed through a Kerr medium of predetermined length. The technical difficulty will be to get a Kerr medium with a high enough non-linearity to produce an evolution till $\gamma = \pi$ within an acceptable time of passage through the Kerr medium. Longer times will essentially introduce losses and the associated noise due to it. In fact, at present

it is precisely this problem which makes the experimental generation of this state difficult. The local oscillator beam at frequency ω forms the other arm of a Mach-Zehnder interferometer which also contains a time delay δ. This beam and the signal

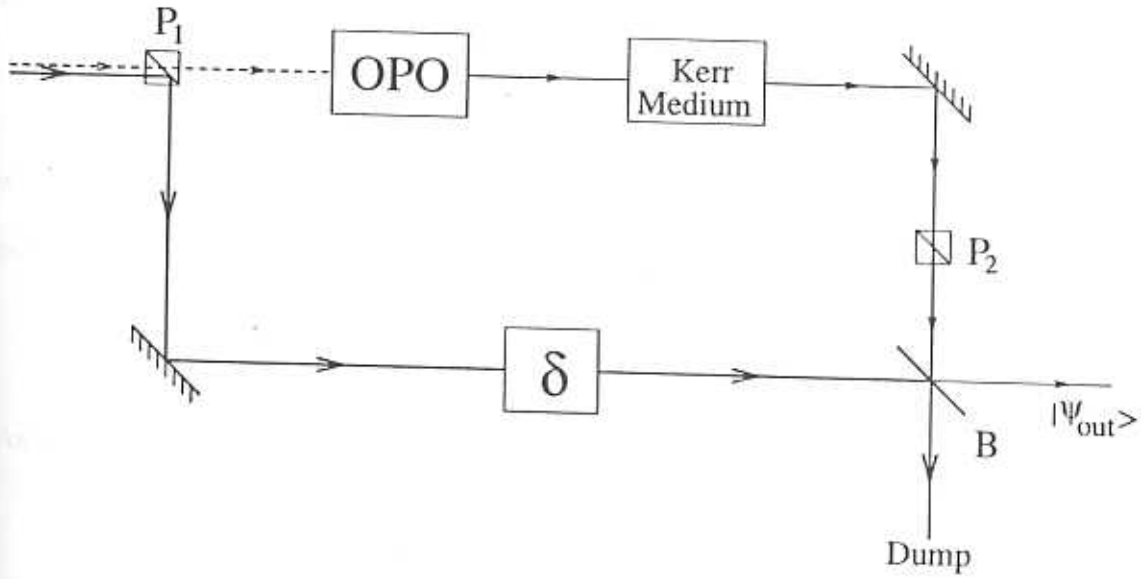

Fig. 1

Fig. 5.1. Schematic of the proposed scheme. The dotted and solid lines represent light at frequencies 2ω and ω respectively. P_1,P_2 are polarizers and B is a highly reflective beam splitter. δ indicates the phase shift introduced into the reference beam.

beam are recombined at the beam splitter B which has a high reflectivity. The high reflectivity prevents the signal from being contaminated by the local oscillator. But at the same time, for a high intensity of the local oscillator beam, the effect of this beam splitter is to produce a displacement in phase space for the signal beam [191]. The angle of this displacement can be adjusted by varying the time delay and the magnitude by adjusting the strength of the reference beam. Typically the OPO operates in the sub-threshold regime[112, 113, 114], and when acting as

an amplifier generates Phase Squeezed Coherent States, and Amplitude Squeezed Coherent States when acting as a deamplifier.

We begin the analysis by rewriting the Hamiltonian for the radiation field in the rotating wave approximation inside the Kerr medium, which is given by[197],

$$H_K = \hbar\omega\hat{a}^\dagger\hat{a} + \chi_{NL}\hat{a}^{\dagger 2}\hat{a}^2 \quad , \tag{5.8}$$

where the anharmonicity parameter χ_{NL} is real and is proportional to the third order non-linear susceptibility. The time evolution operator is written as,

$$U_K(\tau) = \exp(-\frac{i}{\hbar}\widehat{H}\tau) = \exp(-i\omega\hat{a}^\dagger\hat{a}\tau)\,\exp(-i\frac{\chi_{NL}}{\hbar}\hat{a}^\dagger\hat{a}(\hat{a}^\dagger\hat{a}-1)\tau) \quad . \tag{5.9}$$

As seen earlier, this unitary operator acting on a coherent state $|\beta\rangle$ gives,

$$|\beta,\tau\rangle = e^{-|\beta|^2/2}\,e^{-i\omega\widehat{a}^\dagger\widehat{a}\tau}\sum_{n=0}^{\infty}\frac{\beta^n}{\sqrt{n!}}e^{-i\chi_{NL}n(n-1)\tau/\hbar}\,|n\rangle \quad . \tag{5.10}$$

If one chooses the physical dimensions of the Kerr medium in such a way that the beam spends a time $\tau_K = \hbar\pi/2\chi_{NL}$ inside the Kerr medium, the state of the radiation field that emerges out of the Kerr medium is given by[241]

$$\frac{1}{\sqrt{2}}\Big(|i\beta\rangle + e^{i\pi/2}|-i\beta\rangle\Big) \quad , \tag{5.11}$$

where we have ignored the free evolution part.

Since we have written the quadrature squeezed state as a coherent state superposition (Eq. 4.11) [246, 247, 248, 219], the quadrature squeezed state $|\alpha,z\rangle$, after spending a time τ_K ($\gamma=\pi$) evolves out of the Kerr medium as,

$$\begin{aligned}|\psi_K\rangle_{\gamma=\pi} \;=\; & [2\pi\sinh(r)]^{-\frac{1}{2}}\int_{-\infty}^{\infty}dy\,e^{-\frac{1}{2}(\coth(r)-1)y^2} \\ & \frac{1}{\sqrt{2}}\Big(\Big|i\rho e^{i\phi}+iye^{i\theta}\Big\rangle_{\rm coh}+e^{i\pi/2}\Big|-i\rho e^{i\phi}-iye^{i\theta}\Big\rangle_{\rm coh}\Big) \quad .\end{aligned} \tag{5.12}$$

Rewriting in terms of the quadrature squeezed states, we have

$$|\psi_K\rangle_{\gamma=\pi} = \frac{1}{\sqrt{2}}\Big(|i\alpha,-z\rangle + e^{i\pi/2}|-i\alpha,-z\rangle\Big) \quad . \tag{5.13}$$

The first ket has the same relative angle between the squeezing direction and the excitation direction $(\theta-\phi)$ as the original quadrature squeezed state, whereas the second ket has a relative angle differing by π as compared to the first ket. This means that both states are the same quadrature squeezed states as the original quadrature squeezed state, but with second one displaced in the opposite direction to that of the first one in phase space. Using this quantum state, which involves only superposition of quadrature squeezed states, one can readily calculate the mean values of the various field quantities. The beam that comes out of the final beam splitter will be in the quantum state

$$|\psi_d\rangle = \widehat{D}(\xi)\,|\psi_K\rangle \quad , \tag{5.14}$$

where ξ is parameterized as $\eta e^{i\Lambda}$. We now proceed to calculate the photon number uncertainty of the state $|\psi_d\rangle$.

The photon number uncertainty can be described in terms of the Fano factor, defined as

$$f_n = \frac{\langle(\Delta\hat{n})^2\rangle}{\langle\hat{n}\rangle} = 1 + \frac{\left\langle \hat{a}^{\dagger 2}\hat{a}^2\right\rangle - \left\langle \hat{a}^\dagger\hat{a}\right\rangle^2}{\langle\hat{a}^\dagger\hat{a}\rangle} \quad . \tag{5.15}$$

The Fano factor is just the normalized variance which gives the deviation from the Poissonian photon distribution. The value of $f_n = 1$ corresponds to poissonian distribution, and $f_n < 1$ to the sub-poissonian and $f_n > 1$ to the super-poissonian distribution. It is related to the oft quoted Mandel Q parameter[234] by $Q = f_n - 1$. The Fano factor in our case can be written as

$$f_n'(\eta) = 1 + \frac{p_0 + p_1\eta + p_2\eta^2}{q_0 + q_1\eta + \eta^2} \quad , \tag{5.16}$$

where

$$
\begin{aligned}
p_0 &= \frac{1}{\rho^2}\left(\left\langle \hat{a}^{\dagger 2}\hat{a}^2\right\rangle_K - \left\langle \hat{a}^\dagger\hat{a}\right\rangle_K^2\right) \quad , \\
p_1 &= \frac{2}{\rho}\left\{e^{-i\Lambda}\left[\left\langle \hat{a}^\dagger\hat{a}^2\right\rangle_K - \left\langle \hat{a}^\dagger\hat{a}\right\rangle_K\langle\hat{a}\rangle_K\right] + C.C.\right\} \quad , \\
p_2 &= \left\{e^{-2i\Lambda}\left[\left\langle \hat{a}^2\right\rangle_K - \langle\hat{a}\rangle_K^2\right] + C.C\right\} + 2\left[\left\langle \hat{a}^\dagger\hat{a}\right\rangle_K - \left\langle \hat{a}^\dagger\right\rangle_K\langle\hat{a}\rangle_K\right] \quad , \\
\\
q_0 &= \frac{1}{\rho^2}\left\langle \hat{a}^\dagger\hat{a}\right\rangle_K^2 \quad , \\
q_1 &= \frac{2}{\rho}|\langle\hat{a}\rangle_K|\cos(\Lambda) \quad ,
\end{aligned}
\tag{5.17}
$$

In this form, one can immediately minimize the Fano factor with respect to η, the magnitude of ξ, and the optimized value of the Fano factor is then given by

$$f_n = f_n'(\eta_o) \quad . \tag{5.18}$$

Similarly, the photon number distribution of the displaced state can be calculated using the definition,

$$
\begin{aligned}
P_n &= |\langle n\,|\psi_d\rangle|^2 \\
&= \left|\langle n\,|\,\widehat{D}(\xi)\,|\psi_K\rangle\right|^2 \quad .
\end{aligned}
\tag{5.19}
$$

But the action of the displacement operator on the Fock state on the left can be calculated to be

$$
\begin{aligned}
\langle n\,|\,\widehat{D}(\xi) &= e^{-\frac{1}{2}|\xi|^2}\,\langle n\,|\,e^{\xi\hat{a}^\dagger}e^{-\xi^*\hat{a}} \\
&= e^{-\frac{1}{2}|\xi|^2}\sum_{m=0}^{n}\frac{\xi^m}{m!}\sqrt{\frac{n!}{(n-m)!}}\times \\
&\qquad \sum_{k=0}^{\infty}\frac{(-\xi^*)^k}{k!}\sqrt{\frac{(n-m+k)!}{(n-m)!}}\,\langle n-m+k\,| \quad .
\end{aligned}
\tag{5.20}
$$

Using this and the integral representation of the quadrature squeezed state as a coherent state superposition in Eq. (4.11), we have

$$P_n = \frac{n!}{\cosh(r)} e^{-(\rho^2+|\xi|^2)} \left| e^{\frac{1}{2}\tanh(r)\rho^2 e^{2i(\theta-\phi)}} \sum_{k=0}^{\infty} \frac{(-\xi^*)^k}{k!} \times \right.$$
$$\sum_{m=0}^{n} \frac{\xi^m}{m!(n-m)!} e^{-i\frac{\pi}{2}(n-m+k)(n-m+k-1)} \sum_{s=0}^{[\frac{n-m+k}{2}]} \frac{(n-m+k)!}{(n-m+k-2s)!s!} \times$$
$$\left. \left[\frac{e^{2i\theta}\tanh(r)}{2}\right]^s \left\{\rho e^{-i\phi}\left[e^{2i\phi} - e^{2i\theta}\tanh(r)\right]\right\}^{n-m+k-2s} \right|^2 \qquad (5.21)$$

With this general result for the superposition of quadrature squeezed states in the canonical form, we now turn our attention to particular cases of $\theta - \phi$, which show amplitude squeezing.

5.3 Amplitude squeezed states from superposition of phase squeezed coherent states

In this section, we study the state that comes out of the scheme described in the previous section when the initial state is a phase squeezed coherent state. For a phase squeezed coherent state we have $\theta - \phi = 0$, which means that the direction of squeezing is perpendicular to the direction of coherent excitation. As pointed out earlier, the usual Y-S state has a limited scope when it comes to getting an intense amplitude squeezed light. This is because the state can be displaced to a farther position only if the separation between them is large. But a large separation between the states results in very low interference of the states in phase space, and such a state would look more like a statistical mixture of coherent states. But one can avoid this if one is to consider an initial phase squeezed state. Here, one can separate the centers farther away and at the same time keep the interference

between the states at the desired level by increasing the magnitude of squeezing. Hence one can envisage the situation in which one can always find a suitable value of the magnitude of squeezing after which the state will behave like a superposition irrespective of the actual separation between the states.

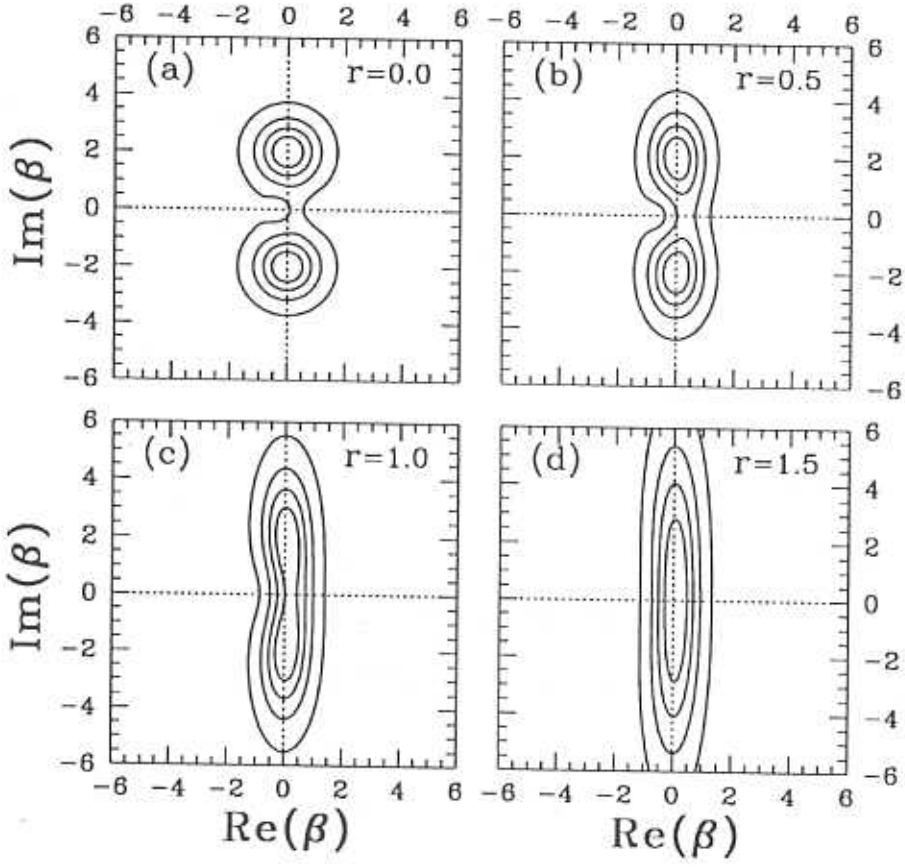

Fig. 5.2. Plot of the contours of the Q-function of an initial phase squeezed coherent state that has evolved through the Kerr medium for $\gamma = \pi$. The contours are at 0.05, 0.25, 0.5, and 0.75 times the maximum value. The value of the magnitude of squeezing is indicated in the figure itself, and in all the figures $\rho = 2$.

We plot the Q-function of this state to demonstrate the above argument pictorially. In Fig.(5.2), we plot the contours of the Q function for a phase squeezed state that has evolved through a Kerr medium to form a macroscopic superposition. The

initial magnitude of displacement ρ is chosen to be 2 in all cases. Here we draw attention to the change in the Q-function as one increases the value of the magnitude of squeezing r. The value of the magnitude of squeezing r is indicated in the figure. Note that when $r = 0$ the initial state is a coherent state and the final state is a Y-S state. The contours in all the figures are at 0.05, 0.25, 0.5, and 0.75 of the maximum value. In all the figures except Fig. (5.2a) we have taken a phase squeezed coherent state ($\theta - \phi = 0$), with the same mean for different values of squeezing r, by choosing an appropriate value for ρ^2. It can be seen that with the increase in the magnitude of squeezing there is a strong interference which results in a slightly curved distribution as in Fig. (5.2c). Further increase in squeezing magnitude straightens this completely, and the resultant state looks more like a quadrature squeezed vacuum as in Fig. (5.2d).

From the figures it is possible to deduce that the ideal direction of displacement for getting the maximum squeezing will be along the x-axis of phase space. Hence we have $\Lambda = 0$. With this Choice of Λ, the coefficients of the powers of k in Eq. (5.17) can be written as

$$\begin{aligned} p_0 &= \sinh^2(r)\cosh(2r) + \rho^2(e^{2r} - 1) \\ p_1 &= \rho e^{-2\rho^2 e^{-2r}}\left(-4\rho^2(e^{-6r} + e^{-2r}) + 2(e^{-4r} - e^{-2r})\right) \\ p_2 &= e^{-2r} - 1 - 4\rho^2 e^{-4\rho^2 e^{-2r}} e^{-4r} \end{aligned}$$

$$q_0 = \sinh^2(r) + \rho^2 \quad , \qquad q_1 = 2\rho e^{-2\rho^2 e^{-2r}} e^{-2r} \quad . \tag{5.22}$$

These values are substituted in Eq. (5.16), and the optimized value of the magnitude of displacement η_o thus obtained, is used in calculating the optimized Fano factor

given by $f_n = f_n'(\eta_o)$.

In Fig. (5.3), the logarithm of the optimized Fano factor f_n is plotted along with the logarithm of the optimum magnitude of displacement η_o, for various values of the separation ρ indicated in the figure. We call the initial displacement of the phase squeezed coherent state ρ as the separation, since the separation of the superposed states has to depend on ρ. The state with the quadrature squeezing $r = 0$ corresponds to a Yurke-Stoler state. In Fig. (5.3), one sees that the Fano factor in

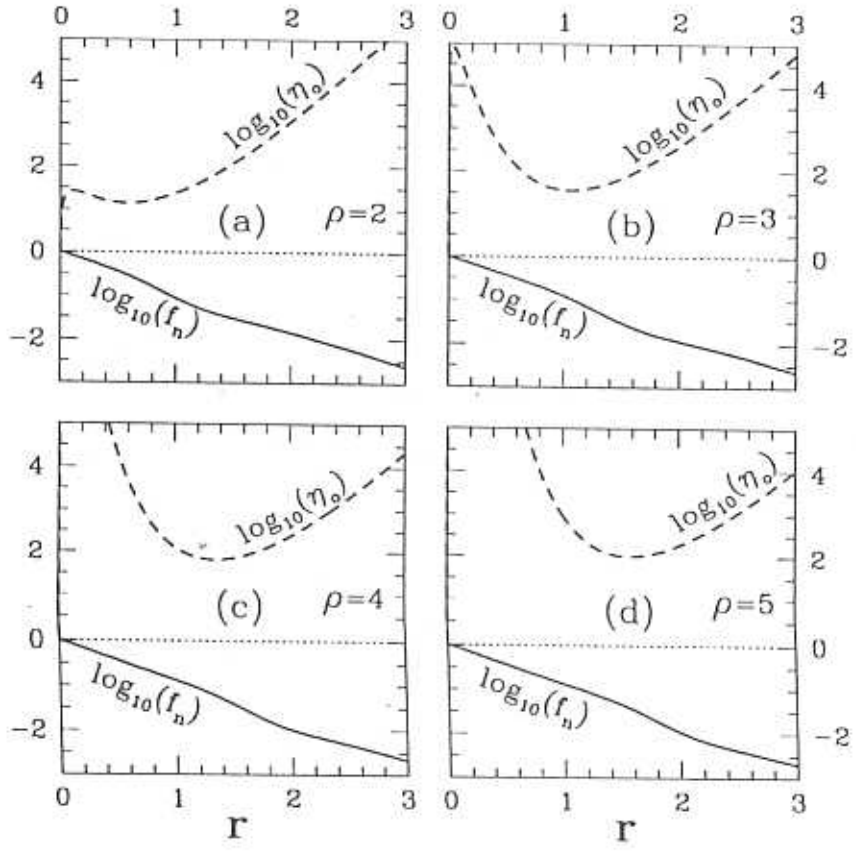

Fig. 5.3. Plot of the logarithm of the optimized Fano factor (Solid line) along with the logarithm of the optimum magnitude of displacement (Dashed line) as indicated in the figure, as a function of quadrature squeezing r for various values of separation ρ. These values are for the state $|\psi_d\rangle$ with an initial phase squeezed coherent state that has evolved through a Kerr medium for $\gamma = \pi$.

this limit goes to one, since the separations are far too large for two coherent states to have any substantial interference in phase space. Hence, at these separations they are more like a statistical mixture of coherent states. On the other hand for very small quadrature squeezing there is a very weak interference and hence one has to displace such a state to a very large distance in phase space to minimize the Fano factor. Hence one sees that η_o rather blows up for small squeezing, especially for large values of the separation ρ [Fig. (5.3c,d)]. This can be judged from the nature of the state $|\psi_K\rangle$ in this regime, by looking at the Q-function given in Fig. (5.2b). Since the squeezing is not large, even though there is interference, it is not effective enough. On the other hand, at very large squeezing, the state $|\psi_d\rangle$ is more like an amplitude squeezed coherent state, as can be seen from the behavior of the Fano factor in Fig. (5.3) and the shape of the Q-function of $|\psi_K\rangle$ in Fig. (5.2d). In between there exists an ideal squeezing value for a given separation ρ, at which the photon number uncertainty goes to a minimum. In the scale of Fig. (5.3) this just appears as a saddle point in the Fano factor.

On the other hand, if one plots the logarithm of the photon number uncertainty, along with the logarithm of the mean photon number, as is done in Fig. (5.4), then it is obvious that the Fano factor goes to a minimum. Since the Fano factor is defined as the ratio of the photon number uncertainty to the mean photon number, for low quadrature squeezing, one can see that the two curves nearly coincide and this implies that the Fano factor is close to its coherent state value of unity. With increasing r, both the mean and the number uncertainty decrease after the initial increase and then increases steadily for large values of r. But it can be seen that as a function of r, the mean photon number starts to increase while the photon number

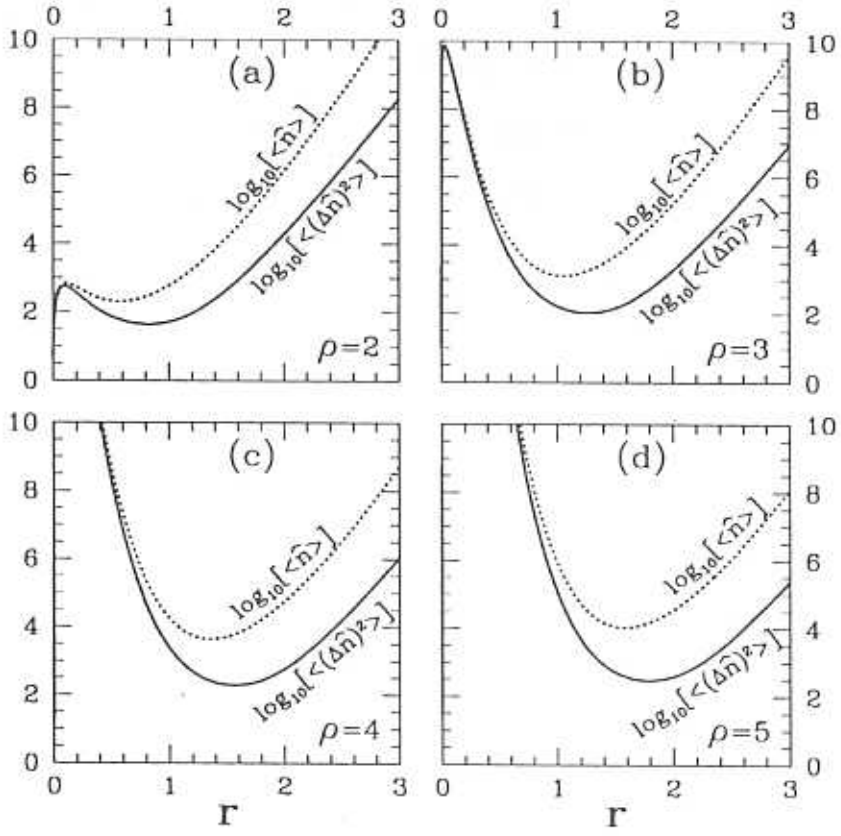

Fig. 5.4. Plot of the logarithm of photon number uncertainty (Solid line) along with the plot of the mean photon number (Dotted line). The other details are same as in the previous figure.

uncertainty is still decreasing, and it is at this region that the Fano factor goes to a minimum.

In Fig. (5.5), the logarithm of the absolute minimum value of the Fano factor is plotted as function of the quadrature squeezing r. Here, for each value of r, the whole range of the separation ρ is scanned numerically and the separation ρ_o corresponding to the minimum value of the Fano factor among these is found. The Fano factor corresponding to this value of ρ_o for a given r is the absolute minimum possible for this given value of squeezing. It can now be seen that the Yurke-Stoler

state, which corresponds to $r = 0$ shows amplitude squeezing. In fact this is the maximum amplitude squeezing that can be got from a Yurke-Stoler state. We see that for small values of r and for $r = 0$ (Y-S state), the optimum value of separation is smaller than unity ($\rho_o < 1$) [whereas in Fig. (5.3) the ρ values are chosen larger

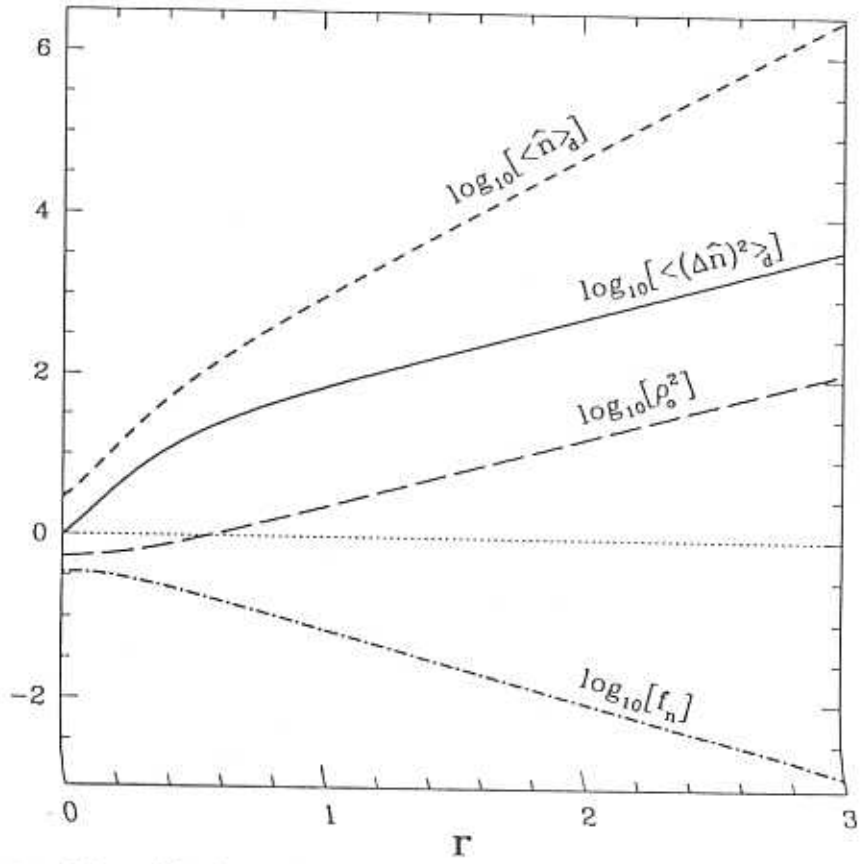

Fig. 5.5. Plot of the logarithm of the absolute minimum of the Fano factor which is got by optimizing the separation ρ. The logarithm of the optimum separation ρ_o for a given value of squeezing is also plotted. The logarithm of the photon number uncertainty and the mean photon number corresponding to the Fano factor obtained in the above way is also plotted.

than one]. It can also be seen that this absolute minimum of the Fano factor for a given value of r, does not show a minimum as a function of r. In this respect the state $|\psi_d\rangle$, which is a superposition of phase squeezed coherent states behaves more

like an amplitude squeezed coherent state. To elaborate further, the slope of the curve corresponding to the Fano factor as a function of r tends to a constant value. The logarithm of the photon number uncertainty and the mean photon number, whose ratio gives the Fano factor is also plotted in the same figure.

In Fig. (5.6), the photon number distribution P_n is plotted for different values of r

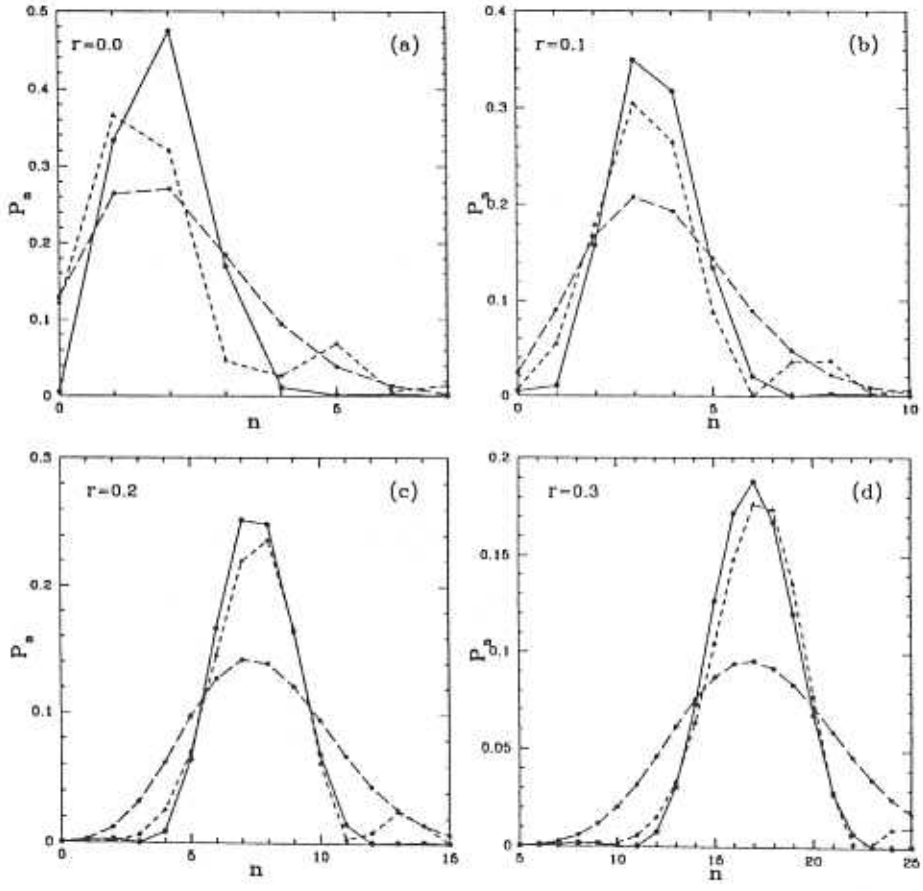

Fig. 5.6. Plot of the photon number distribution P_n Vs. n for different values of squeezing r. For each value of r the optimum separation ρ_o is numerically estimated and the P_n for the corresponding state is plotted (Solid line with Solid circles). For comparison the photon number distribution of an amplitude squeezed coherent state (Dashed line with solid triangles) and a coherent state (Long dashed line with Solid squares) with the same mean is plotted.

for the state $|\psi_d\rangle$, which is in a superposition of phase squeezed coherent states. For

each value of r, the optimum value of the separation ρ_o is estimated numerically [see Fig. (5.5)], at which the Fano factor goes to an absolute minimum, and the photon number distribution P_n, which is given in Eq. (5.21), corresponding to these values is plotted (Solid line with circles). For comparison the photon number distribution of an amplitude squeezed coherent state with the same mean photon number (Dashed line with triangles) and a coherent state with the same mean photon number (Long dashed lines with squares) are also plotted. It can be seen from these figures that this state $|\psi_d\rangle$ is slightly more sub-poissonian than the amplitude squeezed coherent state.

In fact one can analytically show that the photon number uncertainty of this state $|\psi_d\rangle$ is $\langle(\Delta\hat{n})^2\rangle_d < \langle\hat{n}\rangle_d^{2/3}$, which is smaller than that for the amplitude squeezed coherent state. We have mentioned earlier, that for a given separation if the squeezing is increased beyond a certain limit, the resulting state looks more like the squeezed vacuum [Fig. (5.2d)]. If one displaces this state along the direction of squeezing one should get just an amplitude squeezed state, whose photon number uncertainty is bounded from below by $\langle\hat{n}\rangle^{(2/3)}$. But as noticed in [Fig. (5.2c)], there is an intermediate squeezing value where the superposition state has a slight curvature. It is exactly for this curved state that the photon number uncertainty falls below the amplitude squeezed coherent state value. Saying it the other way around, for each given magnitude of squeezing r, there exists a certain range of values for ρ at which the photon number uncertainty falls below the amplitude squeezed coherent state value.

To illustrate, in Fig. 5.7, a plot of the logarithm of the optimized Fano factor f_n for various values of squeezing r is given. The abscissa is proportional to the

separation of the states in phase space and is the phase squeezed coherent state's magnitude of displacement ρ. It should be noted that $\rho = 0$ represents the usual amplitude squeezed coherent state got by displacing the quadrature squeezed vacuum along the direction of squeezing. When the squeezing $r = 0$ it corresponds to the Yurke-Stoler state. It can be seen from the figure that f_n is more or less a constant

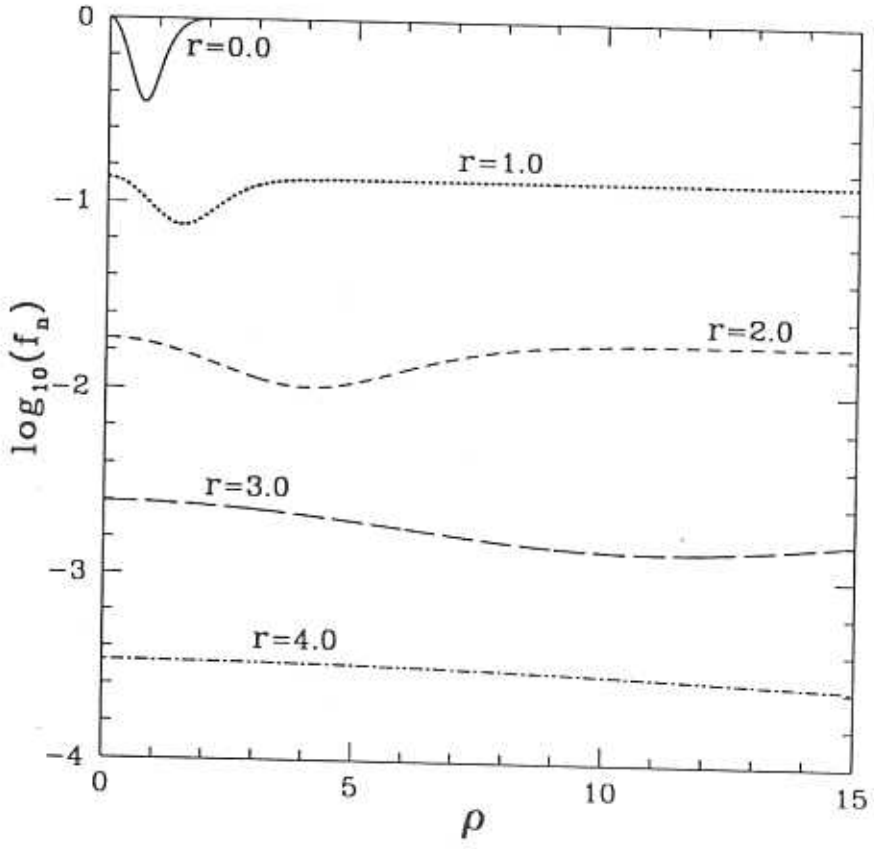

Fig. 5.7. Plot of the logarithm of the optimized Fano factor f_n Vs. the separation ρ for various values of squeezing r indicated in the figure. The curve for $r = 0$ gives the Fano factor for the Yurke-Stoler state. Note that $\rho = 0$ corresponds to the usual amplitude squeezed coherent state.

and equals the value for the amplitude squeezed coherent state for large values of ρ, for a given value of r. In this respect this state differs from the Yurke-Stoler

state for which f_n tends to the coherent state value for large ρ. The dip that occurs for various values of squeezing shows the range of ρ values at which the interference between the constituent states of the macroscopic superposition is maximum. In Fig. 5.8 a plot of the logarithm of $f_n'(\eta)$ against the logarithm of η is given for two representative values of ρ at different squeezing. It shows that for the η values beyond the optimal value, the Fano factor levels off to a constant, and hence the

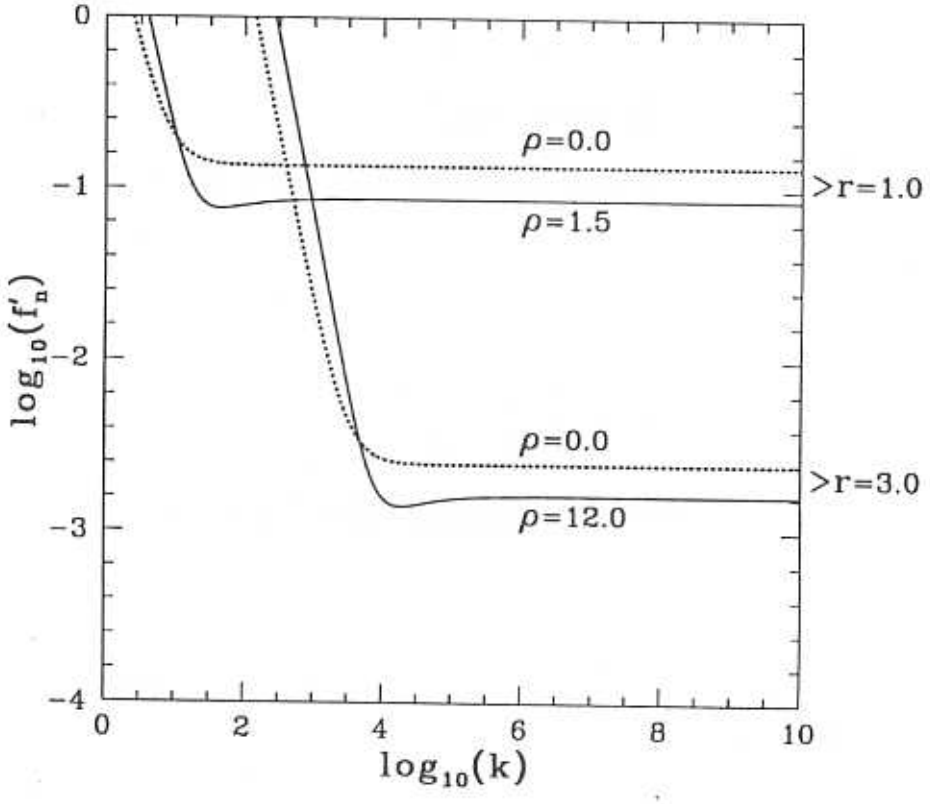

Fig. 5.8. Plot of the logarithm of the Fano factor f_n' Vs. the magnitude of displacement η for two values of squeezing indicated in the figure. For each value of squeezing the dotted line corresponds to the usual amplitude squeezed coherent state and the solid line corresponds to the displaced superposition around the optimal separation indicated in the figure.

photon number uncertainty beyond this η value increases with increasing η. The

value chosen for ρ here is close to the optimal value, which is the value at which the dip occurs in Fig. 5.7. One can see that at the optimal value of η, the Fano factor for the quantum state $|\psi_d\rangle$ is lower than the amplitude squeezed coherent state value. This leads one to suspect the $\langle (\Delta\hat{n})^2 \rangle$ falls below $\langle \hat{n} \rangle^{2/3}$. We now analytically show that this indeed is the case.

Going back to Eq. (5.22), we see that q_0, q_1 and p_0 are always positive and the dip in Fig. 5.7 occurs when p_1 and p_2 are maximum negative. But note that the way in which ρ enters p_1 and p_2 forbids any drastic change. The dip occurs when ρ is approximately in the range $e^r/2 < \rho < e^r/\sqrt{2}$. For small values of r the minimum of f_n' occurs around $\rho \simeq e^r/\sqrt{2}$. But even for moderate values of r the minimum of f_n' occurs around $\rho \simeq e^r/2$. Hence we assume $\rho \simeq e^r/2$. Considering only those terms which are significant when $r > 1$, the Fano factor can be written as,

$$f_n' \simeq \frac{3}{8}\frac{e^{4r}}{\eta^2} - \frac{1}{2}\frac{e^{2r}}{\eta^2} - \frac{1}{2}\frac{e^{r-1/2}}{\eta} \quad . \tag{5.23}$$

Extremising the above equation with respect to r we find that the extremum occurs when

$$e^r(\simeq) > (\frac{e^{-1/2}}{3})^{1/3}\eta^{1/3} \quad , \tag{5.24}$$

where we have used $(\simeq) >$ to denote that e^r is slightly greater than the right hand side. This means that the Fano factor

$$f_n'(\simeq) < \eta^{-2/3} \quad . \tag{5.25}$$

Since the mean photon number is of the order of $\langle \hat{n} \rangle \approx \eta^2$, we have

$$\left\langle (\Delta\hat{n})^2 \right\rangle (\simeq) < \langle \hat{n} \rangle^{2/3} \quad . \tag{5.26}$$

which shows that around the optimal value of ρ for a given amount of squeezing, the photon number uncertainty is smaller than in the usual amplitude squeezed coherent state.

There are many more exciting possibilities, when one considers the superposition of quadrature squeezed states. Much work can be done in this area. Even though experimentally difficult to achieve, superpositions are nevertheless studied to again a deeper insights into the various aspects of the problem, which might lead to a better way of generating more amplitude squeezed states of the radiation field.

In this chapter, we have formulated a general superposition of quadrature squeezed states and then reduced it to the class of superpositions of the Yurke-Stoler type. We then studied the motivations for believing that such superpositions when displaced could show better amplitude squeezing. A scheme was proposed to generate a displaced Yurke-Stoler type of macroscopic superposition of quadrature squeezed coherent states. A particular case, in which a superposition of phase squeezed coherent states was used to generate an amplitude squeezed state, was studied in detail. We have shown analytically that the photon number uncertainty of the displaced superposition of phase squeezed coherent states is smaller than in the usual amplitude squeezed coherent states.

Chapter 6

Highly amplitude squeezed states of the radiation field

In this chapter we study the highly amplitude squeezed states that can be got by evolving an amplitude squeezed coherent state through a Kerr medium and then displacing it to a proper position in phase space. We first describe the scheme with which one can achieve these states, and then calculate the Fano factor and the photon number distribution of the beam coming out of this scheme. We optimize the various parameters involved so as to find the maximum amplitude squeezing that is possible within this scheme. We show that at the maximum possible amplitude squeezing, one can get a state whose photon number uncertainty goes as the fifth root of the mean photon number. We also exhibit the photon number distribution at this maximum amplitude squeezing.

6.1 The proposed scheme

Amplitude squeezed states of the radiation field are characterized by their photon number uncertainty being smaller than their mean photon number. Extensive efforts are being made to generate these states of the radiation field [204, 185, 211, 191, 210, 205, 206, 216, 212, 213, 214]. These states show many inter-related non-classical properties such as sub-poissonian statistics in photon counting, noise

reduction below the shot noise level in direct detection, and photon anti-bunching in Hanbury-Brown-Twiss type of intensity correlation experiments. The quadrature squeezed coherent states do show amplitude squeezing when the direction of squeezing is along the direction of excitation. But the minimum photon number uncertainty that can be obtained is restricted by $\langle (\Delta\hat{n})^2 \rangle \leq \langle \hat{n} \rangle^{2/3}$. Earlier another type of interaction involving the non-linear Kerr medium had been introduced [175, 176, 177, 178, 179], and it was shown that by evolving a coherent state through a Kerr medium, one could generate amplitude squeezed states by the self-phase modulating action of the Kerr medium [174, 190, 185, 197, 241, 191, 139, 140, 193, 141]. In fact the minimum photon number uncertainty that could be got in this way was less than and of the order of $\langle \hat{n} \rangle^{1/3}$ [191]. In this chapter, we propose a quantum state got by evolving a quadrature squeezed coherent state through a Kerr medium, whose photon number uncertainty is smaller than the fifth root of the mean photon number [218]. There were earlier proposals for getting much smaller photon number uncertainties [216], but they are experimentally difficult to achieve compared to the one that is proposed here and in Ref. [191].

In this chapter, we show that a amplitude squeezed coherent state, when allowed to evolve through a non-linear Kerr medium for a small amount of time, shows considerable amplitude squeezing when it is displaced to a proper position in phase space. We have already seen the evolution of an amplitude squeezed coherent state in the Kerr medium in Chapter 4. We have shown there that the Kerr medium interaction term commutes with the photon number operator and hence it leaves the photon number properties unchanged. But we have also seen that the Q-function undergoes quite a change, and compared to the coherent state that has

evolved through the Kerr medium, the quasi probability distribution of the amplitude squeezed coherent state that has evolved through the Kerr medium for the same duration of time is a little flat and is more symmetric. As pointed out earlier and as can be seen from Fig.(4.1) the QPD is situated in such a way that photon number properties remain unchanged on evolution through the Kerr medium. Hence one has to displace such a state to a proper position in phase space to see the effect of the Kerr medium on the amplitude squeezing. Here we do this, and study the effect of the various parameters involved on the amount of amplitude squeezing of the output state.

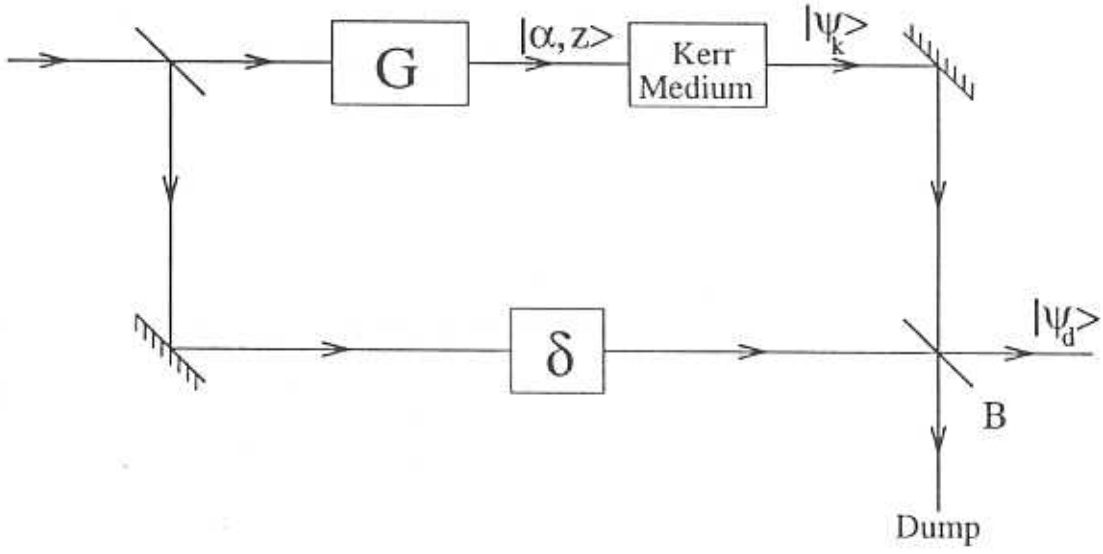

Fig. 1

Fig. 6.1. Schematic. G is the quadrature squeezed light generator, δ is the time delay and B is the final beam splitter.

The schematics of the setup to generate this quantum state is given in Fig. (6.1). Here a coherent light beam is split into two by a beam splitter to make a Mach-Zehnder interferometer configuration. One arm of the interferometer contains a

quadrature squeezed light generator, which is indicated in the figure as G. This generator G can be typically an optical parametric oscillator (OPO) operating in the sub-threshold regime as a deamplifier [214] to generate the amplitude squeezed coherent state. This squeezed state is made to evolve through a Kerr medium for a predetermined small duration of time. The other arm of the interferometer contains a time delay depicted in the figure as δ. These beams are recombined in the final beam splitter B. This beam splitter B has very high reflectivity, which prevents the signal beam from being contaminated with the noise of the reference beam. At the same time this produces a classical displacement of the signal beam's quantum state in phase space [191], when the intensity of the reference beam is high. The angle and the magnitude of this displacement can be adjusted by varying the time delay and the strength of the reference beam respectively. We present in this chapter, the theoretical analysis of this scheme, and calculate the photon number uncertainty and the photon number distribution of the beam coming out of the beam splitter B. Finally, we show that the absolute minimum of the photon number uncertainty is smaller than $\langle \hat{n} \rangle^{1/5}$ [218].

6.2 The displaced state

In this section, we calculate the field quantities needed to access the photon number properties of the beam that comes out of the scheme. The state of the radiation field as it enters the generator G is in a coherent state $|\alpha'\rangle$. The operation of the generator G is to squeeze this initial coherent state, and the quantum state of the

field that comes out of G is given by

$$\hat{S}(z)\,|\,\alpha'\,\rangle = \hat{S}(z)\widehat{D}(\alpha')\,|\,O\,\rangle \quad , \tag{6.1}$$

where $\hat{S}(z) = \exp(\frac{1}{2}(z\hat{a}^{\dagger 2} - z^{*}\hat{a}^{2}))$ is the quadrature squeeze operator [85, 86, 89], and $\widehat{D}(\alpha') = \exp(\alpha'\hat{a}^{\dagger} - \alpha'^{*}\hat{a})$ is the displacement operator [62, 63]. The operators $\hat{a}$, $\hat{a}^{\dagger}$ are the usual boson annihilation and creation operators. It would be convenient if one can rewrite $\hat{S}(z)\widehat{D}(\alpha')\,|\,O\,\rangle$, which is usually called the two-photon coherent state [89], as $\widehat{D}(\alpha)\hat{S}(z)\,|\,O\,\rangle$. This state $\widehat{D}(\alpha)\hat{S}(z)\,|\,O\,\rangle$ is called the *ideal squeezed* state [146], because of its simple properties. These two forms are related [237], and one can go from one to the other by conjugating the displacement operator with the squeeze operator as

$$\hat{S}(z)\widehat{D}(\alpha')\,|\,O\,\rangle = \hat{S}(z)\widehat{D}(\alpha')\hat{S}^{\dagger}(z)\,\hat{S}(z)\,|\,O\,\rangle = \widehat{D}(\alpha)\hat{S}(z)\,|\,O\,\rangle \tag{6.2}$$

where

$$\alpha = \alpha'\cosh(r) + \alpha'^{*}\sinh(r)\,e^{2i\theta} \quad . \tag{6.3}$$

Here we have parameterized z in the usual way as $z = r\,e^{2i\theta}$, and α as $\alpha = \rho\,e^{i\phi}$. From now on, we represent the quadrature squeezed coherent states that evolve out of G as $|\,\alpha, z\,\rangle = \widehat{D}(\alpha)\hat{S}(z)\,|\,O\,\rangle$, and work with this state.

This state $|\,\alpha, z\,\rangle$ is to be evolved through a Kerr medium. The state of the quantum field at the output of the Kerr medium will be

$$|\,\psi_K\,\rangle = \hat{U}(\gamma)\,|\,\alpha, z\,\rangle \quad , \tag{6.4}$$

where

$$\hat{U}_K(\gamma) = e^{i\frac{\gamma}{2}\hat{a}^{\dagger 2}\hat{a}^{2}} \quad . \tag{6.5}$$

We had studied this state in great detail in Chapter 4. This state $|\psi_K\rangle$ undergoes a final displacement in the beam splitter and hence the radiation field that emerges is in the quantum state

$$|\psi_d\rangle = \widehat{D}(\xi)\,|\psi_K\rangle \quad . \tag{6.6}$$

As pointed out earlier, the magnitude of the displacement ξ can be adjusted by changing the intensity of the local oscillator beam and the argument by introducing a time delay.

We find it convenient to re-parameterize the displacement as,

$$\xi = \eta\rho e^{i(\Omega+\delta)} \quad , \tag{6.7}$$

where

$$\Omega = \arg\left[\langle\,\hat{a}\,\rangle_K\right] \quad , \tag{6.8}$$

and η is a real parameter, and $\rho = |\alpha|$ is the magnitude of the initial displacement of the quadrature squeezed state $|\alpha, z\rangle$. The relative angle of displacement δ will be so chosen as to minimize the photon number uncertainty.

The mean photon number of the displaced state is given by

$$\begin{aligned}
\langle\,\hat{n}\,\rangle_d &= \langle\,\psi_d\,|\,\hat{n}\,|\,\psi_d\,\rangle \\
&= \langle\,\psi_K\,|\,\widehat{D}^\dagger(\xi)\hat{n}\widehat{D}(\xi)\,|\,\psi_K\,\rangle \\
&= \left\langle\,\hat{a}^\dagger\hat{a}\,\right\rangle_K + \xi\left\langle\,\hat{a}^\dagger\,\right\rangle_K + \xi^*\langle\,\hat{a}\,\rangle_K + |\xi|^2 \quad ,
\end{aligned} \tag{6.9}$$

where the expectation value of the operators with respect to the state $|\psi_K\rangle$ were calculated earlier in Chapter 4. These and the other expectation values are given in Eq.(4.23–4.26). Using the re-parameterization for ξ, we have

$$\langle\,\hat{n}\,\rangle_d = \left\langle\,\hat{a}^\dagger\hat{a}\,\right\rangle_K + 2\eta\rho\,|\langle\,\hat{a}\,\rangle_K|\cos(\delta) + \eta^2\rho^2 \quad . \tag{6.10}$$

Similarly the photon number uncertainty in the displaced state is given by

$$\begin{aligned}
\left\langle (\Delta\hat{n})^2 \right\rangle_d &= \left\langle \hat{a}^\dagger\hat{a} \right\rangle_d + \left\langle \hat{a}^{\dagger 2}\hat{a}^2 \right\rangle_d - \left\langle \hat{a}^\dagger\hat{a} \right\rangle_d^2 \\
&= \left\langle \hat{a}^\dagger\hat{a} \right\rangle_d + \left\langle \hat{a}^{\dagger 2}\hat{a}^2 \right\rangle_K - \left\langle \hat{a}^\dagger\hat{a} \right\rangle_K^2 \\
&\quad + 2\eta\rho \left\{ e^{-i(\Omega+\delta)} \left[\left\langle \hat{a}^\dagger\hat{a}^2 \right\rangle_K - \left\langle \hat{a}^\dagger\hat{a} \right\rangle_K \langle \hat{a} \rangle_K \right] + C.C. \right\} \\
&\quad + \eta^2\rho^2 \left\{ e^{-2i(\Omega+\delta)} \left[\left\langle \hat{a}^2 \right\rangle_K - \langle \hat{a} \rangle_K^2 \right] + C.C \right\} \\
&\quad + 2\eta^2\rho^2 \left[\left\langle \hat{a}^\dagger\hat{a} \right\rangle_K - \left\langle \hat{a}^\dagger \right\rangle_K \langle \hat{a} \rangle_K \right] \quad , \qquad (6.11)
\end{aligned}$$

where the expectation values $\langle \cdot \rangle_K$ are given in Eq. (4.25,4.26). Hence the Fano factor can be written as

$$f_n'(\eta) = 1 + \frac{p_0 + p_1\eta + p_2\eta^2}{q_0 + q_1\eta + \eta^2} \quad , \qquad (6.12)$$

where the coefficients of the various powers of η are functions of the expectation values of the field operators in the state $|\psi_K\rangle$, and these are given by

$$\begin{aligned}
p_0 &= \frac{1}{\rho^2} \left(\left\langle \hat{a}^{\dagger 2}\hat{a}^2 \right\rangle_K - \left\langle \hat{a}^\dagger\hat{a} \right\rangle_K^2 \right) \quad , \\
p_1 &= \frac{2}{\rho} \left\{ e^{-i(\Omega+\delta)} \left[\left\langle \hat{a}^\dagger\hat{a}^2 \right\rangle_K - \left\langle \hat{a}^\dagger\hat{a} \right\rangle_K \langle \hat{a} \rangle_K \right] + C.C. \right\} \quad , \\
p_2 &= \left\{ e^{-2i(\Omega+\delta)} \left[\left\langle \hat{a}^2 \right\rangle_K - \langle \hat{a} \rangle_K^2 \right] + C.C \right\} + 2 \left[\left\langle \hat{a}^\dagger\hat{a} \right\rangle_K - \left\langle \hat{a}^\dagger \right\rangle_K \langle \hat{a} \rangle_K \right] \quad ,
\end{aligned}$$

$$\begin{aligned}
q_0 &= \frac{1}{\rho^2} \left\langle \hat{a}^\dagger\hat{a} \right\rangle_K^2 \quad , \\
q_1 &= \frac{2}{\rho} |\langle \hat{a} \rangle_K| \cos(\delta) \quad . \qquad (6.13)
\end{aligned}$$

In this form, one can immediately minimize the Fano factor with respect to η, and the optimized η value is given by

$$\eta_o = \frac{-(p_2q_0 - p_0) + \sqrt{(p_2q_0 - p_0)^2 - (p_1q_0 - p_0q_1)(p_2q_1 - p_1)}}{(p_2q_1 - p_1)} \quad . \qquad (6.14)$$

The η optimized value of the Fano factor is then given by

$$f_n = f_n'(\eta_o) \quad . \tag{6.15}$$

The primary task of this chapter is to find the optimum values of the other parameters, such as the scaled duration γ of evolution in the Kerr medium, and the magnitude of squeezing r, etc., which will give the absolute minimum of the Fano factor. But before going into this, we will calculate the photon number distribution and the Q-function of the displaced state. We will be using the Q-function to illustrate the reasoning that we employ in choosing a value of δ that will minimize the photon number fluctuations.

The photon number distribution of this displaced state can be calculated using the definition,

$$\begin{aligned} P_n &= |\langle n \,|\psi_d\rangle|^2 \\ &= \left|\langle n \,|\, \widehat{D}(\xi)\,|\psi_K\rangle\right|^2 \quad . \end{aligned} \tag{6.16}$$

But the action of the displacement operator on the Fock state on the left can be calculated to be

$$\begin{aligned} \langle n \,|\, \widehat{D}(\xi) &= e^{-\frac{1}{2}|\xi|^2} \langle n \,|\, e^{\xi \widehat{a}^\dagger} e^{-\xi^* \widehat{a}} \\ &= e^{-\frac{1}{2}|\xi|^2} \sum_{m=0}^{n} \frac{\xi^m}{m!} \sqrt{\frac{n!}{(n-m)!}} \\ &\qquad \times \sum_{k=0}^{\infty} \frac{(-\xi^*)^k}{k!} \sqrt{\frac{(n-m+k)!}{(n-m)!}} \, \langle n-m+k \,| \quad . \end{aligned} \tag{6.17}$$

Using this and the integral representation of the quadrature squeezed state in Eq. (4.11), we have

$$P_n = \frac{n!}{\cosh(r)} e^{-(\rho^2+|\xi|^2)}$$

$$\times \left| e^{\frac{1}{2}\tanh(r)\rho^2 e^{2i(\theta-\phi)}} \sum_{k=0}^{\infty} \frac{(-\xi^*)^k}{k!} \sum_{m=0}^{n} \frac{\xi^m}{m!(n-m)!} e^{-i\frac{\pi}{2}(n-m+k)(n-m+k-1)} \right.$$
$$\times \sum_{s=0}^{[\frac{n-m+k}{2}]} \frac{(n-m+k)!}{(n-m+k-2s)!s!} \left[\frac{e^{2i\theta}\tanh(r)}{2}\right]^s$$
$$\left. \times \left\{\rho e^{-i\phi}\left[e^{2i\phi} - e^{2i\theta}\tanh(r)\right]\right\}^{n-m+k-2s} \right|^2 \qquad (6.18)$$

We will come back to this expression after we have found the parameter values at which the maximum number squeezing occurs.

The Q-quasi probability distribution function for the displaced state can also be easily calculated, using the fact that

$$\begin{aligned} Q(\beta) &= \frac{1}{\pi}|\langle\, \beta \mid \psi_d \rangle|^2 = \frac{1}{\pi}\left|\langle \beta \mid \widehat{D}(\xi) \mid \psi_K \rangle\right|^2 \\ &= \frac{1}{\pi}\left|e^{(\xi\beta^* - \xi^*\beta)/2} \langle\, \beta - \xi \mid \psi_K \rangle\right|^2 \\ &= Q_K(\beta - \xi) \end{aligned} \qquad (6.19)$$

where we have used $\widehat{D}(\xi) = \widehat{D}^\dagger(-\xi)$ and where Q_K is the Q-function for the state $|\psi_K\rangle$, which is given in Eq. (4.19).

Having calculated these quantities, we now turn to the optimization of the Fano factor.

6.3 Fano factor optimization

We will first reason out the value of δ that will lead to the maximum amplitude squeezing, after which we optimize the remaining two more parameters γ and r. We have earlier seen that the Q-function of the amplitude squeezed coherent state, as it evolves through a Kerr medium becomes crescent shaped [Fig. (4.1)], and the effect

of the initial squeezing is to flatten this crescent a little bit, and to make the tails rather symmetric [Fig. (4.3)]. But we have mentioned before that even though the

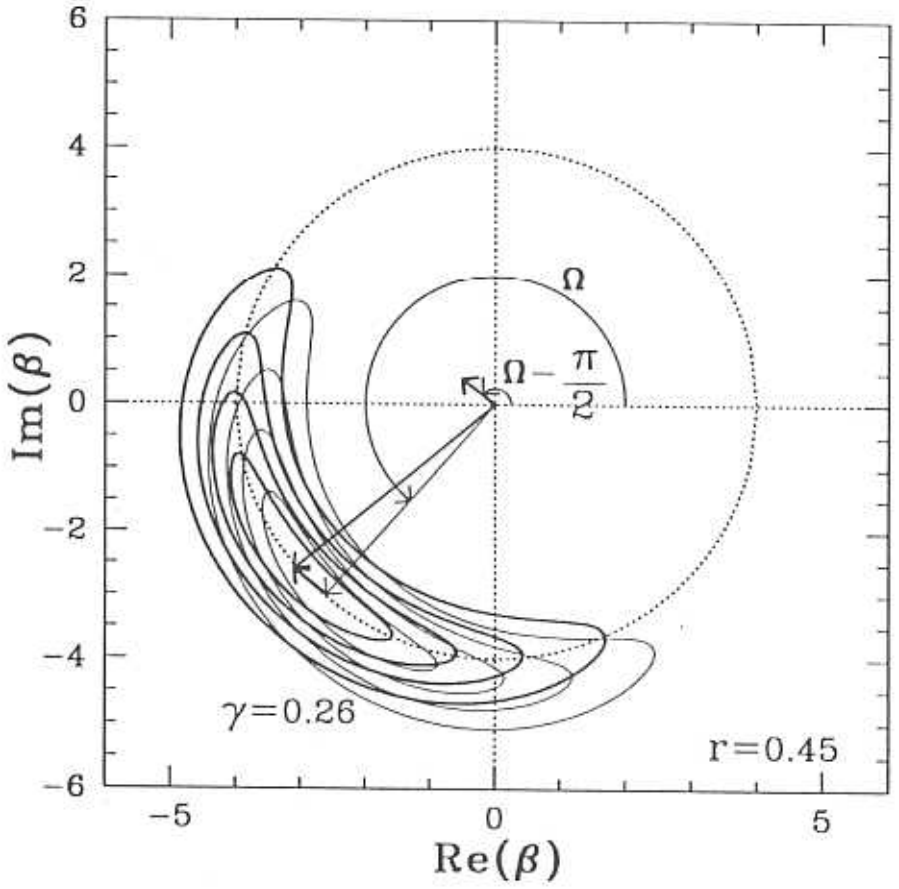

Fig. 6.2. Plot of the contours of the Q-function for the state $|\psi_K\rangle$ (thin lines) and for the state $|\psi_d\rangle$ (thick lines) under the optimum magnitude of displacement η_o along the proper direction in phase space. Ω is the argument of $\langle \hat{a} \rangle_K$. δ, the relative angle of displacement is chosen to be $-\pi/2$. The displacement is represented by a thick arrow and is translated to the origin to show the angle of displacement. The contours are at 0.2, 0.4, 0.6 and 0.8 times the maximum value. The maximum value is connected to the origin by an arrow. The dotted circle is for visual enhancement.

Q-distribution function is curved, the photon number properties remain unchanged because this curved distribution is slightly rotated, and its center of curvature is not in the direction of the phase space origin. This implies that the displacement ξ should

be along the tangent to a circle that is centered at the origin of phase space, and which passes through the center of the distribution. We find that $\delta = -\pi/2$ is the proper choice for the relative angle of displacement. In Fig. (6.2), we convey this idea pictorially. Here, the contours of the Q-function for the state $|\psi_K\rangle$, when $r = 0.45$ and $\gamma = 0.26$, are drawn as thin lines. With the relative angle of displacement $\delta = -\pi/2$, the optimum magnitude of displacement η_o is found. The Q-function for the displaced state $|\psi_d\rangle$ with the above value of displacement is computed using Eq. (6.19), and its contours are plotted as thick lines in the figure. The contours are at 0.2, 0.4, 0.6, 0.8 times the maximum value. The maximum in each case is connected to the origin by an arrow. The action of the displacement in moving the center of the distribution is indicated by a heavy arrow. This is translated to the origin of phase space to show the angle of displacement. The dotted circle centered at the phase space origin is drawn to show that this displacement is tangential to the circle passing through the center of the distribution. This dotted circle also serves the purpose of being a visual guide.

With this value of the relative angle of displacement $\delta = -\pi/2$, the mean photon number of the displaced state goes over to

$$\begin{aligned} \langle \hat{n} \rangle_d &= \left\langle \hat{a}^\dagger \hat{a} \right\rangle_K + \eta^2 \rho^2 \\ &= (1+\eta^2)\rho^2 + \sinh^2(r) \quad . \end{aligned} \tag{6.20}$$

The optimized Fano factor f_n is calculated using Eq. (6.12-6.15). Note that the coefficient q_1 will be zero for this choice of δ.

In Fig. (6.3), we have plotted the logarithm of the optimized Fano factor (Solid line) as a function of the logarithm of γ with a squeezing value $r = 3.4$, for the

initial photon number $|\alpha|^2 = \rho^2 = 10^9$. We have also plotted the logarithm of the optimum value of the displacement magnitude η_o (Dotted line), in the same figure. For comparison, we have plotted for an initial coherent state with the same initial

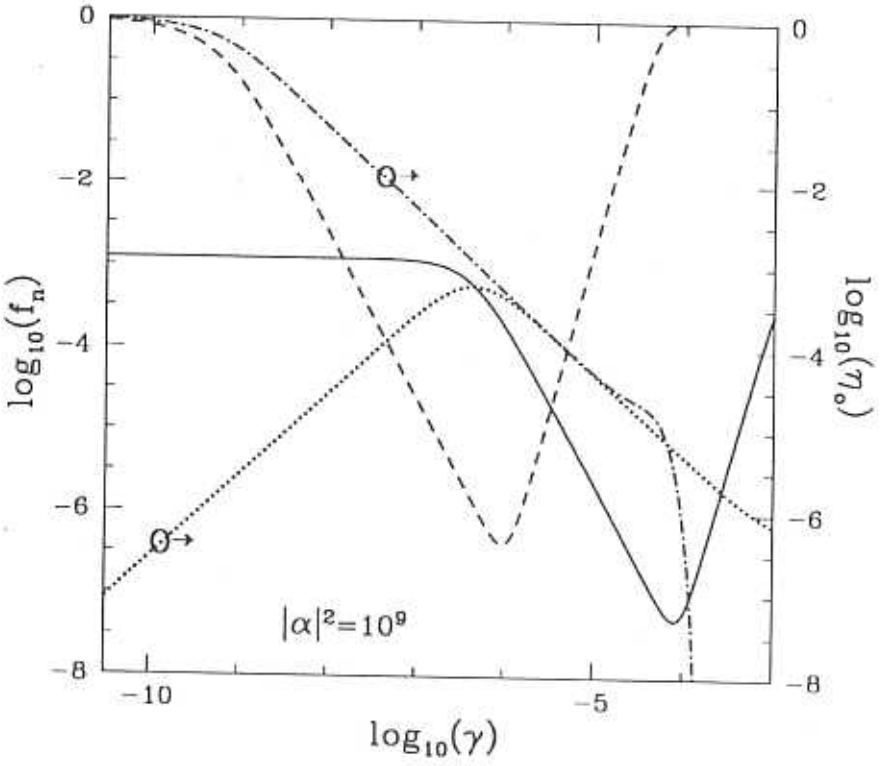

Fig. 6.3. Plot of the logarithm of the optimized Fano factor for the state $|\psi_d\rangle$ (Solid line) for $r = 3.4$ Vs. logarithm of γ. The logarithm of the optimized magnitude of displacement η_o is also plotted (Dotted line) along with. For comparison the logarithm of the Fano factor (Dashed line) and the optimum displacement (Dash-Dotted line) for a coherent state is also plotted.

mean photon number, the logarithm of the optimized Fano factor (Dashed line) and the logarithm of the optimum displacement (Dash-Dotted line) [191]. It can be seen that the Fano factor for an initial amplitude squeezed coherent state is an order of magnitude smaller than for an initial coherent state. Moreover, it could also be

seen that the required non-linearity of the Kerr medium for the maximum amount of amplitude squeezing at a given initial mean photon number is only an order of magnitude higher for an initial amplitude squeezed coherent state. One can see that for a fixed value of ρ and r, the optimized Fano factor as a function of γ has a minimum. Hence, one can optimize γ value for a given initial ρ and r.

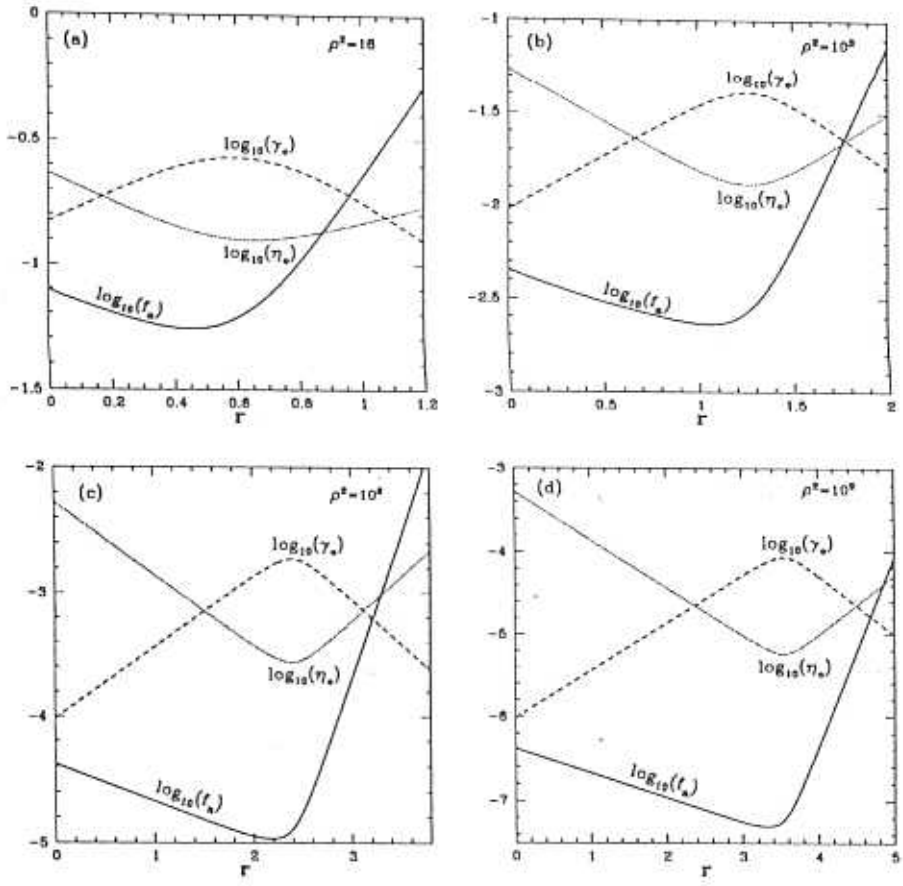

Fig. 6.4. Plot of the logarithm of the minimum of the optimized Fano factor Vs. the squeezing r for various values of the initial displacement ρ, whose value is indicated in the figure. The logarithm of the optimum value of the magnitude of displacement and the logarithm of the optimum non-linearity γ_o at which for a given r and ρ the Fano factor goes to a minimum, is also plotted.

In Fig. (6.4) we do this, where we plot the logarithm of the minimum value of the Fano factor that can be obtained for a given value of ρ^2 and r, as a function of

r for various values of ρ^2. Here, for each value of r, the γ value range is scanned numerically, and for each γ value, the optimized Fano factor value is computed. Among these, the γ value at which the Fano factor is minimum is called here as γ_o and its logarithm is also plotted in the figures. The logarithm of the optimized magnitude of displacement corresponding to this γ_o value is also plotted. The value at $r = 0$ corresponds to the minimum possible value that can be obtained for a coherent state that has evolved through a Kerr medium and suitably displaced. It can be seen from the figures that for each value of ρ^2 there is again a particular value of r at which the Fano factor becomes minimum. This implies that the Fano factor can be absolutely minimized with respect to η, γ and r. This absolute minimum of the Fano factor is seen to occur at higher values of squeezing r for larger initial displacement. But apart from that, the structure of the curves remain the same in all the figures.

In Fig. (6.4), one can see that the absolute minimum of the Fano factor is approximately $f_n^{(a)} = 10^{-4.97}$, which occurs when the squeeze parameter value is around $r = 2.19$, for an initial photon number of 10^6. As can be seen from Eq. (6.20), the mean photon number $\langle \hat{n} \rangle_d$ of the output beam is well approximated by the mean photon number of the input coherent beam, which is $|\alpha|^2 = \rho^2 = 10^6$. Since the Fano factor is defined as the ratio of the photon number uncertainty to the mean photon number, the photon number uncertainty goes as $\langle (\Delta\hat{n})^2 \rangle_d = f_n^{(a)} \rho^2 = 10^{1.03}$. This is slightly greater than, and of the order of, the sixth root of the mean. But one can easily see that $\langle (\Delta\hat{n})^2 \rangle_d < \left\{ (10^6)^{1/5} = 10^{1.2} \right\}$. Hence we conclude that the minimum photon number uncertainty that the output beam can show is in the range

$$\langle \hat{n} \rangle_d^{1/6} < \left\langle (\Delta\hat{n})^2 \right\rangle_d < \langle \hat{n} \rangle_d^{1/5} \quad . \tag{6.21}$$

One can check this in Fig. (6.4) for the input photon number of 10^9. Here, the absolute minimum of the Fano factor is around $f_n^{(a)} = 10^{-7.3}$ which occurs when $r = 3.33$. Hence, the photon number uncertainty goes as $\langle(\Delta\hat{n})^2\rangle_d = 10^{1.7} < \left\{\langle\hat{n}\rangle_d^{1/5} = 10^{1.8}\right\}$, since the mean photon number here is $\rho^2 = 10^9$. In fact, for low mean photon numbers the output beam's photon number uncertainty goes as the sixth root of the mean.

We would like to look at the behavior of the photon number uncertainty and the photon number distribution of the output beam, when the parameters involved are so optimized that the quantum state of this beam has the maximum amplitude squeezing.

6.4 Properties of the state at the maximum possible amplitude squeezing

We have seen in the last section that the Fano factor can be absolutely minimized with respect to all the parameters involved. Even though we have done the γ and r optimization numerically, we have done it in a step by step manner to show the robustness of the procedure. We wish now to plot the absolute minimum of the Fano factor as a function of the input photon number to see its behavior globally. We will then study the photon number distribution of the state which is optimized for the maximum amplitude squeezing in comparison with the other known states.

The absolute minimum of the Fano factor that can be obtained for a given initial displacement ρ^2 is computed numerically by minimizing the optimized Fano factor f_n with respect to γ and r. It should be remembered that what we call

as the optimized Fano factor f_n is by itself got by algebraically optimizing the η variable. The values of the scaled duration of evolution in the Kerr medium and the quadrature squeezing magnitude at which the absolute minimum occurs are

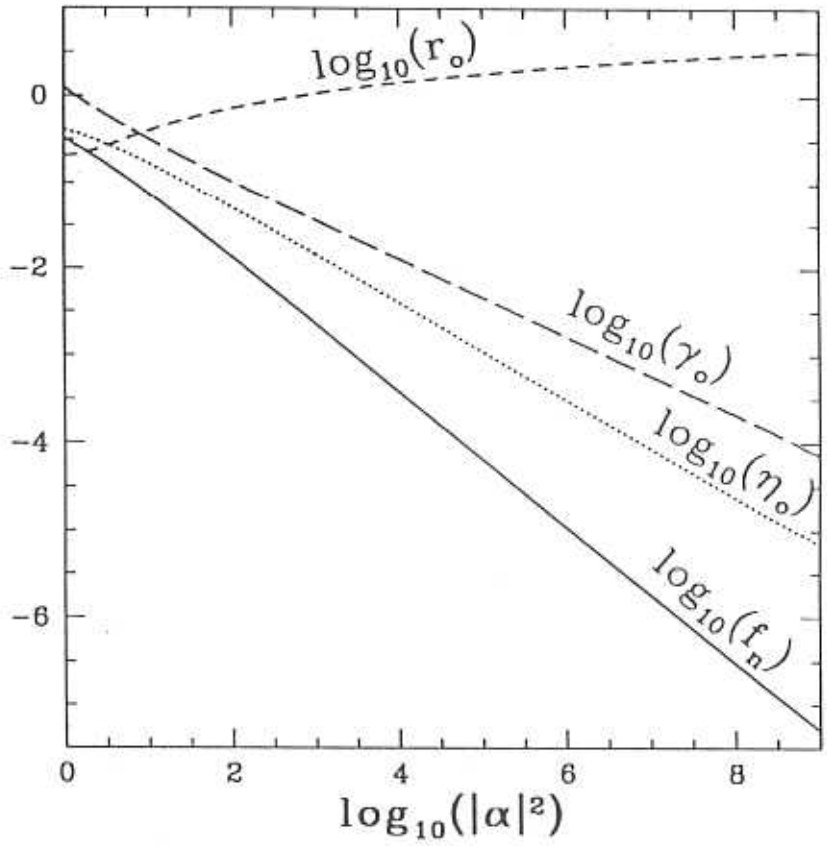

Fig. 6.5. Plot of the logarithm of the absolute minimum of the Fano factor for a given initial displacement $|\alpha|^2 = \rho^2$ is plotted Vs. the logarithm of ρ^2. The optimum values r_o, γ_o, and η_o at which this absolute minimum occurs is also plotted. (See text)

respectively denoted by r_o and γ_o. The logarithms of these are plotted in Fig. (6.5) as a function of the logarithm of ρ^2. The Fano factor corresponding to these r_o and γ_o values is the absolute minimum possible for a given ρ^2, and its logarithm is also plotted in the same figure. The associated optimum displacement η_o is also plotted. It can be seen that the logarithms of γ_o, η_o and f_n are all linear decreasing function

of $\log_{10}(\rho^2)$. One can estimate the behavior of the photon number uncertainty in term of the mean photon number from this figure. It can be seen from the figure that $\log_{10}(f_n)$ as a function of $\log_{10}(\rho^2)$ is linear for large values of ρ^2, with a slope which is slightly greater than $-(4/5)$. Taking this approximation, the linearized line on extrapolation will have an intercept with the ordinate at about -0.3. Hence one could write

$$\begin{aligned} \log_{10}(f_n) &\approx -\frac{4}{5}\log_{10}(\rho^2) - 0.3 \\ \log_{10}(f_n) &< -\frac{4}{5}\log_{10}(\rho^2) \end{aligned} \tag{6.22}$$

$$\begin{aligned} \log_{10}(f_n) &\approx -\frac{4}{5}\log_{10}(\rho^2) - 0.3 \\ \log_{10}(f_n) &< -\frac{4}{5}\log_{10}(\rho^2) \quad . \end{aligned} \tag{6.23}$$

But looking at Eq. (6.20), the mean photon number at large ρ goes as ρ^2 itself, and in this region of large ρ, $\langle \hat{n} \rangle_d \approx \rho^2$. Hence

$$\log_{10}(f_n) < -\frac{4}{5}\log_{10}(\langle \hat{n} \rangle_d) \quad , \tag{6.24}$$

which implies that

$$\left\langle (\Delta\hat{n})^2 \right\rangle_d < \langle \hat{n} \rangle_d^{1/5} \quad . \tag{6.25}$$

Having demonstrated the behavior of photon number uncertainty, we now turn to the photon number distribution of the state which has been optimized to have the highest amplitude squeezing. In Fig. (6.6), we have plotted the photon number distribution for the state $|\psi_d\rangle$. Here we have fixed the mean $\langle \hat{n} \rangle$ at 16. We choose a value of ρ^2 and optimize the squeezing magnitude and Kerr medium non-linearity such that the Fano factor goes to the absolute minimum. Then we check the mean

photon number given by $\langle \hat{n} \rangle_d = (1 + \eta_o^2)\rho^2 + \sinh^2(r)$ and vary ρ^2 till $\langle \hat{n} \rangle_d$ is 16 within the numerical precision available to us. We then use Eq. (6.18) with these

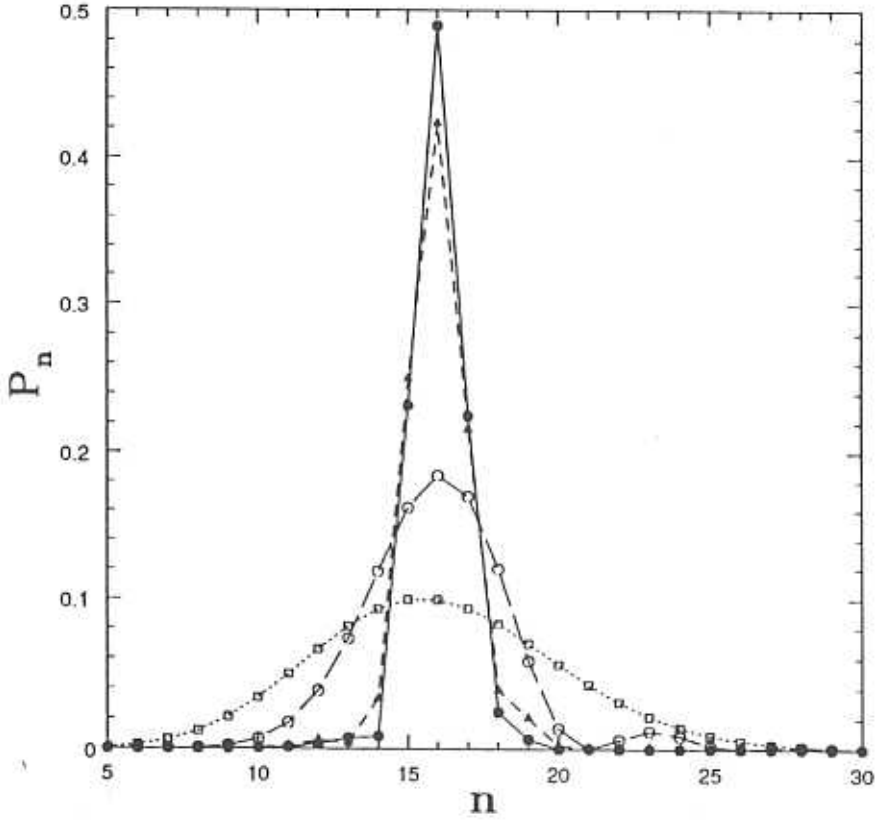

Fig. 6.6. Plot of the photon number distribution (Solid line with Solid Circles) of the state $|\psi_d\rangle$ when the mean is fixed at 16 and the Fano factor is at the absolute minimum (See text and the previous figure). For comparison the photon number distribution of a coherent state that has evolved through the Kerr medium and displaced to a proper position in phase space (Dashed line with Solid Triangles) with the mean photon number fixed at 16 is also plotted. Again for comparison an amplitude squeezed coherent state (Long Dashed line with Open Circles) and a coherent state (Dotted lines with Open Squares) with the same mean photon number is also plotted.

values of ρ^2, η_o, r_o, and γ_o, and compute the photon number distribution, which is plotted in this figure (Solid line with Solid Circles). We have also plotted the photon number distribution (Dashed line with Solid Triangles) when the initial state is a

coherent state, again using Eq. (6.18) with $r = 0$, for computation. Here too we have fixed the mean photon number at 16 and have used the parameter values at which the Fano factor goes to an absolute minimum. Again for comparison, the photon number distribution of an amplitude squeezed coherent state (Long Dashed line with Open Circles) and a coherent state (Dotted lines with Open Squares) are plotted for the same mean photon number. It can be seen from the figure that the state $|\psi_d\rangle$ is more sub-poissonian than the other states. In fact when the mean photon number is 16, the photon number uncertainty for the state $|\psi_d\rangle$, which goes as $16^{1/5}$ is of the order of one, which is only slightly smaller than the corresponding value $16^{1/3}$ for an initial coherent state ($r = 0$) that has evolved through the same Kerr medium. But on the other hand, for large mean photon numbers, say with $\langle \hat{n} \rangle = 10^9$, the photon number uncertainty is of the order of 50 photons for the state $|\psi_d\rangle$, which is two orders of magnitude smaller than the corresponding value of 10^3 for an initial coherent state.

We have presented in this chapter a scheme for generating highly amplitude squeezed states of the radiation field [218]. We have proposed and analyzed the scheme and optimized various parameters involved to obtain maximum amplitude squeezing. This state with the maximum amplitude squeezing is shown to have a photon number uncertainty which goes as $\langle (\Delta\hat{n})^2 \rangle < \langle \hat{n} \rangle^{1/5}$. We have also shown that this state's photon number distribution is much more sub-poissonian than that of other known states. We wish to point out that this scheme has the potential to be experimentally feasible with the existing technology. The availability of Kerr medium with sufficient non-linearity is enough to see the scheme through. A more complete theory which includes the noise and dissipation in the Kerr medium is

desirable. But if sufficiently high non-linearities are available then this only source of noise and loss is minimized and our analysis which doesn't include dissipation and the associated noise will hold. The second point is to treat the output beam splitter in a complete way, rather then the approximate way in which we have done. This too will introduce additional noise but that can be safely neglected. Nevertheless a complete analysis with all the losses and the associated noise is needed. Even with all this, we expect that if this experiment is carried out, the amplitude squeezing that can be got will still be the experimental maximum as of date.

We have in this thesis started with a simple system of superposition of two coherent states in Chapter 2, where we have shown that the relative phase in the Pancharatnam sense between the components of the superposition plays a crucial role in producing a curved quasi probability distribution. In Chapter 3 we have shown the effect of this curvature on amplitude squeezing. Using the insight thus gained, we have proposed a scheme in which an amplitude squeezed coherent state is made to evolve through a Kerr medium, which we believed would result in a quantum state with a highly squeezed photon number fluctuation. We have studied the evolution of a quadrature squeezed coherent state inside a Kerr medium in Chapter 4. After studying some interesting superpositions of quadrature squeezed states that arise in this evolution related to amplitude squeezing in Chapter 5, we moved on to the scheme for getting highly amplitude squeezed states of the radiation field in Chapter 6. Our understanding enables us to

expect much higher amplitude squeezing in some other cases, whose study is currently being undertaken. Much work is also being done on generating highly non-classical light from various semi-conductor devices. It may be expected that the day for getting a Fock state experimentally, and engineering the generation of quantum states with given noise properties, is not very far off. It is this aspect of relatively immediate experimental realization which makes this ever growing field of quantum optics quite exciting and interesting.

Bibliography

The Quantum hypothesis was proposed in

[1] M. Planck, Verh. d. deutsch phys. Ges. **2**, 202, 237, (1900) ; M. Planck, Ann. d. Physik, (4), **4**, 533 (1901).

The quantum hypothesis was used to explain the photo-electric effect by

[2] A. Einstein, Annalen der Physik **17**, 132–148, (1905) ; Eng. trans. by A. B. Arons and M. B. Peppard, Amer. J. Physics **33**, 367–374 (1965).

[3] A. Einstein, Phys. Zeits. **10**, 185–193, (1909).

And in explaining the specific heat of solids as in

[4] A. Einstein, Annalen der Physik **22**, 180–190, (1907).

[5] A. Einstein, Annalen der Physik **35**, 679–694, (1911).

[6] P. Debye, Annalen der Physik **39**, 789–839, (1912).

Beginnings of spectroscopy in

[7] G. Kirchhoff and R. Bunsen, Oswalds Klassiker der exakten Wissenschaften **72** (1860).

Mathematical structure of the lines seen in atomic spectra

[8] J. J. Balmer, Wiedemannsche Annalen der Physik **25**, 80–87, (1885).

[9] J. R. Rydberg, Phil. Mag. **29**, 331-337 (1890).

Planetary model of the atom

[10] M. Rutherford, Phil. Mag. **21**, 669 (1911).

Atomic spectra using quantum hypothesis

[11] N. Bohr, Phil. Mag. **26**, 1–25, 476–502, 857–875, (1913).

A more refined treatment of the adhoc quantum conditions introduced by Bohr

[12] A. Sommerfeld, Annalen der Physik **51**, 1–94,125–167, (1916).

Analytical approach to quantization - 'Matrix mechanics'

[13] W. Heisenberg, Mathematischen Annalen **95**, 694–705, (1925).

[14] M. Born and P. Jordan, Zeitschrift für Physik **34**, 858–888, (1925).

[15] M. Born, W. Heisenberg and P. Jordan, Zeitschrift für Physik **35**, 557–615, (1926).

[16] P. A. M. Dirac, Proc. Roy. Soc. of Lon. **A109**, 642–653, (1925).

[17] P. A. M. Dirac, Proc. Roy. Soc. of Lon. **A110**, 561–579, (1926).

'Wave mechanics'

[18] L. de Broglie, Annales de Physique **3**, 22–128, (1925).

[19] E. Schrödinger, Annalen der Physik **79**, 361–376, 489–527, 734–756 ; **80**, 437–490 ; **81**, 109–139, (1926).

Quantum Mechanics as we use today was introduced in

[20] P. A. M. Dirac, The principles of quantum mechanics Clarendon Press – Oxford (First edition - 1930).

Relativistic quantum theory of the electron

[21] P. A. M. Dirac, Proc. Roy. Soc. **A117**, 610–624 (1928).

Similar attempts to quantize other fields

[22] W. Heisenberg and W. Pauli, Z. Phys. **56**, 1–61 (1929).

Technical details of the usual way of quantizing the radiation field in

[23] E. Fermi, Rev. Mod. Phys. **4**, 87 (1932).

[24] W. Heitler, The Quantum Theory of Radiation, 2nd edition, Oxford University Press – Fair Lawn, N.J. (1944).

[25] E. A. Power, Introductory Quantum Electrodynamics, Longmans – London (1964).

[26] T. W. B. Kimble, in Quantum Optics, edited by *S. M. Kay and A. Maitland*, Academic Press – London (1970).

[27] W. H. Louisell, Quantum Statistical Properties of Radiation, John Wiley & Sons – New York (1973).

[28] D. P. Craig and T. Thirunamachandran, Molecular Quantum Electrodynamics, Academic Press – London (1984).

Classical Electrodynamics and Optics

[29] M. Born and E. Wolf, Principles of Optics, 2 ed., Pergamon Press – Oxford (1964).

[30] L. D. Landau, The Classical Theory of Fields, Pergamon – London (1971).

[31] J. D. Jackson, Classical Electrodynamics, Wiley – New York (1975).

Non-linear Optics

[32] N. Bloembergen, Nonlinear Optics, W. A. Benjamin Inc. – New York (1965).

Quantization of a box filled with a uniform dielectric medium

[33] J. M. Jauch and K. M. Watson, Phys. Rev. **74**, 950 (1948).

Two uniform media with different permittivities : Evanescent field

[34] C. K. Carniglia and L. Mandel, Phys. Rev. **D3**, 280 (1971).

Cavity with output coupling

[35] K. Ujihara, Phys. Rev. **A12**, 148 (1975).

General theory of light propagation in linear medium

[36] I. Abram, Phys. Rev. **A35**, 4661 (1987).

General theory of light propagation in inhomogeneous media

[37] Y. R. Shen, Phys. Rev. **155**, 921 (1967).

[38] L. Knoll, W. Vogel and D. -G. Welsh, Phys. Rev. **A36**, 3803 (1987).

Complete theory of general dispersive inhomogeneous nonlinear media in

[39] P. D. Drummond, Phys. Rev. **A42**, 6845 (1990).

[40] R. J. Glauber and M. Lewenstein, Phys. Rev. **A43**, 467 (1991).

Non-linear time dependent media quantization

[41] Z. Bialynicka-Birula and I. Bialynicka-Birula, J. Opt. Soc. Am. **B4**, 621 (1987).

Quantization of free cavity with moving mirrors (See [142] for squeezing in such case)

[42] G. T. Moore, J. Math. Phys. **11**, 2679 (1970).

Direct consequences of quantization : Casimir force

[43] H. B. G. Casimir, Proc. Kon. Ned. ADad. Wet. **51**, 793 (1948).

See Power's book [25] for a simple way of calculating Casimir force which is also applicable when the radiation field is squeezed. Review of Casimiri force in QED

[44] G. Plunien, B. Muller and W. Greiner, Phys. Rev. **134**, 87 (1986).

In Quantum Optics introduced as radiation pressure by (Some calculation involving radiation pressure due to squeezed states is done in [91])

[45] P. W. Milonni, R. J. Cook and M. E. Goggin, Phys. Rev. **A38**, 1621 (1988).

Phase problem was recognized by Dirac [73] and an approximate phase operator was introduced by

[46] L. Susskind and J. G. Glogower, Physics **1**, 49 (1964).

A measurement scheme to realize the SG phase - phase operator defined using Probability operator measure (POM).

[47] J. H. Shapiro, S. R. Shepard and N. C. Wong, Phys. Rev. Lett. **62**, 2377 (1989).

[48] J. H. Shapiro and S. R. Shepard, Phys. Rev. **A43**, 3795 (1991).

Review article containing different approaches to the phase operator problem

[49] P. Carruthers and M. M. Nieto, Rev. Mod. Phys. **40**, 411 (1968).

Another phase operator approach that is currently much talked about evolved as in

[50] D. T. Pegg and S. M. Barnett, Phys. Rev. **A39**, 1665 (1989).

[51] S. M. Barnett and D. T. Pegg, J. Mod. Opt. **36**, 7 (1989).

The above phase operator was defined using the techniques of discrete-time Fourier transforms which can be found in any communication theory book such as

[52] A. V. Oppenheim and R. W. Schafer, Digital Signal Processing, Prentice-Hall – Englewood Cliffs (1975).

Concept of Coherent states first mentioned in

[53] E. Schrödinger, Naturwiss. **14**, 664 (1926).

Coherent states as Minimum uncertainty states in

[54] E. Schrödinger, Ber. Kgl. Akad. Wiss. – Berlin, 296 (1930).

[55] H. P. Robertson, Phys. Rev. **35**, 667 (1931).

The way we use Coherent states in quantum optics at present was first elucidated in

[56] J. R. Klauder, Ann. of Phys. **11**, 123 (1960).

[57] J. R. Klauder, J. Math. Phys. **4**, 1055 (1963).

Wigner's phase space paper

[58] E. P. Wigner, Phys. Rev. **40**, 749, (1932).

Review of Wigner function

[59] M. Hillery, R. F. O'Connell, M. O. Scully and E. P. Wigner, Phys. Rep. **106**, 121 (1984).

Coherent state description of the radiation field - P representation

[60] R. J. Glauber, Phys. Rev. Lett. **10**, 84, (1963).

[61] E. C. G. Sudarshan, Phys. Rev. Lett. **10**, 277, (1963).

Quantum theory of optical coherence

[62] R. J. Glauber, Phys. Rev. **130**, 2529, (1963).

[63] R. J. Glauber, Phys. Rev. **131**, 2766, (1963).

The present approach to coherent states is based on

[64] J. R. Klauder and E. C. G. Sudarshan, Fundamentals of Quantum Optics, W. A. Benjamin – New York, (1968).

[65] A. M. Perelomov, Commun. Math. Phys. **26**, 222 (1972).

[66] E. Onofrio, J. Math. Phys. **16**, 1087 (1975).

The over-completeness of coherent state basis cannot be undone by removing a countable number of coherent states from it

[67] K. E. Cahill, Phys. Rev. **138**, B1566 (1965).

Overview of coherent states in

[68] J. R. Klauder and B. -S. Skargerstam, Coherent States, World Scientific – Singapore, (1968).

Recent review of coherent states

[69] W. -M. Zhang, D. H. Feng and R. Gilmore, Rev. Mod. Phys. **62**, 867 (1990).

Generalized distribution functions - Showing also the relationship between P, Q and Wigner distribution

[70] K. E. Cahill and R. J. Glauber, Phys. Rev. **177**, 1857 (1969).

[71] K. E. Cahill and R. J. Glauber, Phys. Rev. **177**, 1882 (1969).

Phenomenological theory of radiation, with the new concept of stimulated emission

[72] A. Einstein, Z. Phys. **18**, 121 (1917).

Quantum theory of absorption and emission of radiation

[73] P. A. M. Dirac, Proc. Roy. Soc. **A114**, 243–265 (1927).

Connection of natural line width to the life time of the excited level

[74] V. Weisskopf and E. Wigner, Z. Phys. **63**, 54 ; **65**, 18 (1930).

The invention of maser

[75] A. L. Schawlow and C. H. Townes, Phys. Rev. **112**, 1940 (1958).

The invention of laser

[76] T. H. Maiman, Nature **187**, 493 (1960).

The idea of Holography proposed in

[77] D. Gabor, Nature **161**, 777 (1948).

The first work on rate equation in the quantized form

[78] K. Shimoda, H. Takahasi and C. H. Townes, Proc. Phys. Soc. Japan **12**, 686 (1957).

Quantum theory of laser

[79] H. Haken, Z. Phys. **181**, 96–124 (1964).

[80] H. Haken, Z. Phys. **182**, 346–359 (1965).

[81] J. A. Fleck Jr., Phys. Rev. **141**, 322–329 (1966).

[82] M. Lax, Phys. Rev. **145**, 110–129 (1966).

[83] M. Scully and W. E. Lamb Jr., Phys. Rev. Lett **16**, 853–855 (1966).

The earliest paper that probably talks about quadrature squeezed state

[84] K. Husimi, Prog. Theor. Phys. **9**, 381 (1953).

The quadrature squeezed state through equivalence classes of minimum uncertainty states in

[85] D. Stoler, Phys. Rev **D1**, 3217 (1970).

[86] D. Stoler, Phys. Rev. **D4**, 1925 (1971).

[87] E. Y. C. Lu, Lett. Nuovo Cimento, **2**, 1241 (1971).

[88] E. Y. C. Lu, Lett. Nuovo Cimento, **3**, 585 (1972).

Two photon formulation of quadrature squeezed states

[89] H. P. Yuen, Phys. Rev. **A13**, 2226 (1976).

Introductory article on Squeezed states

[90] D. F. Walls, Nature **306**, 141 (1983).

Review articles on quadrature squeezed states. (See also [96])

[91] R. Loudon and P. L. Knight, J. Mod. Opt **34**, 709 (1987).

[92] M. C. Teich and B. E. A. Saleh, Quant. Opt. **1**, 153 (1989).

[93] M. C. Teich and B. E. A. Saleh, Physics Today **43**, 26 (1990).

Special issues on squeezed states

[94] J. Opt. Soc. Am. **B4** (10) (1987) ; J. Mod. Opt. **34**, (6/7) (1987).

Quadrature squeezed states defined as minimum uncertainty states associated with the generalized Heisenberg inequality

[95] V. V. Dodonov, E. V. Kurmyshev and V. I. Man'ko, Phys.Lett. **A79**, 150 (1980).

And defined as part of Gaussian pure states

[96] B. L. Schumaker, Phys. Rep. **135**, 317 (1986).

A more detailed study of Gaussian pure states in

[97] R. Simon, E. C. G. Sudarshan and N. Mukunda, Phys. Rev. **A36**, 3868 (1987).

[98] R. Simon, E. C. G. Sudarshan and N. Mukunda, Phys. Rev. **A37**, 3028 (1988).

Quadrature squeezed states - Multimode case

[99] G. J. Milburn, J. Phys. **A17**, 737 (1984).

[100] C. M. Caves, Phys. Rev. Lett. **54**, 2465 (1985).

Theory of four-wave mixing

[101] R. W. Hellwarth, J. Opt. Soc. Am. **67**, 1 (1977).

[102] A. Yariv and D. M. Pepper, Opt. Lett. **1**, 16 (1977).

In relation to quadrature squeezing

[103] H. P. Yuen and J. H. Shapiro, Opt. Lett. **4**, 334 (1979).

First experimental observation of quadrature squeezing using four-wave mixing in Sodium vapor

[104] R. E. Slusher, L. W. Hollberg, B. Yurke, J. C. Mertz and J. F. Valley, Phys. Rev. Lett. **55**, 2409 (1985).

Theory of parametric amplification

[105] W. H. Louisell, A. Yariv and A. S. Siegman, Phys. Rev. **124**, 1646 (1961).

[106] A. Yariv, Quantum Electronics, Wiley – New York (1967).

[107] B. R. Mollow, Phys. Rev. **162**, 1256 (1967).

[108] B. R. Mollow and R. J. Glauber, Phys. Rev. **160**, 1076 (1967).

[109] B. R. Mollow and R. J. Glauber, Phys. Rev. **160**, 1097 (1967).

[110] T. G. Giallorenzi, and C. L. Tang, Phys. Rev. **166**, 905 (1968).

[111] B. R. Mollow, Phys. Rev. **A8**, 2684 (1973).

Squeezing in Optical Parametric Oscillator operating in the sub-threshold regime

[112] B. Yurke, Phys. Rev. **A29**, 408 (1984).

[113] M. J. Collett and C. W. Gardiner, Phys. Rev. **A30**, 1386 (1984).

[114] C. W. Gardiner and C. M. Savage, Opt. Commun. **50**, 173 (1984).

Enhancement of non-linearity when the medium is placed in a cavity

[115] L. A. Wu, H. J. Kimble, J. L. Hall and H. Wu, Phys. Rev. Lett. **57**, 2520 (1986).

[116] Ling-Au Wu, Min Xiao and H. J. Kimble, J. Opt. Soc. Am. **B4**, 1465 (1987).

[117] L. A. Wu, Min Xiao and H. J. Kimble, J. Opt. Soc. Am. **B4**, 1465 (1988).

Association of quadrature squeezing to the emission of twin photons

[118] C. K. Hong and L. Mandel, Phys. Rev. **A31**, 2409 (1985).

[119] S. Reynold, C. Fabre and E. Giacobino, J. Opt. Soc. Am. **B4**, 1520 (1987).

Measurement of time lag between the twin photons

[120] S. Friberg, C. K. Hong and L. Mandel, Phys. Rev. Lett. **54**, 2011 (1984).

Squeezing in the difference of intensities due to pair correlation of photons

[121] J. G. Rarity and P. R. Tapster, Phys. Rev. **A41**, 5139 (1990).

Highest noise reduction in such measurements

[122] O. Aytur and P. Kumar, Phys. Rev. Lett. **65**, 1551 (1990).

Second Harmonic generation

[123] P. A. Franken, A. E. Hill, C. W. Peters and G. Weinreich, Phys. Rev. Lett. **7**, 118 (1961).

[124] J. A. Armstrong, N. Bloembergen, J. Ducuing and P. S. Pershan, Phys. Rev. **127**, 1918 (1962).

[125] M. Kozierowski and R. Tanas, Opt. Commun. **21**, 229 (1977).

[126] S. Kielich, M. Kozierowski and R. Tanas, in *Coherence and Quantum Optics*, edited by L. Mandel and E. Wolf, Plenum - New York, (1984), Vol. **IV**.

[127] L. Mandel, Opt. Commun. **42**, **437** (**1982**).

Same squeezing for both the pump and signal fields when the cavity with the medium is at resonance with both the pump and signal frequencies

[128] L. A. Lugiato, G. Strini and F. De Martini, Opt. Lett. **8**, 256 (1983).

Experimental demonstration of squeezing in fundamental mode

[129] S. F. Pereira, Min Xiao, H. J. Kimble and J. L. Hall, Phys. Rev. **A38**, 4931 (1988).

Experimental demonstration of squeezing in the up-converted mode

[130] A. Sizmann, R. H. Horowicz, G. Wagner and G. Leuchs, Opt. Commun. **80**, 138 (1990).

Quadrature squeezing in Short cavity : decay rate of atomic polarization and the cavity modes matched - to achieve which, the cavity has to be only a few millimeters - theory in connection with optical bistability

[131] H. J. Carmichael, Frontiers in Quantum Optics, edited by *E. R. Pike and Sarben Sarkar*, 120 (1986).

The above theory without adiabatic elimination

[132] F. Castelli, L. A. Lugiato and M. Vadacchino, Il Nuovo Cimento **10D**, 183 (1988).

[133] M. D. Reid, Phys. Rev. **A37**, 4792 (1988).

[134] D. M. Hope, D. E. McClelland and C. M. Savage, Phys. Rev. **A41**, 5074 (1990).

Related Experiments - in Sodium atoms, 30% squeezing

[135] M. G. Raizen, L. A. Orozco, Min Xiao, T. L. Boyd and H. J. Kimble, Phys. Rev. Lett. **59**, 198 (1987).

[136] L. A. Orozco, M. G. Raizen, Min Xiao, R. J. Brecha and H. J. Kimble, J. Opt. Soc. Am. **B4**, 1490 (1987).

Without cavity - pulsed high power laser beams

[137] R. E. Slusher, P. Grangier, A. Laporta, B. Yurke, and M. J. Potasek, Phys. Rev. Lett. **59**, 2566 (1987).

[138] T. Hirano and M. Matsuoka, Int. Conf. on Quantum Electronics Technical Digest Series, Vol. 8, p.391, Optical Society of America — Washington DC (1990).

Quadrature squeezing in a Fiber using the χ_3 non-linearity of the fiber to shape the field's fluctuation through self modulation - First Experimental demonstration

[139] R. M. Shelby, M. D. Levenson, S. H. Perlmutter, R. G. De Voe and D. F. Walls, Phys. Rev. Lett. **57**, 691 (1986).

[140] M. Shirasaki and H. A. Haus, J. Opt. Soc. Am. **B7**, 30 (1990).

[141] K. Bergman and M. Shirasaki, Opt. Lett. **16**, 663 (1991).

Squeezed state generation in a cavity with moving walls (See [42] for quantizing such a cavity)

[142] V. V. Dodonov, A. B. Klimov and V. I. Man'ko, Phys. Lett. **A149**, 225 (1990).

Squeezing in harmonic oscillators with time-dependent frequencies

[143] Xin Ma and W. Rhodes, Phys. Rev. **A39**, 1941 (1989).

[144] G. S. Agarwal and S. Arun Kumar, Phys. Rev. Lett. **67**, 3665 (1991).

Squeezed light in connection with gravitational wave detection

[145] J. N. Hollenhorst, Phys. Rev. **D19**, 1669 (1979).

Proposal that the injection of squeezed vacuum into the empty port of the interferometer will improve the sensitivity

[146] C. M. Caves, Phys. Rev. **D23**, 1693 (1981).

[147] L. P. Grishchuk and M. V. Sazhin, Sov. Phys. JETP **57**, 1128 (1983).

Other proposals for increasing the sensitivity of instruments measuring the phase using quadrature squeezed light

[148] R. S. Boudurant and H. J. Shapiro, Phys. Rev. **D30**, 2548 (1984).

[149] M. Shirasaki and H. A. Haus, J. Opt. Soc. Am. **B8**, 681 (1991).

Experimental verification of the above proposal

[150] P. Grangier, R. E. Slusher, B. Yurke and A. LaPorta, Phys. Rev. Lett. **59**, 2153 (1987).

Interferometer with and without non-linear elements can be described in a natural fashion in terms of the usual variables used to describe quadrature squeezing and vice versa. (which suggest that interferometers can be used to measure the amount of quadrature squeezing and quadrature squeezing can be used to improve the interferometer)

[151] B. Yurke, S. McCall and J. Klauder, Phys. Rev. **A33**, 4033 (1986).

Generalized Horne-Shimony-Zeilinger two photon momentum-position interferometer suggested by

[152] M. A. Horne, A. Shimony and A. Zeilinger, Phys. Rev. Lett. **62**, 2209 (1989).

Experimentally implemented by

[153] J. Rarity and P. Tapster, Phys. Rev. Lett. **64**, 2495 (1990).

Three particle version proposed by

[154] D. M. Greenberger *et al*, Am. J. Phys. **58**, 1131 (1990).

Two particle gedanken interferometer that uses the interference between two possible states each of which belongs to a different emission time

[155] J. D. Franson, Phys. Rev. Lett. **62**, 2205 (1989).

Experimentally realized by

[156] Z. Y. Ou, L. J. Wang, X. Y. Zou and L. Mandel, Phys. Rev. Lett. **65**, 321 (1990).

[157] P. Kwiat, W. A. Vareka, C. K. Hong, H. Nathel and R. Y. Chiao, Phys. Rev. **A41**, 2910 (1990).

Multiphoton correlation can lead to more squeezing

[158] S. Braunstein and R. McLachlan, Phys. Rev. **A35**, 1659 (1987).

And more anti-bunching (and also amplitude squeezing)

[159] C. T. Lee, Phys. Rev. **A41**, 1721 (1990).

Also, multi-particle correlation can lead to exponential increase in violation of Bell inequalities

[160] N. D. Mermin, Phys. Rev. Lett. **65**, 1838 (1990).

[161] N. D. Mermin, Physics Today, 9 (June 1990).

EPR paper

[162] A. Einstein, B. Podolsky and N. Rosen, Phys. Rev. **47**, 777 (1935).

Gedanken experiments of spin 1/2 particles discussed in

[163] D. Bohm, Quantum Theory, Prentice Hall – Englewood Cliffs (1951).

Bell's inequality

[164] J. S. Bell, Physics **1**, 195 (1964).

The word 'entanglement' in the context of quantum states was introduced by

[165] E. Schrödinger, Naturwissenschaften **23**, 807-812, 823-828, 844-849 (1935).

An excellent review of experiments to test Bell's inequalities to differentiate between the hidden variable theory and the normal quantum mechanics using light from atomic cascade decay

[166] J. F. Clauser and A. Shimony, Rep. Prog. Phys. **41**, 1881 (1976).

Recent experiments using atomic cascade decay

[167] A. Aspect, P. Grangier and G. Roger, Phys. Rev. Lett. **47**, 460 (1981).

[168] A. Aspect, P. Grangier and G. Roger, Phys. Rev. Lett. **49**, 91 (1982).

[169] A. Aspect, J. Dalibard and G. Roger, Phys. Rev. Lett. **49**, 1804 (1982).

Anyway for many people in the physics community none of these have really demonstrated the phase correlation of the EPR state and consequently not a compelling test of Bell's inequality, and this changed when the first EPR experiment using light quanta pair generated by optical parametric down conversion was used to test the inequalities as in (See also [152]

[170] Y. H. Shih and C. O. Alley, Phys. Rev. Lett. **61**, 2921 (1988).

[171] Z. Y. Ou and L. Mandel, Phys. Rev. Lett. **61**, 50 (1988).

Self-focusing of radiation field

[172] S. A. Akhmanov, R. V. Khokhlov and A. P. Sukhorukov, Laser Handbook, Vol.2, edited by *F. T. Arecchi and E. V. Schulz-Dubois*

Self-trapping...

[173] O. Svelto, Progress in Optics, Vol.XII, edited by *E. Wolf*, p.1, (1974).

Self-phase modulation of radiation field - See also [139], [140], [141]

[174] Y. R. Shen, Rev. Mod. Phys. **48**, 1 (1976).

Dynamics of Kerr medium

[175] Y. R. Shen, in *Quantum Optics*, edited by R. J. Glauber (Academic, New York, 1969), p. 489.

[176] R. H. Stolen and C. Lin, Phys. Rev. **A17**, 1448 (1978).

[177] R. Tanas and S. Kielich, Opt. Commun. **30**, 443 (1979).

[178] P. Tombesi and H. P. Yuen, in *Coherence and Quantum Optics*, edited by L. Mandel and E. Wolf (Plenum, New York, 1984). Vol. V.

[179] M. D. Reid and D. F. Walls, Opt. Commun. **50**, 406 (1984).

Optical Solitons

[180] A. Barthelemy, S. Maneuf and C. Froehly, Opt. Commun. **55**, 193 (1985).

[181] S. Maneuf, R. Desailly and C. Froehly, Opt. Commun. **55**, 193 (1988).

Quantum Solitons

[182] F. Singer, M. .J. Potasek and J. M. Fang and M. C. Teich, Phys. Rev. **A46**, 4192 (1992).

Optical bistability

[183] H. M. Gibbs, Optical Bistability: Controlling light with light, Academic press — New York, (1985).

Applications of Optical bistability

[184] B. E. A. Saleh and M. C. Teich, Fundamentals of Photonics, Wiley — New York, (1991).

Optical non-demolition measurements using Kerr medium

[185] N. Imoto, H. A. Haus and Y. Yamamoto, Phys. Rev. **A32**, 2287 (1985).

[186] M. Kitagawa, N. Imoto and Y. Yamamoto, Phys. Rev. **A35**, 5270 (1987).

[187] N. Imoto and S. Saito, Phys. Rev. **A39**, 675 (1989).

Detailed quantum description of non-destructive measurement of parameters of optical fields using Kerr medium, application in Optical system information capacity, etc - a review

[188] Y. Yamamoto and H. A. Haus, Rev. Mod. Phys. **58**, 1001 (1986).

Review about Kerr medium

[189] V. Peřinová and A. Lukš, Progress in Optics, Vol. XXXIII, edited by *E. Wolf*, p.129, (1994)

Generation of amplitude squeezed states using Kerr medium - Number-phase squeezed state

[190] H. H. Ritze and A. Bandilla, Opt. Commun. **29**, 126 (1979).

[191] M. Kitagawa and Y. Yamamoto, Phys. Rev. **A34**, 3974 (1986).

[192] Y. Yamamoto, S. Machida, N. Imoto, M. Kitagawa, and G. Björk, J. Opt. Soc. Am. **B4**, 1645 (1987).

[193] N. Grønbech and P. S. Ramanujam, Phys. Rev. **A41**, 2906 (1990).

Kerr medium explained as third order non-linear oscillator - Single mode analysis

[194] P. D. Drummond and D. F. Walls, J. Phys. **A13**, 725 (1980).

[195] R. Tanaś, Progress in Optics, Vol. V, edited by *E. Wolf*, p.645, (1984).

[196] M. J. Collett and D. F. Walls, Phys. Rev. **A32**, 2887 (1985).

[197] G. J. Milburn, Phys. Rev. **A33**, 674 (1986).

Inclusion of effect of loss, when the reservoir is at zero temperature

[198] G. J. Milburn and C. A. Holmes, Phys. Rev. Lett. **56**, 2237 (1986).

[199] G. J. Milburn, A. Mecozzi and P. Tombesi, J. Mod. Opt. **36**, 1607 (1989).

Inclusion of effect of loss for a general initial state, when the reservoir is at zero temperature

[200] V. Peřinová and A. Lukš, J. Mod. Opt. **35**, 1513 (1988).

Bath at any temperature with an initial coherent state

[201] D. J. Daniel and G. J. Milburn, Phys. Rev. **A39**, 4628 (1989).

Bath at any temperature with any initial state

[202] V. Peřinová and A. Lukš, Phys. Rev. **A41**, 414 (1990).

[203] S. Chaturvedi and V. Srinivasan, J. Mod. Opt **38**, 777 (1991).

Sub-poissonian light from Hg vapor excited by a space-charge limited electron beam

[204] M. C. Teich and B. E. A. Saleh, J. Opt. Soc. Am. **B2**, 275 (1985).

Amplitude squeezed light ($f_n = 0.98$) from high-efficiency light emitting diode driven by a Johnson-noise-limited high-impedance current source

[205] P. R. Tapster, J. G. Rarity and J. S. Satchell, Europhys. Lett. **4**, 293 (1987).

Amplitude squeezed light from semiconductor laser using sub-poissonian pumping current

[206] S. Machida, Y. Yamamoto and Y. Itacha, Phys. Rev. Lett. **58**, 1000 (1987).

Theoretical analysis of amplitude squeezing in a laser with sub-poissonian pumping

[207] M. A. Marte and D. F. Walls, Phys. Rev. **A37**, 1235 (1988).

[208] S. Machida and Y. Yamamoto, Phys. Rev. Lett. **60**, 792 (1988).

[209] W. H. Richardson and R. M. Shelby, Phys. Rev. Lett. **64**, 400 (1990).

Amplitude squeezing using quantum non-demolition and negative feedback

[210] Y. Yamamoto, N Imoto and S. Machida, Phys. Rev. **A33**, 3243 (1986).

Experimental demonstration of sub-poissonian light with negative feedback

[211] S. Machida and Y. Yamamoto, Opt. Commun. **57**, 290 (1986).

Quantum correlated twin beams showing sub-poissonian statistics in an intensity-intensity correlation measurement using series and parallel coupled light emitting diodes

[212] E. Goobar, A. Karlsson, G. Björk and P.-J. Rigole, Phys. Rev. Lett. **70**,437 (1993).

Quantum repeater by coupling a photo-diode and a light emitting diode to recreate the quantum statistics of the input beam

[213] J.-F. Roch, J.-Ph. Poizat and P. Grangier, Phys. Rev. Lett. **71**, 2006 (1993).

The parametric amplifier generating amplitude squeezed light when used as a deamplifier to deamplify an initial coherent state

[214] M. Koashi, K. Kano, T. Hirano and M. Matsuoka, Phys. Rev. Lett. **71**, 1164 (1993).

Numerical attempts to calculate the evolution of quadrature squeezed state through a Kerr medium

[215] A. Banerjee, Quant. Opt. **5**, 15 (1993).

Theoretical proposals for generating states close to Fock states

[216] M. J. Collett, Phys. Rev. Lett. **70**, 400 (1993).

[217] S. Ya. Kilin and D. B. Horoshko, Phys. Rev. Lett. **74**, 5206 (1995).

Evolution of quadrature squeezed state through Kerr medium and the generation of highly amplitude squeezed states

[218] Kasivishvanathan Sundar, Phys. Rev. Lett. **75**, 2116 (1995).

[219] Kasivishvanathan Sundar, Phys. Rev. **A53**, 1096 (1996).

Using Kerr medium in detection of non-classical states

[220] G. S. Agarwal, Opt. Commun. **72**, 253 (1989).

[221] M. Hillery, Phys. Rev. **A44**, 4578 (1991).

Related concept of photon number amplifier (which preserves the number-phase noise)

[222] H. P. Yuen, Phys. Rev. Lett. **56**, 2176 (1986).

Squeezing gets killed if the intensity gain of an optical amplifier $|G|^2 > 2$. (sort of upper limit for the amplification of light showing non-classical behavior)

[223] C. K. Hong, S. Friberg and L. Mandel, J. Opt. Soc. Am. **B2**, 494 (1985).

Concept of optical amplifier giving $\langle \hat{a}(t) \rangle = G \langle \hat{a}(0) \rangle$ was thoroughly analyzed using the definition that the amplifier consists of a collection of two level atoms of which N_1 are in the ground state and N_2 in the excited state, and $N_2 > N_1$ in

[224] S. Carusotto, Phys. Rev. **A11**, 1629 (1975).

Other types of squeezing : SU(1,1) squeezing, later named by Hillery as amplitude squared squeezing

[225] K. Wodkiewicz and J. H. Eberly, J. Opt. Soc. Am. **B2**, 458 (1985).

Amplitude squared squeezing (See also [243])

[226] M. Hillery, Opt. Commun. **62**, 135 (1987).

[227] J. Bergou, M. Hillery and D. Yu, Phys. Rev. **A43**, 515 (1991).

The representations of SU(1,1) can be used to study higher order squeezing as done in

[228] C. C. Gerry, Phys. Rev. **A31**, 2721 (1985).

[229] P. K. Aravind, J. Opt. Soc. Am. **B5**, 1545 (1988).

[230] V. Bužek, J. Mod. Opt. **37**, 303 (1990).

Difference squeezing : related to SU(2) Lie algebra in that, the operators considered form a SU(2)

[231] M. Hillery, Phys. Rev. **A40**, 3147 (1989).

Bogolibov transformations

[232] N. Bogolibov, J. Phys. USSR **11**, 292 (1947).

Noise matrix is elucidated in

[233] S. Simon and R. Simon, in *Coherence and Quantum Optics*, edited by L. Mandel and E. Wolf, Plenum – New York, (1990), Vol. **VI**.

Definition of Q-parameter, used to access the degree of amplitude squeezing

[234] L. Mandel, Opt. Lett. **4**, 205 (1979).

Higher order squeezing

[235] C. K. Hong and L. Mandel, Phys. Rev. Lett. **54**, 323 (1985).

[236] C. K. Hong and L. Mandel, Phys. Rev. **A32**, 974 (1985).

Impossibility of naively generalizing squeezed states

[237] R. A. Fisher, M. M. Nieto and V. D. Sandberg, Phys. Rev. **D29**, 1107 (1984).

Non-classical states without squeezing or sub-poissonian statistics

[238] G. S. Agarwal and K. Tara, Phys. Rev. **A46**, 485 (1992).

Squeezed number states done in

[239] M. S. Kim, F. A. M. DeOliveira and P. L. Knight, Phys. Rev. **A40**, 2494 (1989).

Superposition of number states

[240] K. Wódkiewicz, P. L. Knight, S. J. Buckle and S. M. Barnett, Phys. Rev. **A35**, 2567 (1987).

Superposition arising due to propagation of coherent states in amplitude-dispersive (Kerr) medium (See also [197, 198])

[241] B. Yurke and D. Stoler, Phys. Rev. Lett. **57**, 13 (1986).

This state when displaced shows amplitude squeezing

[242] A. D. Wilson-Gordon, V. Bužek, and P. L. Knight, Phys. Rev. **A44**, 7647 (1991).

Even-coherent state in connection with amplitude-squared squeezing

[243] M. Hillery, Phys. Rev. **A36**, 3796 (1987).

Even-coherent states show 4th order squeezing

[244] V. Bužek, I. Jex and Tran Quang, J. Mod. Opt. **37**, 159 (1990).

Continuous one dimensional superposition of coherent states

[245] J. Janszky and An. V. Vinogradov, Phys. Rev. Lett. **64**, 2771 (1990).

Quadrature squeezed state as a superposition of coherent states. See also [219]

[246] P. Adam, J. Janszky and An. V. Vinogradov, Opt. Commun. **80**, 155 (1990).

[247] V. Bužek and P. L. Knight, Opt. Commun. **81**, 331 (1991).

[248] G. S. Agarwal and R. Simon, Opt. Commun. **92**, 105 (1992).

Superposition of coherent states situated at the vertices of a polygon - amplitude squeezing in such states

[249] K. Sundar and R. Simon, work in progress

A new superposition $\left|\alpha e^{i\phi/2}\right\rangle + \left|\alpha e^{-i\phi/2}\right\rangle$ of coherent states

[250] W. Schleich, M. Pernigo and Fam Le Kien, Phys. Rev. **A44**, 2172 (1991).

Logarithmic states of the radiation field

[251] R. Simon and M. Venkata Satyanarayana, J. Mod. Opt. **35**, 719 (1988).

Squeezed number states [239] can be expressed as a superposition of displaced number states as in

[252] F. A. M. DeOliveira, M. S. Kim, P. L. Knight and V. Bužek, Phys. Rev. **A41**, 2645 (1990).

Explanation of squeezing in superposition of coherent states in terms of phase space distributions

[253] W. P. Schleich and J. A. Wheeler, J. Opt. Soc. Am. **B4**, 1715 (1987).

[254] W. P. Schleich, D. F. Walls and J. A. Wheeler, Phys. Rev. **A38**, 1177 (1988).

Squeezed superposition states

[255] E. E. Hach III and C. C. Gerry, Jour. of Mod. Opt. **40**, 2351 (1993).

Amplitude squeezing in the superposition of two phase squeezed coherent states

[256] K. Sundar, J. Mod. Opt., in press (1996).

From an initial squeezed state, quantum jumps lead to superposition of coherent states

[257] B. M. Garraway and P. L. Knight, Phys. Rev. **A50**, 2548 (1994).

Geometric phase (Berry–Pancharatnam) : Geometry underlying the residual phase arising in quantum systems that make a closed circuit in parameter space - Formulation in terms of line bundles

[258] B. Simon, Phys. Rev. Lett. **51**, 2167 (1983).

Reformulation of this phase in

[259] M. V. Berry, Proc. R. Soc. **A392**, 45 (1984).

Pancharatnam's phase in connection with Berry phase was pointed out in

[260] S. Ramaseshan and R. Nityananda, Curr. Sci. **55**, 1225 (1986).

[261] R. Bhandari and J. Samuel, Phys. Rev. Lett. **60**, 1211 (1988).

[262] T. H. Chyba, L. J. Wang, L. Mandel, R. Simon, Opt. Lett. **13**, 562 (1988).

Pancharatnam's paper

[263] S. Pancharatnam, Proc. Indian Acad. Sci. Sect. A **44**, 247 (1956) ; Reprinted in Collected works of S. Pancharatnam, Oxford Univ. Press – London (1975).

Geometric phase in Optics

[264] S. Simon and R. Simon, in *Coherence and Quantum Optics*, edited by L. Mandel and E. Wolf, Plenum – New York, (1990), Vol. **VI**.

[265] G. S. Agarwal and R. Simon, Phys. Rev. **A42**, 6924 (1900).

A Quantum kinematic approach to geometric phase

[266] N. Mukunda and R. Simon, Ann. Phys. **228**, 205 (1993).

[267] N. Mukunda and R. Simon, Ann. Phys. **228**, 269 (1993).

Dynamical manifestation of geometric phase as a frequency shift

[268] R. Simon, H. J. Kimble and E. C. G. Sudarshan, Phys. Rev. Lett. **61**, 19 (1988).

Used in Michelson interferometer to see fringes without changing the distance of the arms by a unique arrangement of quarter waveplates inside it

[269] P. G. Kwiat and R. Y. Chiao, Phys. Rev. Lett. **66**, 588 (1991).

BCH Formula

[270] J. E. Campbell, Proc. Lon. Math. Soc. **28**, 381 (1897).

[271] H. F. Baker, Proc. Lon. Math. Soc. **34**, 347 (1902).

[272] H. F. Baker, Proc. Lon. Math. Soc. **35**, 333 (1903).

[273] H. F. Baker, Proc. Lon. Math. Soc. **2**, 293 (1905).

[274] F. Hausdorff, Ber. Verh. Saechs. Akad. Wiss. Leipzig Math. Phys. Kl. **58**, 19 (1906).

In a more accessible form in

[275] R. M. Wilcox, J. Math. Phys. **8**, 962 (1967).

Normal ordering of exponentials quadratic in boson operators

[276] C. L. Mehta, Jour. of Math. Phys. **18**, 404 (1977).

[277] G. P. Agrawal and C. L. Mehta, Jour. of Math. Phys. **18**, 408 (1977).

Author Index

Bhandari R., 1988 [261] (42).

Bialynicka-Birula I., 1987 See [41] (8).

Bialynicka-Birula Z., 1987 [41] (8).

Björk G., 1987 See [192] (32) ; 1993 See [212] (149).

Bloembergen N., 1962 See [124] (23) ; 1965 [32] (4).

Bogolibov N., 1947 [232] (26).

Bohm D., 1951 [163] (31).

Bohr N., 1913 [11] (2).

Born M., 1925 [14] (2) ; 1926 [15] (2) ; 1964 [29] (4).

Boudurant R. S., 1984 [148] (30).

Boyd T. L., 1987 See [135] (24).

Braunstein S., 1987 [158] (31).

Brecha R. J., 1987 See [136] (24).

Buckle S. J., 1987 See [240] (127).

Bunsen R., 1860 See [7] (2).

Bužek V., 1990 [244] (68), [230] (39), See [252] (27) ; 1991 [247] (27, 56, 56, 100, 133), [242] (52, 81, 130).

Cahill K. E., 1969 [70] (19, 51), [71] (19, 51).

Campbell J. E., 1897 [270] (16, 84, 103).

Carmichael H. J., 1986 [131] (24).

Carniglia C. K., 1971 [34] (8).

Carruthers P., 1968 [49] (21).

Carusotto S., 1975 [224] (39).

Casimir H. B. G., 1948 [43] (8).

Castelli F., 1988 [132] (24).

Caves C. M., 1985 [100] (22).

Chaturvedi S., 1991 [203] (33).

Chiao R. Y., 1990 See [157] (31) ; See [269] (42).

Chyba T. H., 1988 [262] (42).

Clauser J. F., 1976 [166] (31).

Collett M. J., 1984 [113] (22, 132) ; 1985 [196] (23, 32, 104) ; 1993 [216] (38, 38, 149, 150).

Cook R. J., 1988 See [45] (9).

Craig D. P., 1984 [28] (3).

Dalibard J., 1982 See [169] (31).

Daniel D. J., 1989 [201] (33).

De Broglie L., 1925 [18] (2).

De Martini F., 1983 See [128] (23).

De Oliveira F. A. M., 1989 See [239] (27, 193) ; 1990 [252] (27).

De Voe R. G., 1986 See [139] (24, 150, 185).

Debye P., 1912 [6] (2).

Desailly R., 1988 See [181] (32).

Dirac P. A. M., 1925 [16] (3) ; 1926 [17] (3) ; 1927 [73] (3, 9, 21, 174) ; 1928 [21] (3) ; 1930 [20] (3).

Dodonov V. V., 1980 [95] (22) ; 1990 [142] (8, 38, 173).

Drummond P. D., 1980 [194] (32, 32, 32, 104) ; 1990 [39] (8).

Ducuing J., 1962 See [124] (23).

Eberly J. H., 1985 See [225] (39).

Einstein A., 1905 [2] (2) ; 1907 [4] (2) ; 1909 [3] (2) ; 1911 [5] (2) ; 1917 [72] (3, 9) ; 1935 [162] (31).

Fabre C., 1987 See [119] (23).

Fam Le Kien, 1991 See [250] (70, 71, 73, 127).

Fang J. M., 1992 See [182] (32).

Feng D. H., 1990 See [69] (13).

Fermi E., 1932 [23] (3, 3, 4, 9).

Fisher R. A., 1984 [237] (27, 39, 153).

Fleck Jr. J. A., 1966 [81] (9).

Franken P. A., 1961 [123] (23).

Franson J. D., 1989 [155] (31).

Friberg S., 1984 [120] (23) ; 1985 See [223] (39).

Froehly C., 1985 See [180] (32) ; 1988 See [181] (32).

Hirano T., 1990 [138] (24) ; 1993 See [214] (149, 152).

Hollberg L. W., 1985 See [104] (22).

Hollenhorst J. N., 1979 [145] (26, 30).

Holmes C. A., 1986 See [198] (33, 52, 192).

Hong C. K., 1984 See [120] (23) ; 1985 [118] (23), [223] (39), [235] (39, 64), [236] (39, 64) ; 1990 See [157] (31).

Hope D. M., 1990 [134] (24).

Horne M., 1989 [152] (30, 185).

Horoshko D. B., 1995 See [217] (38, 38).

Horowicz R. H., 1990 See [130] (23).

Imoto N., 1985 [185] (32, 34, 104, 104, 149, 150) ; 1986 See [210] (38, 149) ; 1987 See [192] (32).

Itacha Y., 1987 See [206] (38, 149).

Jackson J. D., 1975 [31] (4, 4).

Janszky J., 1990 [245] (28), See [246] (27, 100, 133).

Jauch J. M., 1948 [33] (8).

Jex I., 1990 See [244] (68).

Jusimi K., 1953 [84] (21).

Jordan P., 1925 [14] (2) ; 1926 See [15] (2).

Kano K., 1993 See [214] (149, 152).

Karlsson A., 1993 See [212] (149).

Khokhlov R. V., 1972 See [172] (32).

Kielich S., 1978 [126] (23) ; 1979 See [177] (24, 150).

Kilin S. Ya., 1995 [217] (38, 38).

Kim M. S., 1989 [239] (27, 193) ; 1990 See [252] (27).

Kimble H. J., 1986 See [115] (22) ; 1987 See [116] (22, 131), See [135] (24), See [136] (24) ; 1988 See [117] (23), See [129] (23), See [268] (42).

Kimble T. W. B., 1970 [26] (3).

Kirchhoff G., 1860 [7] (2).

Kitagawa M., 1986 [191] (32, 32, 37, 38, 105, 106, 106, 132, 149, 150, 150, 150, 152, 160) ; 1987 See [192] (32).

Klauder J., 1986 See [151] (30).

Klauder J. R., 1960 [56] (13) ; 1963 [57] (13) ; 1968 [64] (13, 13, 14, 42) ; 1985 [68] (13).

Klimov A. B., 1990 See [142] (8, 38, 173).

Knight P. L., 1987 See [91] (9, 24, 174), See [240] (127) ; 1989 See [239] (27, 193) ; 1990 See [252] (27) ; 1991 See [247] (27, 56, 56, 100, 133), [242] (52, 81, 130) ; 1994 See [257] (130).

Knoll L., 1987 [38] (8).

Koashi M., 1993 [214] (149, 152).

Kozierowski M., 1977 [125] (23) ; 1978 See [126] (23).

Kumar P., 1990 See [122] (23).

Kurmyshev E. V., 1980 See [95] (22).

Kwiat P., 1990 [157] (31) ; 1991 [269] (42).

Lamb Jr. W. E., 1966 See [83] (9).

Landau L. D., 1971 [30] (4).

Laporta A., 1987 See [137] (24), See [150] (30).

Lax M., 1966 [82] (9).

Lee C. T., 1990 [159] (31).

Leuchs G., 1990 See [130] (23).

Levenson M. D., 1986 See [139] (24, 150, 185).

Lewenstein M., 1991 See [40] (8).

Lin C., 1978 See [176] (24, 34, 150).

Loudon R., 1987 [91] (9, 24, 174).

Louisell W. H., 1961 [105] (22) ; 1973 [27] (3, 7, 16, 16, 84, 96, 103).

Lu E. Y. C., 1971 [87] (26, 99) ; 1972 [88] (26, 99).

Lugiato L. A., 1983 [128] (23) ; 1988 See [132] (24).

Lukš A., 1988 See [200] (33) ; 1990 See [202] (33) ; 1994 See [189] (38).

Ma X., 1989 [143] (38).

Machida S., 1986 [211] (38, 149), See [210] (38, 149) ; 1987 [206] (38, 149), [208] (38), See [192] (32).

Maiman T. H., 1960 [76] (9).

Mandel L., 1971 See [34] (8) ; 1979 [234] (12, 134) ; 1982 [127] (23) ; 1984 See [120] (23), Ed. See [178] (24, 104, 150) ; 1985 See [118] (23), See [223] (39), See [235] (39, 64), See [236] (39, 64) ; 1988 See [171] (31), See [262] (42) ; 1990 See [156] (31).

Maneuf S., 1985 See [180] (32) ; 1988 [181] (32).

Man'ko V. I., 1980 See [95] (22) ; 1990 See [142] (8, 38, 173).

Marte M. A., 1988 [207] (38).

Matsuoka M., 1990 See [138] (24) ; 1993 See [214] (149, 152).

McCall S., 1986 See [151] (30).

McClelland D. E., 1990 See [134] (24).

McLachlan R., 1987 See [158] (31).

Mecozzi A., 1989 See [199] (33).

Mehta C. L., 1977 [276] (30, 95, 101), See [277] (30, 95, 101).

Mermin N. D., 1990 [160] (31), [161] (31).

Mertz J. C., 1985 See [104] (22).

Milburn G. J., 1984 [99] (22) ; 1986 [197] (32, 32, 52, 104, 130, 133, 150, 192), [198] (33, 52, 192) ; 1989 [199] (33), See [201] (33).

Milonni P. W., 1988 [45] (9).

Mollow B. R., 1967 [107] (22), [108] (22), [109] (22).

Moore G. T., 1970 [42] (8, 38, 182).

Mukunda N., 1987 See [97] (22) ; 1988 See [98] (22) ; 1993 [266] (42, 45), [267] (42, 45).

Muller B., 1986 See [44] (9).

Nathel H., 1990 See [157] (31).

Nieto M. M., 1968 See [49] (21) ; 1984 See [237] (27, 39, 153).

Nityananda R., 1986 See [260] (42).

O'Connell R. F., 1984 See [59] (19).

Onofrio E., 1975 [66] (13).

Oppenheim A. V., 1975 [52] (21).

Orozco L. A., 1987 [136] (24), See [135] (24).

Ou Z. Y., 1988 [171] (31) ; 1990 [156] (31).

Pancharatnam S., 1956 [263] (42).

Pauli W., 1929 See [22] (3).

Pegg D. T., 1989 [50] (21), See [51] (21).

Peppard M. B., 1965 See [2] (2).

Pepper D. M., 1977 See [102] (22).

Pereira S. F., 1988 [129] (23).

Perelomov A. M., 1972 [65] (13, 42).

Pershan P. S., 1962 See [124] (23).

Peters C. W., 1961 See [123] (23).

Peřinová V., 1988 [200] (33) ; 1990 [202] (33) ; 1994 [189] (38).

Perlmutter S. H., 1986 See [139] (24, 150, 185).

Pernigo M., 1991 See [250] (70, 71, 73, 127).

Pike E. R., 1986 Ed. See [131] (24).

Plank M., 1900 [1] (1) ; 1901 [1] (1).

Plunien G., 1986 [44] (9).

Podolsky B., 1935 See [162] (31).

Poizat J. Ph., 1993 See [213] (149).

Potasek M. J., 1987 See [137] (24) ; 1992 See [182] (32).

Power E. A., 1964 [25] (3, 9, 173).

Quang T., 1990 See [244] (68).

Raizen M. G., 1987 [135] (24).

Ramanujam P. S., 1990 See [193] (32, 150).

Ramaseshan S., 1986 [260] (42).

Rarity J. G., 1987 See [205] (149) ; 1990 [121] (23), [153] (30).

Reid M. D., 1984 [179] (24, 34, 104, 150) ; 1988 [133] (24).

Reynold S., 1987 [119] (23).

Rhodes W., 1989 See [143] (38).

Richardson W. H., 1990 [209] (38).

Rigole P. J., 1993 See [212] (149).

Ritze H. H., 1979 [190] (38, 150).

Robertson H. P., 1931 [55] (13).

Roch J. F., 1993 [213] (149).

Roger G., 1981 See [167] (31) ; 1982 See [168] (31), See [169] (31).

Rosen N., 1935 See [162] (31).

Rutherford M., 1911 [10] (2).

Rydberg J. R., 1890 [9] (2).

Saleh B. E. A., 1985 See [204] (149) ; 1989 See [92] (24) ; 1990 See [93] (24) ; 1991 [184] (32).

Samuel J., 1988 See [261] (42).

Sandberg V. D., 1984 See [237] (27, 39, 153).

Sarkar S., 1986 Ed. See [131] (24).

Satchell J. S., 1987 See [205] (149).

Satyanarayana M. V., 1988 See [251] (127).

Savage C. M., 1984 See [114] (22, 132) ; 1990 See [134] (24).

Sazhin M. V., 1983 See [147] (30).

Schafer R. W., 1975 See [52] (21).

Schawlow A. L., 1958 [75] (9).

Schleich W., 1987 [253] (61, 81, 130) ; 1988 [254] (61, 81, 130) ; 1991 [250] (70, 71, 73, 127).

Schrödinger E., 1926 [19] (2), [53] (13) ; 1930 [54] (13) ; 1935 [165] (31).

Schulz-Dubois E. V., 1972 Ed. See [172] (32).

Schumaker B. L., 1986 [96] (22, 24, 178).

Scully M., 1966 [83] (9) ; 1984 See [59] (19).

Shapiro H. J., 1979 See [103] (22) ; 1984 See [148] (30) ; 1991 [48] (21).

Shelby R. M., 1986 [139] (24, 150, 185) ; 1990 See [209] (38).

Shen Y. R., 1967 [37] (8) ; 1969 [175] (24, 33, 35, 150) ; 1976 [174] (24, 32, 150).

Shepard S. R., 1991 See [48] (21).

Shih Y. H., 1988 [170] (31).

Shimoda K., 1957 [78] (9).

Shimony A., 1976 See [166] (31) ; 1989 See [152] (30, 185).

Shirasaki M., 1990 [140] (24, 150, 185) ; 1991 [149] (30), See [141] (24, 150, 185).

Siegman A. S., 1961 See [105] (22).

Simon B., 1983 [258] (42).

Simon R., 1987 [97] (22) ; 1988 [268] (42), [98] (22), [251] (127), See [262] (42) ; 1990 See [264] (45), See [265] (45) ; 1992 See [248] (27, 100, 133) ; 1993 See [266] (42, 45), See [267] (42, 45).

Simon S., 1990 [264] (45).

Singer F., 1992 [182] (32).

Sizmann A., 1990 [130] (23).

Skargerstam B. -S., 1985 See [68] (13).

Slusher R. E., 1985 [104] (22) ; 1987 [137] (24), See [150] (30).

Sommerfeld A., 1916 [12] (2).

Srinivasan V., 1991 See [203] (33).

Stolen R. H., 1978 [176] (24, 34, 150).

Stoler D., 1970 [85] (21, 26, 30, 47, 95, 99, 153) ; 1971 [86] (21, 26, 30, 47, 95, 99, 153) ; 1986 See [241] (52, 77, 81, 121, 127, 130, 133, 150).

Strini G., 1983 See [128] (23).

Sudarshan E. C. G., 1963 [61] (19) ; 1968 See [64] (13, 13, 14, 42) ; 1987 See [97] (22) ; 1988 See [98] (22), See [268] (42).

Sukhorukov A. P., 1972 See [172] (32).

Sundar K., 1995 [218] (32, 32, 37, 38, 108, 112, 150, 152, 167) ; 1996 [219] (27, 32, 32, 38, 100, 106, 108, 109, 112, 122, 130, 131, 133, 192), [256] (108, 130, 131).

Susskind L., 1964 [46] (21).

Svelto O., 1974 [173] (32).

Takahasi H., 1957 See [78] (9).

Tanaś R., 1977 See [125] (23) ; 1978 See [126] (23) ; 1979 [177] (24, 150) ; 1984 [195] (32, 32, 104).

Tang C. L., 1968 See [110] (22).

Tapster P. R., 1987 [205] (149) ; 1990 See [121] (23), See [153] (30).

Tara K., 1992 See [238] (39).

Teich M. C., 1985 [204] (149) ; 1989 [92] (24) ; 1990 [93] (24) ; 1991 See [184] (32) ; 1992 See [182] (32).

Thirunamachandran T., 1984 See [28] (3).

Tombesi P., 1984 [178] (24, 104, 150) ; 1989 See [199] (33).

Townes C. H., 1957 See [78] (9) ; 1958 See [75] (9).

Ujihara K., 1975 [35] (8).

Vadacchino M., 1988 See [132] (24).

Valley J. F., 1985 See [104] (22).

Vareka W. A., 1990 See [157] (31).

Vinogradov An. V., 1990 See [246] (27, 100, 133), See [245] (28).

Vogel W., 1987 See [38] (8).

Wagner G., 1990 See [130] (23).

Walls D. F., 1980 See [194] (32, 32, 32, 104) ; 1983 [90] (24) ; 1984 See [179] (24, 34, 104, 150) ; 1985 See [196] (23, 32, 104) ; 1986 See [139] (24, 150, 185) ; 1988 See [207] (38), See [254] (61, 81, 130).

Wang. L. J., 1988 See [262] (42) ; 1990 See [156] (31).

Watson K. M., 1948 See [33] (8).

Weinreich G., 1961 See [123] (23).

Weisskopf V., 1930 [74] (9).

Welsh D. -G., 1987 See [38] (8).

Wheeler J. A., 1987 See [253] (61, 81, 130) ; 1988 See [254] (61, 81, 130).

Wigner E., 1930 See [74] (9) ; 1932 [58] (19).

Wigner E. P., 1984 See [59] (19).

Wilcox R. M., 1967 [275] (16, 84, 103).

Wilson-Gordon A. D., 1991 [242] (52, 81, 130).

Wódkiewicz K., 1985 [225] (39) ; 1987 [240] (127).

Wolf E., 1964 See [29] (4) ; 1974 Ed. See [173] (32) ; 1984 Ed. See [195] (32, 32, 104), [178] (24, 104, 150) ; 1994 Ed. See [189] (38).

Wu H., 1986 See [115] (22).

Wu L. A., 1986 [115] (22) ; 1987 [116] (22, 131) ; 1988 [117] (23).

Xiao M., 1987 See [116] (22, 131), See [135] (24), See [136] (24) ; 1988 See [117] (23), See [129] (23) ; 1990 See [209] (38).

Yamamoto Y., 1985 See [185] (32, 34, 104, 104, 149, 150) ; 1986 [188] (37), [210] (38, 149), See [191] (32, 32, 37, 38, 105, 106, 106, 132, 149, 150, 150, 150, 152, 160), See [211] (38, 149) ; 1987 [192] (32), See [206] (38, 149), See [208] (38).

Yariv A., 1961 See [105] (22) ; 1967 [106] (22) ; 1977 [102] (22).

Yu D., 1991 See [227] (39).

Yuen H. P., 1976 [89] (22, 26, 27, 47, 95, 99, 153, 153) ; 1979 [103] (22) ; 1984 See [178] (24, 104, 150) ; 1986 [222] (39).

Yurke B., 1984 [112] (22, 132) ; 1985 See [104] (22) ; 1986 [241] (52, 77, 81, 121, 127, 130, 133, 150), [151] (30) ; 1987 See [137] (24), See [150] (30).

Zeilinger A., 1989 See [152] (30, 185).

Zhang W. -M., 1990 [69] (13).

Zou X. Y., 1990 See [156] (31).